4-22-2008

MonoAminergic Receptors in the Stomatogastric Nervous System: Characterization and Localization in Panulirus Interruptus

Merry Christine Clark

MONOAMINERGIC RECEPTORS IN THE STOMATOGASTRIC NERVOUS SYSTEM: CHARACTERIZATION AND LOCALIZATION IN *PANULIRUS INTERRUPTUS*

by

MERRY C. CLARK

Under the direction of Deborah J. Baro, Ph.D.

ABSTRACT

Neural circuit flexibility is fundamental to the production of adaptable behaviors. Invertebrate models offer relatively simple networks consisting of large, identifiable neurons that are useful for investigating the electrophysiological properties that contribute to circuit output. In particular, central pattern generating circuits within the crustacean stomatogastric nervous system have been well characterized with regard to their synaptic connectivities, cellular properties, and response to modulatory influences.

Monoaminergic modulation is essential for the production of adaptable circuit output in most species. Monoamines, such as dopamine and serotonin, signal via metabotropic receptors, which activate intracellular signaling cascades. Many of the neuronal and network targets of monoaminergic modulation in the crustacean stomatogastric nervous system are known, but nothing is known of the signal transduction cascades that mediate the biophysical response.

This work represents a thorough characterization of monoaminergic receptors in the crustacean stomatogastric nervous system. We took advantage of the close phylogenetic relationship between crustaceans and insects to clone monoaminergic receptors from the spiny lobster. Using a novel database mining strategy, we were able to identify several uncharacterized monoaminergic receptors in the *Panulirus interruptus* genome. We cloned one serotonin (5-

$HT_{2\beta Pan}$) and three dopamine receptors ($D_{1\alpha Pan}$, $D_{1\beta Pan}$, and $D_{2\alpha Pan}$), and characterized them with regard to G protein coupling and signal transduction cascades. We used a heterologous expression system to show that G protein couplings and signaling properties of monoaminergic receptors are strongly conserved among vertebrate and invertebrate species. This work further shows that DAR-G protein couplings in the stomatogastric nervous system are unique for a given receptor subtype, and receptors can couple to multiple signaling pathways, similar to their mammalian homologs.

Custom made antibodies were used to localize monoamine receptors in the stomatogastric ganglion, and in identified neurons. Pyloric neurons show unique receptor expression profiles, which supports the idea of receptor expression as an underlying mechanism for cell-type specific effects of a given modulator. Receptors are localized to the synaptic neuropil, but are not expressed in the membrane of large diameter processes or the soma. The localization of dopamine receptors in identified pyloric neurons suggests that they may respond to synaptic, paracrine or neurohormonal dopamine signals. This work also supports the idea that different types of signals can be generated by a single receptor.

INDEX WORDS: Central Pattern Generator, Stomatogastric, Monoamine, Dopamine, cAMP Serotonin, Signal transduction, GPCR, *Panulirus interruptus*, Crustacean, Heterologous expression, Invertebrate Neuromodulation

MONOAMINERGIC RECEPTORS IN THE STOMATOGASTRIC NERVOUS SYSTEM: CHARACTERIZATION AND LOCALIZATION IN *PANULIRUS INTERRUPTUS*

by

MERRY C. CLARK

A Dissertation Submitted in Partial Fulfillment of the Requirements for the Degree of

Doctor of Philosophy

in the College of Arts and Sciences

Georgia State University

2008

MONOAMINERGIC RECEPTORS IN THE STOMATOGASTRIC NERVOUS SYSTEM: CHARACTERIZATION AND LOCALIZATION IN *PANULIRUS INTERRUPTUS*

by

MERRY C. CLARK

Committee Chair: Deborah J. Baro, Ph.D.

Committee: Charles D. Derby, Ph.D.
Teryl K. Frey, Ph.D.
Susanna F Greer, Ph.D.
Paul S. Katz, Ph.D.

Electronic Version Approved:

Office of Graduate Studies
College of Arts and Sciences
Georgia State University
May 2008

DEDICATION AND ACKNOWLEDGEMENTS

This dissertation is dedicated to my parents, whose constant neutrality and unwavering support have rendered me capable of walking many paths.

Throughout the past five years, I have leaned on many people. My husband has been my reality touchstone. He found humor in the parts of the science that he/we didn't understand, an ability that kept me smiling and pushed me to look for answers. My sister shared her thoughts with me when I was discouraged and frustrated. Her words helped me stay grounded and focused on what is most important. Mark and Julie provided an oasis where I could truly relax a few times a year, and they have helped me continue to evolve. Nadja Spitzer helped me beyond words.

I have some patient friends that still make time when I have it to share: Zillah, Mara, Emily, Frisch, Lauren, Tom, Brian & Brandi, Syd, Mike B, Elzea, and my extended family: Joe and Audrey, Warren and Abby. These people have collectively kept me in check.

I feel that my committee is comprised of the absolute ideal for scientific assessment. I am sincerely honored to have worked with each of them. I would also like to acknowledge Dr Robert Simmons, and Dr. Don Edwards for their guidance along the way. Additionally, I am grateful for the financial support provided to me by the Molecular Basis for Disease program at Georgia State.

Dr. Deborah Baro has truly been the catalyst for my success. My experience with her has strengthened me both personally and professionally, and will prove invaluable in my future endeavors, whatever they may be.

TABLE OF CONTENTS

LIST OF TABLES

LIST OF FIGURES

LIST OF ABBREVIATIONS

DTT	1,4-dithiothreitol
Et-18-OCH_3	1-O-Octadecyl-2-O-methyl-rac-glycero-3-phosphorylcholine
CHAPS	3-[(3 cholamidopropyl)dimethylammonio]-1-propanesulfonate
IBMX	3-isobutyl-1-methylxanthine
Ach	acetylcholine
AC	adenylyl cyclase
AB	anterior burster
I_{KCa}	calcium activated potassium current
I_{Ca}	calcium-dependent outward current
CabTRP Ia	*Cancer borealis* tachykinin-related peptide-Ia
CPG	central pattern generator
CCK	cholecystokinin
MHC1	class 1 major histocompatibility complex
COG	commissural ganglia
CCAP	crustacean cardioactive peptide
cAMP	cyclic 3', 5'-adenosine monophosphate
$I_{K(v)}$	delayed rectifier potassium current
DAG	diacyl glycerol
DA	dopamine
DAR	dopamine receptor
dvn	dorsal ventricular nerve

dvn	dorsal ventricular nerve
DMEM	Dulbecco's modified eagle's medium
ER	endoplasmic reticulum
EOG	esophageal ganglion
Epac	exchange protein activated by cAMP
el	extracellular loop
ERK	extracellularly regulated kinase
FSK	forskolin
GPCR	G protein-coupled receptor
GIRK	G protein-regulated inwardly rectifying K^+ channel
GPR	gastropyloric receptor
GRK	GPCR kinase
GEF	guanine nucleotide exchange factor
GDP	guanosine diphosphate
GTP	guanosine-5'-triphosphate
HIS	histamine
HEK	human embryonic kidney
I_h	hyperpolarization-activated inward current
ICC	immunocytochemistry
IC	inferior cardiac
ion	inferior esophageal nerve
IPSP	inhibitory post-synaptic potential
IP_3	inositol 1,4,5-triphosphate

IP	inositol phosphate
il	intracellular loop
LP	lateral pyloric
lpn	lateral pyloric nerve
lvn	lateral ventricular nerve
LTD	long term depression
LTP	long term potentiation
mvn	medial ventricular nerve
MAPK	mitogen activated protein kinase
MAP	mitogen-activated protein
MCN	modulatory commissural neuron
MCN1	modulatory commissural neuron 1
MPN	modulatory proctolin neuron
NMJ	neuromuscular junction
OCT	octopamine
pFRG	parafacial respiratory group
PTX	pertussis toxin
PMA	phorbol 12-myristate 13-acetate
PDE	phosphodiesterase
PLC	phospholipase C
PI	phosphotidylinositol
PIP_2	phosphotidylinositol 4,5 bisphosphate
PIR	post inhibitory rebound

PBC	preBotzinger complex
PBC	preBotzinger complex
PKA	protein kinase A
PKC	protein kinase C
PP2B	protein phosphatase-2-B
PY	pyloric constrictor
PD	pyloric dilator
pdn	pyloric dilator nerve
pyn	pyloric nerve
PK	pyrokinin
RSA	receptor specific antibody
RT	reverse transcription
5-HT	serotonin
STG	stomatogastric ganglion
stn	stomatogastric nerve
stn	stomatogastric nerve
STNS	stomoatogastric nervous system
son	superior esophageal nerve
TTX	tetrodotoxin
I_A	transient potassium current
TM	transmembrane
TM	transmembrane
TEVC	two electrode voltage clamp

TYR	tyramine
V_1R	vasopressin-1 receptor
V_2R	vasopressin-2 receptor
VD	ventricular dilator
β_1AR	β-1-adrenergic receptor
β_2AR	β-2-adrenergic receptor
GABA	γ-aminobutyric acid

CHAPTER ONE

GENERAL INTRODUCTION

Central pattern generators

Rhythmicity is a fundamental property necessary for all living organisms. For example, gas exchange in the plant kingdom, patterns of bioluminescence in cyanobacteria, and animal behaviors such as sleeping and eating all rely on environmentally induced rhythms. In many cases, rhythmic physiological or behavioral activities are driven by coordinated electrophysiological oscillations produced by central pattern generators (CPGs). A CPG is a neuronal network that drives a set of muscles to produce a rhythmic activity. CPGs produce a wide variety of rhythmical motor patterns, including continuous activities, such as respiration, and intermittent behaviors, such as walking or chewing (Feldman et al. 2003; Selverston 2005). CPG output does not require rhythmic sensory or patterned central input. Rather, oscillatory behavior arises as a property of the CPG network components and/or the connectivities among them. Circuit input induces variability in the motor pattern and adapts output to changing demands. For example, walking, trotting and galloping are all produced by the same motor circuit, but each behavior is induced in response to different input, or intensity of input (Kiehn 2006).

In some cases, a CPG contains one or more endogenously oscillatory neurons, termed "bursting pacemaker" neurons, which generate the rhythm. In a pacemaker-driven CPG, one or more cells spontaneously and rhythmically depolarizes, fires bursts of action potentials, then repolarizes. In this case, the oscillatory behavior intrinsic to the pacemaker neuron(s) is determined by membrane currents that drive the periodic depolarization-repolarization cycle

(Gola and Selverston 1981; Harris-Warrick and Flamm 1987; reviewed in Harris-Warrick 2002). Coupling of a pacemaker neuron to other neurons in a CPG network forces follower neurons to exhibit oscillatory behavior, and the resulting motor pattern is shaped by additional intrinsic neuronal properties, such as post inhibitory rebound (PIR) or plateau potential (reviewed in Marder and Bucher 2001).

Endogenous bursting behavior is not associated with all CPG circuits. In some cases, neural rhythmicity emerges as a consequence of synaptic connectivity among the component neurons. In this type of CPG, termed a half-center oscillator (Brown 1924), reciprocal inhibitory connections between two neurons cause alternating bursts of activity. The mammalian locomotor CPG, for example, is a half center oscillator: populations of interneurons in the flexor or extensor half-centers excite flexor or extensor muscles, respectively. Simultaneous activity of flexors and extensors is prevented by mutual inhibitory connections between the half-centers (Kiehn 2006). Oscillations result as firing slows in one half-center, releasing the other half-center from inhibition and allowing for activity in antagonist motoneurons (Grillner et al. 1998). As is the case in pacemaker driven networks, the half-center oscillations are sculpted by intrinsic membrane properties that dictate the transition between activated and inactivated states. For example, the calcium activated potassium current (I_{KCa}) causes a progressive hyperpolarization following a burst that slows firing, consequently releasing the opposing half center oscillator from inhibition (Grillner et al. 2001). Alternatively, neuronal ionic currents that are activated by hyperpolarization often underlie escape from inhibition in the opposing oscillator (Kiehn et al. 2000). Thus, a full understanding of reciprocally inhibitory networks includes defining synaptic coupling as well as identifying the constellation of ionic conductances expressed in component neurons.

Often, CPGs have multiple mechanisms that sustain the rhythmic output. For example, mammalian respiratory rhythms appear to arise from multiple, mechanistically distinct CPG elements that are each capable of producing the same motor output, allowing for functional transitioning from a pacemaker-driven network to one driven by purely reciprocal synaptic interactions (Smith et al. 2000). Over the past decade, there has been a great deal of debate regarding the mechanism for respiratory rhythmogenesis, but the current consensus is that two brain regions are critical for generating the respiratory motor pattern: a subregion of the ventrolateral medulla termed the preBotzinger complex (PBC), and another region in the parafacial respiratory group (pFRG), located rostral to the PBC (Rekling and Feldman 1998; Onimaru and Homma 2003; Ramirez et al. 2004). Originally, experimental attempts to identify the respiratory rhythm generator focused on the PBC, showing that neural circuits located in this region were sufficient for generating respiratory motor patterns *in vitro*, and PBC neurons were capable of intrinsic bursting oscillations (Smith et al. 1991; Koshiya and Smith 1999). Moreover, lesioning of a subpopulation of PBC neurons led to an uncoordinated, non-rhythmic respiration in awake, adult rats (Gray et al. 2001). These results suggested that neurons present in the PBC generate the respiratory rhythm. However, subsequent studies indicated that the rhythm may be an emergent property of the network rather than being dependent on the bursting properties of the neurons, as abolishing bursting behavior in PBC neurons had no effect on respiratory-related rhythm in neonatal PBC slices (Del Negro et al. 2002). Furthermore, Thoby-Brisson and Ramirez found that the pacemaker neurons within the PBC displayed significantly different bursting properties (2001), and different responses during hypoxia (2000) which contributed to the idea of a distributed network that encompasses multiple pacemaker “kernels”. Indeed, Mellen et al. (2003) showed that neurons in the PBC and pFRG represent two synaptically coupled

pacemaker networks, each sufficient for generating the respiratory rhythm. Moreover, each of the oscillatory centers is differentially sensitive to modulatory input: opiates alter the pattern of the pFRG kernel but have no effect on PBC bursting (Mellen et al. 2003). Janczewski and Feldman (2006) further showed that these two rhythm generators are normally coupled but can function independently in juvenile rats *in vivo*, and suggested that the role of pFRG neurons is to drive the expiratory rhythm, while the PBC group controls inspiration. Despite significant advances in delineating the underlying mechanisms for respiratory rhythm generation, major researchers in this field do not share a common view on the mechanisms that drive rhythmical activity, and this remains a subject for debate (Feldman and Janczewski 2006a, b; Onimaru and Homma 2006).

Many of the operating principles for CPGs are the same for vertebrates and invertebrates (Marder and Calabrese 1996; Marder and Bucher 2001). As such, the relative simplicity of invertebrate nervous systems provides a means of investigating the molecular basis of rhythmic behaviors. Indeed, much of the conceptual work that has provided some understanding of vertebrate CPG circuits is derived from invertebrate systems. For example, the first evidence that rhythmic motor patterns are centrally generated came from studies on the locust nervous system (reviewed in Marder and Calabrese 1996). Studies on the *Tritonia* swim circuit were the first to show that neuromodulation can be intrinsic to a CPG circuit (Katz et al. 1994; Katz and Frost 1997), and the leech heartbeat CPG has offered insight into intersegmental coordination of CPG circuits, and circuits with multiple mechanisms for generating rhythmic output (Arbas and Calabrese 1987b, a; Angstadt and Calabrese 1989; Arbas and Calabrese 1990; Angstadt and Calabrese 1991; Cymbalyuk et al. 2002). Moreover, the CPG that controls feeding behavior in *Aplysia* not only represents a useful model for examining sensorimotor integration, but is also

providing new insights into the neural networks and subcellular mechanisms that mediate two important forms of associative learning (reviewed in Cropper et al. 2004).

The stomatogastric system

One of the best characterized model systems for investigating rhythm generating neuronal networks is the crustacean stomoatogastric nervous system (STNS), which contains multiple CPGs that control rhythmic feeding and digestive activities such as swallowing, chewing, and filtering of food particles. The crustacean foregut consists of a short, muscular esophageal tube, and a stomach. The stomach is further subdivided into three regions: the cardiac sac, gastric mill, and pylorus (Figure 1-1). Unlike the mammalian foregut, which is comprised of an epithelium surrounded by smooth muscle, the crustacean foregut is surrounded by striated muscles. Motor neurons in the STNS CPGs innervate these muscles. The motor nerves have multiple terminals widely distributed over the muscle fiber, and contraction of the muscle is a graded function of synaptic input. Muscle contractions direct food taken in through the mouth through the esophagus to the cardiac sac, where it is combined with digestive juices. Partially digested food is then directed to the gastric mill region, which contains three interlocking teeth that facilitate mechanical breakdown. Smaller pieces pass into the pylorus, where filtering occurs (Johnson and Hooper 1992). Solid particles are passed into the animal's hindgut for excretion, while fluid nutrients are taken up by a system of glands functionally similar to the liver and pancreas (Ceccaldi 1989).

All of the muscles directing these rhythmic movements are controlled by four CPG circuits found within the STNS. The esophageal circuit controls muscles to allow alternating constrictions and dilations of the esophagus, while the cardiac sac circuit innervates muscles

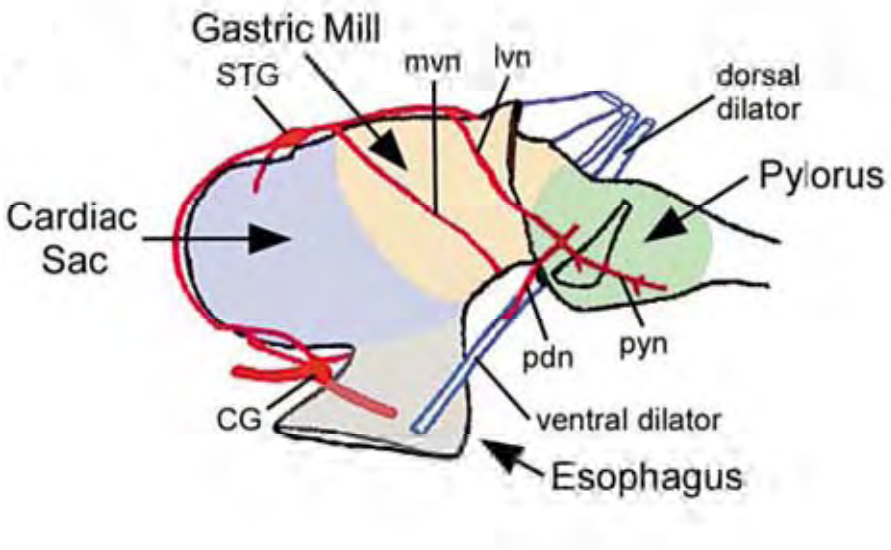

Figure 1-1: Diagrammatic view of the lobster foregut. Schematic shows the esophagus, the 3 regions of the stomach (cardiac sac, gastric mill, pylorus), the stomatogastric nervous system (red), and 2 pyloric muscles (the dorsal and ventral dilators). Nerve abbreviations: pdn = pyloric dilator; pyn = pyloric; lvn = lateral ventricular; mvn = medial ventricular. Ganglion abbreviations: STG = stomatogastric; CG = commissural. From (Hooper and DiCaprio 2004).

that control the size of the cardiac sac region of the stomach (Johnson and Hooper 1992). Contraction of these muscles expands the cardiac sac, which allows food to enter. The gastric mill CPG circuit participates in constriction of the cardiac sac, which directs food to the gastric mill, and also controls the stomach teeth to facilitate chewing. The pyloric network controls movements of the pyloric filtering machinery. Movement of food particles occurs bidirectionally from the gastric mill to the pylorus and vice versa, such that chewing and filtering activities are repeated to ensure thorough digestion (Ceccaldi 1989).

The STNS is a peripheral nervous system comprised of four ganglia and their associated nerves (Figure 1-2). The paired commissural ganglia (CoG) each contain roughly 400 neurons, while the unpaired esophageal ganglion (OG) contains approximately 18 neurons (Marder and Bucher 2007). Among other things, descending input from these centers controls activity in the fourth ganglion, the stomatogastric ganglion (STG), comprised of roughly 30 neurons, depending on the species (Bucher et al. 2007). The esophageal and cardiac sac CPG circuitries lie in the CoG and the OG, while the gastric and pyloric networks are localized to the STG (Figure 1-2). The distribution of esophageal and cardiac sac component neurons among multiple ganglia has made them difficult to identify, and while the rhythms produced by these CPGs are known, the circuitry has not been completely mapped out. On the other hand, the gastric and pyloric networks have been extensively characterized, and are among the best understood neural circuits to date.

The gastric mill circuit is inactive *in vivo* and *in vitro,* except when it receives input from CoG projection neurons (Blitz and Nusbaum 1997; Clemens et al. 1998a; Blitz et al. 1999). The gastric mill rhythm does not emerge as the result of pacemaker activity, but is instead the result

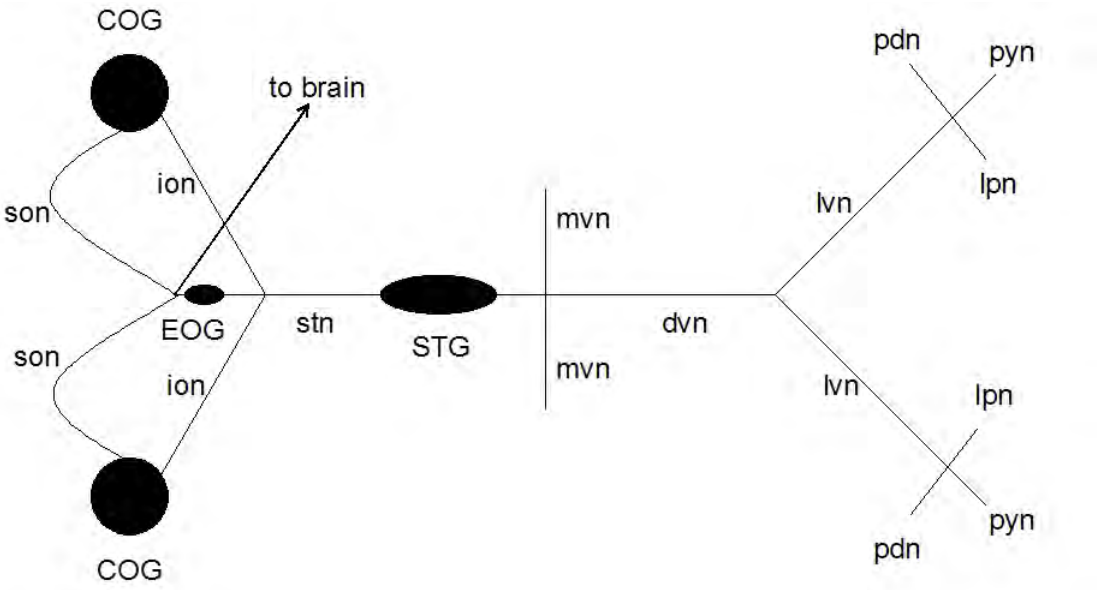

Figure 1-2: Diagram of the STNS. Ganglia are represented as *filled ovals* and *circles*. Ganglia contain the somatodendritic compartments of neurons. Neurons in one ganglion project their axons to another ganglion or to muscles via identified nerves, which are represented as *lines*. Monopolar neurons in the STG send their axons down the *dvn* to terminate on muscle fibers, or up the stn to terminate in the neuropil of higher ganglia (i.e. commissural ganglia, *COG*). *EOG*, esophageal ganglion; *ion*, inferior esophageal nerve; *son*, superior esophageal nerve; *stn*, stomatogastric nerve; *dvn*, dorsal ventricular nerve; *mvn*, medial ventricular nerve; *lvn*, lateral ventricular nerve; *lpn*, lateral pyloric nerve; *pyn*, pyloric nerve; *pdn*, pyloric dilator nerve.

of synaptic interconnectivity within the network (Selverston and Mulloney 1974; Hartline and Russell 1984). The resulting motor pattern is variable, depending on how the rhythm is initiated (Coleman and Nusbaum 1994; Blitz et al. 1999; Beenhakker and Nusbaum 2004; Blitz et al. 2004). For example, two different gastric mill rhythms are elicited *in vitro* in the crab, *Cancer borealis*, depending on whether projection neurons in the CoGs are stimulated by mechanoreceptor or proprioceptor input (Beenhakker and Nusbaum 2004; Blitz et al. 2004). Proprioceptor input additionally plays a regulatory role during gastric mill activity via direct connections with gastric mill neurons to further influence the motor output (Beenhakker et al. 2005).

Unlike the gastric mill circuit, the pyloric CPG is continuously active in the intact animal, producing alternating dilations and constrictions of the pylorus (Rezer and Moulins 1983). The pyloric rhythm is pacemaker-driven, though the complete motor pattern results from the connectivity and membrane properties of all network components (Miller 1987). Pyloric activity is conditional on the presence of one or more neuromodulators, and removal of modulatory input to this network abolishes rhythmic output (Nagy and Miller 1987). Several variations of the pyloric rhythm can be elicited, depending on the exact modulatory input (reviewed in Dickinson 2006). The pyloric CPG is the subject of this dissertation and is discussed in more detail below.

One characteristic of CPGs within the STNS is a great deal of internetwork connectivity. Activity in one STNS circuit often influences activity in another. For example, gastric mill and cardiac sac activity alter the motor pattern produced by pyloric network (Thuma and Hooper 2002, 2003). The result is that pyloric muscles can display gastric or cardiac motor patterns even though they are not innervated by neurons from these CPGs (Morris et al. 2000). While the functional relevance of these internetwork interactions is not completely understood, it is thought

that they coordinate muscle contractions among the foregut compartments, and thus the directionality of food movement, to ensure adequate digestion (Thuma et al. 2003).

Another type of internetwork interaction results in circuit reconfigurations. Meyrand et el. (1991) showed that modulatory input elicits a rhythmic, swallowing-like behavior that mediates the transfer of food from the esophagus to the cardiac sac (Figure 1-1), and the motor pattern for this behavior is produced by a single CPG constructed *de novo* from components of the esophageal, gastric mill, and pyloric circuitries. The *de novo* circuit produces a single motor output that overrides the individual esophageal, gastric and pyloric patterns, ensuring that valve openings are synchronized and food is moved posteriorly. Thus, CPGs are not necessarily hard-wired.

In light of these examples of CPG flexibility, an increasing number of studies address CPGs not as the sum of the network components and their cellular and synaptic properties, but as complex, dynamic systems with multiple mechanisms for generating rhythmic output. Studies regarding the cellular and molecular basis for CPG flexibility are rapidly growing in number. We are particularly interested in how monoaminergic signal transduction cascades contribute to circuit flexibility. Indeed, a complete understanding of CPG function will necessarily include such information.

The pyloric network

In the spiny lobster, *Panulirus interruptus*, the pyloric network is a 14-neuron circuit containing 6 cell types: the anterior burster (AB), two pyloric dilators (PDs), the ventricular dilator (VD), the inferior cardiac (IC), the lateral pyloric (LP), and eight pyloric constrictors (PYs) (Miller 1987). The somatodendritic compartments of these neurons lie within the STG. All

of these neurons, except the pacemaker AB, project their axons to a muscle(s) via identified motor nerves as shown in Figure 1-2. The AB neuron projects its axon up the stomatogastric nerve (*stn*) and makes connections with higher ganglia, such as the CoG. A more detailed description of neuron and STG anatomy is provided in Chapter 2.

As shown in Figure 1-3, the extensive chemical and electrical connections of the pyloric neurons are known. All of the chemical synapses within the network are inhibitory (indicated by small, filled circles in Figure 1-3). Electrical couplings are either rectifying, as in the case of the LP-PY, PY-PY, and VD-PD synapses (Figure 1-3, diode symbols), or nonrectifying, such as those between the AB neuron and the two PD neurons, and between the PD neurons themselves (resistor symbols, Figure 1-3). Some connections are mixed, as in the case of the AB-VD, which has both a chemical and a rectifying electrical synapse (Eisen and Marder 1982).

In vitro, the pyloric motor pattern is similar to that recorded *in vivo* (Miller 1987). The characteristic triphasic pyloric output (Hartline and Maynard 1975; Selverston 1977) is shown in Figure 1-4. Figure 1-4A shows intracellular recordings from the somata of six pyloric cell types. PD and AB fire in the first phase, LP and IC in the second phase, and PY and VD in the third phase. Figure 1-4B shows extracellular recordings from identified motor nerves containing the axons of these neurons. Spikes seen on the nerve recordings correspond to bursts of action potentials generated by neurons whose axons are contained within the nerve. For example, the pyloric dilator nerve (*pdn*) contains axons from the two PD neurons, and the *pdn* recording shown in Figure 1-4B depicts spikes generated by the PD neurons. The lateral ventricular nerve (*lvn*) contains the LP, PY and the PD axons; hence there are three distinct sets of spikes on the *lvn* recording. The medial ventricular nerve (*mvn*) contains the VD and IC axons; action potentials generated by the VD and IC neurons are represented on the *mvn* recording. The spikes

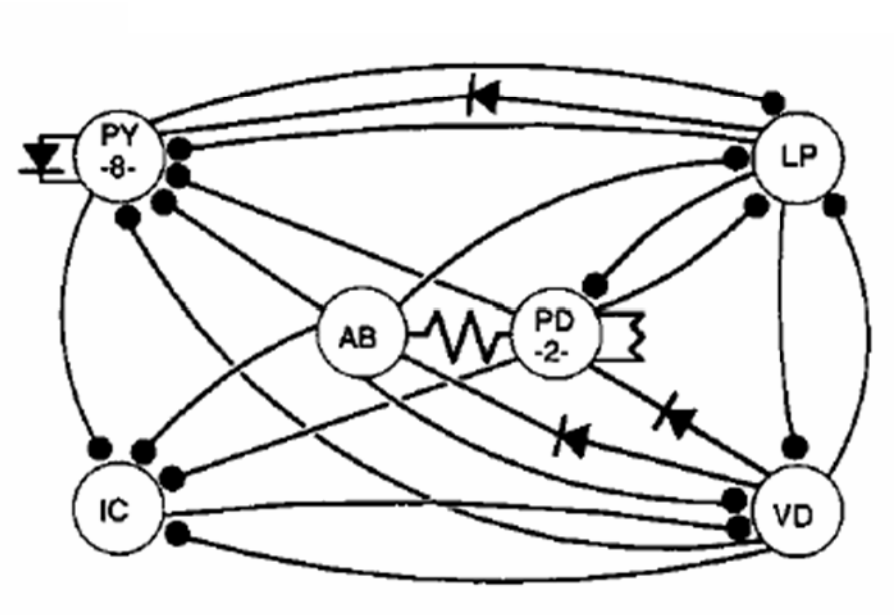

Figure 1-3: The neuronal complement and synaptic interconnectivity of the pyloric network. There are 8 PY neurons, 2 PD neurons, and one each of the other pyloric neurons. Small, filled circles indicate inhibitory chemical synapses, resistor symbols indicate nonrectifying electrical synapses, diodes indicate rectifying electrical synapses, with the direction of the arrow representing the preferred direction of positive current flow. From (Johnson et al. 1995).

seen in a burst presumably regulate muscle contractions, but there is not necessarily a linear correlation between spiking and contraction, as contraction properties are modified in some cases by the number or the frequency of action potentials, (Morris and Hooper 1997) or the pyloric cycle period (Morris and Hooper 1998).

Pyloric neurons interact to generate a triphasic rhythm (Figure 1-4) in the following manner: the dilator phase (Phase I) of the pyloric rhythm is driven by a three-neuron electrically coupled pacemaker kernel, consisting of an endogenous burster (the AB neuron) and the two PD neurons. These three neurons inhibit all the other neurons in the network (Figure 1-3). Next is the two-part constriction phase. When PD inhibition wanes, the LP is first to recover and it inhibits PY, VD and PD (Phase II). IC fires in phase with LP. As LP begins to repolarize, PY and VD escape from inhibition and inhibit LP (Phase III). Inhibition of LP allows PD to depolarize and the cycle begins again. Thus, the sequential firing of LP and PY drives the two-part constriction phase of the motor pattern.

The triphasic pyloric motor output drives a sequence of muscle contractions that underlie the filtering activities in the pylorus. In phase one, the PD induces contraction of the cardiopyloric valve muscles, which dilate the pylorus and open the cardiopyloric valve, allowing liquefied food to enter the pylorus (Johnson and Hooper 1992; Selverston 2005). In the two part constriction phase, a rostral to caudal wave of pyloric muscle constriction directs food toward the. midgut or digestive gland (Selverston 2005). In the case of large food particles that require further processing, muscles innervated by additional STNS circuits participate in opening the cardiopyloric valve and directing food anteriorly (Johnson and Hooper 1992).

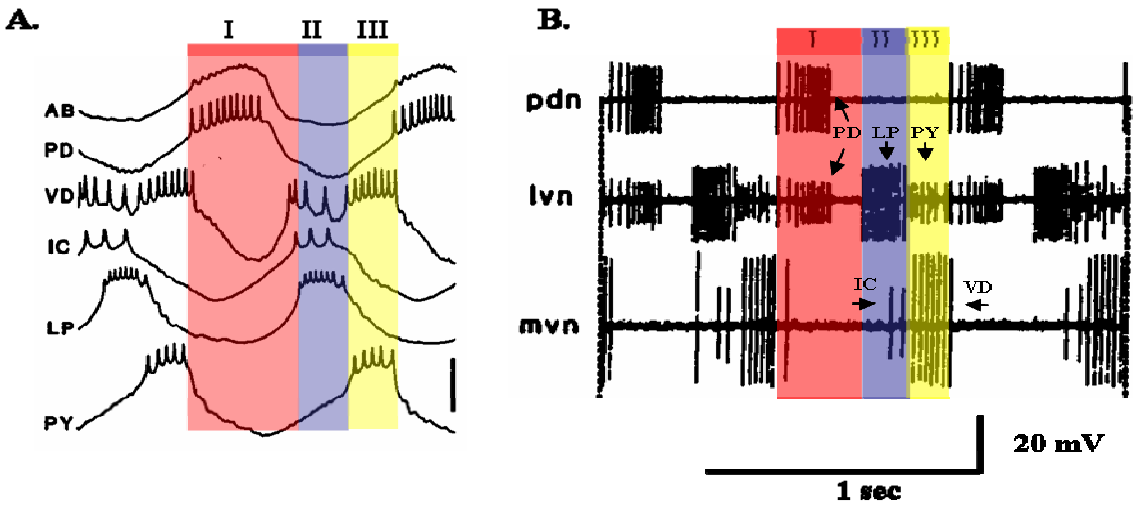

Figure 1-4: The pyloric motor pattern. **A)** Intracellular glass microelectrodes were used to record *in vitro* from the somata of six pyloric neurons. The duration of the recording shown is 1 sec. Scale bar = 20 mV for PD and LP, 10 mV for AB, VD, IC, and PY. **B)** Extracellular recordings from the peripheral motor nerves *in vitro*. The *pdn* contains axons from the two PD neurons. The *lvn* contains the LP axon (large spikes), the PY axons (small spikes), and the PD axons (intermediate spikes). The *mvn* contains the VD axon (large spikes) and IC axon (small spikes). The triphasic pyloric rhythm consists of bursts of action potentials from the PD neurons (Phase I, orange), followed by bursts of action potentials in the LP neuron (Phase II, blue), then by bursts in the PY neurons (Phase III, yellow). Phases are indicated by roman numerals and highlighted for clarity in A and B. Recordings are from *P. interruptus* preparations with CoGs intact. Adapted from (Miller 1987).

Neuromodulatory input to the STG

Natural selection favors animals capable of producing adaptive behaviors. Feedback or input to CPG circuits refines the motor output pattern, thus enabling continuous behavioral flexibility. For example, cerebellar input influences locomotor CPG output, such that limb movements are coordinated within each step cycle (Grillner 1985). Likewise, sensory and neuromodulatory inputs coordinate respiratory rhythms with changing metabolic demands (Mitchell and Johnson 2003). As mentioned above, the range of flexibility afforded to STG circuits by modulatory inputs is extensive. In some cases, modulatory input is necessary to initiate a motor pattern, while in other cases, modulators alter an active motor pattern. Modulators can also enable neurons to switch from one CPG to another, or form new circuits capable of generating a distinct motor pattern. Thus, the STG circuits provide attractive models for studying CPG modulation.

Modulatory substances are delivered to the STG via projection neurons in the OG or CoGs, which send their axons to the STG via the *stn* (Figure 1-2) (reviewed in Nusbaum and Beenhakker 2002). Within the STG, the input fibers can arborize extensively, sending process throughout the entire ganglion (Nusbaum et al. 1992). In the crab, *Cancer borealis*, there are roughly 25 different modulatory input fibers to the STG, which is approximately half the number of input fibers seen the spiny lobster (Coleman et al. 1992). These fibers deliver neuropeptides and small molecule transmitters, and in some cases amines, to the STG (reviewed in Marder and Bucher 2007). Modulatory inputs contain both conventional and nonconventional transmitter release profiles. Electron microscopy studies have revealed that, within the STG, modulatory neuron terminals contain classical, fast-synaptic neurotransmitter release profiles, as well as

neurohemal profiles, which are associated with release at a distance from the target (Marder et al. 1995). Thus, projection neurons can have both synaptic and paracrine effects on STG neurons.

Primary sensory neurons can also be sources of modulatory input to the STG, and can induce fast excitatory responses, as well as slow, prolonged modulation of STG neurons (Katz and Harris-Warrick 1990b). In the crab *Cancer borealis*, the gastropyloric receptor (GPR) cells are proprioceptive cells that sense the movement of foregut muscles (Katz et al. 1989). GPR cells send input fibers containing both serotonin (5-HT) and acetylcholine (Ach) to the STG to modify the pyloric and gastric rhythms (Katz and Harris-Warrick 1990a). The presence of co-transmitters in modulatory neurons is not uncommon in this system, and indeed serves to enhance the range of responses that can be elicited (see below) (Nusbaum et al. 2001). GPR stimulation has 5-HT-mediated, modulatory effects on all of the pyloric neurons, but only elicits Ach-mediated, synaptic responses in two of the cells (Katz and Harris-Warrick 1990a). These findings suggest that the GPRs do not synapse directly onto all pyloric neurons, because all pyloric cells respond to Ach (Marder and Eisen 1984). Thus, sensory inputs to the STG likely have both synaptic and paracrine effects.

The STG is located in a blood vessel, and is therefore constantly bathed in hemolymph. As such, modulatory substances can reach the STG as circulating hormones. Indeed, many of the same neuroactive chemicals that are delivered to the STG by modulatory neurons are also found concentrated in varicosities within neurosecretory structures (Christie et al. 1995; reviewed in Marder and Bucher 2007), and freely circulating in the hemolymph at nanomolar concentrations (Livingstone et al. 1980). In the crab, one pair of projection neurons in the CoGs contain a cholecystokinin (CCK)-like peptide within their STG terminals, and this same neuropeptide is found the pericardial organs, which are the major neurohemal structures in the crab (Christie et

al. 1995). In *Panulirus interruptus*, levels of a CCK-like peptide in the hemolymph increase fourfold after feeding, peaking at 1.6 x 10^{-9} M, and gradually decrease over 4 hours (Turrigiano and Selverston 1990). Thus, a single neuroactive chemical can have effects with different time scales (i.e., short-term or long-term) depending on how it is released.

For a given modulator, the release mechanism may vary within species. In adult *Homarus americanus*, 5-HT modifies pyloric network activity, and the threshold for producing physiological effects is 10^{-6}M, which is much greater than the 10^{-9}M concentration of 5-HT in the circulating hemolymph (Beltz et al. 1984). As such, 5-HT is presumed to exert its modulatory influence via direct input fibers to the STG. Indeed, 5-HT immunoreactivity is observed in the *stn* and within the STG neuropil in the adult (Beltz et al. 1984). During embryonic development, however, 5-HT modulates the motor patterns produced by STG neurons well before 5-HT is found in projection inputs to the STG (Fenelon et al. 1999), suggesting that hormonally released 5-HT plays a predominant role in regulating STG output early in *H. americanus* development, while direct 5-HT input becomes relevant at later stages.

For a given modulator, the modulatory release mechanism may vary across species. As mentioned above, 5-HT is found in input fibers to the STG in the lobster *H. americanus*, and high concentrations (10^{-6} M) of this monoamine modulate pyloric activity. In the spiny lobster, *Panulirus interruptus*, however, the threshold for 5-HT-mediated modulation of pyloric activity is 10^{-9} M (Beltz et al. 1984). Indeed, this monoamine is not found in descending modulatory input fibers, but only in the neurosecretory structures, and thus acts strictly as a hormone in this species. The neuromodulatory content of input neurons can also differ across species: the GPR cells contain 5-HT in the crab, but not in the spiny lobster, for example (reviewed in Katz and Harris-Warrick 1990b).

Effects of modulatory input

Several modulatory inputs to the STG have been described (reviewed in Katz and Harris-Warrick 1990b; Nusbaum and Beenhakker 2002). Research on one of the most well studied modulatory neurons, the modulatory commissural neuron (MCN)-1, has revealed many basic principles related to neuromodulation. One such principle is that the effect of a modulatory neuron is not limited to one CPG. Some modulatory neurons, when stimulated, can simultaneously modify the pyloric, gastric mill and cardiac sac activities and thereby coordinate the functions of the different circuits. As an example, MCN-1 excites the pyloric network (Coleman and Nusbaum 1994) and elicits gastric mill activity (Coleman et al. 1995). Thus, modulatory neurons can have multiple targets which comprise different CPGs.

A second basic principle regarding MCN-1 studies is that a neuron may contain multiple transmitters; however, a given cotransmitter may act on only a subset of all of that neuron's modulatory targets. In the crab, MCN-1 contains multiple modulatory substances, or co-transmitters: γ-aminobutyric acid (GABA), proctolin and *Cancer borealis* tachykinin-related peptide-Ia (CabTRP Ia), and each of these can modify gastric mill activity when bath applied (Blitz et al. 1999). However, the MCN-1 uses only CabTRP Ia and GABA to initiate the gastric mill rhythm, and MCN-1-released proctolin has no direct influence on the gastric mill CPG (Stein et al. 2007). Conversely, the effects of MCN-1 on the pyloric network are mediated by proctolin and CabTRP Ia (Wood and Nusbaum 2002).

There are several mechanisms that could restrict a modulator's actions to only a subset of all possible post-synaptic targets. The most obvious explanation is that a target cell lacks the appropriate receptor. As I show in my dissertation work, this is possible, because STG neurons can display unique receptor expression profiles. However, in the case of MCN-1 and its targets,

there are examples of neurons that do not respond to an MCN-1 released neuropeptide but do respond to the same focally applied peptide (Stein et al. 2007); thus, other mechanisms must exist. Another explanation is that the modulatory substance may never reach the target cell's receptors due to differential release and/or diffusion barriers. In some cases, a neuron will not release a given modulator from all terminals. Neuropeptides can be targeted to only a subset of terminals (Sossin et al. 1990). Similarly, transmitter release may differentially depend on neuronal firing patterns. Neuropeptide release often requires higher firing frequency than small molecule transmitter (i.e., GABA) release (Vilim et al. 1996). Often, this is due to the fact that the peptides are localized at a distance from the release site (Karhunen et al. 2001). Diffusion barriers may also prevent neuroactive substances from reaching receptors on target cells. Several types of diffusion barriers can exist, including physical (Kilman and Marder 1996), cellular (e.g. glial wrap) or molecular barriers, such as reuptake mechanisms (Iversen 2006), and enzymes that degrade the neuroactive substance (Wood and Nusbaum 2002). This brings us to the next principle: Neuromodulatory influences can be locally regulated.

Paracrine or long distance effects are mediated by neuroactive substances, which in most cases, are not released directly into the synaptic cleft, and are therefore not subject to the classical reuptake mechanisms operating for neurotransmitters (reviewed in Nusbaum 2002). Instead, these modulatory substances can diffuse within the STG and exert a wider range of influence over longer time scales than synaptic transmitters. Interestingly, the same neuropeptide released in a paracrine fashion by one or more neurons does not necessarily reach the same set of receptors. Rather, the extent of neuromodulatory control can be dictated by extracellular aminopeptidase activity. For example, MCN-1 and MPN differentially modulate the pyloric rhythm in the crab, even though the different effects are partially mediated by the same

modulator, proctolin. When proctolin actions are prolonged by blocking aminopeptidase activity, the pyloric circuit response to these two projection neurons is similar (Wood and Nusbaum 2002). Thus, modulatory influences are spatially and functionally restricted, in some cases, by peptidase activity.

A fourth organizing principle revealed by studies on MCN-1 is that cotransmitters can act over different time scales, and this is often essential for pattern generation. For example, the MCN-1-mediated actions of CabTRP Ia and GABA on gastric mill neurons have different time courses of action (Stein et al. 2007). The fast GABAergic actions initiate bursting in one of the gastric mill neurons, while the peptidergic actions slowly excite a gastric mill neuron that in turn inhibits MCN-1. The temporally distinct responses of MCN-1's targets in this case lead to phasic inhibition of MCN-1 transmitter release, which is critical for shaping the gastric mill rhythm (Coleman et al. 1995).

A fifth principle of neuromodulation is that different projection neurons containing the same neuroactive substance can elicit distinct STG rhythms depending upon the complement of cotransmitters (Nusbaum et al. 2001). For example, three pair of proctolin containing neurons innervate the STG and modulate circuit activity: MCN-1, MCN-7, and modulatory proctolin neuron (MPN) (Coleman et al. 1992; Blitz et al. 1999). These three proctolinergic neurons have distinct cotransmitters, and this contributes to their distinct actions on the STG circuits. As mentioned above, MCN-1 uses CabTRP Ia and GABA to differentially modulate gastric mill neurons, while proctolin and CabTRP Ia mediate its effect on the pyloric circuit. Stimulation of MPN or MCN-7 elicits distinct pyloric rhythms but does not activate the gastric mill rhythm. The distinct effects are due, in part, to the fact that MPN uses GABA and proctolin, while MCN-7 has no known co-transmitter (Blitz and Nusbaum 1999).

A sixth principle is that the same motor pattern can be elicited by different modulatory inputs. In *Cancer borealis,* pyrokinin (PK) peptides are found in modulatory inputs to the STG and in neurohemal release sites, and bath applied PK elicits gastric mill activity *in vitro* (Saideman et al. 2007b). The PK-elicited gastric mill rhythm is nearly identical to the MCN-1-elicited gastric mill rhythm, even though MCN-1 does not use PK as a cotransmitter. However, despite the similarities in the two elicited gastric mill motor patterns, they are different. This is because bath applied PK targets distinct sets of STG neurons to elicit the gastric mill motor pattern than MCN-1 stimulation (Saideman et al. 2007a). MCN-1 stimulation targets a pyloric neuron, the AB, and so alters the pyloric rhythm, but PK has no effect on pyloric neurons, which leads to differences in gastro-pyloric coordination in response to PK- versus MCN-1-mediated modulation. Since the coordination of circuit activities is variable under different physiological conditions (i.e., before or after feeding) (Clemens et al. 1998b), these results highlight the functional relevance of convergent modulatory actions.

A seventh principle is that neuromodulators can converge onto the same current. Indeed, six neuromodulatory substances have been found to activate the same voltage dependent current in pyloric neurons (Swensen and Marder 2000). The response to one of the six modulators is nonetheless variable among neurons. For example, all six substances elicit the same current in the LP neuron, while the VD neuron responds to only a subset of the modulators. Indeed, each of the modulators targets a distinct set of pyloric neurons, and therefore elicits a unique motor pattern, despite sharing a common target (Swensen and Marder 2001).

The preceding discussion focused on modulatory influences that acted over the short term. However, the last principle to be discussed is that modulatory neurons can have long term effects. In the absence of modulatory inputs, neurons reorganize their ionic current densities to

maintain a constant firing pattern (Mizrahi et al. 2001; Thoby-Brisson and Simmers 2002). This suggests that modulatory inputs somehow help to control gene expression in the target neuron. The observed changes in current densities are partly due to changes in neuronal activity (Golowasch et al. 1999; Watt et al. 2000; Mee et al. 2004). However, it appears that neuromodulators also have activity independent effects and can directly regulate current densities (Khorkova and Golowasch 2007). Modulatory inputs can also exert long-term regulatory effects on their target networks during development. In *Homarus gammarus*, modulatory inputs play a critical role in the maturation of motor networks, by maintaining a unique embryonic neuronal network while masking the adult circuit until appropriate stages in development (Le Feuvre et al. 1999).

Effects of hormonal input

Hormonal input also influences STG motor patterns. In *Homarus americanus*, hormonal concentrations of DA evoke action potentials in the PD neuron, and these spikes are generated in the axon, where no direct DA input exists (Bucher et al. 2003). These spikes travel orthodromatically toward the PD muscle and antidromatically toward the PD soma where they can influence PD bursting behavior. Interestingly, the effects of DA-induced peripheral spikes are state-dependent: with modulatory input removed, centrally generated spikes increase in response to DA, but then gradually decline and cease. On the other hand, peripheral spikes increase in DA up to a steady state level, such that they generate the majority of the overall spikes. In preparations with modulatory inputs intact, centrally generated spikes decrease with increasing peripheral spikes in response to DA, and both reach a steady level. Thus, the

hormonal influence on pyloric motor patterns depends on the state of the circuit that is established by modulatory inputs.

In some cases, hormonal inputs expand the range of flexibility of the CPG circuits beyond that provided by neuronal modulation. For example, crustacean cardioactive peptide (CCAP), influences the STG only as a circulating hormone (Marder and Bucher 2007). At low concentrations (10^{-10}M), CCAP does not elicit gastric mill activity, but does modify the MCN-1-elicited gastric mill rhythm in *C. borealis* (Kirby and Nusbaum 2007). Interestingly, gastric mill neurons that exhibit altered activity during these CCAP-influenced rhythms do not correspond completely to the set of CCAP-responsive neurons. Moreover, if gastric mill activity is triggered by direct mechanoreceptor stimulation, CCAP also modifies the resulting gastric rhythm, though it targets a different subset of neurons than those targeted during the MCN1-elicited rhythm. Thus, despite having multiple targets within the gastric mill circuit, CCAP acts on only a subset of neurons, depending on the state of the circuit.

Hormonal influences provide long term effects that may outlast the presence of the hormone. As mentioned above, increasing levels of a CCK-like peptide are found in the hemolymph following feeding in *Panulirus interruptus* (Turrigiano and Selverston 1990). The levels of this hormone coincide neatly with gastric mill activity over the same time period: at one hour post-feeding, gastric mill cycle frequency and CCK levels peak, then both decline over a period of three hours, suggesting that CCK regulates gastric mill activity. Postprandial gastric mill activity can be blocked if a CCK antagonist is administered within two hours of the initiation of feeding behavior, but the antagonist has little effect if administered more than two hours after the start of feeding, suggesting that the intracellular effects of the hormone are long lasting. Moreover, gastric mill activity triggered by CCK injections is not identical to that seen

after feeding, indicating that this hormone contributes to feeding behavior in the lobster, similar to its role in vertebrate systems, but gastric mill activity is influenced by additional, state-dependent modulatory sources *in vivo*.

The role of neuromodulators in homeostatic maintenance of CPG activity

As discussed above, neuromodulators can produce both short-term (e.g., differences in phosphorylation states) and long-term (e.g., differences in transcript and protein abundance) changes in intrinsic neuronal properties and synaptic strengths. In addition, activity-dependent mechanisms can produce long-term changes in these same properties (Golowasch et al. 1999; Mee et al. 2004). This leads to significant preparation-to-preparation variability in ion channel mRNA abundance and ion current maximal conductance in identified neurons (Schulz et al. 2006; Schulz et al. 2007), as well as variability in synaptic strengths (Watt et al. 2000; Watt et al. 2004). Despite this, circuit activity is remarkably constant over the long-term. This begs the question: How is it that stable firing properties and variable ion channel densities are not mutually exclusive?

Modeling studies have shown that multiple combinations of synaptic strengths and neuronal properties can produce a constant circuit output (Prinz et al. 2004). Thus it is likely that multiple ionic currents and synaptic strengths, which are constantly changing over the short term, are balanced over the long term to maintain a constant circuit output. Our lab is testing the idea that modulators contribute to the maintenance of a stable output over the long term by continually controlling the phosphorylation state and transcription of a given ion channel, Further, that a change in modulator concentration will evoke opposite effects on channel function and abundance, e.g., an increase in conductance and a decrease in gene expression. We are

testing this hypothesis for the monoamines dopamine (DA) and serotonin (5-HT), because a great deal of background information exists on their cellular and circuit effects in the STNS (see below). An understanding of DA and 5-HT receptors and their signaling cascades is therefore a prerequisite for testing the hypothesis. When I began my dissertation work, the signaling cascades mediating the neuromodulatory effects in the STG were completely unknown. Moreover, in general, there is no clear understanding of the spatio-temporal organization of transduction cascades in any neurons. Thus, I set out to characterize the DA and 5-HT signal transduction cascades operating in the pyloric network.

Serotonergic modulation of the pyloric network in Panulirus interruptus

Among the more than 30 different modulatory substances that have an effect on the pyloric network (Marder and Bucher 2007), monoamines play a central role in reconfiguring the circuit. They can alter both the strength of synaptic interactions and the intrinsic firing properties of neurons within the network to influence motor output. The monoamines octopamine (OCT), 5-HT, and dopamine (DA), are delivered via ascending or descending input fibers, or as circulating hormones. Their effects on pyloric motor output have been characterized in detail (Flamm and Harris-Warrick 1986b, a; Katz and Harris-Warrick 1990b; Johnson et al. 1994, 1995; Ayali et al. 1998; Ayali and Harris-Warrick 1999; Kloppenburg et al. 1999; Kloppenburg et al. 2000; Johnson et al. 2003; Gruhn et al. 2005; Peck et al. 2006). Each monoamine evokes a unique suite of changes in the motor pattern. For example, each of the three monoamines elicits bursting in a quiescent AB by acting on different ionic currents, resulting in distinguishable differences in burst frequency and amplitude (Harris-Warrick and Flamm 1987).

In the spiny lobster, *Panulirus interruptus*, 5-HT acts strictly as a circulating neurohormone to alter the intrinsic firing properties and synaptic strengths of pyloric network components over the long term (Beltz et al. 1984; Flamm and Harris-Warrick 1986b, a). Over two decades ago, Flamm and Harris-Warrick (1986a) showed that a 10 minute bath application of 10^{-5}M 5-HT, intending to mimic neurohormonal transmission in *P. interruptus*, has differential effects on pyloric neurons. In a synaptically intact circuit, with endogenous modulatory inputs removed, 5-HT elicits bursting in AB and PD, has a weakly excitatory effect on IC, inhibits LP and VD, and has no effect on the PY neuron.

In isolated cells (i.e., all modulatory and synaptic inputs blocked), the effects of 5-HT are consistent with those recorded in intact circuits, with the exception of the PD neuron: 5HT has no effect on the isolated PD (Figure 1-5) (Flamm and Harris-Warrick 1986b). Thus, PD activity is enhanced in the intact circuit due to electrical coupling with the AB, which is excited by 5-HT. The cell-type specific responses to 5-HT observed in the AB, IC, LP and VD neurons are due, in part, to differential modulation of ionic conductances. However, the specific 5-HT targets in each cell are not completely understood. The ionic conductances targeted by 5-HT in the AB neuron to elicit bursting are unknown (Harris-Warrick and Flamm 1987; Ayali and Harris-Warrick 1999). 5-HT enhances I_h in the IC neuron, (Peck et al. 2006) but has no effect on this current in any of the other pyloric neurons. I_A is decreased in the IC neuron in response to 5-HT, consistent with 5-HT's enhancement of IC firing, but I_A in the AB and VD neurons is unaffected by 5-HT (Peck et al. 2001).

5-HT additionally modulates the strength of electrotonic coupling and chemical synapses within the pyloric circuit (Figure 1-5) (Johnson and Harris-Warrick 1990; Johnson et al. 1993b, 1994, 1995). 5-HT alters the strength of graded synaptic transmission from the PD neurons: it

reduces graded transmission from the PD to LP and PY neurons, and enhances the PD-IC synapse (Johnson and Harris-Warrick 1990). Graded transmission from the AB neuron to the IC, LP, and PY neurons is increased by 5-HT, while graded transmission at all other pyloric synapses is either decreased or not effected (Johnson et al. 1995). 5-HT also alters the strength of electrical connections between pyloric neurons (Johnson et al. 1993b, 1994). Thus, in addition to the cellular effects described above, 5-HT enhances circuit flexibility by acting on a network level, supporting the idea that circuit reconfiguration encompasses multiple distributed changes within the circuitry.

Electrophysiological data have provided a great deal of understanding regarding the actions of 5–HT on the pyloric motor pattern; however, little is known about the underlying cellular mechanisms that mediate these actions. Pharmacological studies suggest that 5-HT responses in the pyloric network are mediated by multiple receptors (Zhang and Harris-Warrick 1994), but the signal transduction cascades operating in pyloric cells were largely unknown. As part of my dissertation work, I investigated the organization of the crustacean 5-HT receptor family and provided the first characterization of a crustacean 5-HT_2 receptor (Chapter 2). My research laid the foundation for subsequent studies on the components of the 5-HT response system that provide flexibility in 5-HT regulation of pyloric network cycle frequency (Chapter 7).

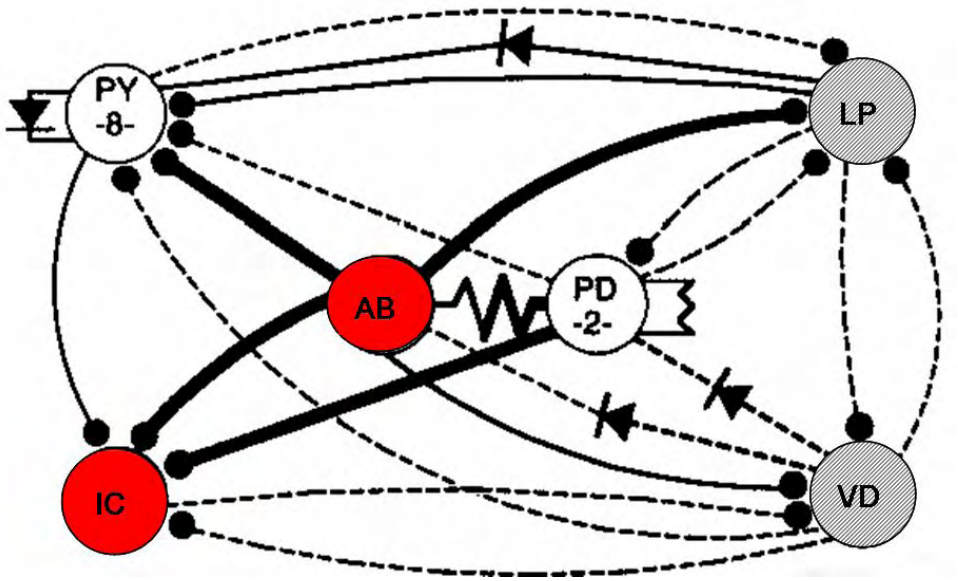

Figure 1-5: 5-HT effects in the pyloric network. Experiments were conducted in the absence of modulatory input using bath applied 10^{-5}M 5-HT. Neuronal targets were identified by synaptically isolating each cell (Flamm and Harris-Warrick 1986b). Small, filled circles indicate inhibitory chemical synapses, resistor symbols indicate nonrectifying electrical synapses, diodes indicate rectifying electrical synapses, with the direction of the arrow representing the preferred direction of positive current flow. The direct effect of 5-HT on synaptic strength is indicated as follows: thin lines = no change; thickened lines = enhanced; dashed lines = weakened. The effect of 5-HT on pyloric neurons is indicated as follows: red = excitatory; grey = inhibitory; white = no effect. Modified from (Johnson et al. 1995).

Dopaminergic modulation of the pyloric network

Since STG neurons are constantly bathed by hemolymph, they receive neurohormonal DA input via secretion into the hemolymph by the pericardial organs (Sullivan et al. 1977; Fort et al. 2004). DA is also found in descending modulatory input fibers from cells in the commissural ganglia and the brain (Barker et al. 1979; Kushner and Barker 1983). It is not known whether these modulatory projections make direct synaptic connections with pyloric neurons, or if their effects are paracrine.

The effects of DA on the pyloric network have been extensively characterized. When bath applied, DA dramatically alters the pyloric motor pattern by differentially altering the cellular properties and synaptic strengths within the network (Figure 1-6) (Eisen and Marder 1984; Flamm and Harris-Warrick 1986b, a; Harris-Warrick and Flamm 1987; Johnson and Harris-Warrick 1990; Johnson et al. 1993a, b; Harris-Warrick et al. 1995b; Harris-Warrick et al. 1995a; Johnson et al. 1995; Kloppenburg et al. 1999; Peck et al. 2001; Johnson et al. 2003; Gruhn et al. 2005; Peck et al. 2006). DA inhibits the PD and VD neurons, while exciting the AB, IC, LP and PY neurons (Figure 1-6). The overall effect of bath-applied 10^{-4}M DA is a phase-advance for the LP, IC and PY neurons, and a marked decrease in cycle frequency.

Electrophysiological data show that differential DA modulation occurs via cell-type specific targeting of ionic currents in each of the neurons in the network (Table 1-1) Additionally, DA has been shown to alter the efficacy of every graded chemical synapse within the pyloric network (Figure 1-6). However, since changes in synaptic strengths were determined by recording IPSPs (inhibitory post-synaptic potentials) in the somata, it is not clear whether DA acts directly on synaptic proteins, or whether it alters the cellular input resistance and thereby indirectly alters synaptic strengths. Interestingly, DA can differentially modulate spike-mediated

and graded synaptic inhibition at a particular synapse. For example, at the LP-PD synapse, graded inhibition is enhanced in the presence of DA, but spike-mediated inhibition is reduced due to DA's effect on the postsynaptic PD cell (Ayali et al. 1998). As graded release occurs at lower thresholds than spike-mediated release in pyloric neurons (Graubard et al. 1983), these findings suggest that, as seen in the leech (Ivanov and Calabrese 2006), Ca^{2+} currents with different voltage thresholds may underlie graded versus spike mediated transmission at pyloric synapses, and DA may predominantly target low-threshold Ca^{2+} channels.

An understanding of how DA evokes distinct responses from each cell type requires a characterization of the DA signal transduction cascades operating in each cell. Nothing was known about the molecular aspects of DA signal transduction in the pyloric network. As part of my thesis dissertation I have characterized the dopaminergic transduction cascades (Chapters 3-5) and dopamine receptor expression patterns in pyloric neurons (Chapter 6). This work has led to the realization that in response to bath applied DA, highly localized DA receptors alter local protein function and generate global signals that act throughout the cell.

G protein-coupled receptors

Most monoaminergic signals are transduced to the intracellular milieu via transmembrane receptors coupled to trimeric G proteins. These aptly named G protein-coupled receptors (GPCRs) constitute a superfamily with an estimated 791 members in the human genome (Bjarnadottir et al. 2006). GPCRs are activated by an enormous number of ligands, including odorants, light, proteins, nucleotides and Ca^{++}. All GPCRs share a common central core domain, comprised of 7 α–helically arranged transmembrane domains (TM1 through TM7) connected by alternating intracellular and extracellular peptide loops (Figure 1-7). Thus, there are 3

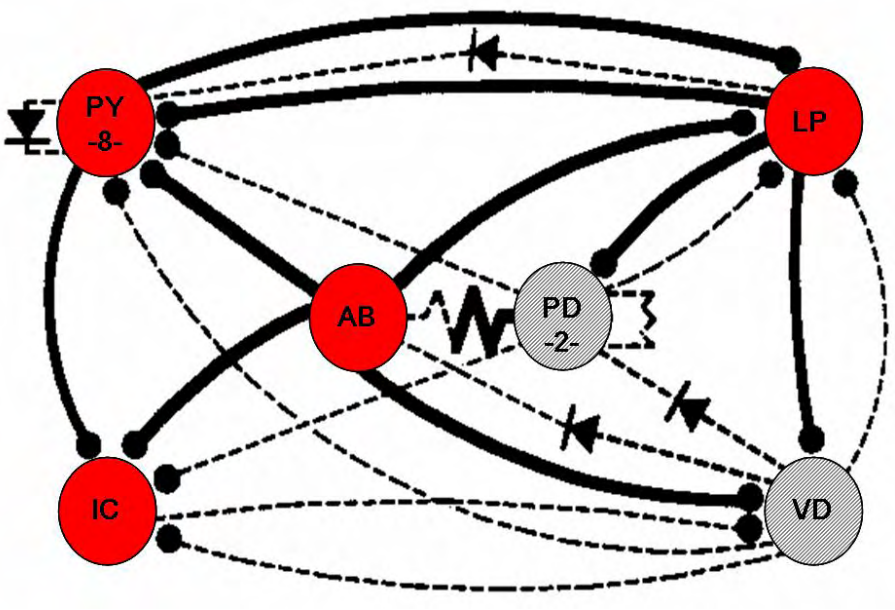

Figure 1-6: DA effects in the pyloric network. Experiments were conducted in the absence of modulatory input using bath applied 10^{-4}M DA. Neuronal targets were identified by synaptically isolating each cell (Flamm and Harris-Warrick 1986b). Small, filled circles indicate inhibitory chemical synapses, resistor symbols indicate nonrectifying electrical synapses, diodes indicate rectifying electrical synapses, with the direction of the arrow representing the preferred direction of positive current flow. The direct effect of DA on synaptic strength is indicated as follows: thin lines = no change; thickened lines = enhanced; dashed lines = weakened. The effect of DA on pyloric neurons is indicated as follows: red = excitatory; grey = inhibitory. Modified from (Johnson et al. 1995).

Table 1-1: Ionic targets of DA in pyloric neurons

[1](Harris-Warrick et al. 1995b); [2](Harris-Warrick et al. 1995a); [3](Kloppenburg et al. 1999); [4](Peck et al. 2001); [5](Peck et al. 2006); [6](Johnson et al. 2003); [7](Gruhn et al. 2005)

Cell	I_A	I_{OCa}	I_h	I_{Ca}	I_{Kv}
AB	↓ [4]	not tested	↑ [5]	↓ [6]	↑ [7]
VD	no effect [4]	not tested	↑ [5]	↓ [6]	no effect [7]
IC	↓ [4]	not tested	no effect [5]	↑ [6]	no effect [7]
LP	↓ [2]	not tested	↑ [2]	↑ [6]	no effect [7]
PY	↓ [1]	not tested	↑ [5]	↑ [6]	↑ [7]
PD	↑ [3]	↑ [2]	no effect [5]	↓ [6]	no effect [3]

intracellular loops (i1-3) and 3 extracellular loops (e1-3), as well as the intracellular C- and extracellular N- terminal domains (Yeagle and Albert 2007). It is thought that a change in the conformation of the core domain is responsible for receptor activation in all GPCRs (Bockaert and Pin 1999).

A number of different approaches have been taken toward classifying GPCRs. Some classification systems group the receptors according to where ligand binding occurs, while others use sequence or motif-based analysis, or statistical models that predict G protein couplings (Bockaert and Pin 1999; Fredriksson et al. 2003; Sgourakis et al. 2005; Gao and Wang 2006). Currently, GPCR protein sequences are divided into six families: Family A: rhodopsin-like, Family B: secretin-like, Family C: metabotropic glutamate, Family D: fungal pheromone, Family E: cAMP receptor and Family F: frizzled/smoothened. (Fredriksson and Schioth 2005; Gao and Wang 2006). Each family contains several subfamilies of GPCRs. Family A contains the most GPCRs, including receptors for odorants, small ligands, biogenic amines, peptides, and glycoprotein hormones. Family B includes secretin and adhesion-like receptors, and ligands include high molecular weight hormones and large peptides. Family C contains calcium sensing receptors, GABA and glutamate receptors, and a group of putative pheromone receptors. Family D comprises pheromone receptors linked to Gi, and family F contains receptors involved in embryonic development, as well as some taste receptors (Bockaert and Pin 1999; Schioth and Fredriksson 2005; Gao and Wang 2006).

An intriguing point from an evolutionary perspective is that while function (i.e., alteration of G protein activity in response to extracellular ligands) and global structure of GPCRs are highly conserved, receptors from different families share little sequence similarity.

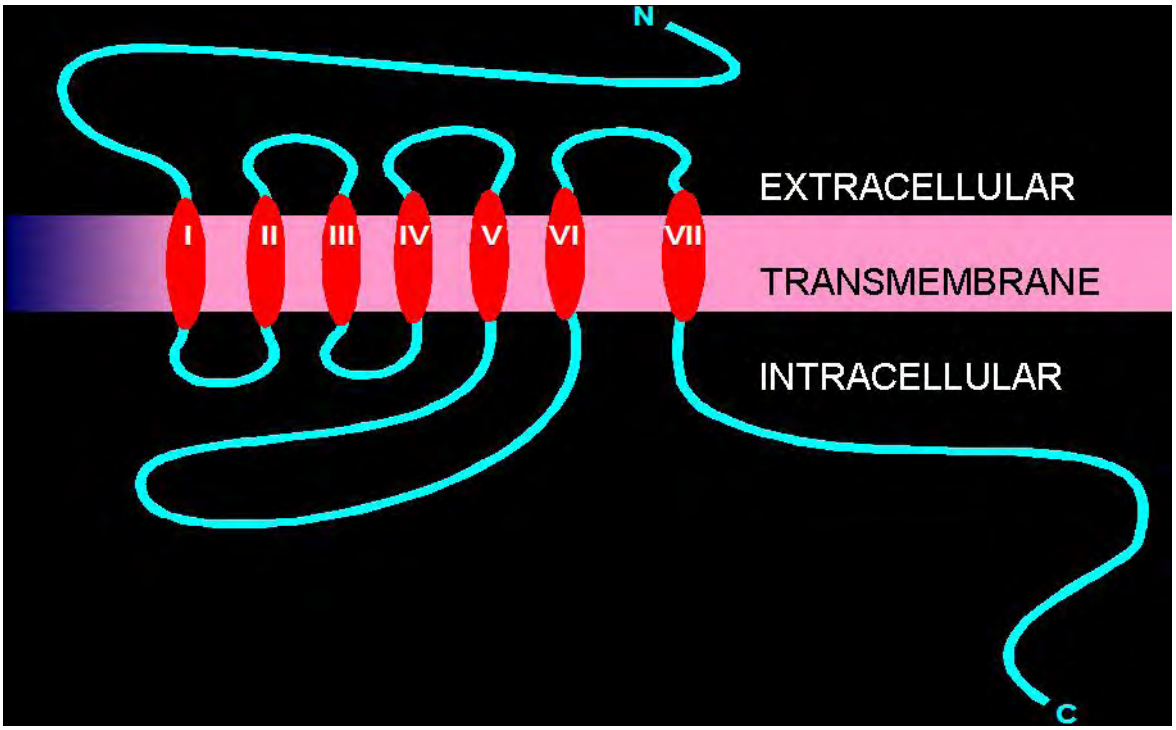

Figure 1-7: Structure of a GPCR. Seven transmembrane (TM) helices (I through VII) divide the protein into three domains, the cytoplasmic, the TM and the extracellular domains.

Thus, the various families achieve similar functions through distinct means. For example, although a similar change in conformation of the core domain is presumably associated with GPCR activation in most GPCR families, a great variety of mechanisms have evolved to allow the natural ligand to induce this change in conformation. For some Family A GPCRs, the ligand binding occurs in a cavity formed by TM3-TM6, while the N terminal region is critical for ligand binding in some Family B receptors (Bockaert and Pin 1999). Moreover, no predicative motif has been identified in GPCRs to explain receptor coupling to a specific G protein (Sgourakis et al. 2005). For example, the C-terminal region and il-2 are both required for the type-1 vasopressin receptor (V_1R) to activate a G_q-mediated signaling cascade (Liu and Wess 1996; Berrada et al. 2000; Thibonnier et al. 2001), whereas il-3 and a short sequence at the N-terminus are required for activation of G_s by the type-2 vasopressin receptor (V_2R) (Erlenbach and Wess 1998). Thus, G protein coupling appears to be due to distinct combinations of receptor regions.

GPCR families are further divided into subfamilies, classes, subclasses and subtypes. For example, amine receptors are one subfamily of the Family A group of GPCRs. The amine subfamily is further divided into classes: muscarinic acetylcholine, dopamine histamine, octopamine, serotonin, and adrenoreceptors (Gao and Wang 2006). Within a class, receptors are divided into subclasses based on pharmacological profiles and sequence similarities, as in the case of the DA receptor class, which has D_1 and D_2 subclasses (Missale et al. 1998). Pharmacology and signaling pathways are unique to each subclass, and a given subclass may contain multiple receptor subtypes. In mammals, the D_1 receptor subclass contains two receptor subtypes, D_1 and D_5, and the D_2 subclass contains D_2, D_3 and D_4 receptor subtypes. Within a given subclass, signaling mechanisms and structure are conserved.

GPCR signaling

GPCR activation causes GPCRs to act as guanine nucleotide exchange factors (GEFs), prompting trimeric G proteins to exchange GDP for GTP, resulting in dissociation of Gα from Gβγ subunits. These subunits then interact with effectors, initiating signaling cascades and second messenger production. There are at least 18 different Gα subtypes that are classified into four subfamilies (Gαi/o, Gαq, Gαs, and Gα12/13) based on sequence homology and the downstream effector molecules they associate with (Table 1-2) (Wong 2003). Members of the Gs family traditionally couple to adenylate cyclase (AC) in a stimulatory manner to increase cAMP production, while Gi proteins have an inhibitory effect on AC. Phospholipase C (PLC) β is the classical downstream effector for Gq family members, while Gα12/13 stimulates p115RhoGEF, a regulatory protein (Cabrera-Vera et al. 2003).

Table 1-2: Traditional Gα effectors

	effector	**effect**	**2nd messenger**
Gαs	adenylate cyclase	stimulatory	cAMP
Gαi	adenylate cyclase	inhibitory	cAMP
Gαq	phospholipase C β	stimulatory	IP3/Ca++/DAG
Gα12/13	phospholipase D/ p115RhoGEF	stimulatory	

While the traditional view of G protein signaling attributes changes in second messenger levels to α subunit interactions with effector molecules, there are additionally five β subtypes and twelve γ subunits that can mediate intracellular signaling cascades. In general, Gβγ dimers can form from many Gβ-Gγ combinations, but there is evidence that the dimerization process is not random. Some Gβ and Gγ isoforms do not dimerize *in vitro*, and Gβγ dimerization may also exhibit cell-type specificity (Cabrera-Vera et al. 2003). Additionally, different Gβγ dimers can have different effectors. Gβγ effectors include many of the same targets of Gα, including PLCβ and AC, as well as additional kinases and regulatory proteins (Cabrera-Vera et al. 2003). Gβγ subunits can modulate ion channels by direct binding (Yamada et al. 1998), and are also implicated in altering the function of vesicle fusion machinery. For example, PC12 cells release catecholamines from dense core vesicles. In response to Ca^{2+}, the SNARE complex, which consists of 3 proteins (synaptobrevin, sxntaxin, SNAP-25), interacts with synaptotagmin, a Ca^{2+} sensor, leading to transmitter release. Gβγ interacts with the SNARE complexes to prevent their interaction with synaptotagmin, and secretion in these cells is attenuated with βγ treatment (Blackmer et al. 2005). This inhibitory mechanism appears to be evolutionarily conserved, to some degree. In the lamprey spinal cord, Gβγ similarly targets Ca^{2+} dependent assembly of the synaptic vesicle fusion machinery. Specifically, βγ binds the C-terminus of SNAP-25 to mediate GPCR-induced presynaptic inhibition (Gerachshenko et al. 2005).

GPCRs can exhibit promiscuity with regard to G protein coupling and thus couple to multiple signaling pathways in a cell. For example, the human thyrotropin receptor can couple to members of all four Gα protein families with equal potency (Laugwitz et al. 1996). In some cases a given agonist can differentially activate a subset of all possible pathways, a phenomenon termed agonist-directed trafficking (Pauwels 2000). In addition, GPCRs can switch coupling in

the continued presence of an agonist. Studies have revealed that phosphorylation of β_2ARs by PKA decreases coupling to Gαs and switches receptor coupling to Gαi (Daaka et al. 1997).

Some GPCR functions do not involve G proteins. For example, in hippocampal neurons, human D_5 receptors regulate synaptic strength via direct interaction with $GABA_A$ receptors (Liu et al. 2000). In some cases, G protein independent signaling involves an adaptor protein, such as β-arrestin. β-arrestins regulate GPCR signaling cascades first by uncoupling the receptor and G protein (see below), and second, by recruiting additional signaling proteins to the GPCR, such as signal terminating phosphodiesterases (PDEs) (Perry et al. 2002) or tyrosine kinases (Luttrell et al. 1999). In the latter case, β-arrestin switches receptor signaling from a G protein-dependent to a G protein-independent, MAP kinase cascade (Luttrell et al. 2001; Baillie et al. 2003).

The physiological consequences of β-arrestin binding are not limited to intracellular signaling, but encompass receptor expression as well: β-arrestins play a key role in controlling GPCR internalization and recycling (Lefkowitz 1998). Agonist-induced GPCR stimulation leads to GPCR kinase- (GRK) mediated phosphorylation, which enhances the affinity of the receptor for interaction with β-arrestins rather than G proteins, a process termed desensitization. β-arrestins bind to the GPCR and recruit clathrin and additional adaptor proteins, which leads to the co-localization of the GPCR and β-arrestin in clathrin coated pits at the cell surface. GPCRs are then internalized to acidic endosomes, where they are either recycled to the cell surface or degraded in a process known as downregulation (Pierce and Lefkowitz 2001). The carboxy-terminal tail of the GPCR is important in determining how the receptor is internalized. In the case of the β_2AR, the receptor and β-arrestin co-localize in clathrin-coated pits at or near the cell surface, and rapidly dissociate before the GPCR travels to endosomes; thus, the receptor is quickly recycled and returned to the cell surface in about 30 minutes (Oakley et al. 2001; Pierce

and Lefkowitz 2001). V_2Rs, on the other hand, bind tightly to β-arrestins and may remain complexed in endosomes for extended periods of time before being recycled or degraded (Tohgo et al. 2003).

In addition to β-arrestin, a diverse plethora of adaptor proteins exist to regulate signal specificity and receptor localization. Some adaptors have been shown to tether signaling components at discrete subcellular locations such as an organelle or the dendritic cytoskeleton (Hall and Lefkowitz 2002; Bockaert et al. 2003; Wong and Scott 2004; Dodge-Kafka et al. 2005). Additionally, signaling components can be compartmentalized within the membrane by sequestering them to caveolae or lipid rafts. In neonatal rat cardiac myocytes, studies have identified caveolin-enriched microdomains that contain GPCRs, G protein subunits, and downstream effectors (reviewed in Insel et al. 2005). Moreover, there is evidence that the compartmentalization of GPCRs and effector molecules is cell-type specific: in rat cardiac myocytes, β_2ARs associate with AC in caveolin-rich membrane fractions, but in vascular smooth muscle cells, these signaling components are not associated with caveolae (Ostrom et al. 2002).

As a result of the subcellular compartmentalization of GPCR signaling components and protein-protein interactions described above, GPCR signals can be spatially restricted. A second mechanism for restricting a signal involves physical barriers, such as the endoplasmic reticulum (ER). A third mechanism involves molecular barriers. The inclusion of signal terminating molecules within a GPCR microdomain restricts a large proportion of the signal to the membrane, resulting in distinct local and global signals. The function of molecular barriers has been best studied for GPCRs that couple with Gs to increase cAMP and thereby increase PKA activity.

It has been demonstrated that GPCRs that couple with Gs can simultaneously generate large, complex local changes in cAMP at or near the plasma membrane, as well as small, sustained global changes in distal cellular compartments (Rich et al. 2001; Nikolaev et al. 2006). Figure 1-8 shows temporal changes in cAMP that occur in a two compartment model cell upon GPCR activation. Trace 1 represents the signal generated within the local compartment, near the receptor. Trace 2 indicates the global signal, which is received in the distal compartment. Due to restricted diffusion out of the local compartment, the local cAMP signal is substantially larger then the global signal. The local signal is transient, due to signal terminating molecules (i.e., PDEs) that are activated as a result of dramatic changes in PKA activity that accompany the large increase in cAMP (see below). On the other hand, some diffusion out of the local compartment results in a small, sustained cAMP signal in the distal compartment.

The extent and form of local and global signaling largely depend on diffusion barriers within the cell. For example, it has been shown that in HEK cells and cardiac myocytes, scaffolding proteins can simultaneously bind PDE and PKA near the GPCR. When PDE is phosphorylated by PKA, its activity increases. In this arrangement, receptor mediated increases in PKA activity trigger PDE-mediated cAMP degradation (Michel and Scott 2002; Zaccolo and Pozzan 2002). This negative feedback loop (1) ensures that the increase in PKA activity is transient and (2) reduces cAMP diffusion away from the membrane (Willoughby et al. 2006). This is exactly what is observed in the model described above (trace 1, Figure 1-8).

While GPCR signals can be highly restricted, evidence also suggests that a signal can travel across compartments. The global signal is only a small fraction of the signal observed near the GPCR (compare trace 1 and 2 in Figure 1-8) (Rich et al. 2001), yet it does not represent non-specific second messenger diffusion. Instead, it appears that the extent of a global signaling is

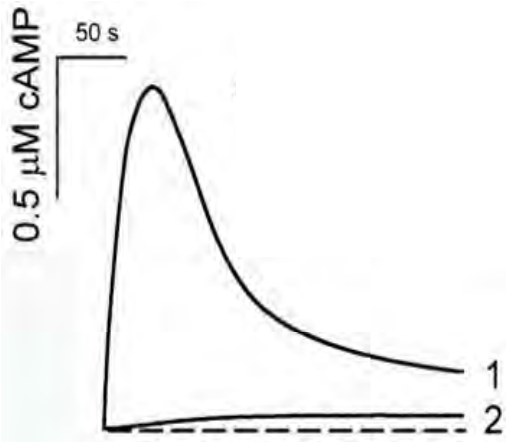

Figure 1-8: Rich-Karpen model of local and global signaling. The dashed line represents [cAMP] when no agonist is present. The traces represent temporal changes in [cAMP] in local (1) vs. distant (2) compartments during constant agonist application. Modified from (Rich et al. 2001).

controlled. In rat cardiomyocytes, both β_1- and β_2ARs couple to Gs to produce an increase in cAMP, though the signals are markedly different: β_1AR stimulation generates a cAMP signal that diffuses throughout the cell, while β_2AR stimulation does not elicit cAMP diffusion (Nikolaev et al. 2006). It has been argued that the differences in diffusion are indirectly due to differences in signal strength, because the β_2AR-mediated cAMP signal is smaller than that generated by the β_1AR. However, when a portion of the β_1AR-mediated cAMP signal is blocked to achieve levels comparable to those generated by β_2ARs, the cAMP signal is still propagated over long distances throughout the cell. Surprisingly, restriction of the β_2AR–mediated cAMP signal is independent of PDE activity, suggesting that additional barriers or regulatory mechanisms are in place to preferentially restrict β_2AR- but not β_1AR-mediated cAMP signals. Thus, global signals, while far reaching, are nonetheless tightly controlled.

An interesting example of the importance of PDE barriers in controlling local and global signaling involves glucagon-like peptide-1 receptors in pancreatic β-cells. Receptor stimulation produces cAMP oscillations at the membrane that are temporally coordinated with Ca^{2+} oscillations in rat pancreatic cells. Inhibiting PDE activity in these cells prevents the oscillations, and results in a stable cAMP elevation that promotes PKA translocation to the nucleus (Dyachok et al. 2006).

Summary

This dissertation describes the use of a crustacean model to address mechanisms that impart flexibility on a rhythmic system. A first step in understanding circuit flexibility and rhythm generation is to understand how GPCRs signal in rhythmic neurons. My dissertation work is consistent with recent findings regarding both traditional and non-traditional GPCR

signaling. In particular, the data presented here indicate that monoaminergic receptor-G protein couplings are conserved across vertebrate and invertebrate lines, but multiple signaling cascades can be initiated by a given receptor, depending on the cellular milieu. This work is the first to report on monoamine receptor expression or localization in pyloric neurons, and differential receptor expression patterns are described that firmly support previous electrophysiological work. My results suggest that GPCRs produce global signals and provide a platform for further investigation into the subcellular compartmentalization and/or regulation of GPCR signaling cascades. My work will also provide the basis for future studies on how monoaminergic response systems provide flexibility to the pyloric network over the short term while contributing to stability over the long-term. Finally, novel laboratory protocols and tools are described that will aid future investigations in this and other rhythmogenic systems.

CHAPTER TWO

ARTHROPOD 5-HT$_2$ RECEPTORS: A NEUROHORMONAL RECEPTOR IN DECAPOD CRUSTACEANS THAT DISPLAYS AGONIST INDEPENDENT ACTIVITY RESULTING FROM AN EVOLUTIONARY ALTERATION OF THE DRY MOTIF

PUBLICATION: MERRY C. CLARK, TIMOTHY E. DEVER, JOHN J. DEVER, PING XU, VINCENT REHDER, MARIA A. SOSA, AND DEBORAH J. BARO (2004) *JOURNAL OF NEUROSCIENCE 24(13):3421-3435*

NOTE: I PERFORMED ALL OF THE EXPERIMENTS IN THIS CHAPTER, EXCEPT FOR THE INITIAL CLONING AND IMMUNOCYTOCHEMISTRY

Introduction

As mentioned in Chapter 1, the effects of 5-HT on the pyloric network have been investigated at the cellular and circuit levels (Figure 1-5). However, the wealth of information on the electrophysiological responses to 5-HT modulation contrasts sharply with the dearth of information on how these signals are transduced in pyloric neurons. The data suggest that there are a minimum of three 5-HT receptors (Zhang and Harris-Warrick 1994; Krenz et al. 2000), but little is known about the signaling cascades operating in stomatogastric neurons (Flamm et al., 1987, Hempel et al., 1996, Scholz et al., 1996; 2001), and there is no information linking any crustacean monoamine receptor to a specific second messenger pathway in any cell type.

5-HT receptor classification is based upon primary sequence homologies and, to a lesser degree, second messenger responses. Four different subclasses of mammalian 5-HT GPCR have been identified: 5-HT_1, 5-HT_2, 5-HT_5, and 5-$HT_{4/6/7}$. There are five members in the 5-HT_1 subclass (5-HT_{1A}, 5-HT_{1B}, 5-HT_{1D}, 5-HT_{1E}, 5-HT_{1F}), and three members in 5-HT_2 subclass (5-HT_{2A}, 5-HT_{2B}, 5-HT_{2C}) (Albert and Tiberi 2001). The remaining subtypes (i.e., 5-$HT_{4/6/7}$ and 5-HT_5) are less understood, and have been established due to the discovery of 5-HT receptors that share little sequence homology or signaling properties with 5-HT_1 or 5-HT_2 receptors (Wong 2003). Members of the 5-HT_1 receptor subclass traditionally couple with Gαi/Gαo proteins to produce a net decrease in cAMP, while most 5-$HT_{4/6/7}$ members couple to Gs proteins to increase AC activity. The canonical signaling pathway associated with 5-HT_2 receptors is a Gαq-mediated activation of PLCβ. The coupling for 5-HT_5 receptors is still uncertain (Bockaert et al. 2006).

The pharmacological profiles for invertebrate receptors differ from those of vertebrate receptors, although protein sequences and second messenger couplings are relatively well conserved. For example, the 5-HT_{2Lym} receptor, cloned from the pond snail, *Lymnaea stagnalis*,

displays 57% homology with its drosophila homolog and 46–49% homology with mammalian 5-HT_2 receptors. Furthermore, when 5-HT_{2Lym} was expressed in HEK293 cells, stimulation with 5-HT elicited inositol phosphate (IP) production, indicating that, like vertebrate 5-HT_2 receptors, 5-HT_{2Lym} activates PLCβ (Tierney 2001). Likewise, invertebrate 5-HT_1 receptor sequences are most homologous to the mammalian 5-HT_1 receptor subclass, and couple with Gαi/o-mediated decreases in cAMP (Tierney 2001; Hoyer et al. 2002; Spitzer et al. 2008).

As mentioned above, nothing is known regarding the receptors that mediate the 5-HT response in the STNS. In this chapter, we begin to elucidate 5-HT signal transduction in pyloric neurons. We have used a bioinformatics approach to identify 8 novel arthropod monoamine receptors that have never been cloned or characterized in any species. We clone and characterize one of these monoamine receptors from the spiny lobster, and show that it is a serotonin receptor. Here, we describe the 5-$HT_{2\beta Pan}$ receptor, which couples to the traditional Gαq signaling cascade when expressed in HEK293 cells. This receptor is constitutively active due to a mutation in TM3, and is expressed by most STG neurons.

Materials and Methods

Cloning and mutagenesis of the 5-$HT_{2\beta Pan}$ receptor

Total RNA was extracted from *Panulirus interruptus* nervous system using Trizol (Ambion) according to the manufacturer's instructions. RNA quality was assessed with denaturing gel electrophoresis and quantified with a biophotometer (Fisher). Multiple RNA extractions were performed. When necessary, mRNA was isolated with an oligotex kit (Qiagen). cDNA was obtained from total and/or mRNA preparations by performing reverse transcription reactions using Superscript II (Invitrogen) according to the manufacturer's instructions. The

following degenerate primers (written 5' to 3') were designed based on conserved regions of the *Drosophila* and *Anopheles* orthologs of a putative monoamine receptor, as described in results:

5a: TGGATITGYYTIGAYGTNYTNTTYTG

5b TITTYTGYACIGCIWSNATNATG

5c: ACIGCIWSATNATGCAYYTNTGYAC

3a: GGIATRTARAARCAIACIATNSWNCC

3b: CATIACICCNARNGGNATRTARAARCA

3c: TAIGTIARIARCATIACNCCNARNGG

Fragments of the lobster ortholog were amplified from multiple cDNA preparations using various combinations of the degenerate primers in nested PCR experiments (only 2 degenerate primers for any given PCR) as previously described (Baro et al. 1994). Nested PCR products were size fractionated on acrylamide gels. Appropriate bands of expected size were gel isolated. DNA was eluted (Ausubel et al. 1990) and cloned using a TA cloning kit (Invitrogen). Forty-four independent clones were sequenced (Georgia State University Biotechnology Facility). Twenty-five clones from nine independent nested PCR experiments representing multiple cDNA templates fell into a single contig that displayed strong amino acid identity with the previously identified *Drosophila* protein that served as the template for the design of the degenerate primers. A DNA fragment from these twenty-five clones was amplified with specific primers in a standard PCR. The resulting fragment was gel isolated and used as the template in a primer extension reaction containing ^{32}P, according to the manufacturer's instructions (ladderman kit, TaKaRa). Unincorporated nucleotides were removed from the reaction by ethanol precipitation, and the resulting product was used to probe 5 different *Panulirus interruptus* nervous system cDNA libraries as previously described (Baro et al. 1996b). The conventional library screen

yielded 5 clones all missing the start methionine codon. DNA fragments containing the 5' end of the full-length cDNA were obtained using a SMART™ RACE cDNA amplification kit (BD Biosciences Clontech) according to the manufacturer's instructions. The following primers (written 5' to 3') were used in the reaction:

GSPAM1: CGTGACGGCCAGGGAGAGCAGGAAGTAGTTG

NGSPAM1: GCCAGGATGAGGAGGATGTTGCCGAAGAGTGTC

ProbeAM1: CAACCTATCTTACGGGAGGGAGAACGAGACGT

To guard against PCR induced sequence errors, four different RNA preparations were used in separate experiments, and multiple, independent RACE fragments were isolated. Fragments were cloned and sequenced as described above. Criteria used to identify clones containing the complete 5' end of the ORF were: 1) The clone must be bounded by the primers used in the experiment and contain a region of overlap with the library clones, 2) The clone must contain multiple stop codons in all three reading frames 5' to the start methionine in the amino terminus region (sequence 5' to TM1), 3) The translation start site should conform to the Kozak consensus sequence. Five independent clones from multiple cDNA preparations contained the same DNA fragment representing the 5' end of the transcript. The Kozak consensus sequence was recognizable but not optimal; nevertheless, protein expression levels were adequate in HEK 293 cells using this endogenous site (see below). The full length of the isolated cDNA was 3.92kb and included a polyA tail. Constructs containing the complete open reading frame (2.426 kb in length) were assembled using standard procedures (Ausubel et al. 1990). Both strands of the constructs were sequenced with the following primers, written 5' to 3':

U1: TGTTTCCCCACTTACCCACCAG

U2: TGCGGAGGTCCCACTGTCG

U3: CTCCTGTGGGCTCCGTTCTTCATC

U4: TCGGAGTTGATGGCTTCTTGTG

U5: GAATTAGTGCTGTGCTCCGTGTG

U6: GCTGAGTTGTGCTTTGGAAGTGA

L1: ACACAGCTCCTTACCCAACTTCACAC

L2: GTTGACCATGGAGGAGGCGTAGC

L3: ACGAGGTCCGGGGTGGTTCTG

L4: TCGGTGGAGCGGGGAAGT

L5: TCGGTGATGGAGACGGCAGTG

L6: ATGAGGAGGATGTTGCCGAAGAGT

L7: GGAGGAGGCGTAGCCCAGCCAGGTCACCAAGTTGA

Two independent constructs were used to establish permanent cell lines as described below. These constructs also served as templates in site directed mutagenesis experiments that were performed with the Quickchange kit (Stratagene) according to the manufacturer's instructions. Both strands of multiple mutagenized clones were sequenced, and one clone was used to establish permanent cell lines as described below. Sequence data was analyzed and manipulated using Sequencher (Gene Codes) and Lasergene (DNAStar) software.

Generation of HEK293 cell lines stably expressing 5HT receptors

HEK293 cells were maintained in DMEM supplemented with 10% horse serum, penicillin (50 units/ml), streptomycin (50 μg/ml) at 37°C, 5% CO_2. Cells were grown to 90-95% confluency in 35mm dishes and transfected with 2 μg DNA using 10μl Lipofectamine in 100μl opti-MEM. After varying amounts of time (6 to 24 hours), the media was replaced with DMEM

supplemented with 10% horse serum, according to the manufacturer's suggestions. After two days in culture, cells expressing the transfected genes were selected in media containing 10% dialyzed fetal bovine serum and 500 μg/ml neomycin (Sigma). Cells were maintained in selection media for $\geq$ 28 days, after which each plate was expanded to produce a cell line. Each cell line was assayed for receptor expression, by performing western blot experiments on proteins extracted from each cell line, using anti-5-$HT_{2BCrust}$ to probe the membranes (see below). All experiments reported in this manuscript were conducted on the cell line with the highest 5-HT_{2BPan} expression level. However, the same results were obtained with a second line. The same procedure was used to establish two 5-HT_{2BPan} (F171Y) cell lines. All tissue culture lines and reagents were purchased from American Type Culture Collection (ATCC), except the dialyzed serum, Lipofectamine, and opti-MEM (Invitrogen).

PKC assay

We used a modified version of a previously described procedure to fractionate cells and measure total PKC activity in each fraction (Setterblad et al. 1998). A 100mm plate of confluent cells was trypsinized and cells were recovered by centrifugation. The pellet was resuspended in DMEM, and cell numbers were determined. Aliquots of 5×10^5 resuspended cells were removed to separate 1.5ml tubes and exposed to varying concentrations of monoamines (usually 0 to 10^{-2} M) for 15 minutes at 37°C in a total volume of 1 ml DMEM. Normally, one plate would yield enough cells for an entire concentration series for a given drug (i.e., 9 aliquots ranging from 0 to 10^{-2} M). After exposure to the drug, cells were pelleted in a centrifuge for 2 minutes, the media was removed and replaced with liquid nitrogen. Tubes were stored on dry ice and assayed immediately, or tubes could be stored at –70°C for up to one month with similar results in both

cases. For the PKC assay, frozen pellets were resuspended in 500µl lysis buffer (25mM Tris-HCl, 0.5mM EDTA, 0.5mM EGTA, 0.05% Triton X-100, 10mM β-mercaptoethanol, 1µg/ml leupeptin, 1µg/ml aprotinin, 2mM PMSF), and centrifuged at 100,000 × g for 1 hour. The supernatant (soluble fraction) was collected, and the pellet (membrane fraction) was resuspended in 500µl of lysis buffer containing 1% Triton X-100. Total PKC activity in each fraction was determined using a PKC assay system (Promega), which measures ^{32}P-phosphorylation of a PKC-specific substrate. Briefly, 5 nmol of a biotinylated PKC peptide substrate [neurogranin (28-43)] was mixed with 5µl of a given cell lysate in the presence of ^{32}P-ATP, activation buffer (1.6mg/ml phosphatidylserine, 0.16mg/ml diacylglycerol, 100mM Tris-HCl, 50mM $MgCl_2$), and coactivation buffer (1.25mM EGTA, 2mM $CaCl_2$, 0.5mg/ml BSA). Following a 5 minute incubation at 30°C, the reaction was terminated by the addition of 7.5M guanine hydrochloride. Samples were applied to streptavidin-coated discs, to which the biotinylated substrate is specifically bound. Excess free ^{32}P-ATP and nonbiotinylated cellular components are removed by several washes in 2M NaCl. A phosphorimaging system (FUJI) was used to determine the radioactivity incorporated into the substrate. The signal was expressed in units of PSL (photo-stimulated luminescence). Protein concentrations in each cell fraction were determined using a BCA Protein Assay Kit (Pierce) and the residual cell lysate from the fractionation procedure described above. The specific activity in each fraction was expressed as PSL/µg protein. The total specific activity for a given aliquot of 5×10^5 cells is equal to the specific activity of the membrane fraction plus the specific activity of the soluble fraction. In some experiments 10^{-7} M phorbol 12-myristate 13-acetate (PMA; Sigma), a PKC activator, was substituted for a monoamine, or 5-HT application was preceded by a 15 minute application of 10µM 1-O-Octadecyl-2-O-methyl-rac-glycero-3-phosphorylcholine (Et-18-OCH_3; Calbiochem), a PLC

inhibitor, or prior to removing cells from the plate, a 24 hour application of 100ng/ml pertussis toxin (PTX; Calbiochem), a $G_{i/o}$ inhibitor.

Assay for inositol phosphate (IP) formation or phosphatidyl inositol (PI) hydrolysis

Measurement of IP formation in cultured cells was performed using a slight modification of a previously described protocol (Li et al. 1995). Briefly, confluent cells in 24-well plates were labeled with [^{3}H]-myoinositol (1.3μCi/ml; Perkin Elmer) for 48 hr. They were washed with PBS and preincubated with 10mM LiCl (Sigma) in PBS for 30 minutes. Cells were incubated an additional 60 minutes in either 10^{-3}M 5-HT, 20mM NaF, or no drug (control). Cells were lysed by adding 0.75 ml ice-cold 20mM formic acid to the wells and incubating the plates at –20°C for 1 hour. The lysate was loaded on to AG1-X8 columns (BioRad) that were pre-equilibrated with formic acid (20mM). Care was taken not to disturb the membranes that remained attached to the plate. The columns were washed with 3ml 50mM ammonium hydroxide. IP_1 and IP_2 were collected with 10ml of 0.1M formic acid/0.4M ammonium formate. IP_3 was eluted with 10ml of 0.1M formic acid/1M ammonium formate. The IP fractions were then combined, and radioactivity in the samples was quantified by scintillation counting. The cell membranes attached to the bottom of the wells were dissolved in 1 M NaOH and counted as total phosphatidyl inositols, as previously described (Agretti et al., 2003). Results are expressed as percentage radioactivity incorporated in inositol phosphates (IP_1 + IP_2 + IP_3) over the sum of radioactivity in inositol phosphates and phosphatidyl inositols.

[cAMP] determinations

1×10^5 cells were plated in 35mm dishes and grown to confluency. Cells were washed with 2 ml phosphate-buffered saline and preincubated at 37°C for 10 minutes in the presence of the phosphodiesterase inhibitor, 3-isobutyl-1-methylxanthine (2.5mM) (Sigma). Cells were incubated an additional 30 minutes at 37°C with either 5-HT (10^{-3}M) or forskolin (2.5μM) or forskolin and 5-HT. The media was removed and 0.5ml of 0.1M HCl with 0.8% Triton X-100 was added to the plates. After a 30 minute incubation at room temperature, the lysate was removed from the plates and spun in a centrifuge for 2 minutes. Supernatant was collected and assayed for cAMP levels using a direct cAMP enzyme immunoassay kit (Assay Designs, Inc.) according to the manufacturer's instructions. Protein concentrations in each sample were determined using a BCA Protein Assay Kit (Pierce). For some experiments, cells were pretreated with pertussis toxin (100ng/ml) for 24 hours prior to the experiment. Data are expressed as pmol cAMP/mg protein.

Antibody production

Two affinity purified antibodies were synthesized by Bethyl labs against sequences that are conserved across crustacean orthologs of the 5-HT_{2B} receptor (lobster and prawn, Sosa and Baro, unpublished). Since these antibodies will recognize the 5-HT_{2B} receptor in multiple species of Crustacea, we call them anti-5-$HT_{2BCrust}$. Anti-5-$HT_{2BCrust}$.A was made against the peptide: DRFLSLRYPMKFGRHKTRRR. Anti-5-$HT_{2BCrust}$.B was generated against the peptide: DPHSTIVDGVCQIPVSLFQI. When necessary, a C was appended to the end of the sequence for conjugation to a carrier.

Protein extractions and western blots

Protein extractions and western blots were performed as previously described (Sosa et al., 2004). For preabsorption experiments, blots contained mirror images of the same protein extracts on either side of a prelabeled molecular weight marker (Biorad). Blots were cut down the midline of the lane containing the visibly labeled molecular weight marker (Biorad) and incubated with either the antibody, or the antibody preabsorbed with its peptide antigen for $\geq$ two hours at room temperature. The ratio of peptide to antibody was 1:50 (w/w), respectively. Blots were reassembled just prior to chemiluminescent detection.

Immunocytochemistry

Whole mount immunocytochemistry with stomatogastric ganglia was as previously described (Baro et al., 2000). Controls included preabsorption of the primary antibody with the peptide used to generate the antibody for 2hours at room temperature prior to incubation with the prep (peptide to antibody = 1:50, w/w), and omission of the primary antibody. In all cases the 5-HT_{2BPan} signals were lost, indicating specificity of the antibody (data not shown). To determine whether the receptor was present at neuromuscular junctions (NMJs), a double label protocol involving anti-5-$HT_{2BCrust}$ and anti-synaptotagmin, which labels NMJs (Littleton et al. 1993; Cooper et al. 1995; Quigley et al. 1999) and was a kind gift from Dr. Hugo Bellen, was performed on identified muscles (Govind and Atwood 1975). Muscles were dissected without the ganglion and fixed intact in 3.2% paraformaldehyde in PBS (0.14 M NaCl, 0.27mM KCl, 10mM Na_2 HPO_4, and 0.18mM KH_2 PO_4, pH 7.3) for 2 hours at 4°C. The fixed muscle was then pulled into strips (and for the PD cut in half to reduce the length) and washed in 8 changes of PBST (PBS plus 0.3% Triton X-100) over 2-8 hours. The primary antibody was added [1:1000

dilution of rabbit anti-synaptotagmin in PBST containing 5% normal goat serum (NGS)] and incubated overnight at 4°C. The prep was then washed in 8 changes of PBST over 2-8 hours. The secondary antibody, goat anti-rabbit IgG Fab fragments conjugated to FITC or tetramethyl rhodamine (JacksonImmuno Research) was added at a dilution of 1:50 in PBST containing 5% NGS and incubated overnight at 4°C. The prep was washed in 8 changes of PBST over 2-8 hours. The second primary antibody was added (1-10µg/ml rabbit anti-5-$HT_{2BCrust}$ in PBST containing 5% NGS) and the prep was incubated overnight at 4°C. The primary antibody was washed out with 8 changes of PBST over 2-8 hours, and a second secondary antibody was added [goat anti-rabbit IgG conjugated to Texas Red (Jackson Immuno Research) or Oregon Green 488 (molecular probes) in PBST containing 5% NGS] and incubated overnight at 4°C. The secondary antibody was washed out in 8 changes of PBS over 2-8 hours. The preparations were placed on a poly-lysine coated cover slip, dehydrated in an ethanol series, cleared in xylene, and mounted on a glass slide with DPX (Fluka) as previously described (Baro et al., 2000). In some experiments the order of the primary antibodies was reversed. Negative controls included preparations in which the second primary antibody, (always rabbit anti- 5-$HT_{2BCrust}$), was omitted or preabsorbed for at least 2 hours with the peptide that served as the antigen in antibody production (antibody to antigen ratio was 50:1, w/w). Negative controls always included sequential addition of <u>both</u> secondaries. In the negative controls, NMJs were still identified by robust synaptotagmin staining, but unlike the experimental preparations, the NMJs in the negative controls never showed double-labeling. In addition, single-label experiments using only one primary and one secondary confirmed the findings of the double-label experiments. Similarly, double label experiments were performed on the STG using the same protocol, except that the additional primary antibody was anti-shal 1.b, instead of anti-synaptotagmin.

All images were obtained with a Zeiss LSM510 confocal imaging system and manipulated with Adobe Photoshop 5.5 software.

Experimental animals

Pacific spiny lobsters (*Panulirus interruptus*) were obtained from the Don Tomlinson Commercial Fishing (San Diego, CA). Lobsters were maintained at 16°C in constantly aerated and filtered seawater. All animals were anesthetized by cooling on ice prior to experiments.

Statistical analyses

Student t-tests were performed with Excel software, alpha = 0.05. Results are given as mean ± SEM.

Results

Bioinformatics and Cloning of 5-HT$_{2\beta Pan}$

We took advantage of the fly genome projects (*Drosophila* and *Anopheles*) to clone a novel arthropod 5-HT type 2 receptor. First, we mined the *Drosophila* database for potential monoamine GPCRs, and identified several candidates including nine previously cloned monoamine receptors (Table 2-1). We next used one of the uncloned candidates (NP_731257/NP_649806) in a protein-protein blast against the *Anopheles* database to identify the mosquito ortholog. An alignment of the two protein sequences revealed highly conserved regions that were then used as templates in the design of degenerate primers. Nested PCRs with the degenerate primers and a spiny lobster cDNA template produced fragments of the lobster ortholog. These fragments were used as probes to screen five *Panulirus* cDNA libraries.

We obtained 5 partial library clones, all missing the amino terminus. RACE was used to obtain the missing 5' ends.

Table 2-1: Monoamine GPCRs in *Drosophila*
Dopamine (DA); serotonin (5-HT); tyramine (TYR); octopamine (OCT)

Protein Accession Number(s)	Subtype	Reference(s)	original name(s)	Renamed according to the new nomenclature rules
NP_524548	DA_1	(Feng et al. 1996; Han et al. 1996)	DAMB, DopR99B	$D_{1\alpha Dro}$
NP_733299	DA_1	(Gotzes et al. 1994; Sugamori et al. 1995)	Dm*dop1*, dDA1	$D_{1\beta Dro}$
NP_477007	DA_2	(Hearn et al. 2002)	DD2R	D_{2Dro}
NP_524419	TYR	(Arakawa et al. 1990; Saudou et al. 1990)	Dm*oct/tyr*	
NP_732541	OCT	(Han et al. 1998)	OAMB	
NP_524599	$5\text{-}HT_7$	(Witz et al. 1990)	5HT-dro1	$5\text{-}HT_{7Dro}$ (Colas et al. 1995)
NP_476802	$5\text{-}HT_1$	(Saudou et al. 1992)	5HT-dro2A	$5\text{-}HT_{1ADro}$ (Colas et al. 1995); $5\text{-}HT_{1\alpha Dro}$ (present study)
NP_523789	$5\text{-}HT_1$	(Saudou et al. 1992)	5HT-dro2B	$5\text{-}HT_{1BDro}$ (Colas et al. 1995); $5\text{-}HT_{1\beta Dro}$ (present study)
NP_524223	$5\text{-}HT_2$	(Colas et al. 1995)	$5\text{-}HT_{2Dro}$	$5\text{-}HT_{2\alpha Dro}$ (present study)
NP_731257 + NP_649805	$5\text{-}HT_2$	Present study	$5\text{-}HT_{2\beta Dro}$	
NP_651057	putative			
NP_650651	putative			
NP_650652	putative			
NP_650754	putative			
NP_651772	putative			
NP_647897	putative			
NP_572358	putative			
NP_731719 to 731721; NP_650212 to 650213	putative			

The predicted protein sequence from the complete lobster cDNA (Figure 2-1) was used in a stringent protein-protein blast against the *Drosophila* database. To our surprise, this returned two adjacent genes on chromosome arm 3R (FLYBASE, http://flybase.bio.indiana.edu). The first was our candidate gene, NP_731257/NP_649806, situated at cytological location 85A5. The second, NP_649805, mapped to cytological position 85A4 and was among the remaining genes from our mining expedition. Closer inspection of the two protein sequences revealed that TM regions 3-7 (TM 3-7) and the carboxy terminus of the receptor were contained in the original candidate gene, while the amino terminus and TM1-2 were contained in the second candidate gene. Clearly the algorithms used to annotate the database and identify introns and gene boundaries did not detect the very large intron between TM2 and 3, because instead of identifying one large, sprawling gene, the program defined two smaller genes. As a result, we reanalyzed all candidate genes resulting from the mining expedition for the presence of all 7 TM regions. Complete predicted receptors currently represented by multiple genes in the databases are indicated as such in Table 2-1. This work makes two important points: 1) the existing genome projects (2 or more) can be used effectively to clone orthologs from related species for which no sequence data is available, and 2) cloning genes from related organisms helps to annotate existing databases.

5-HT$_{2\beta Pan}$ sequence analyses and comparisons

A protein-protein blast of the complete genbank with the predicted amino acid sequence of the newly identified lobster monoamine receptor revealed that this novel receptor is a homolog of mammalian 5-HT$_2$ receptors, with e-values ranging from e-33 to e-31 for mammalian type 2 receptors, e-26 for 5-HT$_{2\alpha Dro}$ (Colas et al. 1995), and e-23 for an arthropod 5-

HT type 7 receptor. Arthropod 5-HT type 1 receptors were not listed in the results, but a paired protein - protein blast against 5-$HT_{1\alpha Dro}$ returned an e-value of 6e-16. Since one 5-HT type 2 receptor has already been identified in *Drosophila* (Colas et al. 1995), we named the two new proteins 5-$HT_{2\beta Pan}$ (lobster) and 5-$HT_{2\beta Dro}$ (fruit fly) according to a modification of the suggested nomenclature rules (Colas et al. 1995; Tierney 2001). With this nomenclature, homology to the mammalian subtypes is indicated by a subscripted number immediately after 5-HT (i.e., 5-HT_1-5-HT_7). This number is meant to imply conservation between vertebrate and invertebrate receptors at the level of the DNA sequence and the signaling pathway. Thus, the arthropod 5-HT1 receptors, originally named 5-HT2A and 5-HT2B (Table 2-1) (Saudou et al. 1992; Colas et al. 1995), are most homologous to the mammalian 5-HT1 receptors and all negatively couple with cAMP. Similarly, the arthropod 5-HT7 receptor, originally named 5-HTdro1 (Table 2-1) (Witz et al. 1990; Colas et al. 1995), positively couples with cAMP like its mammalian homologs. When there is more than one known gene within a subtype, individuals are represented by subscripted letters that immediately follow the number. At this point, we modified the original nomenclature scheme to include Greek letters for arthropod receptors (i.e., 5-$HT_{1\alpha}$, 5-$HT_{1\beta}$, etc.), rather than the Roman letters used in the mammalian nomenclature (i.e., 5-HT_{1A}, 5-HT_{1B}, etc.). This is because the subscripted letter is not meant to imply orthology across vertebrate/invertebrate lines. It is generally accepted that the paralogs within a subtype (i.e., 5-HT1A, 5-HT1B, etc.) evolved independently for mammals and invertebrates (Tierney 2001); thus, the arthropod 5-$HT_{2\beta}$ receptor has no real ortholog among the three vertebrate type 2 receptors: 2A, 2B, 2C. To emphasize this fact and thereby reduce confusion, here we indicate paralogs within a subtype using Greek letters for arthropods and Roman letters for vertebrates. Species is indicated immediately after the subscripted letter.

Table 2-2: 5-HT_2 receptor transmembrane region (TMR) amino acids with known functions.

LB, Ligand binding; HBP, hydrophobic binding pocket.

TMR	Position in receptor	Function	Conserved	References
TM1	2CHum55W	LB	No	(Roth et al. 1997a; Roth et al. 1997b)
TM2	2CHum104L	LB	No	(Wang et al. 1993;
	2CHum111L	LB	No	Choudhary et al. 1995;
	2CHum113A	LB	No	Sealfon et al. 1995; Roth
	2βPan118D	LB and G-protein coupling, binds to residue 2BPan697N in TM7	Yes	et al. 1997b; Manivet et al. 2002)
TM3	2βPan152D	LB and membrane targeting	Yes	(Kristiansen et al. 2000;
	2CHum138S	LB	No	Visiers et al. 2001;
	2βPan169D	Activation (see text)	Yes	Kroeze et al. 2002;
	2βPan170R	Activation (see text)	Yes	Manivet et al. 2002;
	2βPan171F	Activation (see text)	No	Shapiro et al. 2002); present study
TM5	2βPan236S	LB	Yes	(Almaula et al. 1996b;
	2βPan240F	LB contributes to HBP	Yes	Almaula et al. 1996a;
	2βPan242I	LB	Yes	Johnson et al. 1997;
	2CHum222A	LB	No	Shapiro et al. 2000;
	2CHum224F	LB	No	Manivet et al. 2002)
	2CHum228T	LB	No	
TM6	2CHum305N	Activation	No	(Choudhary et al. 1993;
	2CHum310S	Activation	No	Choudhary et al. 1995;
	2βPan644E	Activation (see text)	Yes	Roth et al. 1997a; Roth
	2βPan645Q	Activation	Yes	et al. 1997b; Shapiro et
	2βPan646K	Activation (see text)	Yes	al. 2000; Visiers et al.
	2βPan650V	Activation	Yes	2001; Manivet et al.
	2βPan651L	Activation	Yes	2002)
	2βPan654V	Activation	Yes	
	2βPan662W	LB contributes to HBP	Yes	
	2βPan664P	Activation: hinge allowing TM3/TM6 association-dissociation	Yes	
	2β an665F	LB contributes to HBP	Yes	
	2βPan666F	LB contributes to HBP	Yes	
	2βPan669N	LB	Yes	
TM7	2βPan688W	LB contributes to HBP	Yes	(Sealfon et al. 1995;
	2βPan691Y	LB contributes to HBP	Yes	Roth et al. 1997a; Roth
	2CHum353F	LB	No	et al. 1997b; Rosendorff
	2βPan697N	LB/coupling, interacts with 2Bpan118D	Yes	et al. 2000; Manivet et
	2βPan701Y	Activation	Yes	al. 2002)

A prosite scan revealed that both arthropod 2β orthologs contain N-linked glycosylation sites in their amino termini (Figure 2-1) and multiple phosphorylation sites (data not shown). Figure 2-1 shows an alignment of the arthropod 5-$HT_{2\beta}$ receptors with a mammalian 5-HT_{2C} receptor, as well as 5-$HT_{2\alpha Dro}$ and a 5-HT subtype 1 homologue from lobster (5-HT_{1Pan}) (Sosa et al. 2004). Only the TM regions were aligned, thereby emphasizing the differences in the lengths of the extracellular amino termini, the third intracellular loops (i3) and the intracellular carboxy termini. Though characteristic and expected, the lack of i3 conservation between 2β orthologs is somewhat baffling given that G protein coupling and receptor targeting are conserved functions of the i3 domain (Kroeze et al. 2002). The other intracellular loops (i1 and i2) are well conserved across arthropod 2β orthologs, whereas the extracellular loops (e1-e3) are not. G protein coupling is partially determined by i2 (Burns et al. 1997; Lembo et al. 1997; Niswender et al. 1999), e2 functions in ligand selectivity (Kroeze et al. 2002), but the functions of the other loops are unknown.

The amino termini of 5-HT receptors are usually not conserved in sequence or length, and their role remains undefined. The conserved proximal portion of the C-terminus (2βPan, 706K-717K) is predicted to form a helix parallel to the membrane surface, and the adjacent conserved cysteine (2βPan, 718C) represents a putative palmitoylation site that may play a role in anchoring this presumed eighth cytoplasmic helix at the membrane surface (Palczewski et al. 2000; Kroeze et al. 2002). The terminal amino acids of the human 2C receptor form a type 1 PDZ domain that interacts with the MUPP1 scaffold protein to form a multi-protein signaling complex (Becamel et al. 2001; Becamel et al. 2002). Similarly, this domain helps to determine functional activity and receptor trafficking of 5-HT_{2A} receptors (Xia et al. 2003).

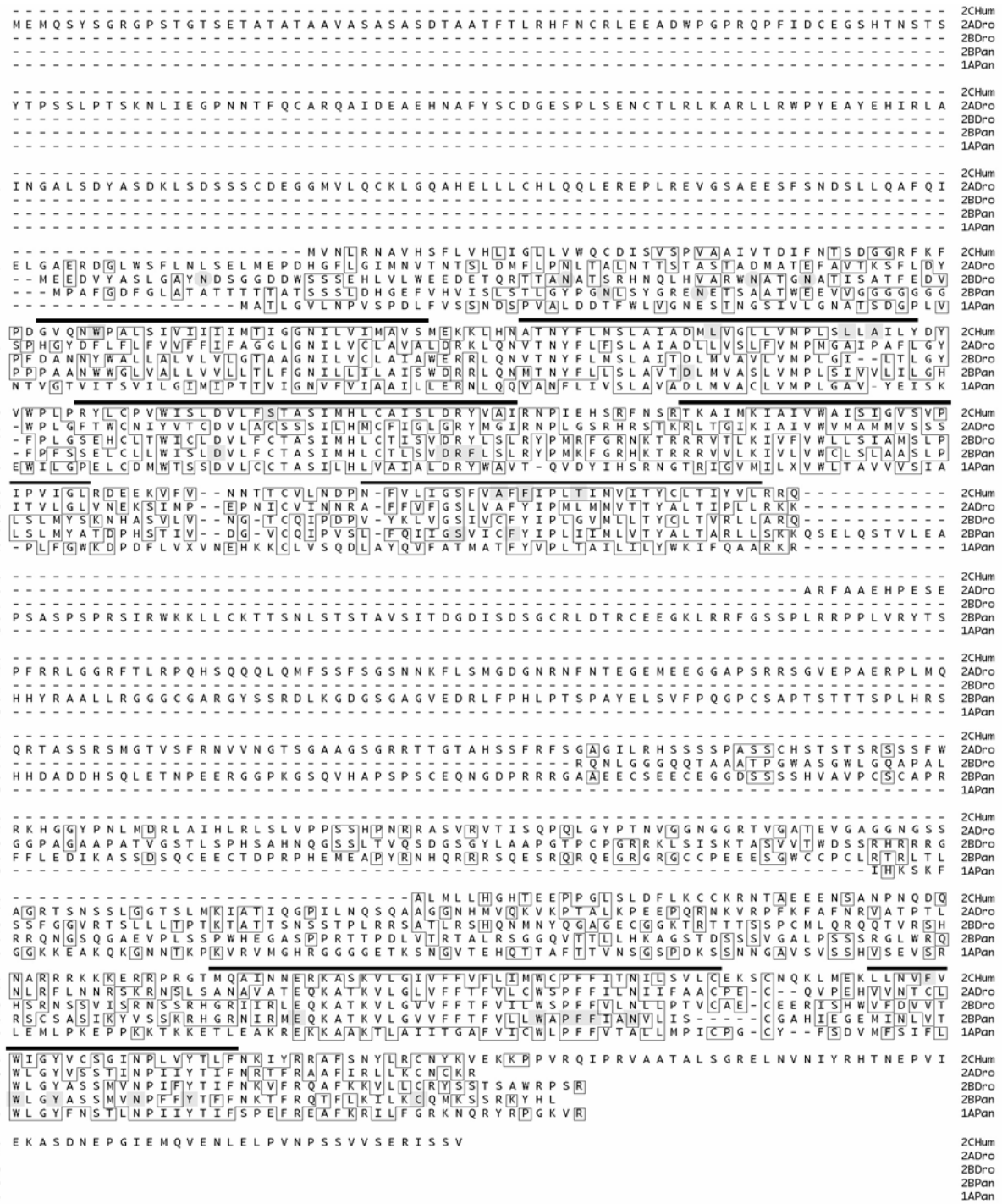

Figure 2-1: Conservation of 5-HT receptors. The predicted protein sequences for the two arthropod 5-HT_{2B} receptors are aligned with those predicted for the human type 2C receptor, the arthropod 5-HT_{2A} paralog and a lobster 5-HT type 1 receptor. Amino acids are numbered such that the start methionine is +1 in each sequence. Heavy black bars above the sequence approximate the seven transmembrane regions. Amino acids matching the consensus sequence are boxed. Amino acids discussed in the text are highlighted. Highlighted circles represent N-linked glycosylation sites.

In contrast, this domain is not present in the arthropod 2β orthologs, although the terminal amino acids of the lobster receptor form an atypical PDZ domain (Bezprozvanny and Maximov 2001).

There is a great deal of conservation of structure and function in the 5-HT receptor TM regions, which function both in ligand binding and receptor activation. Residues known to be important to these functions are listed in Table 2-2. Amino acids in the TM helices near the extracellular surface are thought to interact and form a binding pocket for ligands (Kroeze et al. 2002). Roughly half of the amino acids known to be involved in ligand binding are conserved between the human 2C and lobster 2β receptors (Table 2-2), which is consistent with the fact that pharmacological profiles are not fully preserved across species. It has been suggested that the cytoplasmic regions of TM3 and TM6 are closely associated in the inactive receptor but that these helices move apart in the activated receptor (Visiers et al. 2001; Kroeze et al. 2002; Shapiro et al. 2002). The highly conserved DRY motif in TM3 is partially responsible for mediating this effect. The conserved arginine residue (2βPan: 170R) is thought to interact with the neighboring conserved aspartate in TM3 (2βPan: 169D) and a conserved glutamate in TM6 (2βPan: 644E). Mutations that disrupt this triad cause constitutive activity in mammalian receptors. Although the tyrosine (Y) in the DRY motif is highly conserved among most monoamine receptors, to our knowledge, its function in receptor activation has not been characterized by mutagenic analyses. Interestingly, this residue is not conserved in the lobster 2β ortholog (2βpan: 171F).

The 5-HT$_{2\beta Pan}$ signaling pathway: Gq to PLC to PKC

While a 5-HT type 2 receptor has been cloned in *Drosophila* (Colas et al. 1995), its G protein coupling(s) is unknown. Conservation of a given receptor subtype across species usually

extends beyond the sequence to the primary signaling pathway. Traditionally, mammalian 5-HT type 2 receptors are thought to couple via G_q to PLC. Activated PLC hydrolyses phosphotidylinositol 4,5 bisphosphate (PIP_2), thereby producing inositol 1,4,5-triphosphate (IP_3) and diacyl glycerol (DAG). IP_3 goes on to release calcium stores, and together, the Ca^{2+} and DAG bind to the C2 and C1 sites on protein kinase C (PKC), respectively, thereby linking PKC to the membrane where it is activated by association with phosphotidyl serine (Liu and Heckman 1998; Newton 2001). It has now been shown that 5-HT_2 receptors can additionally couple to multiple pathways (Berg et al. 1998; Pauwels 2000; Kurrasch-Orbaugh et al. 2003) and that there are three subtypes of PKC isozymes that vary with respect to their substrates and requirements for DAG and Ca^{2+} (Way et al. 2000). In the next series of experiments, we investigated whether 5-$HT_{2\beta Pan}$ is coupled to the G_q signaling pathway.

Using standard cloning techniques we generated full-length constructs for 5-$HT_{2\beta Pan}$ and used them to establish permanent HEK cell lines expressing 5-$HT_{2\beta Pan}$ (HEK 5-$HT_{2\beta Pan}$). We then assayed cells for PKC activation in response to increasing concentrations of 5-HT (Figure 2-2). PKC translocates from the cytosol to the membrane where it is activated, and translocation is a standard assay for PKC activation in response to GPCR activity (Burgess 1992). We exposed cells to 10^{-9} to 10^{-2} M 5-HT for 15 minutes, lysed and fractionated the cells (membrane vs. cytosol), and then measured total PKC activity in each of the two fractions using an assay that detects phosphorylation of neurogranin, a substrate for conventional PKC isozymes that are sensitive to both [DAG] and $[Ca^{2+}]_i$ (Huang et al. 1993; Ramakers et al. 1999). Figure 2-2A demonstrates that for HEK 5-$HT_{2\beta Pan}$ cells there is a significant, dose-dependent translocation of PKC to the membrane in response to increasing concentrations of 5-HT. On the other hand, the parental, nontransfected HEK cells show no response to 5-HT application (Figure 2-2B).

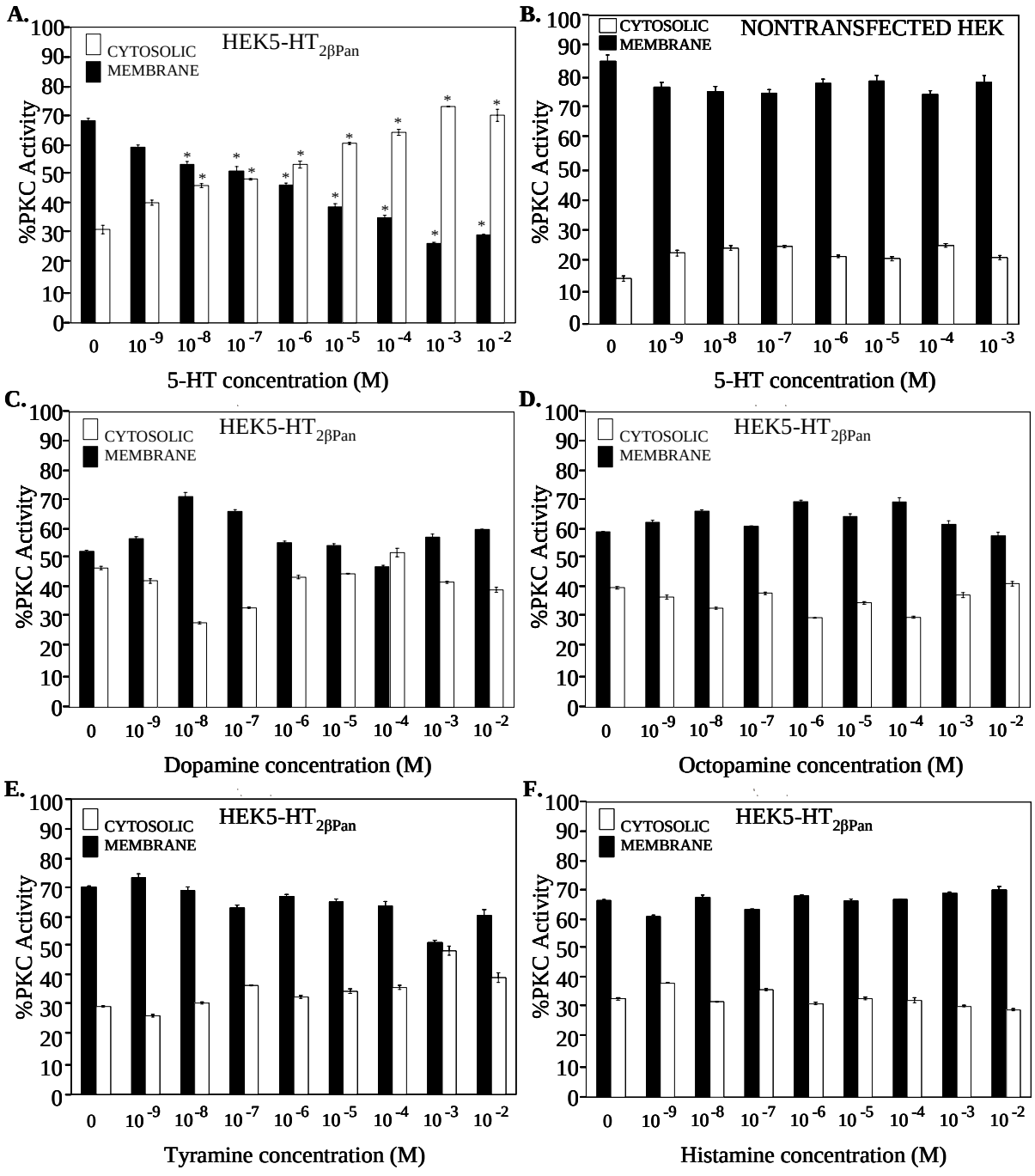

Figure 2-2: The effect of biogenic amines on PKC translocation. HEK 5-$HT_{2\beta Pan}$ or nontransfected HEK cells were exposed to the indicated drug for 15 minutes. Cytosolic and membrane fractions were separated, and PKC specific activity in each fraction was measured. The percent of total PKC specific activity associated with the cytosolic (filled bars) vs. membrane (open bars) fractions is indicated. Data are expressed as mean $\pm$ SEM and n=3 for all experiments except panels A & B, where n=8 for 0 5-HT. * significantly different ($p < 0.05$) when compared to the same fraction in the absence of drug.

Since some monoamine receptors can be activated by multiple ligands (Hearn et al. 2002), we next asked if other monoamines that normally function as modulators in the lobster nervous system could activate the 5-$HT_{2\beta Pan}$ receptor. Neither dopamine (Figure 2-2C), octopamine (Figure 2-2D), tyramine (Figure 2-2E) nor histamine (Figure 2-2F) produced significant PKC translocation in HEK5-$HT_{Pan2\beta}$ cells, even at concentrations as high as 10mM. These results are consistent with the classification of our newly discovered GPCR as a 5-HT_2 receptor.

To show that PLC activation led to the previously observed PKC translocation in cells expressing the 5-$HT_{2\beta Pan}$ receptor, we applied the PLC inhibitor, ET-18-OCH_3, 15 minutes prior to incubation with 5-HT, and assayed the cells for PKC translocation. Figure 2-3 demonstrates that application of the PLC inhibitor precludes the 5-HT evoked PKC translocation, suggesting that the signaling cascade activated by the 5-$HT_{2\beta Pan}$ receptor includes PLC.

In order to further test this hypothesis, we measured inositol phosphate (IP) accumulation in response to 5-HT. Figure 2-4 illustrates that HEK5-$HT_{2\beta Pan}$ cells displayed a significant, 2.75-fold increase in PI hydrolysis (or IP accumulation) in response to 10^{-3} M 5-HT ($p < 0.01$), while the parental HEK cells showed no significant change. However, both cell lines responded to the nonspecific activator of trimeric G proteins, NaF, with roughly a 3-fold increase in PI hydrolysis. Collectively, these data suggest that the 5-$HT_{2\beta Pan}$ receptor transduces signals via PLC. (Figure 2-5), and both showed the same basal level of cAMP, approximately 300pmol/mg, which was similar to that previously reported from other groups (Sadou et al., 1992). However, both cell lines responded to the AC activator, forskolin, with equivalent increases in $[cAMP]_i$ (Figure 2-5). These data suggest that 5-$HT_{2\beta Pan}$ does not activate G_s, which positively couples to AC.

PLC can be activated by the α subunit of G_q or through the $\beta\gamma$ subunits of other G proteins. Three pieces of data suggest that PLC is activated via G_q. First, both nontransfected

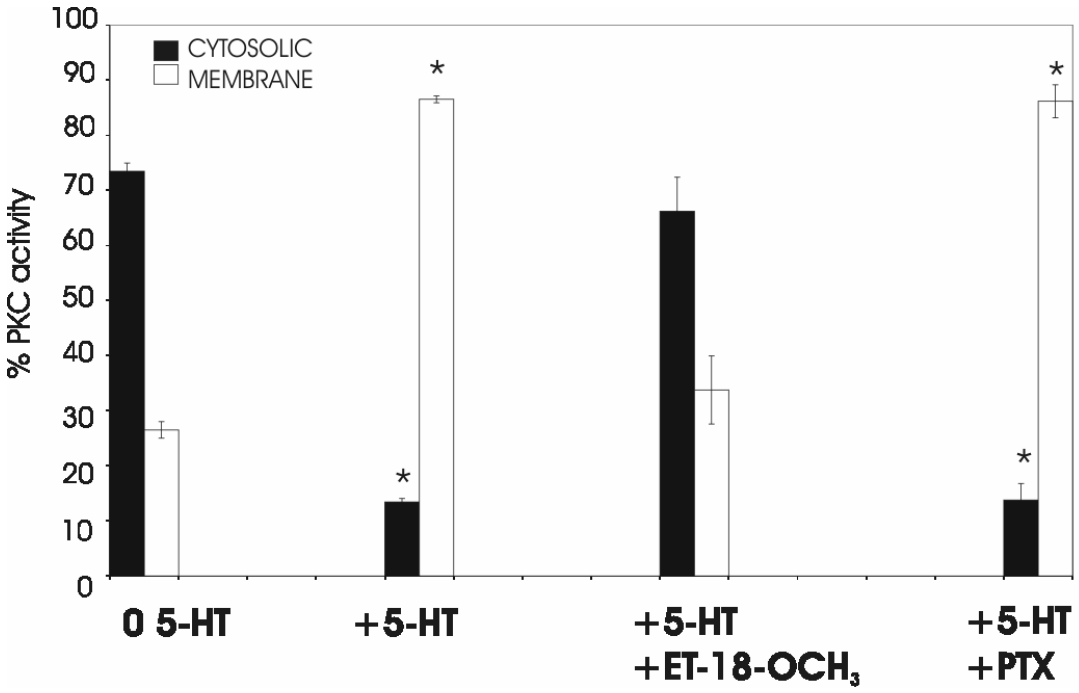

Figure 2-3: The PLC inhibitor, ET-18-OCH_3, but not pertussis toxin, blocks the 5-$HT_{2\beta Pan}$ receptor-mediated translocation of PKC. Following pretreatment with an inhibitor, cells were incubated an additional 15 minutes with 5-HT (10^{-3}M). PKC activity was measured in the cytosolic and membrane fractions. Data are expressed as the mean $\pm$ SEM, n = 3 per condition. * significantly different ($p < 0.05$) when compared to 0 5-HT.

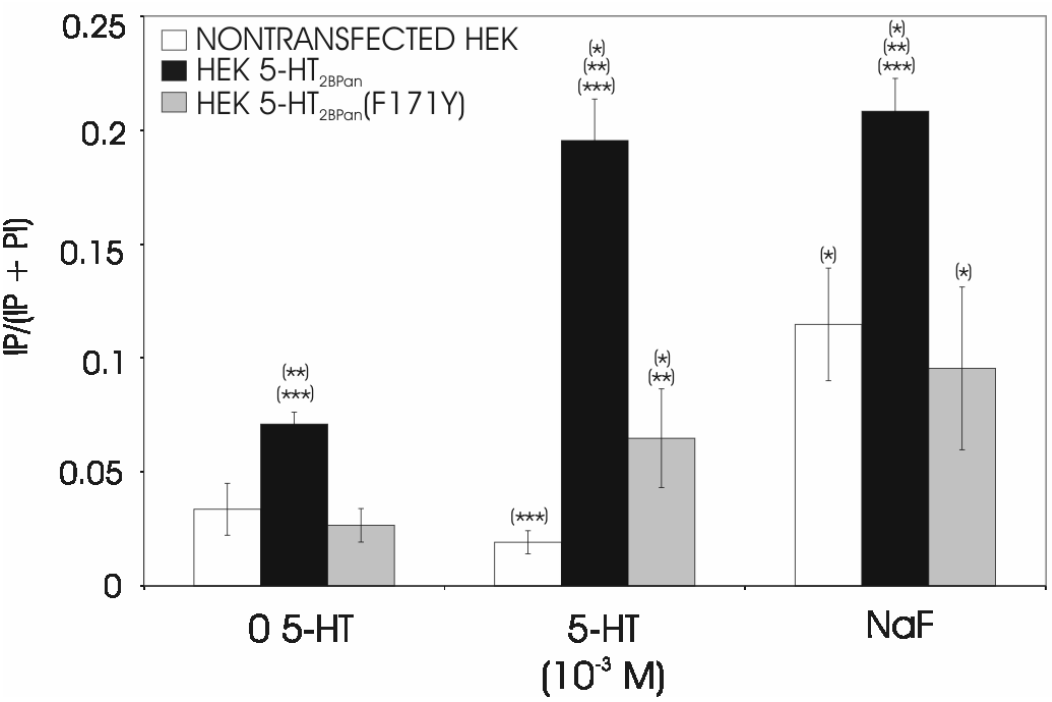

Figure 2-4: 5-HT stimulates inositol phosphate production in cells expressing the 5-HT$_{2\beta Pan}$ receptor, but not in the parental HEK cell line. Total PI and IP were assayed in nontransfected HEK (white), HEK 5-HT$_{2\beta Pan}$ (black), and HEK 5-HT$_{2\beta Pan}$ (F171Y) cells (gray). Three conditions are shown: control (no drug), 5-HT (60 minute exposure to 10^{-3} M 5-HT) and NaF (60 minute exposure to the nonspecific trimeric G protein activator, 20 mM NaF). Results are expressed as a ratio of IP/(PI + IP). Data represent mean $\pm$ SEM from three separate experiments. * significantly different ($p < 0.05$) for drug vs. control for a given cell line. ** significantly different from HEK cells under the same condition (i.e., comparisons within each of the groups: control, 5-HT, NaF). *** significantly different from HEK 5-HT$_{2\beta Pan}$ (F171Y) under the same condition.

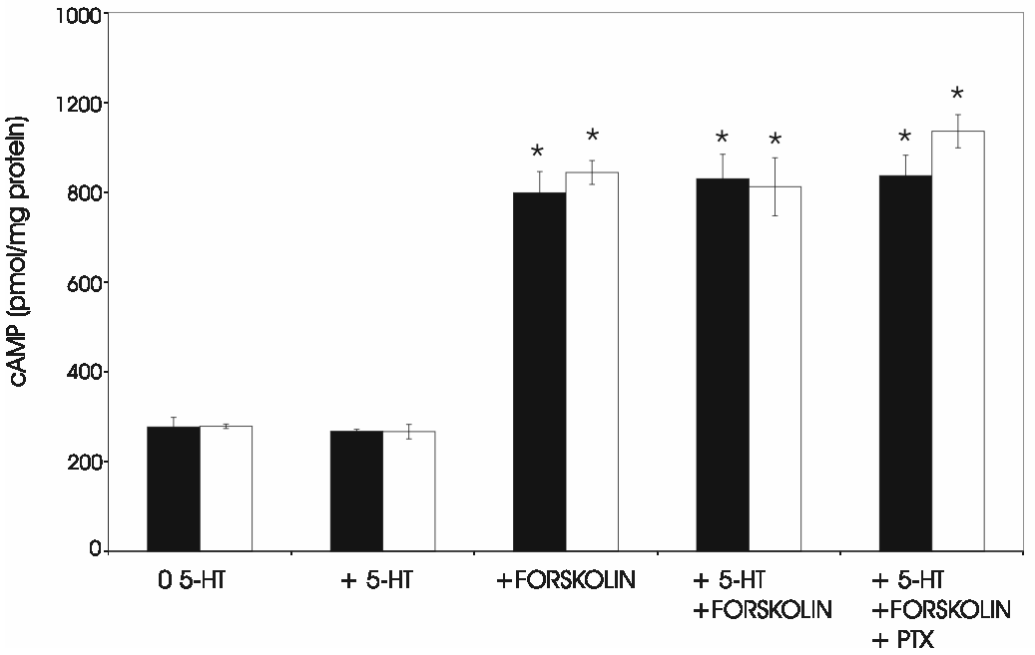

Figure 2-5: cAMP levels do not change in response to 5-HT treatment. cAMP levels were measured in 5-$HT_{2\beta Pan}$ transfected (shaded bars) and nontransfected cells (open bars), or cells exposed to 5-HT (10^{-3}M), or forskolin (2.5mM), or forskolin (2.5mM) with 5-HT(10^{-3}M), or forskolin (2.5mM) with 5-HT(10^{-3}M) following pretreatment with pertussis toxin. Results are expressed as pmol cAMP/mg protein. Data are mean $\pm$ SEM from three separate experiments. * significantly different ($p < 0.05$) for drug vs. control for a given cell line. There were no significant differences between any treatments containing forskolin within or between cell lines.

HEK and HEK 5-$HT_{2\beta Pan}$ cells showed no increase in cAMP levels in response to 10^{-3} M 5-HT Second, exposure to 5-HT did not significantly alter the forskolin response in either cell line, suggesting that $G_{i/o}$, which inhibits AC, was not activated by 5-HT in either cell line (Figure 2-5). Third, pertussis toxin, which specifically blocks $G_{i/o}$ dissociation into G_{α} and $G_{\beta\gamma}$ subunits, had no significant effect on the 5-HT evoked PKC translocation in HEK 5-$HT_{2\beta Pan}$ cells (Figure 2-3), or on levels of cAMP in cells exposed to both forskolin and 5-HT (Figure 2-5). This further demonstrates that the $\beta\gamma$ subunit of $G_{i/o}$ does not activate PLC in response to 5-HT. Collectively, these data are consistent with a mode of action by which the 5-$HT_{2\beta Pan}$ receptor couples to what has been designated as the traditional pathway for 5-HT_2 receptors in mammals: G_q to PLC to PKC.

Agonist independent activity of the 5-$HT_{2\beta Pan}$ receptor

It is well documented that GPCRs can demonstrate agonist independent activity (Seifert and Wenzel-Seifert 2002; Mustard et al. 2003). This is usually detected as an increase in signaling pathway activity under baseline conditions (no agonist present) in cells expressing the GPCR (HEK 5-$HT_{2\beta Pan}$) relative to the nontransfected parental cell line (HEK). In all experiments we noticed that in the absence of agonist, the PKC activity associated with the membrane fraction was significantly higher in HEK 5-$HT_{2\beta Pan}$ cells relative to nontransfected HEK cells ($p < 2 \times 10^{-5}$: compare the first set of bars in Figure 2-2A, 2-2C, 2-2D, 2-2E, and 2-2F to 2-2B). The average PKC activity associated with the membrane fraction was 11 $\pm$ 1.4 % for nontransfected HEK cells and 35 $\pm$ 4.0% for HEK5-$HT_{2\beta Pan}$ cells under baseline conditions. Since PKC activation is associated with translocation to the membrane, we conclude that there is roughly a 3-fold increase in the basal level of PKC activity in cells expressing the 5-$HT_{2\beta Pan}$

receptor. Similarly, in the absence of agonist we observed a significant, 2.3-fold increase in IP levels in cells expressing the 5-$HT_{2\beta Pan}$ receptor relative to the parental cell line (Figure 2-4; $p < 0.05$). The most parsimonious interpretation of these data is that when the 5-$HT_{2\beta Pan}$ receptor is expressed in HEK cells, it displays some agonist independent activity.

Phorbol esters, like PMA, can substitute for DAG, as they associate with the DAG binding site, C1, on the PKC enzyme. Thus, both PMA and DAG serve as hydrophobic anchors that can recruit conventional PKC isozymes to the membrane even in the absence of Ca^{2+} (Newton 2001). A 15 minute application of 0.1μM PMA alone caused 90% of the PKC to translocate to the membrane in HEK 5-$HT_{2\beta Pan}$ cells, but not in the parental, nontransfected cells (Figure 2-6). A sixty minute exposure to PMA was required to obtain the same level of translocation in the parental cell line. The average PKC specific activity was not significantly different between HEK5-$HT_{2\beta Pan}$ and HEK cells (0.11 ± 0.02 psl/μg vs. 0.095 ± 0.03 psl/μg; $p = 0.2$). Thus, the average number of PKC molecules is probably similar in the two cell lines. Since the level of PKC's membrane affinity is linearly related to the mol fraction of C1 ligand in the bilayer (i.e., DAG and/or PMA), and since Ca^{2+} binding at the C2 site on conventional PKC enzymes acts synergistically with binding at the C1 site to facilitate PKC association with the membrane (Newton 1995, 2001), the potentiated response of the transfected cells to PMA is consistent with the idea of a constitutively active receptor.

Blocking constitutive activity by restoring the DRY motif

As discussed earlier, it has been suggested that the highly conserved DRY motif in TM3 helps to mediate receptor activation, and mutation of the D and/or R in this motif is known to cause constitutive receptor activity in mammalian type 2 receptors

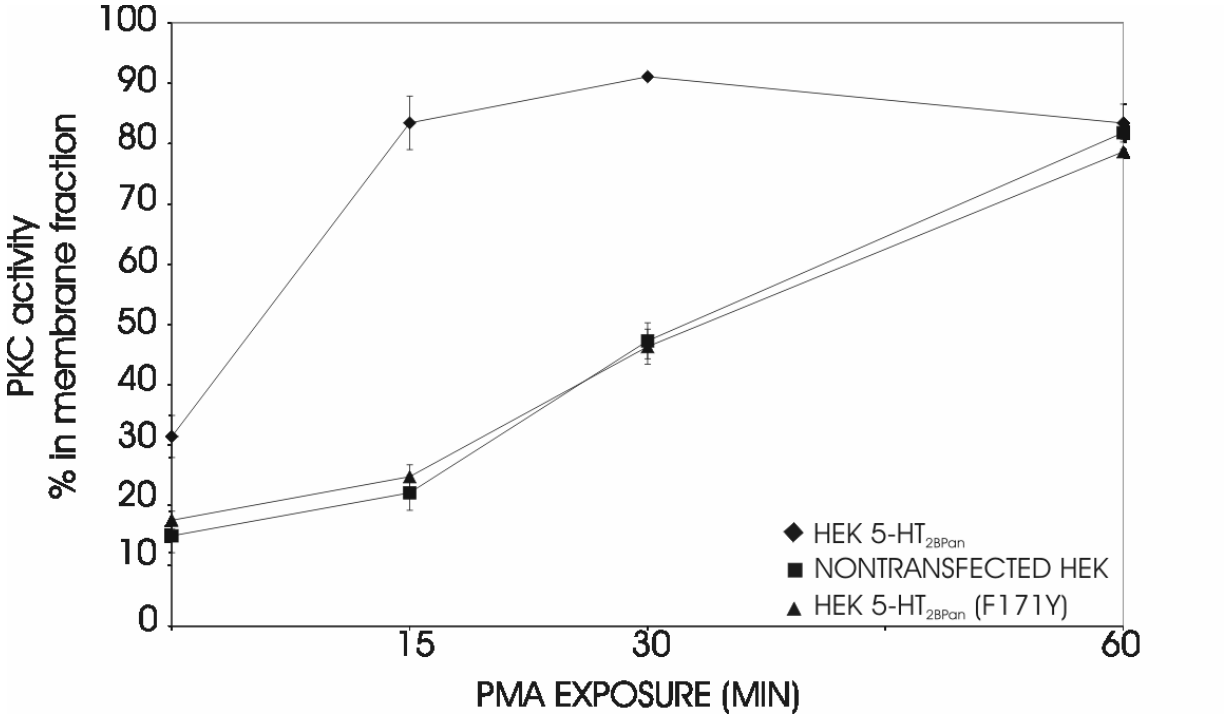

Figure 2-6: The PMA response is potentiated in HEK 5-HT$_{2\beta Pan}$ cells. The PKC activator, PMA (0.1µM), was applied for 15, 30, or 60 minutes to each of three cell lines [HEK 5-HT$_{2\beta Pan}$, diamonds; HEK, squares; HEK 5-HT$_{2\beta Pan}$ (F171Y), triangles]. The PKC specific activity associated with the cytosolic and membrane fractions was measured, and the percent of the total specific activity associated with a given fraction was determined. The percent of PKC specific activity associated with the membrane is plotted for each time point in each cell line. Each data point represents the mean $\pm$ SEM, n=3 per data point.

(Kroeze et al. 2002; Shapiro et al. 2002). In the 5-$HT_{2\beta Pan}$ receptor, the DRY motif has evolved into DRF (Figure 2-1). This same alteration has also occurred in a nematode receptor, 5-HT_{2As} (Huang et al. 2002). Restoration of the DRY motif in the nematode receptor caused a reduction in its affinity for 5-HT, but the effect on activation was not considered (Huang et al. 2002). We hypothesized that the Y to F transition might contribute to the observed constitutive activity of the lobster receptor. To test this hypothesis, we used site directed mutagenesis (F171Y) on our original construct to restore the DRY motif to the 5-$HT_{2\beta Pan}$ receptor. We used this new construct to stably transfect HEK cells and establish a second cell line, HEK 5-$HT_{2\beta Pan}$(F171Y). We then assayed the cell line for PKC activity and PI hydrolysis as previously described. Figure 2-7 demonstrates that HEK 5-$HT_{2\beta Pan}$(F171Y) cells still show a dose-dependent translocation of PKC in response to increasing levels of 5-HT. However, in the absence of agonist only 17 $\pm$ 2.0% of the total PKC specific activity was associated with the membrane fraction of HEK 5-$HT_{2\beta Pan}$(F171Y) cells, which was not significantly different from the 11$\pm$ 1.4% observed for the parental, nontransfected HEK cell line, but was significantly different from the 35 $\pm$ 4.0% observed for the wild type receptor containing the DRF motif ($p<0.002$). Similarly, although cells expressing the mutated receptor still respond to 10^{-3}M 5-HT with a significant, roughly 2.4-fold increase in PI hydrolysis (Figure 2-4, $p < 0.05$), under baseline conditions IP levels were not significantly different between the HEK 5-$HT_{2\beta Pan}$(F171Y) and the parental HEK cell lines, but were significantly lower for cells expressing the mutated versus wild type receptor ($p < 0.003$). Finally, Figure 2-6 illustrates that restoration of the DRY motif abolishes the potentiated PMA response associated with the wild type receptor. All of these results strengthen the idea that the wild type 5-$HT_{2\beta Pan}$ receptor is constitutively active when expressed in HEK cells, and suggest that the residue at position 171 plays a role in receptor activation.

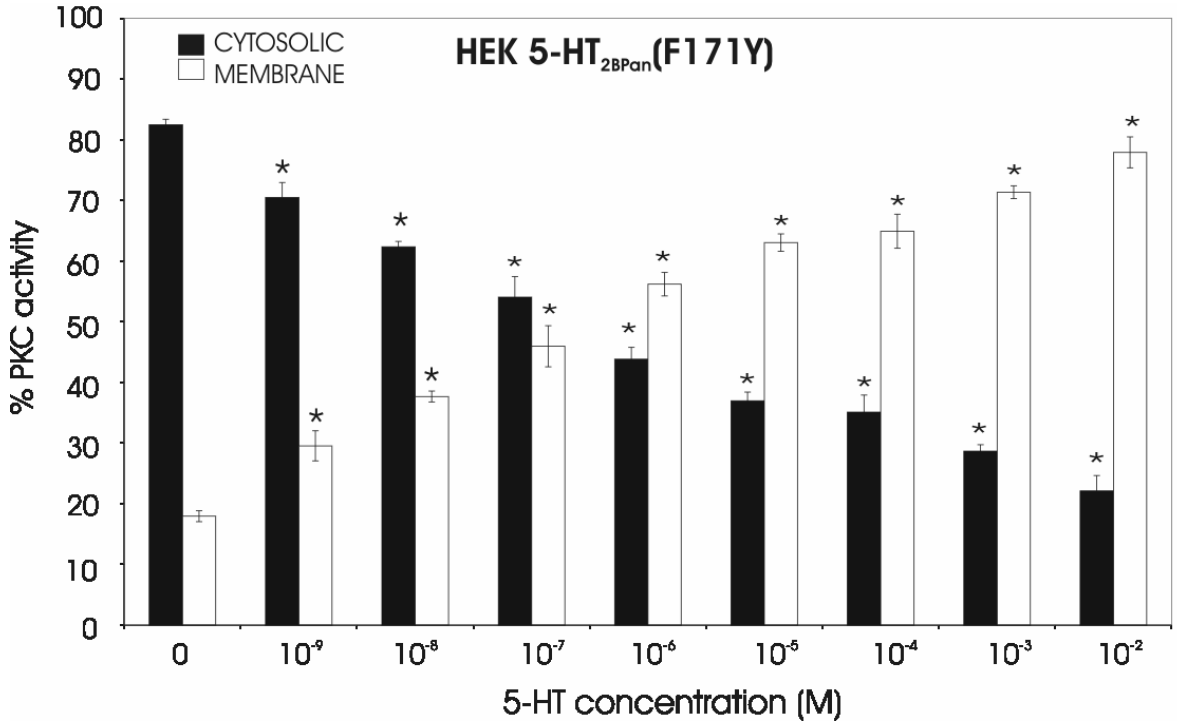

Figure 2-7: Restoration of the DRY motif disrupts the agonist independent activity associated with the 5-HT$_{2\beta Pan}$ receptor, but not the response to 5-HT. HEK 5-HT$_{2\beta Pan}$ (F171Y) cells were assayed for PKC translocation after a 15 minute exposure to varying concentrations of 5-HT, as indicated. Data are expressed as mean $\pm$ SEM from three separate experiments, except for the 0 5-HT data point where n = 5. *, $p < 0.05$ when compared to activity in the same fraction in the absence of drug treatment.

Interestingly, in addition to triggering constitutive activity, the Y to F transition at position 171 also seems to increase evoked PI hydrolysis. Figure 2-4 shows that PI hydrolysis in response to 5-HT was significantly higher in cells expressing the wild type versus the mutant receptor. Similarly, the response of 5-$HT_{2\beta Pan}$ cells to NaF was significantly greater than for either of the other two cell lines. There did not appear to be a potentiation of the evoked PKC response in 5-$HT_{2\beta Pan}$ relative to 5-$HT_{2\beta Pan(F171Y)}$ cells; however, the 5-HT exposure time varied between the two assays: 15 minutes for the PKC assay versus 60 minutes for the IP assay, as did the state of the cells during exposure to the drug (resuspended versus plated, respectively).

5-HT_{2BPan} localization in the stomatogastric nervous system (STNS)

In *Panulirus interruptus*, stomatogastric neurons are modulated by bath application of 5-HT (Flamm and Harris-Warrick 1986b, a). There are no serotonergic input fibers to the STG. Instead, a short distance away is a neurohemal plexus that releases 5-HT into the hemolymph that constantly bathes the ganglion (Sullivan et al. 1977b; Beltz et al. 1984; Beltz 1999). The 5-HT receptors in *P. interruptus* have a high affinity for 5-HT and respond to physiological concentrations contained in the hemolymph (Beltz 1999). Thus, it is generally thought that 5-HT acts as a neurohormone in this system. We were interested in whether 5-$HT_{2\beta Pan}$ could potentially serve as a neurohormonal receptor mediating some of the actions of 5-HT on pyloric neurons. We therefore asked if 5-$HT_{2\beta Pan}$ was expressed in stomatogastric neurons, and if so, where this potential neurohormone receptor might be located.

We generated affinity purified antibodies against the receptor as detailed in Materials and Methods. Figure 2-8 shows that the antibody recognizes a single band around the predicted molecular weight of 79kD, and the signal is lost upon preabsorption with the peptide used to

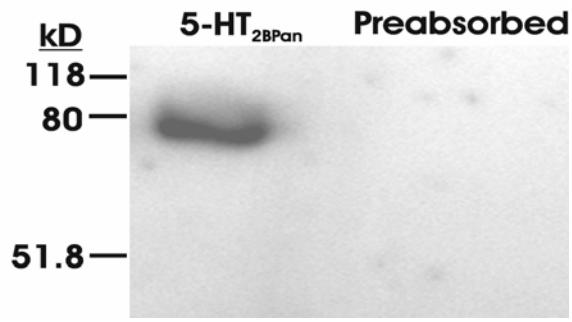

Figure 2-8: Anti-5-HT$_{2BCrust}$ specifically recognizes the 5-HT$_{2\beta Pan}$ receptor in lobster nervous tissue. The figure shows a representative western blot experiment. The blot containing protein extracts from lobster nervous tissue was probed with an antibody against 5-HT$_{2BCrust}$ (5-HT$_{2\beta Pan}$) or the same antibody preabsorbed with the peptide antigen used to generate the antibody (Preabsorbed). Molecular weight standards are indicated. The antibody produces a signal corresponding to the predicted size of the protein, which is lost upon preabsorption.

generate the antibody, suggesting that the antibody is specific for the 5-$HT_{2\beta Pan}$ protein. To determine if this receptor is expressed in pyloric neurons, we used the antibody to perform whole mount immunocytochemistry experiments on the STG and identified muscles, followed by confocal microscopy, as previously described (Baro et al., 2000).

The STG is a sphere containing a core of coarse neuropil, which is encompassed by a layer of fine neuropil, which in turn, is surrounded by the peripheral layer that contains neuronal cell bodies, nerve fibers, blood vessels, and blood cells interspersed among numerous glial elements (see Baro et al., 2000; Wilensky et al., 2003 for a more complete perspective). A perineural sheath covers the entire ganglion. Each of the 14 monopolar pyloric neurons have their cell bodies in the peripheral layer, and send a primary process into the central coarse neuropil that then branches into secondary and tertiary neurites. Processes from the coarse neuropil enter and branch in the more peripheral fine neuropil, where synapses occur between stomatogastric neurons as well as modulatory input fibers. Afferent fibers mainly enter the ganglion through the peripheral layer, and then go on to form synapses in the fine neuropil (Friend, 1976; King, 1976a,b). The stomatogastric nerve (stn) and dorsal ventricular nerve (dvn) are associated with the ganglion anteriorly and posteriorly, respectively. The13 pyloric motoneurons all send an axon out the dvn, each of which goes on to innervate identified muscles.

Figure 2-9 shows receptor distribution in the STG. We found that the receptor was expressed in what appears to be the somatic endomembrane compartment of 98% of the neurons (n=6 ganglia), but expression levels varied across neurons (Figures 2-9A and 2-9B). In an attempt to determine whether the receptor might be in the somatodendritic plasma membrane, we performed double-label experiments (Figure 2-9C) using anti-5-$HT_{2BCrust}$ and an antibody against

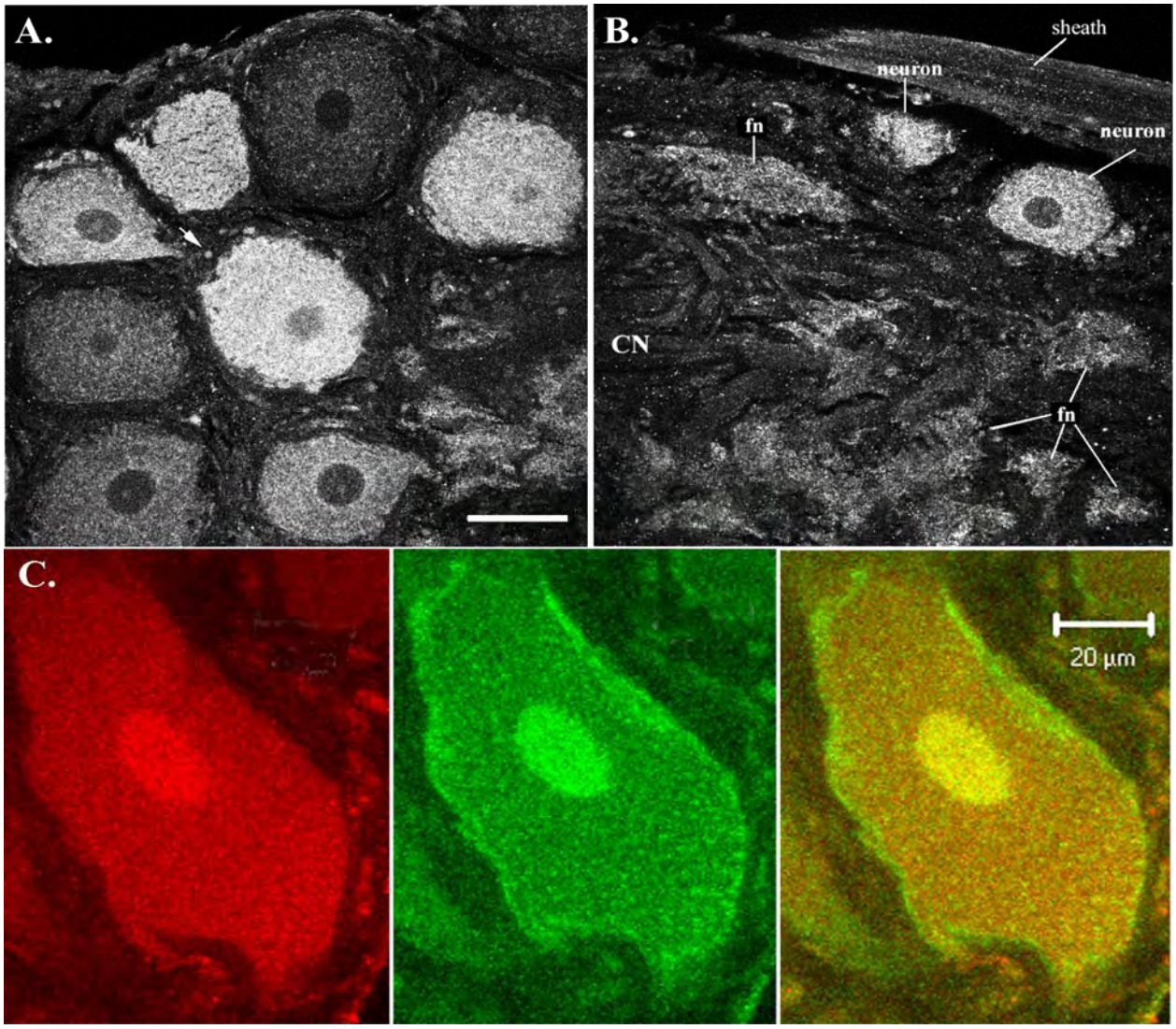

Figure 2-9: Most stomatogastric neurons express 5-$HT_{2\beta Pan}$ to varying degrees. Panels A and B each represent a 5.45µm confocal slice from different representative ganglia. The scale bar represents 50µm for both panels. A. Anterior left quadrant roughly 20µm from the dorsal-most aspect of the ganglion. This slice depicts mostly the peripheral layer showing 8 neuronal cell bodies; however, the fine, synaptic neuropil containing tufts of neurites from stomatogastric and modulatory input neurons can be seen in the lower right corner, (above scale bar). The arrow points to one of many profiles most likely representing transport of the receptor in fibers that are entering/leaving the ganglion through the peripheral layer. B. Optical slice representing posterior left quadrant of the ganglion approximately 35µm from the ventral-most aspect. All layers of the ganglion appear in this slice: the triangular course neuropil (CN) jutting out from the left, surrounded by several tufts of fine neuropil (fn), sourrounded by the peripheral layer containing somata, sourrounded by the perineural sheath. C. Confocal projection representing roughly 1.5µm in depth, showing a single neuron double-labeled for the 5-$HT_{2\beta Pan}$ receptor (red) and the K^+ channel, shal 1.b (green). The third panel represents the merged image. Note the ring of protein in the plasma membrane that is present in the K^+ channel profile but absent in the receptor profile.

the terminal exon of the K^+ channel, Shal 1.b (Baro et al., 2001). Though shal channels have previously been shown to reside in the somatodendritic plasma membranes of stomatogastric neurons and glial cells (Baro et al., 2000), this particular isoform is expressed only in neurons (Baro, unpublished). The typical shal channel profile, which is an intense ring around the somata, can be seen in Figure 2-9C. This ring, which suggests that the protein is concentrated in the plasma membrane, was missing in the receptor profile for all single and double label experiments. Thus, the receptor does not appear to be well represented in the somatic plasma membrane. Similarly, an intense ring surrounding the large diameter process in the coarse neuropil was seen only in the K^+ channel profiles (not shown). On the other hand, the receptor was observed in higher branch order processes of the fine neuropil, and in what we interpret to be the endomembrane system of a fraction of fibers throughout the ganglion (Figure 2-9A and 2-9B). The receptor was not observed in the membranes of axons leaving the ganglion via the dorsal ventricular nerve (dvn) or in glial cells surrounding the neurons.

Flamm and Harris-Warrick (1986) demonstrated that all pyloric neurons except the pyloric dilators (PD) and pyloric constrictors (PY) respond to bath applied 5-HT, as determined by somatic intracellular recordings from synaptically isolated cells. The PD and PY cell types comprise roughly 30% of all stomatogastric neurons (i.e., approximately 10 out of 30 neurons). Our immunocytochemistry data suggest that the 5-$HT_{2\beta Pan}$ receptor is detected in the somatic endomembrane compartment of nearly all stomatogastric neurons. Thus, most PD and PY neurons must express the 5-$HT_{2\beta Pan}$ receptor. The signals detected in the endomembrane system most likely represent turnover, processing, and/or transport of the receptor protein. Since the PD and PY neurons send axons out the dvn that go on to innervate distant, identified muscles that are centimeters away from the somata, one explanation for the presence of immunoreactivity but

absence of an electrophysiological response, is that some cell types, like PD and PY, transport the receptors to axon terminals at neuromuscular junctions (NMJs) where their presence would not be detected by somatic intracellular recordings. To test this hypothesis, we examined receptor distribution at two identified NMJs: the PD NMJ (PD neurons exclusively innervating the paired ventral PD muscles (cpv2; n =5 animals) and the PY NMJ (PY neurons exclusively innervating the paired P8 muscles; n = 4 animals). In these experiments we used a second antibody against synaptotagmin, which has previously been used to identify the axon terminals at crustacean NMJs (Littleton et al. 1993; Cooper et al. 1995; Quigley et al. 1999). Figure 2-10 illustrates that the 5-$HT_{2\beta Pan}$ receptor is observed at both identified NMJs. Consistent with our hypothesis, the strong colocalization with synaptotagmin, an integral, synaptic vesicle membrane protein, suggests that the receptor is located presynaptically. We occasionally observed receptor staining without counterpart synaptotagmin staining (arrows in Figure 2-10). We do not know if this staining represents extra-synaptic receptors in the muscle and/or terminal, or simply "nonspecific" sticking of the antibody; however, this staining was not observed when the anti-5-$HT_{2BCrust}$ antibody was preabsorbed. In addition, receptor staining at the PD NMJ was always robust, while at the PY NMJ staining intensities varied with the animal. We do not know if this variability was biological or technical; however, synaptotagmin staining at all NMJs was always robust in all animals.

Discussion

We have successfully used a bioinformatics approach to clone a novel 5-HT receptor from arthropods, and in particular, from a crustacean that lacks a sequenced genome. This illustrates that the profusion of data existing for model genetic organisms, like *Drosophila*, can

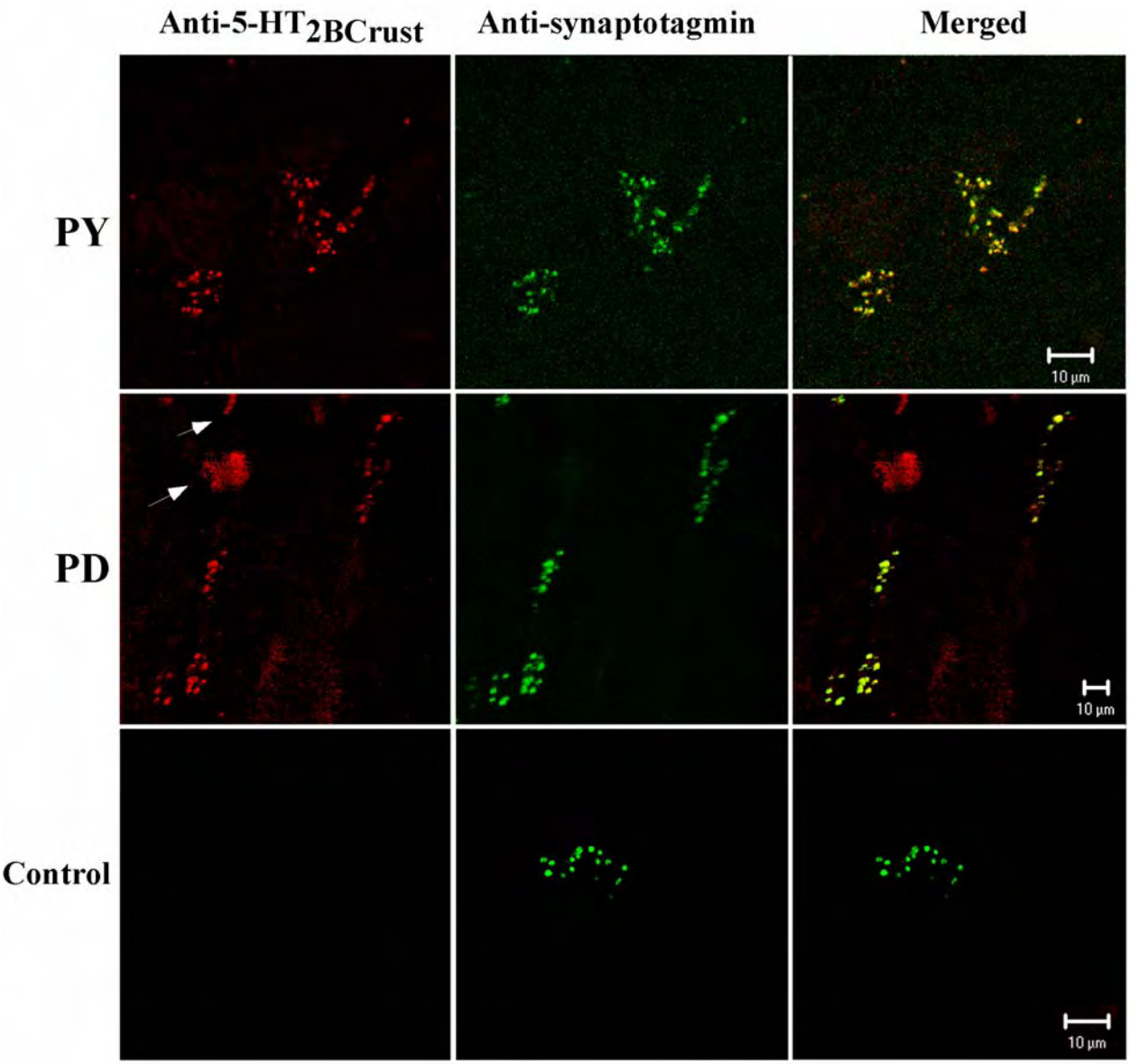

Figure 2-10: Colocalization of 5-HT$_{2\beta Pan}$ receptors with synaptotagmin at identified NMJs. Double-label immunocytochemistry was performed on PD and PY muscles, using the antibodies indicated above the panels. Control represents the same double-label experiment except that the ant-5-HT$_{2BCrust}$ antibody was preabsorbed. Each row displays representative NMJs from one experiment, where identified muscles and control are as indicated. Arrows point to 5-HT2$_{\beta Pan}$ staining that is not localized to the synapse. The PD panels represent a projection of 5 confocal slices representing approximately 5µm in depth. Each set of PY and preabsorbed panels represent a single 1.0µm confocal slice.

be exploited to the advantage of other important, but genetically intractable arthropod models used to study physiological processes like motor pattern generation. The number of potential monoamine receptors identified by this approach suggests that a little over half of the existing arthropod monoamine receptors have been cloned and characterized (10 of the predicted 18), and that invertebrate receptor numbers may parallel those observed for vertebrates.

The 5-$HT_{2\beta}$ receptor that we identified in fly and spiny lobster is a paralog of the 5-HT_{2A} receptor previously cloned from *Drosophila* (Colas et al. 1995). Thus, there are two known arthropod 5-HT_2 genes to date. We have demonstrated, for the first time, that arthropod 5-HT_2 receptors couple to the G_q signaling pathway, like their mammalian homologs. This is consistent with most comparisons of monoamine receptor subtypes across vertebrate/invertebrate lines (Blenau and Baumann 2001; Tierney 2001), and it upholds the emerging concept that for a given receptor subtype, both sequence and primary signaling pathways will be conserved across species, while pharmacological profiles may not.

Similar to many other GPCRs, the 5-$HT_{2\beta Pan}$ receptor displays agonist-independent activity when heterologously expressed in a mammalian cell line. Our data suggest that the Y to F transition that evolved in the highly conserved TM3 DRY motif contributes to the observed agonist-independent activity; and therefore, this residue is implicated in receptor activation. Inverse agonists stabilize GPCRs in the inactive conformation and thereby reduce agonist-independent activity. Inverse agonists (synthetic and/or endogenous) have been identified for the majority of constitutively active GPCRs (Seifert and Wenzel-Seifert 2002). Since endogenous inverse agonists exist (Ango et al. 2001; Bockaert et al. 2002; Seifert and Wenzel-Seifert 2002), much of the constitutive activity displayed in heterologous systems may be absent in the native system where the inverse agonists also reside. Still, there have been demonstrations of agonist

independent activity for endogenous GPCRs in native cells (Morisset et al. 2000; Seifert and Wenzel-Seifert 2002), and it has been further shown that constitutive activity can be regulated by cellular processes. For example, neuronal activity can disrupt the interaction between mGluR and the scaffold protein/inverse agonist, homer 3, thereby activating the associated G protein in the absence of ligand with a time constant that is different from that of agonist mediated stimulation (Ango et al. 2001). Important issues that we will address in future experiments include whether the 5-$HT_{2\beta Pan}$ receptor can display agonist independent activity in pyloric neurons, under what conditions, and how this might affect network properties and motor output.

The presence of 5-HT receptors in the STG supports 2 decades of electrophysiological and anatomical experimentation showing that 5-HT modulates neural circuits located in this ganglion (Beltz et al. 1984; Marder and Eisen 1984b; Flamm and Harris-Warrick 1986a, b; Harris-Warrick and Flamm 1987; Katz et al. 1989; Katz and Harris-Warrick 1989; Johnson and Harris-Warrick 1990; Katz and Harris-Warrick 1990b; Kiehn and Harris-Warrick 1992a, b; Meyrand et al. 1992; Johnson et al. 1993a; Turrigiano and Marder 1993; Zhang and Harris-Warrick 1994; Christie et al. 1995; Zhang and Harris-Warrick 1995; Zhang et al. 1995; Hempel et al. 1996b; Ayali and Harris-Warrick 1999; Kilman et al. 1999; Tierney et al. 1999; Peck et al. 2001; Birmingham et al. 2003; Richards et al. 2003). A minimum of three pharmacologically distinct 5-HT receptors exist in these neurons (Zhang and Harris-Warrick 1994). To date, we have localized two serotonin receptors, 5-$HT_{2\beta Pan}$ and 5-HT_{1Pan} (Baro and Clark, Society for Neuroscience Abstract, 2003), to the STG and another 3 arthropod 5-HT receptors have been cloned and characterized in insects [5-HT_{1B} (Saudou et al. 1992); 5-HT_7 (Witz et al. 1990); 5-HT_{2ADro} (Colas et al., 1995)]. It may be the case that other uncharacterized 5-HT receptors exist in arthropods (Table 2-1). Whether all or only a subset of arthropod 5-HT receptors are

expressed in the STG has yet to be determined, but our results suggest that a single cell can express multiple 5-HT receptors and that cells differentially express a given receptor, which is consistent with previously demonstrated cell-specific responses to the neuromodulator.

Stomatogastric neurons do not target detectable numbers of 5-$HT_{2\beta Pan}$ receptors to the *plasma* membrane surrounding the somatic compartment and the large diameter, lower branch order processes in the coarse neuropil, though receptors are seen in the *endo*membrane system throughout the cells. Furthermore, the collective data suggest that PD and PY neurons exclusively localize plasma membrane 5-$HT_{2\beta Pan}$ receptors to distal compartments outside the ganglion, including axon terminals at NMJs. This finding is consistent with a previous study showing that 5-HT can regulate the amplitude of nerve evoked, stomatogastric muscle contractions (Jorge-Rivera et al. 1998), and other pharmacological and electrophysiological studies demonstrating the existence of presynaptic 5-HT_2 receptors at crustacean NMJs (Dixon and Atwood 1989; Tabor and Cooper 2002; Cooper et al. 2003). We do not yet know whether all stomatogastric neurons target the 5-$HT_{2\beta Pan}$ receptor exclusively to axon terminals, or whether some neurons localize this receptor to distal neurites in the fine neuropil and/or peripheral spike initiation zones (Meyrand et al. 1992; Bucher et al. 2003b) in addition to, or instead of axon terminals. In this regard, it is interesting to note that pyloric neurons show a stereotyped distribution of K^+ channels. That is to say, all neuronal cell types target shal channels to the plasma membrane surrounding the somatodendritic compartment and shaker channels to the plasma membrane surrounding the axonal compartment (Baro et al., 2000). Thus, it is possible that all stomatogastric neurons target 5-$HT_{2\beta Pan}$ to the NMJ, and that most ganglionic, plasma membrane bound 5-$HT_{2\beta Pan}$ receptors are located in the modulatory neurons that synapse on stomatogastric neurites in the fine neuropil. Indeed, we observed profiles that are consistent with

receptor transport in modulatory neurons. We should be able to address the likelihood of this possibility once we have the pharmacological profile for this receptor in hand.

The interactions between ion channels and GPCRs are key to maintaining neurons as distinct, yet malleable components of a dynamic cellular ensemble, and recent work suggests that ion channels and GPCRs can be physically organized into functional units. One question to emerge from this work is whether GPCRs modulate only those ion channels that exist in the same multiprotein complex, or whether, by diffusional mechanisms, they act on distant channels throughout the cell. The answer has important implications for how pyloric neurons operate, as distinct tasks such as nonspiking dendrodendritic graded synaptic transmission, axonal spike and somal voltage oscillation generation may reside in discrete cellular compartments that are differentially decorated with receptors. Indeed, out data suggest that the 5-$HT_{2\beta Pan}$ receptor is not obviously expressed in the plasma membrane surrounding the soma and lower branch order processes, while it is clearly expressed in fine neurites and axon terminals.

Interestingly, bath application of DA or 5-HT to the STG alters the biophysical properties of ion channels located in pyloric somata, as determined by voltage clamp recording from the somata (Hartline et al. 1993; Harris-Warrick et al. 1995a; Harris-Warrick et al. 1995b; Kloppenburg et al. 1999; Peck et al. 2001). However, three pieces of data apart from the current study suggest modulatory receptors are located only in the distal dendritic processes of pyloric neurons and not in the somata: 1) a diffusionally restrictive glial sheath covers the entire neuron, except at sites of synaptic contact (Friend 1976; King 1976a, b; Atwood et al. 1977); 2) a cAMP imaging study shows that stimulation of modulatory inputs causes an initial accumulation of second messenger in the fine neurites that can eventually diffuse to the somata of stomatogastric neurons (Hempel et al. 1996b); and 3) puffing monoamines onto the somata instead of into the

neuropil fails to elicit modulation. Collectively, these data suggest that ion channels participating in a compartmentalized cellular task, restricted to the soma or lower branch order processes, for example, can be regulated by distant GPCRs via voltage-independent mechanisms. Future work will be aimed at elucidating the different types of GPCR multi-protein complexes that exist in pyloric neurons, and ascertaining whether any type can modulate the cell globally, with or without local effects.

In summary, there are roughly 18 monoamine receptors in arthropods, including multiple dopamine and serotonin receptors. We cloned and characterized a novel arthropodal metabotropic 5-HT receptor, 5-$HT_{2\beta Pan}$. Sequence comparisons illustrate both conservation and dissimilarity across vertebrate/invertebrate lines. The 5-$HT_{2\beta Pan}$ receptor signals via G_q to activate PLC, which activates PKC in HEK 293 cells. There is clear evidence that the receptor can be constitutively active and that this agonist independent activity in HEK cells is dependent on an evolutionary alteration to the monoaminergic signature sequence, DRY. This receptor is localized to the synaptic neuropil of the STG and axon terminals of stomatogastric neurons, and therefore, is most likely involved in modulating the motor output of stomatogastric networks. Taken together, these data represent an important step toward understanding the molecular mechanisms underlying modulation of an adaptive motor output.

CHAPTER THREE

MOLECULAR CLONING AND CHARACTERIZATION OF CRUSTACEAN TYPE ONE DOPAMINE RECEPTORS: $D_{1\alpha Pan}$ AND $D_{1\beta Pan}$

PUBLICATION: MERRY C. CLARK AND DEBORAH J. BARO (2006) *COMPARATIVE BIOCHEMISTRY AND PHYSIOLOGY PART B: BIOCHEMISTRY AND MOLECULAR BIOLOGY 143(3): 294-301*

NOTE: I PERFORMED ALL OF THE EXPERIMENTS DESCRIBED IN THIS CHAPTER, EXCEPT FOR THE INITIAL CLONING.

Introduction

The role of neuromodulation in fashioning multiple outputs from a single circuit has long been appreciated. In this regard, important insights have been realized from studies on the STNS in Decapod crustaceans (Nusbaum and Beenhakker 2002; Hooper and DiCaprio 2004). Peptidergic and monoaminergic modulation of STNS circuits have been studied extensively at the anatomical and electrophysiological levels (Harris-Warrick et al. 1992a; Beltz 1999; Nusbaum 2002). DA is known to alter both synaptic and intrinsic properties of stomatogastric neurons in a cell specific manner (Cleland and Selverston 1997; Harris-Warrick et al. 1998; Kloppenburg et al. 1999; Peck et al. 2001; Bucher et al. 2003b; Johnson et al. 2003a); however, little is known about the signal transduction cascades that generate these physiological responses.

Dopaminergic responses are mediated through multiple DA receptors (DARs) that comprise an evolutionarily conserved family of GPCRs. DARs are thought to have evolved initially from gene duplication and drift leading to 2 related paralogous genes defining two different subfamilies: D_1 and D_2 (Callier et al. 2003; Kapsimali et al. 2003; Le Crom et al. 2003). To date, all DARs can be broadly classified into these two subfamilies on the basis of conserved structure and signaling mechanisms. In general, type-1 DARs preferentially couple to Gs to increase AC activity while type-2 receptors preferentially couple with Gi/o to decrease AC activity (Neve et al. 2004). Pharmacology is also used to classify vertebrate DARs. Pharmacological profiles are not conserved across vertebrate/invertebrate lines; thus, vertebrate pharmacology cannot be used when classifying arthropod receptors as D_1 vs. D_2.

The natural history of D_1 receptors has been well studied for vertebrates, but much less is known for vertebrate D_2 receptors. In addition, the orthologous relationships for vertebrate and invertebrate DARs are unknown (Kapsimali et al. 2003). Seven DAR subtypes exist in the

phylum chordata: four D_1 subtypes (D_1/D_{1A}, D_{1B}/D_5, D_{1C}, D_{1D}) and three D_2 subtypes (D_2, D_3, D_4). A given class (e.g., mammal, teleost, reptile, etc.) may possess only a subset of the seven. For example, only five DAR subtypes are represented in mammals: D_1/D_{1A}, D_{1B}/D_5, D_2, D_3 and D_4. There are three well-characterized DARs in the phylum arthropoda (Gotzes et al. 1994; Sugamori et al. 1995; Feng et al. 1996; Han et al. 1996; Blenau et al. 1998; Hearn et al. 2002). Two of these receptors can be classified as type 1, and one of these receptors can be classified as type 2. A fourth arthropod receptor that responds to DA with a slight, but significant increase in cAMP has recently been cloned (Srivastava et al. 2005). This receptor also responds strongly to ecdysteroids, and further characterization is necessary to determine if this receptor should be classified as belonging to the DAR family.

As a first step toward defining the dopaminergic transduction cascades operating in the STNS, we have cloned and characterized the two known arthropod type 1 receptors from the spiny lobster, *Panulirus interruptus*: $D_{1\alpha Pan}$ and $D_{1\beta Pan}$. In the work presented in this chapter, we define the G protein and second messenger couplings for each receptor, and examine which monoamines activate these receptors.

Materials and Methods

Cloning and expression in a heterologous system

The three lobster DARs were cloned from nervous tissue of *Panulirus interruptus* using a degenerate PCR strategy with conventional library screening and RACE technology as previously described (Clark et al. 2004). Full length constructs were created and inserted into a pIRESneo3 vector (B.D. Biosciences Clontech, Palo Alto, CA) using standard recombinant techniques. Constructs were stably expressed in HEK cells using methods previously described

(Clark et al. 2004). The data have been submitted to Genbank under accession numbers DQ295790 ($D_{1\alpha Pan}$) and DQ295791 ($D_{1\beta.1Pan}$).

Membrane preparations

Stably transfected cells were harvested with trypsin (ATCC, Manassas, VA) or cell stripper (Media Tech, Herndon, VA). Pellets were homogenized in 20mM HEPES (pH 7.4) containing 2mM $MgCl_2$, 1 mM EDTA, 2mM 1,4-dithiothreitol (DTT), 1µg/ml leupeptin, 1µg/ml aprotinin, and 2mM PMSF. The homogenate was centrifuged at 2500 rpm for 5 minutes. The supernatant was recovered and centrifuged at 15,000 rpm for 30 minutes at 4°C. Pellets were resuspended in 20mM HEPES (pH 7.4) containing 0.5% 3-[(3 cholamidopropyl)dimethylammonio]-1-propanesulfonate (CHAPS), and 2mM EDTA. For some experiments, samples were stored at -70°C until assayed. Protein concentrations in each sample were determined using a BCA Protein Assay Kit (Pierce).

G protein activation assay

Agonist-induced activation of specific G proteins was determined using an assay based on a well-established, previously described protocol (Zhou and Murthy 2004). In these experiments, individual wells of a 96-well break-apart plate (Fisher Scientific) were UV sterilized in a tissue culture hood for 15 minutes. At this point, wells were denoted either as blanks or coated. Coated wells received an antibody against one human Gα subunit [EMD/Calbiochem catalog #371778 ($G_{12}\alpha$), #371723 ($G_{i1/2}\alpha$), #371751 ($G_q\alpha$), #371726 ($G_{i3/o}\alpha$), #371732 ($G_s\alpha$), or #371741 ($G_z\alpha$)]. Antibodies were diluted to a concentration of 20µg/ml in sterile phosphate-buffered saline, and 50µl were aliquotted to separate wells. Plates were

incubated on ice. After 2 hours, the liquid was removed from the coated wells. Both coated and blank wells were then completely filled with blocking solution (3%BSA, 0.06% sodium azide in phosphate-buffered saline) and incubated on ice for 2 hours. During this time, reactions were performed as follows. Membrane preparations from cell lines (1.5µg/ul of protein) were incubated at 37°C for 15 minutes in 10mM HEPES (pH 7.4) containing 10mM $MgCl_2$, 100µM EDTA and 10nM GTPγ^{35}S (Amersham) with or without DA. Reactions were terminated with ten volumes of termination buffer [10mM $MgCl_2$, 100µM GDP, 200mM NaCl in 100mM Tris (pH 8.0)]. Fifty µl of each terminated sample were then aliquotted in triplicate to both coated wells and blank wells (i.e., there are a total of six wells for each sample when measuring the activity of one G protein, nine wells for each sample when measuring the activity of two different G proteins, etc.). Plates were incubated on ice for 2 hours. Wells were then rinsed three times with phosphate-buffered saline containing 0.3% Tween-20. Individual wells were placed in scintillation vials containing ScintiSafe Econo 1 (Fisher) and the radioactivity in each well was quantified with a scintillation counter. Resulting cpm from the blank wells were averaged and used as a measure of non-specific binding. Nonspecific binding was subtracted from the average cpm obtained from the coated wells. Data are expressed as cpm/µg of protein.

cAMP assays

cAMP levels were measured as previously described (Clark et al. 2004). Briefly, 1×10^5 cells were plated in 35mm dishes and grown to confluence. Cells were washed with 1 ml of media and preincubated at 37°C for 10 minutes in the presence of the phosphodiesterase inhibitor 3-isobutyl-1-methylxanthine (2.5mM) (Sigma). In some cases, cells were incubated an additional 30 minutes at 37°C with or without FSK (2.5µM), and varying concentrations of DA. In some

experiments, cells were pretreated for 24 hours with pertussis toxin (PTX, Calbiochem) or 15 minutes with 1-O-Octadecyl-2-O-methyl-rac-glycero-3-phosphorylcholine (Et-18-OCH_3, Calbiochem). The media was removed and 0.5ml of 0.1M HCl (Sigma) with 0.8% Triton X-100 (Sigma) was added to the plates. After a 30 minute incubation at room temperature, the lysate was removed from the plates and centrifuged for 2 minutes. The supernatant was collected and assayed for cAMP levels using a direct cAMP enzyme immunoassay kit (Assay Designs, Inc.) according to the manufacturer's instructions. Protein concentrations in each sample were determined using a BCA Protein Assay Kit (Pierce). Data are expressed as picomoles of cAMP/milligram of protein.

Statistical analyses and curve fitting

Student t-tests were performed with Excel software. Curve fitting and Kruskall-Wallis (ANOVA on ranks) tests were performed with Prism (GraphPad Software, San Diego, CA, www.graphpad.com). In all cases, statistical significance was determined as $p < 0.05$.

Results

The family of DA receptors is conserved across different classes of arthropods

To begin to elucidate the dopaminergic systems in the STNS, we cloned the two known arthropod type-one DARs from *Panulirus interruptus*: $D_{1\alpha Pan}$ and $D_{1\beta Pan}$. The $D_{1\alpha Pan}$ receptor is orthologous to the *Drosophila* receptor DAMB/DopR99B (Feng et al. 1996; Han et al. 1996) and the $D1_{\beta Pan}$ receptor is orthologous to the *Drosophila* receptor Dm*dop*1/dDA1 (Gotzes et al. 1994; Sugamori et al. 1995; Blenau et al. 1998). Figure 3-1 illustrates that orthologs show high homology. Paired alignments of lobster and *Drosophila* $D_{1\alpha}$ and $D_{1\beta}$ orthologs revealed 44% and

37% amino acid identity over the entire protein, respectively. Most differences across species occur in the amino and carboxy termini and intracellular loop 3, which is typical for GPCRs (Clark et al. 2004; Sosa et al. 2004). Indeed, the idea of divergent termini is emphasized by the fact that the gene for the $D_{1\beta}$ receptor is alternately spliced to produce two proteins with different amino termini, $D_{1\beta.1Pan}$ and $D_{1\beta.2Pan}$ (Table 3-1; Figure 3-1). Interestingly, and contrary to the idea that the carboxy termini often diverge, both $D_{1\beta Pan}$ orthologs end in a conserved PDZ domain. However, we have not performed an exhaustive search for alternate splice forms, and it is possible that there are additional alternately spliced exons for both $D_{1\alpha Pan}$ and $D_{1\beta Pan}$ receptors.

$D_{1\alpha Pan}$ couples with Gs in HEK cells to produce an increase in $[cAMP]_i$

We next characterized receptor-G protein couplings in a heterologous expression system. When bound by ligand, activated DARs function as guanine nucleotide exchange factors (GEFs), causing inactive heterotrimeric G proteins to exchange GDP for GTP. The trimeric G protein then dissociates into Gα and Gβγ subunits, each of which interacts with downstream effectors (Cabrera-Vera et al. 2003). Since vertebrate and insect D_1 receptors preferentially couple with Gs to stimulate AC and increase cAMP levels (Feng et al. 1996; Han et al. 1996; Neve et al. 2004), we predicted that the $D_{1\alpha Pan}$ receptor should do likewise. To test this prediction, full-length $D_{1\alpha Pan}$ constructs were assembled using standard recombinant techniques. The constructs were then stably expressed in HEK cells, and the resulting cell line, HEK $D_{1\alpha Pan}$, was assayed for changes in G protein activity and cAMP levels.

We first developed and performed a "G protein activation assay" based on minor modifications to a previously described protocol (Zhou and Murthy 2004). In this assay, the wells of a break-apart 96-well plate are pre-coated with commercially available antibodies

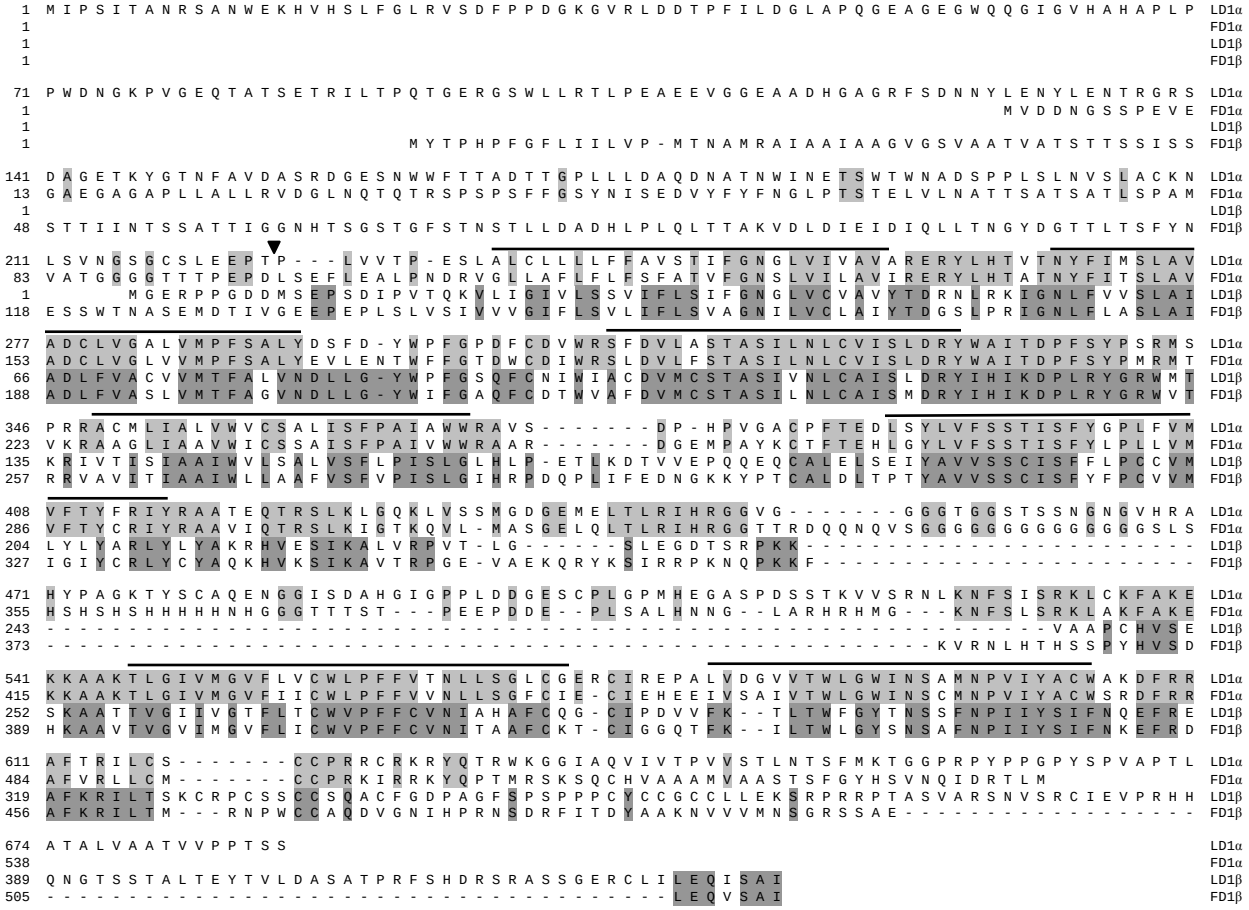

Figure 3-1: The DAR family is conserved across arthropods. The *Panulirus* (L) and *Drosophila* (F) DAR orthologs are aligned. Amino acids that are identical in fly and lobster orthologs are highlighted for each pair of DARs. Black bars approximate the seven transmembrane regions. The point of alternate splicing on lobster $D_{1\beta Pan}$ is indicated by a black arrowhead. The accession numbers are as follows: $LD_{1\alpha Pan}$, DQ295790; $FD_{1\alpha Pan}$, U34383; $LD_{1\beta.1Pan}$, DQ295791; $FD_{1\beta Pan}$, X77234.1.

Table 3-1: Alternate splicing of $D_{1\beta Pan}$
Capital letters represent alternately spliced exons, lower case letters represent amino acids present in all isoforms examined.

Location	Isoform	Exon Configuration	Amino Acid Sequence
N-terminus	$D_{1\beta.1Pan}$	$D_{1\beta}$ N-terminal exon 1	MGERPPGDDMSepsdi...
	$D_{1\beta.2Pan}$	$D_{1\beta}$ N-terminal exon 2	MKTVIESSAMTNITDDQepsdi...

against the various human G proteins. Membrane fractions of a human cell line stably expressing a lobster receptor are prepared and incubated with or without DA in a solution containing GTPγ^{35}S, a labeled, nonhydrolyzable form of GTP. Activated DARs cause coupled G proteins to exchange GDP for GTPγ^{35}S. The reactions are terminated and dispensed into the pre-coated wells. After two hours the wells are washed to remove material that is not recognized by the anti-G protein antibody, and the bound radioactivity is quantified with a scintillation counter. The cpm associated with each antibody-coated well are a measure of the activation of the corresponding G protein. Figure 3-2 illustrates that $D_{1\alpha Pan}$ couples exclusively with $G\alpha_s$. Exposure to 10^{-5}M DA for 15 minutes induced a ~ 4-fold increase in $G\alpha_s$ activity ($p < 0.03$), but did not significantly increase the activity of any of the other G proteins examined ($G\alpha_q$, $G\alpha_{i1}$, $G\alpha_{i2}$, $G\alpha_{i3}$, $G\alpha_o$, $G\alpha_z$, $G\alpha_{12}$).

DA induced activation of Gs should produce an increase in cAMP via the positive coupling of Gαs to AC. We therefore measured cAMP levels in HEK$D_{1\alpha Pan}$ and parental HEK cells in response to DA. Figure 3-3 illustrates that DA caused a dose dependent increase in HEK $D_{1\alpha Pan}$ cAMP levels, with an EC_{50} of 1.1 x 10^{-8}M. However, DA had no effect on cAMP levels in the parental HEK cell line. Constitutive activity, or agonist independent activity, is a well documented characteristic of many GPCRs (Seifert and Wenzel-Seifert 2002). It can be identified as a significant increase in second messenger levels under baseline conditions (no ligand in media) in transfected cell lines expressing a GPCR relative to the parental cell lines that do not express the receptor. In the absence of DA, levels of cAMP are not significantly different between the HEK $D_{1\alpha Pan}$ and HEK cell lines (Figure 3-3), suggesting $D_{1\alpha Pan}$ is not constitutively

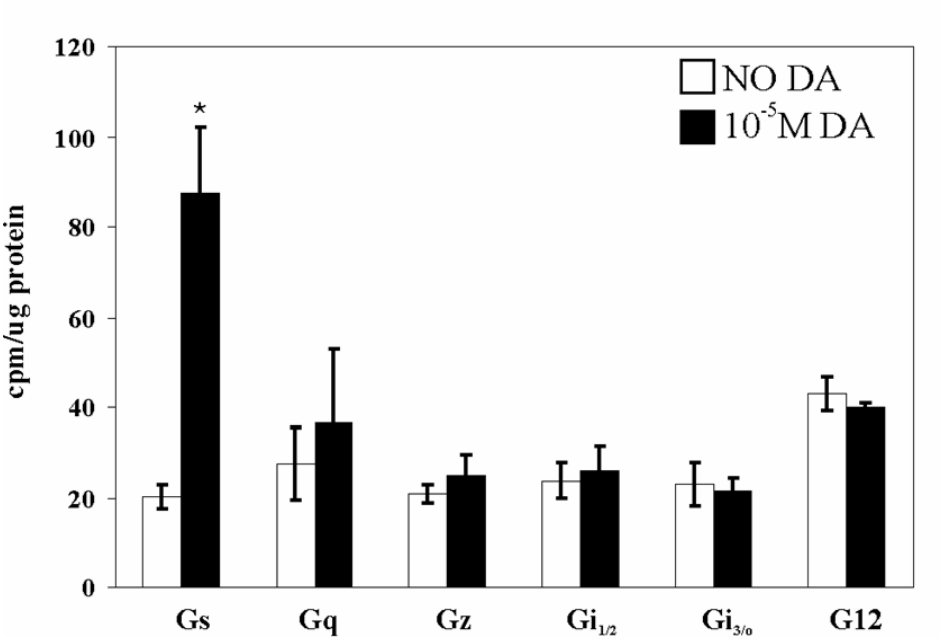

Figure 3-2: The $D_{1\alpha Pan}$ receptor couples with Gs. G protein activities in HEK $D_{1\alpha Pan}$ membrane preparations were measured in the absence (open bar) vs. the presence (filled bar) of 10^{-5}M DA for eight G proteins: Gs, Gq, Gz, Gi_1, Gi_2, Gi_3, Go, G12. Data represent the mean $\pm$ S.E.M., n = 3. Statistically significant differences in the activity of a given G protein are indicated with an asterisk ($p < 0.05$).

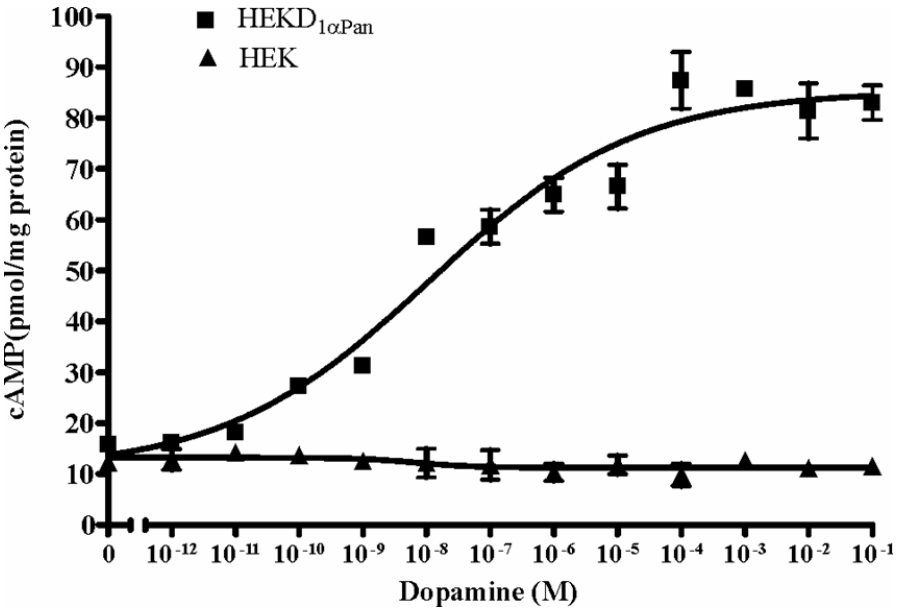

Figure 3-3: DA activation of the $D_{1\alpha Pan}$ receptor increases [cAMP]. Changes in cAMP levels in response to increasing [DA] were measured in a stably transfected cell line expressing the $D_{1\alpha Pan}$ receptor ($HEKD_{1\alpha Pan}$, squares) and in the nontransfected parental cell line (HEK, triangles). Data are represented as the mean $\pm$ S.E.M, n = 3.

active when expressed in HEK cells. Similarly, the mammalian $D_{1/1A}$ receptor does not appear to be constitutively active in heterologous expression systems (Missale et al. 1998).

$D_{1\beta Pan}$ couples with Gs and Gz in HEK cells, resulting in increased [cAMP]i

Insect orthologs of the arthropod $D_{1\beta}$ receptor have previously been shown to positively couple with AC, suggesting that this receptor couples to Gs (Gotzes et al. 1994; Sugamori et al. 1995; Blenau et al. 1998). We performed the G protein activation assay on the HEK$D_{1\beta Pan}$ cell lines to determined $D_{1\beta Pan}$ receptor-G protein coupling. Figure 3-4 indicates that the $D_{1\beta Pan}$ receptor couples with multiple G proteins. A 15 minute exposure to 10μM DA produced a ~5-fold increase in $G\alpha_s$ activity ($p < 0.002$). DA also produced a significant 1.6-fold increase in the activity of $G\alpha_z$ ($p < 0.004$), a PTX insensitive member of the Gi/o family that negatively couples with AC to reduce cAMP levels (Ho and Wong 2001). The stimulation of Gs was roughly 3 times larger than that of Gz. The human D_{1B}/D_5 receptor has also been shown to couple with Gs and Gz in GH_4C_1 cells (Sidhu et al. 1998).

Figure 3-3 indicates that the $D_{1\beta Pan}$ receptor couples with G proteins that regulate AC in opposing directions (i.e., Gs increases AC activity while Gz decreases AC activity). Since DA induced Gs activity was three times larger than DA induced Gz activity, we predicted that DA should elicit a net increase in cAMP in HEK$D_{1\beta Pan}$ cell lines. Figure 3-5 illustrates that stable cell lines expressing different isoforms of the full-length lobster $D_{1\beta}$ receptor (HEK $D_{1\beta.1Pan}$ and HEK $D_{1\beta.2Pan}$) show a dose dependent increase in cAMP in response to increasing concentrations of DA, with EC_{50}s between 1-1.4 x 10^{-6}. In addition, the $D_{1\beta Pan}$ isoforms appear to be constitutively

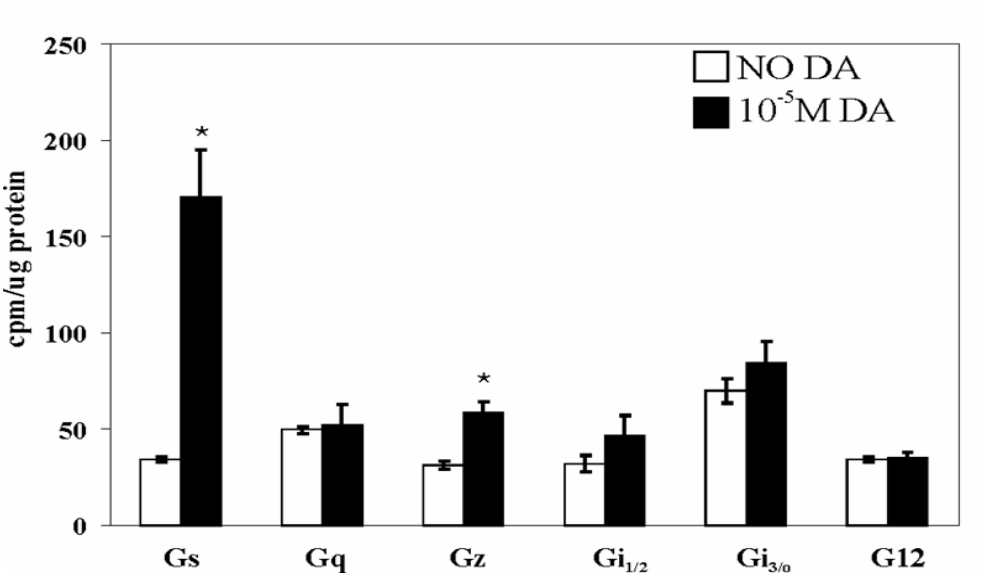

Figure 3-4: The $D_{1\beta Pan}$ receptor couples with Gs and Gz. G protein activities in HEK $D_{1\beta Pan}$ membrane preparations were measured in the absence (open bar) vs. the presence (filled bar) of 10^{-5}M DA for eight G proteins: Gs, Gq, Gz, Gi_1, Gi_2, Gi_3, Go, G12. Data represent the mean $\pm$ S.E.M., $n \geq 3$. Statistically significant differences in the activity of a given G protein are indicated with an asterisk ($p < 0.05$).

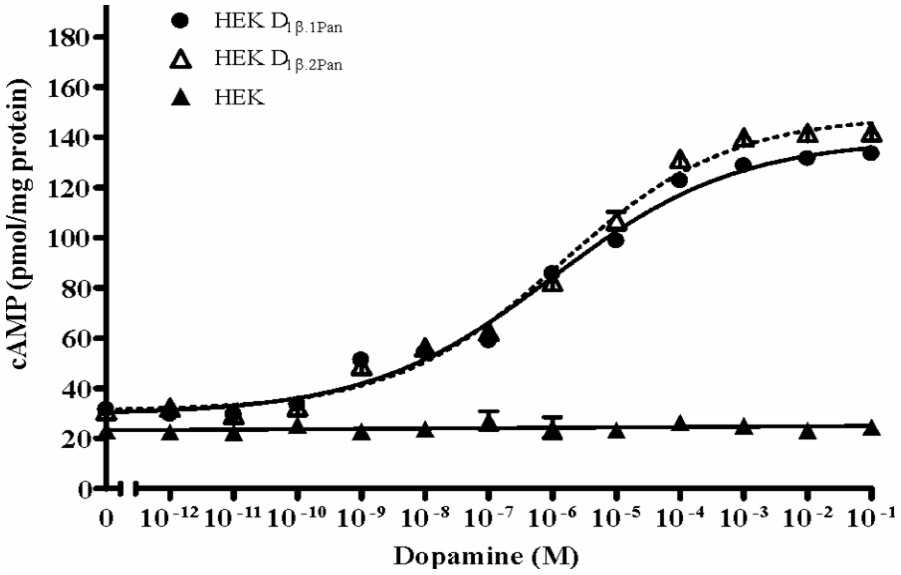

Figure 3-5: DA activation of the $D_{1\beta Pan}$ receptor produces a net increase in cAMP. The $D_{1\beta Pan}$ receptor couples positively with cAMP. Changes in cAMP levels in response to increasing [DA] were measured in the nontransfected parental cell line (HEK, filled triangles) and in two stably transfected cell lines expressing the $D_{1\beta Pan}$ receptor. We identified two isoforms for the $D_{1\beta Pan}$ receptor, and established cell lines for each: HEK $D_{1\beta.1Pan}$ (circles) and HEK $D_{1\beta.2Pan}$ (open triangle). Data represent the mean $\pm$ S.E.M., n = 5.

active. As shown in Figure 3-5, in the absence of DA cAMP levels were significantly higher in HEK $D_{1\beta Pan}$ cells relative to parental cells ($p < 10^{-5}$ for both isoforms). Thus, both isoforms of the $D_{1\beta Pan}$ receptor display agonist independent activity like the mammalian D_{1B}/D_5 receptor (Demchyshyn et al. 2000). The data do not indicate whether coupling with Gz was also constitutive.

Dopamine activates lobster type 1 DA-Rs

Monoamines act as circulating neurohormones and neurotransmitters in the STNS. Five endogenous biogenic amines can modulate STNS neurons: DA, 5-HT, tyramine (TYR), OCT and histamine (HIS). It has been reported that in some cases, arthropod DARs can respond to multiple monoamines in heterologous expression systems (Hearn et al. 2002). Activation of lobster DARs by multiple monoamines could have important implications for monoaminergic signal transduction in the STNS. We therefore asked which of the endogenous monoamines could activate $D_{1\alpha Pan}$ and $D_{1\beta Pan}$ receptors.

Levels of cAMP were measured in three cell lines (HEK, $HEKD_{1\alpha Pan}$ and $HEKD_{1\beta.2Pan}$) before and after exposure to one of the five monoamines. Figure 3-6 illustrates that DA activation of $D_{1\alpha Pan}$ and $D_{1\beta Pan}$ produced significant, approximately 5.3- and 3.6-fold increases in cAMP levels in the HEK $D_{1\alpha Pan}$ and $HEKD_{1\beta Pan}$ cell lines, respectively, but had no significant effect on the parental HEK cell line. Thus, the heterologously expressed receptors are responsible for the DA-induced increase in cAMP in $HEKD_{1\alpha Pan}$ and $HEKD_{1\beta Pan}$ cell lines.

At a concentration of 1mM, OCT and TYR had no significant effect on any of the three cell lines examined. On the other hand, Figure 3-6 demonstrates that 1mM 5-HT produced a significant, roughly 3-fold increase in cAMP in HEK cells, suggesting that the parental cell line

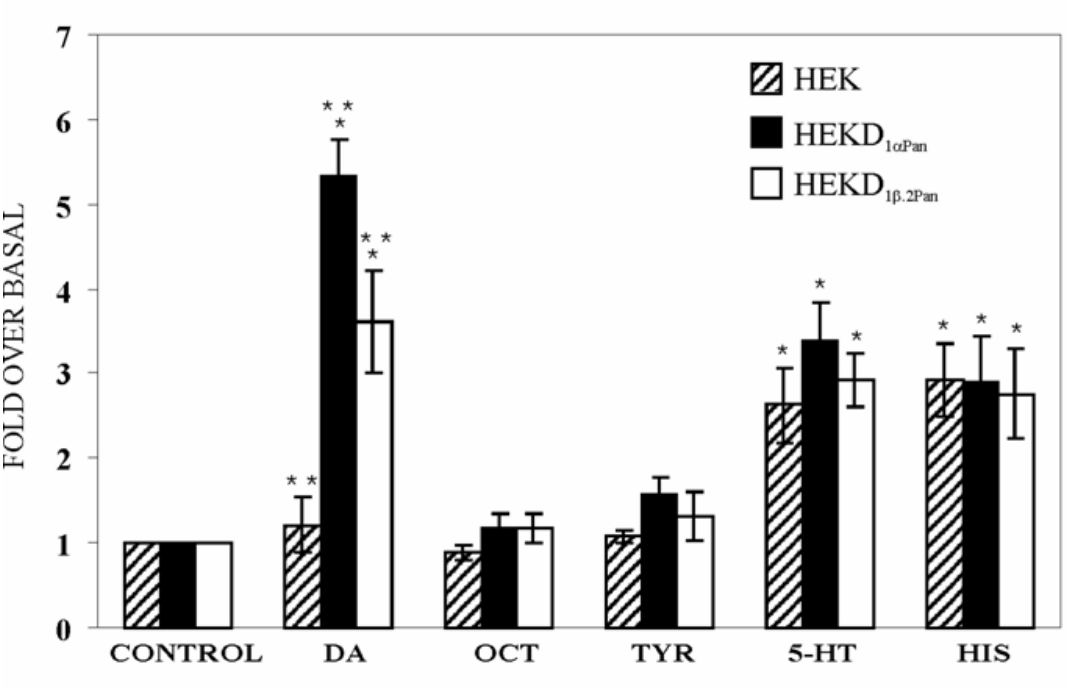

Figure 3-6: DA is the only endogenous monoamine that activates the $D_{1\alpha Pan}$ and $D_{1\beta Pan}$ receptors. Levels of cAMP were measured in HEK (hatched bars), $HEKD_{1\alpha Pan}$ (filled bars) and $HEKD_{1\beta Pan.2}$ (open bars) cell lines under control conditions (no monoamines present) or in the presence of 1mM of the indicated monoamine. The cAMP levels measured in the presence of the indicated monoamine were normalized by cAMP levels under control conditions. Average fold changes over basal cAMP levels are plotted, error bars indicate the S.E.M, $n \geq 3$. * indicates significant increases in cAMP over basal levels ($p < 0.05$). ** indicates significant differences ($p < 0.05$) between cell lines within the same condition (e.g., differences between cell lines exposed to DA).

contains endogenous 5-HT receptors that are positively coupled to AC, as has been previously reported (Johnson et al. 2003b). The same increase was observed in the $HEKD_{1\alpha Pan}$ and $HEKD_{1\beta Pan}$ cell lines. The 5-HT induced cAMP increases in all three cell lines were not significantly different from one another, suggesting that the responses are due to the endogenous 5-HT receptors and not the heterologously expressed DARs.

Similarly, the parental HEK cell line appears to express endogenous HIS receptors, as 1mM HIS produced a significant, approximately 3-fold increase in cAMP in HEK cells. This increase was also observed in the $HEKD_{1\alpha Pan}$ and $HEKD_{1\beta Pan}$ cell lines. The responses in the three cell lines were not significantly different from one another, suggesting that they were due to the endogenous histamine receptors and not the heterologously expressed DARs. In summary, DA activates $D_{1\alpha Pan}$ and $D_{1\beta Pan}$ receptors, but 5-HT, HIS, OCT and TYR do not.

Discussion

The work presented here represents the first step toward defining the molecular underpinnings of dopaminergic neuromodulation in the STNS. We have shown that the structure and function of the spiny lobster DARs, $D_{1\alpha Pan}$ and $D_{1\beta Pan,}$ are conserved across class and phyla. $D_{1\alpha Pan}$ couples with Gs to increase cAMP while $D_{1\beta Pan}$ couples with Gs and Gz to produce a net increase in cAMP. Moreover, of the 5 biogenic amines tested, only DA activated these receptors.

In all systems, dopaminergic effects are mediated through GPCRs that interact with G proteins. Both G proteins and GPCRs are well conserved across vertebrate/invertebrate lines, especially with regard to interaction domains. Indeed, Table 3-2 shows that the C-terminal domain of the G protein, which physically interacts with the GPCR, is identical for homologous G proteins in lobsters and humans! There are 6 $G\alpha$ proteins in arthropods: $G\alpha_s$, $G\alpha_f$ (Gs-like at

Table 3-2: Comparisin of G protein C-termini across species

H = human, L = lobster, F = fly

$G\alpha_s$	H: RMHLRQYELL
	L: RMHLRQYELL
$G\alpha_q$	H: QLNLKEYNLV
	L: QLNLKEYNLV
$G\alpha_{i1/2}$	H: KNNLKDCGLF
	L: KNNLKDCGLF
$G\alpha_o$	H: AKNLRGCGLY
	F: ANNLRGCGLY
$G\alpha_{12}$	H: QENLKDIMLQ
	F: QRNLNALMLQ
Gαf	
	F: SENVSSMGLF

the DNA level), $G\alpha_q$, $G\alpha_i$, $G\alpha_o$, $G\alpha_{12}$ (http://flybase.net/). Three of the G proteins have been cloned from lobster (McClintock et al. 1992; McClintock et al. 1997; Xu et al. 1997). As shown in Table 3-2, the C-termini of lobster $G\alpha_s$, $G\alpha_q$ and $G\alpha_i$ are completely conserved with their human homologs. Thus, it is reasonable to probe the coupling specificity of lobster GPCRs in human cell lines.

Traditionally, DARs were thought to couple only with Gs to increase $[cAMP]_i$ and Gi/o to decrease $[cAMP]_i$; however, recent studies in heterologous expression systems, including the one presented here, suggest that DAR-G protein coupling can be much more diverse (Sidhu and Niznik 2000). For example, D_1/D_{1A} can couple with Gs and Go in reconstitution experiments or in overexpression experiments with rat pituitary GH_4C_1 cells (Kimura et al. 1995b; Kimura et al. 1995a). D_{1B}/D_5 can couple with Gs and Gz in GH_4C_1 cells (Sidhu et al. 1998), or with Gs and G12 in immortalized rat renal proximal tubule cells (Zheng et al. 2003). D_2 receptors couple with multiple members of the Gi/o family (Ghahremani et al. 1999; Obadiah et al. 1999; Banihashemi and Albert 2002). When expressed in CHO cells, human D_3 receptors may couple with the Gi/o and Gq families (Newman-Tancredi et al. 1999). Studies in native systems also suggest non-classical coupling such that D_1 receptors may couple with Gs and Gq in the mammalian and *C. elegans* CNS (Undie et al. 2000; Wersinger et al. 2003; Chase et al. 2004; O'Sullivan et al. 2004; Zhen et al. 2004).

It is interesting that the lobster $D_{1\beta Pan}$ receptor, like the human D_{1B}/D_5 receptor can couple with both Gs and Gz. We do not know the proteins that interact with the lobster DARs to facilitate multiple couplings. Both post-translational modifications and receptor-interacting proteins can cause a receptor to switch G protein coupling. As mentioned in chapter 1, when phosphorylated by protein kinase A, the β_2-adrenergic receptor switches its coupling from Gs to

Gi (Daaka et al. 1997; Baillie et al. 2003). Receptor coupling can also be extended by receptor-interacting proteins, like calcyon, which regulates receptor cross-talk and allows D_1 receptors to switch coupling between Gs and Gq (Lezcano et al. 2000). It is not obvious why this receptor would couple to multiple cascades that have opposing effects on cAMP. It is possible that the population of cells is heterogeneous so that there is only one type of coupling per cell. On the other hand, when simultaneously activated, opposing cascades in a single cell may be highly localized so that microdomains of cAMP gradients are created (Zaccolo and Pozzan 2002). Alternatively the cascades may function with different kinetics and interact to generate feedback loops and/or multiphasic responses.

CHAPTER FOUR

ARTHROPOD D_2 RECEPTORS POSITIVELY COUPLE WITH CAMP THROUGH THE Gi/o PROTEIN FAMILY

PUBLICATION: MERRY C. CLARK AND DEBORAH J. BARO (2007) *COMPARATIVE BIOCHEMISTRY AND PHYSIOLOGY PART B: BIOCHEMISTRY AND MOLECULAR BIOLOGY 146(1):9-19.*

NOTE: I PERFORMED ALL OF THE EXPERIMENTS DESCRIBED IN THIS CHAPTER, EXCEPT FOR THE INITIAL CLONING.

Introduction

As previously mentioned, DARs are traditionally classified as type-1 or type 2: type-1 DARs couple to Gs proteins, leading to a Gα-mediated increase in [cAMP]i and PKA activity, while type-2 DARs couple to Gi/o proteins to decrease [cAMP]i and PKA activity (Missale et al., 1998;Neve et al., 2004). It is now clear that this traditional view of DAR signaling is much too simple. First, DARs have been shown to couple with multiple G proteins in various heterologous and native systems (Kimura et al., 1995a;Sidhu et al., 1998;Zheng et al., 2003;O'Sullivan et al., 2004;Zhen et al., 2004;Kimura et al., 1995b). Moreover, GPCRs, including DARs, can switch G protein coupling over time in response to constant agonist application (Daaka et al., 1997;Baillie et al., 2003;Lezcano et al., 2000). Second, both the Gα and Gβγ subunits are known to mediate individual responses (Cabrera-Vera et al., 2003). Third, activated G protein subunits can directly interact with target proteins such as ion channels without altering second messenger levels (Dascal, 2001;Ivanina et al., 2004). Fourth, GPCRs are known to interact directly with target proteins. For example, DARs can physically interact with, and activate ionotropic glutamate receptors (Zou et al., 2005;Lee and Liu, 2004;Pei et al., 2004;Liu et al., 2000). Fifth, GPCRs can activate additional cascades, like the mitogen activated protein kinase (MAPK) cascade via crosstalk (Werry et al., 2005). Finally, GPCRs can directly activate G protein-independent cascades via recruitment of β-arrestin scaffolds (Lefkowitz and Shenoy, 2005). In this regard, it was recently shown that the D_2 receptor modulates locomotor activity in mice via a β–arrestin 2-mediated signaling complex involving Akt and PP2A, as well as by traditional G protein cascades (Beaulieu et al., 2005).

We have previously cloned and characterized the two type-1 DARs from the spiny lobster (Clark and Baro, 2006). Here we describe the cloning and characterization of the lobster D_2 receptor, $D_{2\alpha Pan}$.

Materials and Methods

Cloning and expression in a heterologous system

The lobster $D_{2\alpha Pan}$ cDNA was cloned from nervous tissue of *Panulirus interruptus* using a degenerate PCR strategy with conventional library screening and RACE technology as previously described (Clark et al., 2004). The $D_{2\alpha.1Pan}$ sequence has been submitted to Genbank under accession number DQ900655 (Figure 4-1). Full length constructs were created and inserted into a pIRESneo3 vector (B.D. Biosciences Clontech, Palo Alto, CA) using standard recombinant techniques. $D_{2\alpha Pan}$ and *Am*Dop3 constructs were stably expressed in HEK293 cells using methods previously described (Clark et al., 2004). *Am*Dop3 was kindly provided by Dr. Allison Mercer, University of Otago. All tissue culture reagents were purchased from Invitrogen except the DMEM and the penicillin streptomycin solution (American Type Culture Collection), and the neomycin (Sigma).

In some experiments, the Gβγ scavengers, dexras1 (UMR cDNA resource center, University of Missouri-Rolla) or $\beta ARK_{495-689}$ (kindly provided by Dr. Robert Lefkowitz, Howard Hughes Medical Institute), were transiently expressed. In these cases, cells were maintained in DMEM supplemented with 10% dialyzed fetal bovine serum plus 600µg/mL neomycin ($HEKD_{2\alpha Pan}$ or HEK*Am*Dop3) or 50 units/mL penicillin and 50µg/mL streptomycin (parental HEK cells) at 37°C, 5% CO_2, and were grown to 90-95% confluency in 26x33mm wells of an 8-well plate (Fisher Scientific). One day prior to transfection, the cells received media without

antibiotic. Cells were transfected with 2 μg DNA using 10μL lipofectamine in 100uL opti-MEM according to the manufacturer's instructions. After 6 hours at 37°C, 5% CO_2, cells received 1mL of DMEM containing 20% dialyzed serum. Cells received normal media (with antibiotic) 24 hours following transfection, and were assayed 24-48 hours later.

The experiments described in this manuscript were conducted over the course of 2 years, during which time the properties of the parental HEK cell line varied. During the first year the parental line was insensitive to DA, even at a concentration of 100mM. The assays shown in Figures 4-2, 4-4, 4-6 and 4-7 were conducted during this initial period. There was then a long hiatus from experimentation during which time all cell lines were frozen in liquid nitrogen. Experiments were resumed during year 2. Parental HEK and $HEKD_{2\alpha.1Pan}$ cells were thawed and the assays shown in Figures 4-3 and 4-5 were performed. In addition, the parental line was transfected to generate stable HEK*Am*Dop3, $HEKD_{2\alpha.2Pan,}$ and $HEKD_{2\alpha.3Pan}$ lines, and the assays shown in Figures 4-8 and 4-9 were performed. At some point during the second year, the parental line began to express low and variable levels of an endogenous human D_1 receptor that in some assays produced a significant increase in cAMP in response to 10^{-4}M DA or the D_1 selective agonist, 6-chloro-PB ($n= 3$, $p< 0.05$). The pharmacology of the human D_1 receptor was distinct from the $D_{2\alpha Pan}$ receptor. The $D_{2\alpha Pan}$ receptor produced an increase in cAMP in response to 10^{-5}M quinpirole ($n=3$, $p < 0.05$), a selective D_2 agonist, while the parental D_1 receptor did not ($n=3$, $p> 0.05$). Furthermore, the signaling properties of the two receptors were distinct: The arthropod D_2 receptor relies on the Gβγ subunit to produce an increase in cAMP while the human D_1 receptor does not (Figures 4-5 and 4-8).

Membrane preparations

Stably transfected cells were harvested with trypsin (ATCC, Manassas, VA). Pellets were homogenized in 20mM HEPES (pH 7.4) containing 2mM $MgCl_2$, 1 mM EDTA, 2mM 1,4-dithiothreitol (DTT), 1µg/ml leupeptin, 1µg/ml aprotinin, and 2mM PMSF. The homogenate was centrifuged at 2500 rpm for 5 minutes. The supernatant was recovered and centrifuged at 15,000 rpm for 30 minutes at 4°C. Pellets were resuspended in 20mM HEPES (pH 7.4) containing 0.5% 3-[(3 cholamidopropyl)dimethylammonio]-1-propanesulfonate (CHAPS), and 2mM EDTA. Protein concentrations in each sample were determined using a BCA Protein Assay Kit (Pierce).

G protein activation assay

Agonist-induced activation of specific G proteins was determined using our previously described G protein activation assay (Clark and Baro, 2006). Briefly, membrane preparations from cell lines (1.5µg/ul of protein) were incubated at 37°C for 15 minutes in 10mM HEPES (pH 7.4) containing 10mM $MgCl_2$, 100µM EDTA and 10nM GTPγ^{35}S (Amersham) with or without DA. Reactions were terminated with ten volumes of termination buffer [10mM $MgCl_2$, 100µM GDP, 200mM NaCl in 100mM Tris (pH 8.0)]. Fifty µl of each terminated sample were then aliquotted in triplicate to wells precoated with one antibody against a human Gα subunit [$G_{12}\alpha$, $G_{i1/2}\alpha$, $G_q\alpha$, $G_{i3/o}\alpha$, $G_s\alpha$, or $G_z\alpha$ (EMD/Calbiochem)] and to uncoated wells (blanks). Plates were incubated on ice for 2 hours. Wells were then rinsed three times with phosphate-buffered saline containing 0.3% Tween-20. Individual wells were placed in scintillation vials containing ScintiSafe Econo 1 (Fisher) and the radioactivity in each well was quantified with a scintillation counter. Resulting cpm from the blank wells were averaged and used as a measure

of non-specific binding. Nonspecific binding was subtracted from the average cpm obtained from the coated wells. Data are expressed as cpm/µg of protein.

cAMP assays

cAMP levels were measured as previously described (Clark et al., 2004). Briefly, 1×10^5 cells were plated in 35mm dishes and grown to confluence. Cells were washed with 1 ml of media and preincubated at 37°C for 10 minutes in the presence of the phosphodiesterase inhibitor 3-isobutyl-1-methylxanthine (2.5mM) (Sigma). Cells were incubated an additional 30 minutes at 37°C with or without forskolin (2.5µM), and varying concentrations of monoamine (DA, 5-HT, TYR, HIS, or OCT). In some experiments, cells were pretreated for 24 hours with pertussis toxin (PTX, Calbiochem) or 15 minutes with 1-O-Octadecyl-2-O-methyl-rac-glycero-3-phosphorylcholine (Et-18-OCH_3, Calbiochem). The media was removed and 0.5ml of 0.1M HCl with 0.8% Triton X-100 (Sigma) was added to the plates. After a 30 minute incubation at room temperature, the lysate was removed from the plates and centrifuged for 2 minutes. The supernatant was collected and assayed for cAMP levels using a direct cAMP enzyme immunoassay kit (Assay Designs, Inc.) according to the manufacturer's instructions. Protein concentrations in each sample were determined using a BCA Protein Assay Kit (Pierce).

Statistical analyses and curve fitting

Student t-tests were performed with Excel software. Curve fitting, Kruskall-Wallis (ANOVA on ranks) tests, and Bonferroni posttests were performed with Prism (GraphPad Software, San Diego, CA, www.graphpad.com). In all cases, statistical significance was determined as $p < 0.05$.

Results

DARs are conserved across species

Using total lobster nervous system cDNA and a combination of conventional library screening and RACE technologies, we cloned a type 2 DAR from the spiny lobster, *Panulirus interruptus*. We found that this receptor, $D_{2\alpha Pan}$, is alternately spliced (see arrowheads in Figure 4-1) to produce four distinct proteins: $D_{2\alpha.1Pan}$, $D_{2\alpha.2Pan}$, $D_{2\alpha.3Pan}$, and $D_{2\alpha.4Pan}$ (Table 4-1). We did not conduct an exhaustive search for $D_{2\alpha Pan}$ isoforms, and it is likely that additional splice forms exist (Hearn et al., 2002).

The $D_{2\alpha Pan}$ receptor is orthologous to the *Drosophila* receptor DD2R (Hearn et al., 2002) and the *Apis* receptor *Am*Dop3 (Beggs et al., 2005). A BLAST against the *Homo sapien* Reference Proteins database showed that the $D_{2\alpha Pan}$ receptor was most homologous to the long form of the human D_2 receptor (NP_000786) with an E value of 3e-58. Figure 4-1 illustrates that all D_2 receptors are well conserved across species. When compared to its fly, honeybee and human homologs, the $D_{2\alpha Pan}$ receptor shows 45%, 39% and 37% amino acid identity over the entire protein, respectively. As expected, the 7 TM regions are among the most conserved portions of the protein. In addition, the cytoplasmic domains known to interact with G proteins show a fairly high degree of identity, including intracellular loops 1 and 2, the amino and carboxy portions of intracellular loop 3, and the cytoplasmic C-terminal domain (Limbird, 2004;Cabrera-Vera et al., 2003). Most amino acid substitutions in these regions are conservative (Figure 4-1).

$D_{2\alpha.1Pan}$ couples with multiple members of the Gi/o family in HEK cells

As stated above, the G protein interaction domains are well conserved between arthropodal and mammalian D_2 receptors. Similarly, the G protein domains that interact with

Figure 4-1: The DAR family is conserved across arthropods. The *Panulirus* (lob), *Drosophila* (fly), *Apis* (bee), and human (hum) DAR proteins are aligned. Amino acids that are identical are highlighted. Black bars approximate the seven transmembrane regions. The points of alternate splicing on lobster DARs are indicated by black arrowheads. The accession numbers are as follows: lobster: DQ900655; fly: AAN15955; bee: NP_001014983; human: NP_000786.

Table 4-1: Alternate splicing of $D_{2\alpha Pan}$
Capital letters represent alternately spliced exons, lower case letters represent amino acids present in all isoforms examined. The * represents a stop codon.

Location	Isoform	Exon Configuration	Amino Acid Sequence
Intra-cellular loop 3	$D_{2\alpha Pan.1}$	+ i3 alternately spliced exon	...qdeeEEEGEDVMGLGGeenc...
	$D_{2\alpha Pan.2}$	+ i3 alternately spliced exon	...qdeeEEEGEDVMGLGGeenc...
	$D_{2\alpha Pan.3}$	- i3 alternately spliced exon	...qdeeeenc...
	$D_{2\alpha Pan.4}$	- i3 alternately spliced exon	...qdeeeenc...
C-terminus	$D_{2\alpha Pan.1}$	$D_{2\alpha}$ C-terminal exon 1	...ilisqS*
	$D_{2\alpha Pan.4}$	$D_{2\alpha}$ C-terminal exon 1	...ilisqS*
	$D_{2\alpha Pan.2}$	$D_{2\alpha}$ C-terminal exon 2	...ilisqMTISSNSFSLETVVLENHASC*
	$D_{2\alpha Pan.3}$	$D_{2\alpha}$ C-terminal exon 2	...ilisqMTISSNSFSLETVVLENHASC*

receptors are conserved across species (reviewed in Cabrera-Vera et al., 2003). The last five residues of the Gα C-terminus is an important mediator of receptor-G protein interactions. This domain shows 100% amino acid identity between human and arthropod Gs, Gi, Go and Gq homologs (reviewed in Clark and Baro, 2006). While receptor-G protein interactions are not mediated solely by this structural feature, the extreme conservation suggests that the mechanisms for receptor-G protein interactions will be similar in mammals and arthropods. This predicts that arthropodal GPCRs will activate the same G protein(s) as homologous mammalian receptors when expressed in mammalian cell lines. Mammalian type-2 DARs (Ghahremani et al. 1999; Obadiah et al. 1999; Banihashemi and Albert 2002) stimulate both PTX sensitive ($G\alpha_o$, $G\alpha_{i1}$, $G\alpha_{i2}$, $G\alpha_{i3}$) and insensitive ($G\alpha_z$) members of the $G\alpha_{i/o}$ family (Obadiah et al., 1999;Banihashemi and Albert, 2002;Ghahremani et al., 1999). We stably expressed the $D_{2\alpha.1Pan}$ construct in a HEK cell line ($HEKD_{2\alpha.1Pan}$) and performed our previously described G protein activation assay (Clark and Baro, 2006) to determine receptor-G protein coupling. Figure 4-2 illustrates that $D_{2\alpha.1Pan}$ couples with both PTX-sensitive and PTX-insensitive members of the $G\alpha_{i/o}$ family, but not with $G\alpha_s$, $G\alpha_q$, or $G\alpha_{12}$. The receptor appeared to couple most strongly with $G\alpha_{i3/o}$, producing a significant 2.4-fold increase in activity in response to a 15-minute application of 10μM DA ($p < 0.007$). There was also significant coupling with $G\alpha_z$ (1.8-fold increase in activity, $p < 0.02$) and $G\alpha_{i1/2}$ (1.4-fold increase in activity, $p < 0.02$).

DA activates $D_{2\alpha.1Pan}$ to produce an increase in cAMP

$D_{2\alpha Pan}$ orthologs have been shown to respond to multiple monoamines. In addition to DA, TYR stimulates the DD2R and *Am*Dop3 receptors, and DD2R responds to serotonin (5-HT) (Hearn et al., 2002;Beggs et al., 2005). $G\alpha_{i/o}$ proteins are known to decrease AC activity and

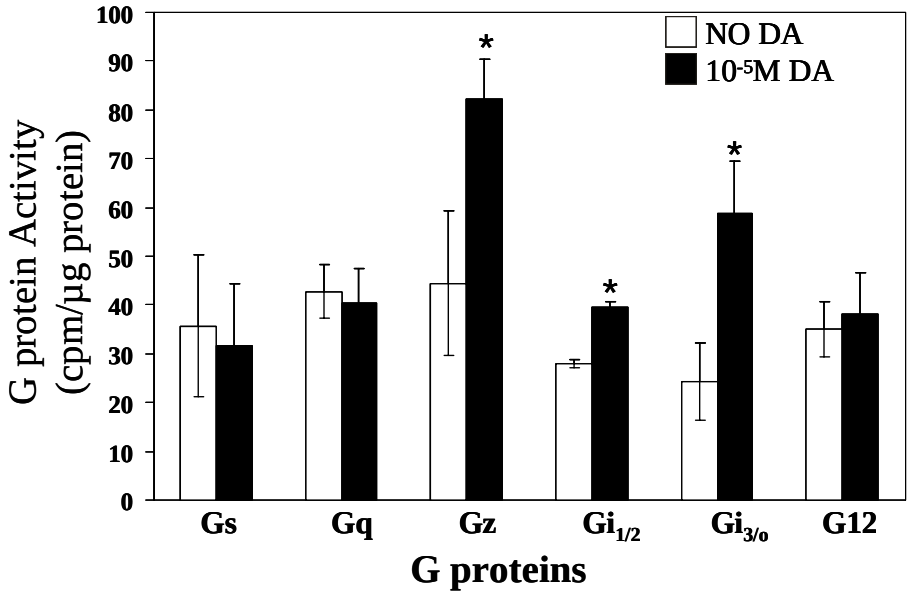

Figure 4-2: The $D_{2\alpha.1Pan}$ receptor couples with Gi/o family members. G protein activities in $HEKD_{2\alpha.1Pan}$ membrane preparations were measured in the absence (open bar) vs. the presence (filled bar) of 10^{-5}M DA for eight G proteins: Gs, Gq, Gz, Gi_1, Gi_2, Gi_3, Go, G12. Data represent the mean $\pm$ S.E.M., n = 3. Student t-tests were performed. Statistically significant differences in the activity of a given G protein in the presence vs. absence of DA are indicated (*; $p < 0.05$).

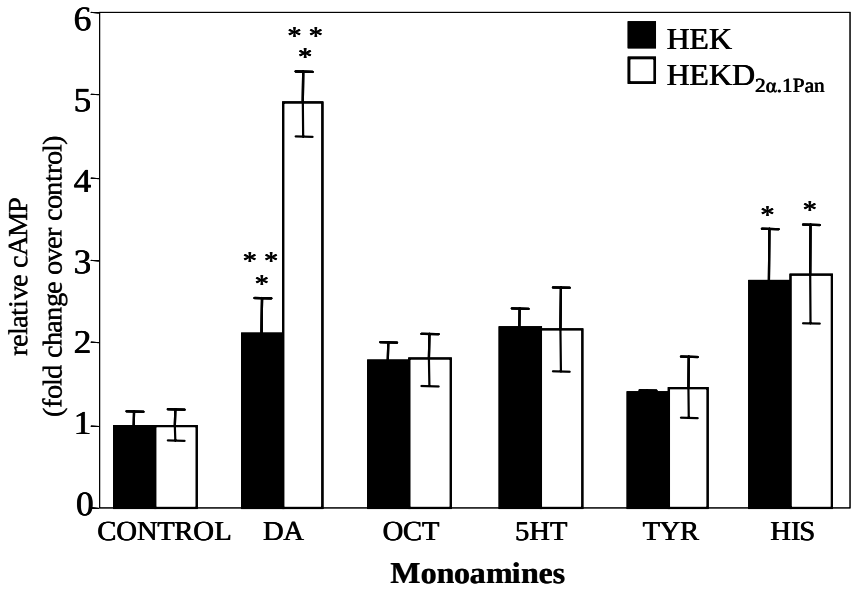

Figure 4-3: DA is the only monoamine that activates $D_{2\alpha.1Pan}$. Levels of cAMP (pmol cAMP/mg protein) were simultaneously measured in HEK and $HEKD_{2\alpha.1Pan}$ cell lines under control conditions (no monoamine present) or in the presence of 1mM of the indicated monoamine. cAMP levels measured in the presence of the indicated monoamine were normalized to control [cAMP] for each cell line, and the $HEKD_{2\alpha.1Pan}$ response was normalized by the HEK response. Average fold changes in the transfected cell line relative to the parental cell line are shown. Error bars indicate the S.E.M, $n \geq 3$. The data were subjected to a one-way ANOVA.* indicates significant differences from cAMP levels measured in the control ($p < 0.05$). ** indicates significant differences in HEK vs. $HEKD_{2\alpha.1Pan}$ for the same condition.

reduce [cAMP]i. We therefore further characterized the $D_{2\alpha.1Pan}$ receptor by measuring [cAMP]i in cells after a 30 minute exposure to one of five monoamines that are endogenous to lobster nervous tissue. Figure 4-3 illustrates that at a concentration of 1mM, 5-HT, OCT, TYR and HIS had no significant effect on [cAMP]i in $HEKD_{2\alpha.1Pan}$ relative to parental cells. On the other hand, DA produced a significant 2.3-fold increase in [cAMP]i in $HEKD_{2\alpha.1Pan}$ relative to parental cells ($p < 3 \times 10^{-4}$). Collectively, these data suggest that DA is the only endogenous monoamine that activates the $D_{2\alpha.1Pan}$ receptor when expressed in HEK cells.

The DA-induced increase in [cAMP]i is mediated by Gi/o proteins

Interestingly, DA produced an increase in cAMP levels (Figure 4-3), despite the fact that the $D_{2\alpha.1Pan}$ receptor couples with the Gi/o family (Figure 4-2). This is contrary to previous studies on the fly and bee orthologs of $D_{2\alpha Pan}$, which show that when these receptors are expressed in HEK cell lines, exposure to DA produces a decrease in cAMP (Beggs et al., 2005;Hearn et al., 2002). It is not clear whether the difference lies in the cell lines or the arthropod D_2 receptors. In order to elucidate the mechanism responsible for this difference, we further characterized the lobster D_2 signaling cascade(s) in HEK cells.

DARs can signal through mechanisms independent of the traditional, G protein mediated pathways (Beaulieu et al., 2005;Zou et al., 2005;Lee and Liu, 2004;Pei et al., 2004;Liu et al., 2000;Lefkowitz and Shenoy, 2005). To determine if the DA-induced increase in cAMP is due to Gi/o proteins (Figure 4-2) and/or G protein independent cascades, we examined the effect of DA in the presence of PTX, which specifically blocks the activation and dissociation of all members of the Gi/o family, except Gz. We hypothesized that if PTX can partially block the DA-induced increase in cAMP, it would suggest that Gi/o proteins help to mediate the response.

Figure 4-4 (solid line) shows that HEK$D_{2\alpha.1Pan}$ cells produced a dose-dependent increase in cAMP levels in response to DA, with an EC_{50} of 9.2 x 10^{-7}M, while the parental HEK cell line did not respond to DA. The dashed line illustrates that application of PTX significantly attenuated the DA response, and reduced the maximal fold change in cAMP from 4.4 to 3 ($p < 0.0008$). On the other hand, PTX had no effect on cAMP levels in the parental HEK cell line. These data, along with Figure 4-2, suggest that the DA-evoked increase in cAMP depends, in part, on PTX sensitive trimeric Gi/o proteins. The DA response was not completely eliminated despite the fact that a saturating concentration of PTX was applied (500 ng/ml; see Figure 4-4 inset for PTX dose response curve). This is at least partially due to coupling between the $D_{2\alpha.1Pan}$ receptor and the PTX insensitive Gz protein (Figure 4-2); however, we cannot rule out the possibility that the $D_{2\alpha Pan}$ receptor activates additional G protein independent cascades to increase [cAMP]i.

The Gβγ subunits of Gi/o proteins contribute to DA-induced alterations in [cAMP]i

AC can be regulated by both Gα and Gβγ subunits (Federman et al., 1992). While $G\alpha_{i/o}$ subunits decrease or have no effect on AC activity, Gβγ can increase or decrease AC activity depending on the AC and Gβγ isozymes involved (Cabrera-Vera et al., 2003). We tested the hypothesis that Gβγ subunits mediate the DA-induced increase in [cAMP]i in the HEK$D_{2\alpha.1Pan}$ cell line by blocking the Gβγ pathway with known Gβγ scavengers. Dexras1 has been shown to specifically block agonist-stimulated GPCR activation of Gβγ signaling (Nguyen and Watts, 2005). Similarly, the carboxyl-terminal domain of βARK1 and βARK2 ($\beta ARK_{495-689}$) suppresses Gβγ-mediated responses by scavenging free βγ subunits (Koch et al., 1994). We transiently expressed $\beta ARK_{495-689}$ or dexras1 in HEK and HEK$D_{2\alpha.1Pan}$ cell lines and measured

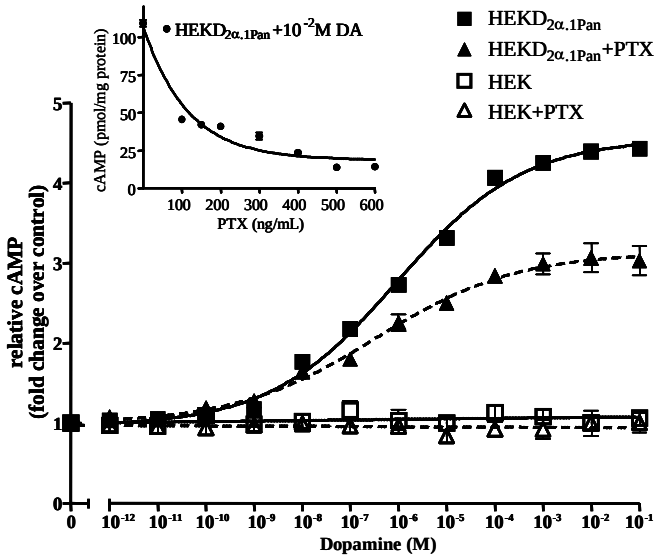

Figure 4-4: The $D_{2\alpha.1Pan}$ receptor couples positively with cAMP through PTX-sensitive Gi/o proteins, as well as PTX insensitive cascades. [cAMP] (pmol/mg protein) was simultaneously measured in $HEKD_{2\alpha.1Pan}$ (solid symbols) and HEK (open symbols) cells in the presence of increasing DA. All data points are normalized to [cAMP] measured in the absence of DA (control) in the same experiment, and the fold change over control is plotted on the y axis. Experiments were conducted in the presence (dashed line) vs. the absence (solid line) of the Gi/o inhibitor, PTX (500ng/ml). Inset represents a PTX dose-response curve for the HEK $D_{2\alpha.1Pan}$ cell line. Data represent the mean $\pm$ S.E.M, n=3.

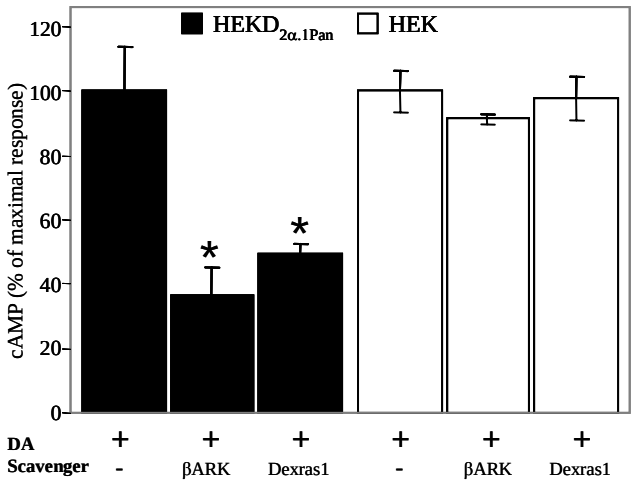

Figure 5-5: The increase in cAMP in $HEKD_{2\alpha.1Pan}$ is mediated by Gi/o βγ subunits. The Gβγ scavengers dexras1 or $\beta ARK_{495-689}$ were transiently expressed in $HEKD_{2\alpha.1Pan}$ (black bars) and HEK (white bars) cells, as indicated below each bar. Cells were exposed to 10^{-4}M DA, and [cAMP] (pmol cAMP/mg protein) was measured. Data are normalized to the average [cAMP] in the presence of DA for each cell line. Data represent the mean $\pm$ S.E.M., n = 3. Student t-tests were performed, and asterisks indicate significant differences from cAMP levels measured in the absence of dexras1or $\beta ARK_{495-689}$ within a cell line ($p < 0.04$).

[cAMP]i in the presence of 10^{-4}M DA. Figure 4-5 shows that expression of either $\beta ARK_{495-689}$ or dexras1 significantly inhibited the DA-induced increase in cAMP in $HEKD_{2\alpha.1Pan}$ cells by 64 $\pm$ 9% ($p < 0.04$) and 51 $\pm$ 3% ($p < 0.008$) respectively, but had no significant effect on the parental cell line ($p > 0.7$). These data suggest that Gβγ subunits contribute to the DA-induced changes in [cAMP] in $HEKD_{2\alpha Pan}$ cells.

Blocking the Gβγ cascade reveals a DA-induced, $G\alpha_{i/o}$ mediated decrease in cAMP

Gβγ can have many immediate effectors, including PLCβ, ACs, ion channels, kinases and components of the synaptic vesicle release machinery (Blackmer et al., 2005;Cabrera-Vera et al., 2003;Stehno-Bittel et al., 1995;Sullivan, 2005;Gerachshenko et al., 2005). It has been previously demonstrated that D_2 receptors can regulate ACII activity via Gβγ–mediated activation of PLCβ (Tsu and Wong, 1996). To determine whether Gβγ subunits act via PLCβ in $HEKD_{2\alpha Pan}$ cells, we applied the PLCβ inhibitor, ET-18-OCH_3, and measured cAMP levels in the presence of increasing concentrations of DA. Figure 4-6 (dashed line) demonstrates that inhibiting PLCβ also inhibited the DA induced increase in cAMP, and revealed a dose-dependent decrease in cAMP.

The dose-dependent decrease in cAMP was largely PTX sensitive. Figure 4-7 illustrates that in the presence of forskolin (an AC activator) and ET-18-OCH_3, DA evokes a clear dose dependent decrease in cAMP in $HEKD_{2\alpha.1Pan}$ cells with an EC_{50} of 1.4 x 10^{-7}M. The total inhibition by saturating levels of PTX was 77% of the maximal response. The response that remained in the presence of PTX was most likely mediated by Gz (Figure 4-2). Collectively, these data suggest that DA initiates parallel signaling cascades in $HEKD_{2\alpha.1Pan}$ cells with

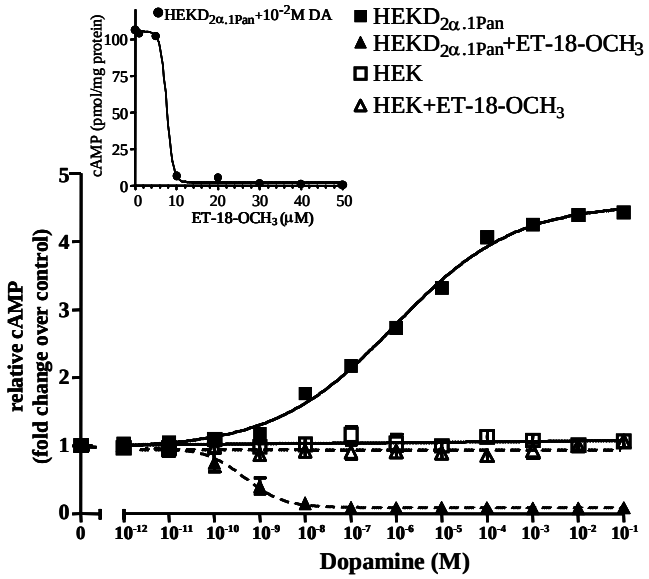

Figure 4-6: Blocking PLCβ reveals a negative coupling between the $D_{2\alpha.1Pan}$ receptor and cAMP. [cAMP] was simultaneously measured in pmol cAMP/mg protein for both $HEKD_{2\alpha.1Pan}$ (solid symbols) and HEK (open symbols) cells in the presence of increasing DA. All data points are normalized to [cAMP] measured in the absence of DA (control) in the same experiment, and the fold change over control is plotted on the y-axis. Experiments were conducted in the presence (dashed line) vs. the absence (solid line) of the PLCβ inhibitor, ET-18-OCH_3 (50μM). The inset represents an ET-18-OCH_3 dose-response curve for the HEK $D_{2\alpha.1Pan}$ cell line. All experiments were repeated 3 times. Data represent the mean $\pm$ S.E.M.

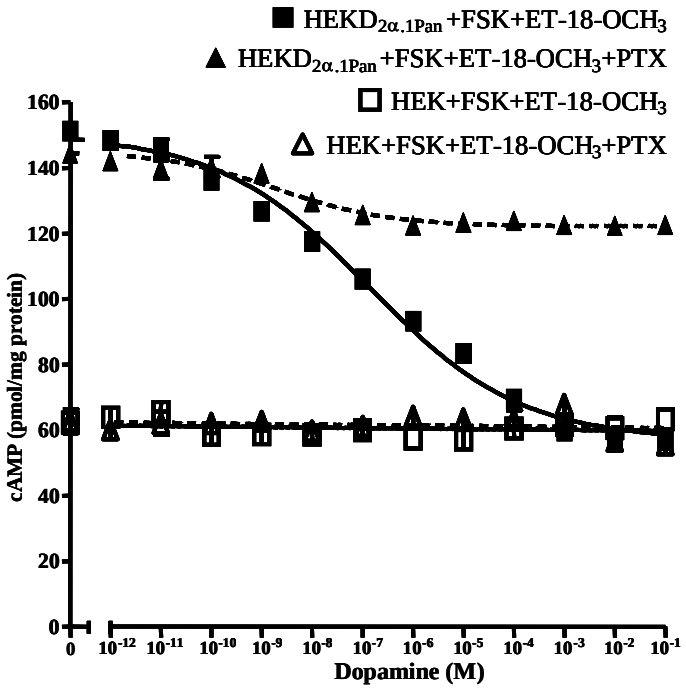

Figure 4-7: The negative coupling to cAMP is mediated by PTX-sensitive and PTX-insensitive G proteins.All cells were exposed to forskolin (2.5µM) and ET-18-OCH_3 (50 µM). [cAMP] was simultaneously measured in pmol cAMP/mg protein for both $HEKD_{2\alpha.1Pan}$ (solid symbols) and HEK (open symbols) cells in the presence of increasing DA. Experiments were conducted in the presence (dashed line) vs. the absence (solid line) of the Gi/o inhibitor, PTX (500ng/ml). All experiments were repeated 3 times. Data represent the mean $\pm$ S.E.M.

opposing effects on cAMP levels: the $G\alpha_{i/o}$ subunits cause a decrease in cAMP while $G\beta\gamma$ subunits activate PLCβ to cause an increase in cAMP.

Figure 4-7 also suggests that the $D_{2\alpha.1Pan}$ receptor, like its mammalian and *Drosophila* homologs, may constitutively activate Gi/o proteins. The forskolin activated cAMP levels are significantly higher in $HEKD_{2\alpha.1Pan}$ relative to the parental HEK cell line (Figure 4-7; 150pmol/mg vs. 60pmol/mg; $p < 10^{-4}$). This compensatory mechanism is known as heterologous sensitivity or supersensitivity (Watts, 2002;Vortherms et al., 2004;Watts and Neve, 2005). Several studies have demonstrated that chronic Gi/o activity ultimately leads to a paradoxical increase in AC activity (supersensitivity) through a number of different molecular mechanisms.

The intracellular milieu determines whether arthropod D_2 receptors positively or negatively couple with cAMP

As previously stated, when expressed in HEK293 cells, the lobster versus fruit fly and honeybee orthologs of the D_2 receptor produce opposite changes in cAMP levels in response to DA: the lobster D_2 receptor positively couples with cAMP (Figure 4-3) while the fly and bee orthologs of the D_2 receptor negatively couple with cAMP (Beggs et al., 2005;Hearn et al., 2002). We predicted that if the cellular background determines whether D_2 receptors positively or negatively couple with cAMP, then expressing the honeybee ortholog of the D_2 receptor, *Am*Dop3, in our parental HEK293 cell line should produce an increase, rather than the previously described decrease in cAMP. To test the hypothesis we obtained the *Am*Dop3 clone from the Mercer lab, transformed our HEK293 cells to generate a stable cell line, HEK*Am*Dop3, and measured changes in cAMP in response to DA. Figure 4-8 shows that the HEK*Am*Dop3 cells responded to 10^{-4}M DA with a significant increase in cAMP ($p < 0.0001$). The DA-induced

increase in HEK*Am*Dop3 cells is roughly 7-fold greater than that observed in the parental HEK line ($p < 0.009$, HEK*Am*Dop3 vs. HEK). The increase was attenuated by transiently expressing the Gβγ scavenger $\beta ARK_{495-689}$. Together these data suggest that the cellular milieu greatly influences D_2 mediated changes in [cAMP] and that there are no obvious functional differences between the signaling properties of the honeybee and lobster D_2 orthologs.

Alternate splicing changes the potency and efficacy of $D_{2\alpha Pan}$ isoforms

Figure 4-1 and Table 4-1 indicate that the $D_{2\alpha Pan}$ receptor can be alternately spliced to create multiple isoforms with differences in their carboxy termini and/or intracellular loop 3. The carboxy terminus and intracellular loop 3 are involved in G protein coupling (Wong, 2003). Changes in amino acid sequence in these regions can alter the strength or specificity of G protein signaling (Franke et al., 1990;Cotecchia et al., 1990). The C-terminus of GPCRs also determines the rate of receptor recycling and receptor coupling to β-arrestin mediated cascades (Oakley et al., 1999). To determine whether alternate splicing produces functional differences in G protein signaling, we established stable HEK cell lines expressing $D_{2\alpha.2Pan}$ or $D_{2\alpha.3Pan}$ and obtained DA dose-response curves for the resulting cell lines: $HEKD_{2\alpha.2Pan}$ and $HEKD_{2\alpha.3Pan}$. Figure 4-9A shows that in all cases the receptor produces a dose-dependent increase in [cAMP]i that is significantly higher than in the parental HEK cell line (2.5-fold and 2-fold greater, respectively, at 10^{-4}M DA; $p < 0.05$). Altering the carboxy terminal domain ($D_{2\alpha.1Pan}$ vs. $D_{2\alpha.2Pan}$) reduced the EC_{50} by more than an order of magnitude (from 9.2×10^{-7}M to 2.4×10^{-6}M, respectively). In addition, removing the alternately spliced intracellular loop 3 exon ($D_{2\alpha.2Pan}$ vs. $D_{2\alpha.3Pan}$) once again changed the EC_{50} by more than an order of magnitude (from 2.4×10^{-6} to 4×10^{-7}, respectively) and significantly altered receptor efficacy. Thus, these data suggest that

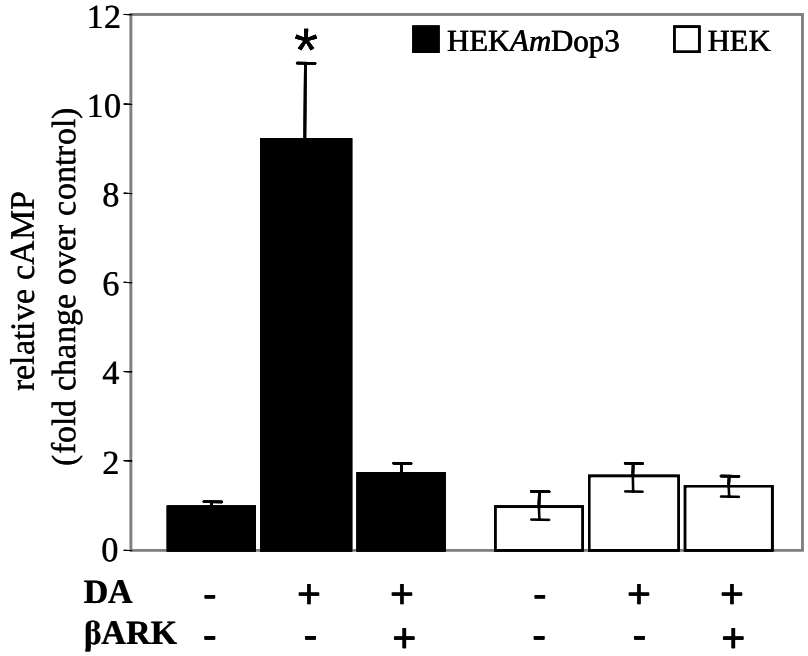

Figure 4-8: *Am*Dop3 positively couples to cAMP through the Gβγ cascade. Levels of cAMP (pmol cAMP/mg protein) were simultaneously measured in HEK cells expressing the *Am*Dop3 receptor (HEK*Am*Dop3, black bars) and in the parental HEK cell line (white bars) in the presence or absence of 10^{-4}M DA and in the presence or absence of the Gβγ scavenger $\beta ARK_{495-689}$, as indicated below each bar. All data were normalized to average [cAMP] in the absence of DA (control) for the same experiment, and fold change over control is plotted on the y axis. All experiments were repeated 3 times. Data represent the mean $\pm$ S.E.M. Data were analyzed using Student t-tests. * indicates significant differences from cAMP levels measured in the control for the same cell line ($p < 0.0001$).

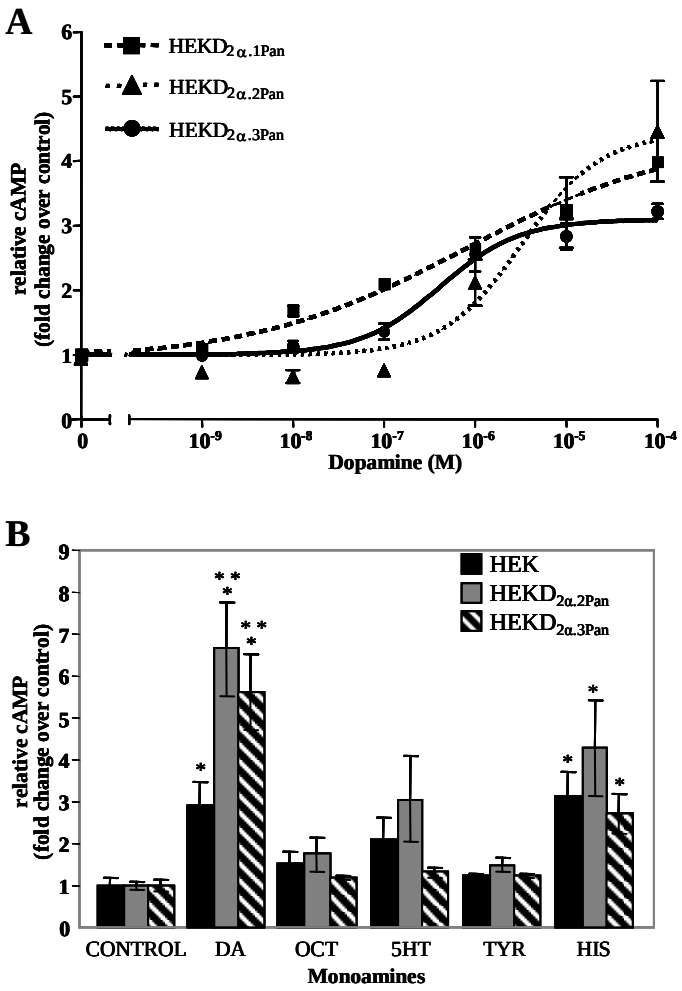

Figure 4-9: Alternate splicing changes the potency and efficacy of $D_{2\alpha Pan}$ isoforms. A. Changes in cAMP levels (pmol cAMP/mg protein) in response to increasing [DA] were measured in $HEKD_{2\alpha.1Pan}$ (squares, dashed line) $HEKD_{2\alpha.2Pan}$ (triangles, dotted line) and $HEKD_{2\alpha.3Pan}$ (circles, solid line) cell lines. All data are normalized to [cAMP] in the absence of DA (control) and fold changes over control are plotted on the y axis. Data represent the mean $\pm$ S.E.M, n=3. B. Levels of cAMP (pmol cAMP/ mg protein) were simultaneously measured in HEK, $HEKD_{2\alpha.2Pan}$ (grey bars) and $HEKD_{2\alpha.3Pan}$ (hatched bars) cells under control conditions (no monoamines present) or in the presence of 1mM of the indicated monoamine. Data were first normalized to control, and then the responses of the transfected cell lines were normalized to that of the parental HEK cell line. Average fold changes in the transfected relative to parental line are plotted, error bars indicate the S.E.M, $n \geq 3$. * indicates significant differences from cAMP levels measured in the control ($p < 0.05$).

alternate splicing may change the potency of the $D_{2\alpha Pan}$ receptor. We also tested the effect of 5HT, OCT, TYR, and HIS on [cAMP]i in $HEKD_{2\alpha.2Pan}$ and $HEKD_{2\alpha.3Pan}$ cell lines. Figure 4-9B shows that, like the $D_{2\alpha.1Pan}$ receptor (Figure 4-3), $D_{2\alpha.2Pan}$ and $D_{2\alpha.3Pan}$ respond only to DA when expressed in HEK cells. Thus, alternate splicing does not affect the monoamine specificity of these receptors.

Discussion

CPGs are highly modulated neural circuits that rely on GPCRs to produce a rhythmic output (Ramirez et al., 2004;Marder and Bucher, 2001). The effects of DA on a model CPG, the pyloric network, have been extremely well characterized (Harris-Warrick et al., 1998;Gruhn et al., 2005;Johnson et al., 2003;Kloppenburg et al., 2000;Kloppenburg et al., 1999;Peck et al., 2001); however, the molecular mechanisms by which DA exerts its effects are completely unknown. To begin to investigate the molecular underpinnings of the dopaminergic response in pyloric neurons, we cloned and characterized the only known arthropod type-2 DAR from *Panulirus interruptus*: $D_{2\alpha Pan}$. Heterologous expression in HEK cells indicates that this receptor is specifically activated by DA, as opposed to other monoamines known to be endogenous to the lobster nervous system. Alternate splicing in intracellular loop 3 and at the carboxy terminus alters the potency and efficacy of the receptor.

Surprisingly, we found that when expressed in HEK cells the $D_{2\alpha Pan}$ receptor positively couples with cAMP. The increase in cAMP is mediated, in part, by multiple Gi/o proteins. $D_{2\alpha Pan}$ stimulation of Gi/o activity results in the activation of two discrete pathways: 1) a Gα mediated inhibition of AC, leading to a decrease in cAMP and 2) a Gβγ mediated activation of PLCβ, leading to an increase in cAMP. We also found that contradictory to previous reports (Beggs et

al., 2005), the honeybee D_2 receptor can positively couple with cAMP via the Gβγ subunits of Gi/o proteins, suggesting that the intracellular environment can alter receptor coupling to cAMP. We conclude that arthropod and mammalian D_2 receptor signaling is very similar, and that D_2 mediated signaling is determined by both the functional properties of the receptor and the intracellular milieu.

The $D_{2\alpha Pan}$ receptor simultaneously activates multiple cascades

It is not clear whether the $D_{2\alpha Pan}$ receptor response is mediated entirely by G proteins in HEK cells. Figure 4-7 suggests that a PTX insensitive protein, probably $G\alpha_z$, mediates roughly 23% of the DA induced decrease in cAMP while the PTX sensitive $G\alpha_{i/o}$ subunits are responsible for 77% of the response. However, saturating levels of PTX only reduced the DA induced increase in cAMP from 4.4- to 3-fold, rather than the predicted 1.8-fold (Figure 4-4). Furthermore, the EC_{50} for the increase in cAMP (9.2×10^{-7}; Figure 4-4) is 6.6-fold lower than the EC_{50} for the decrease in cAMP (1.4×10^{-7}; Figure 4-7). There are at least two possible explanations for these findings, and they are not mutually exclusive. First, $D_{2\alpha Pan}$ receptors may simultaneously activate multiple cascades, including G protein independent cascades (Beaulieu et al., 2005;Lefkowitz and Shenoy, 2005). Second, $G\alpha_z$ may donate the majority of Gβγ subunits that interact with PLCβ to increase cAMP. Specific Gα donors for Gβγ subunits have previously been observed in certain cell types. For example, GIRK channels are activated by Gβγ subunits that are exclusively donated by $G\alpha_{i2}$ and $G\alpha_{i3}$ in native tissues, though any Gα subunit can donate the Gβγ subunits in studies utilizing heterologous expression systems (Dascal, 2001). Specificity in native tissues appears to be conferred by binding of the α-subunit to the GIRK effector (Ivanina et al., 2004) and the fact that upon activation, Gi and Gz proteins undergo a

conformational change, but do not dissociate into physically independent Gα and Gβγ subunits (Frank et al., 2005). Although Gα donor specificity has never to our knowledge been observed for Gβγ regulation of PLCβ, we cannot dismiss this concept a priori.

Unexpectedly, the $D_{2\alpha Pan}$ receptor-initiated cascades regulate cAMP in opposing directions in the same cells. These cascades may be highly localized to create microdomains of cAMP gradients (Zaccolo and Pozzan, 2002;Rich et al., 2001). On the other hand, the cascades may function with different kinetics and interact to generate feedback loops. In addition, there are examples of G protein mediated cascades dominating the early portion of a response to constant agonist application, while β-arrestin cascades predominate in later portion (Ahn et al., 2004). Thus, distinct $D_{2\alpha Pan}$ mediated cascades may operate in different timeframes to generate multiphasic responses.

Receptor signaling varies with the intracellular milieu

Interestingly, a D_2 receptor can produce opposite responses even when expressed in the "same" cell type. When *Am*Dop3, the honeybee ortholog of the arthropod D_2 receptor, is expressed in HEK293 cells in the Mercer lab, it produces a decrease in cAMP; however, when it is expressed in HEK293 cells in the Baro lab, it produces an increase in cAMP. Such a finding is not unique to the arthropod D_2 receptor. For example, isoproterenol induced β_2-adrenergic receptor signaling in HEK293 cells varies across labs (Daaka et al., 1997;Friedman et al., 2002;Lefkowitz et al., 2002). Tissue culture cell lines can often rearrange their genetic material and/or alter their genetic programs, most likely because culture conditions provide little selective pressure for maintaining a constant genome/transcriptome/proteome. Thus, receptor signaling in a given cell type may vary with the lab because cell lines diverge within and across labs over

time. Indeed, in our hands the parental HEK cell line could alter its response to DA, despite the fact that it was cultured under constant conditions. Differences in the expression, localization and/or interactions of downstream effectors of the D_2 receptor could account for the differences in the *Am*Dop3 response in each HEK cell line. All of these findings reinforce the idea that GPCR signaling is context dependent. Based on these studies, we cannot predict how the $D_{2\alpha Pan}$ receptor will affect cAMP levels in pyloric neurons; though the data suggest that the $D_{2\alpha Pan}$ receptor will most likely couple with Gi and Go proteins to alter cAMP levels in pyloric neurons.

Monoaminergic GPCR signaling is conserved across species

Relatively little is known about invertebrate monoaminergic GPCRs compared to their vertebrate homologs. Data mining studies suggest that there are roughly 19 monoamine receptors in arthropods (Clark et al., 2004;Roeder, 2003). By the year 2004, 10 of these receptors had been cloned and characterized (Tierney, 2001;Blenau and Baumann, 2001;Clark et al., 2004). Several recent efforts have reduced the number of uncharacterized monoaminergic receptors to roughly 3 out of 19 (Balfanz et al., 2005;Srivastava et al., 2005;Maqueira et al., 2005;Cazzamali et al., 2005;Evans and Maqueira, 2005).

Both receptors and G proteins show strong amino acid sequence conservation in functional domains across species. Here we have demonstrated that the arthropod D_2 receptor can regulate second messenger levels by coupling to both AC, via Gα subunits, and PLCβ, via Gβγ subunits of Gi/o proteins. Similar findings were previously published for mammalian D_2 receptors expressed in HEK293 cells (Tsu and Wong, 1996) and in native neurons (Hernandez-Lopez et al., 2000). In addition, we have previously shown that comparable to mammalian type-1 DARs, the $D_{1\alpha Pan}$ receptor couples with Gs and the $D_{1\beta Pan}$ receptor couples with both Gs and Gz

when expressed in HEK cells (Clark and Baro, 2006). Likewise, we have shown that the 5-$HT_{2\beta Pan}$ receptor couples with Gq (Clark et al., 2004) and the 5-$HT_{1\alpha Pan}$ receptor couples with Gi/o (Spitzer and Baro, submitted), as is the case for their respective mammalian homologs. Collectively, these data strongly suggest that signaling mechanisms for homologous receptors are well conserved across species.

In conclusion, receptor expression studies in heterologous systems are important as they help to define key structure/function relationships for homologous receptors across species. Such studies are also useful and necessary in that they reveal organizing principles for signal transduction and more specifically, the repertoire of cascades available to a given receptor. However, heterologous expression studies are limited by the fact that receptor signaling is context dependent. In order to understand the function of a receptor in a specific cell type, the receptor must ultimately be studied in that cell type. We have found that when the $D_{2\alpha Pan}$ receptor is heterologously expressed, it couples with Gi/o proteins and can modulate cAMP levels through both $G\alpha$ and $G\beta\gamma$ subunits, like all of its homologs. The data also suggest that $D_{2\alpha Pan}$ receptor signaling may involve additional Gi/o-independent mechanisms. These results set the stage for future studies aimed at understanding the role of D_2 receptors in native neurons involved in rhythmic motor pattern generation.

CHAPTER FIVE

CRUSTACEAN DARS: LOCALIZATION AND G PROTEIN COUPLING IN THE STG

PUBLICATION: MERRY C. CLARK, REESHA KHAN, AND DEBORAH J. BARO (2008) *JOURNAL OF NEUROCHEMISTRY 104(4):1006-1019*

NOTE: I PERFORMED ALL EXPERIMENTS IN THIS CHAPTER EXCEPT FOR THE DAR WESTERN BLOTS AND QUANTIFICATION OF RECEPTOR STAINING IN CONFOCAL STACKS

Introduction

The neurotransmitter DA is associated with motor control in a variety of systems (Sidhu et al. 2003). In order to better understand how DA modulates motor behaviors, we study the well-established model system: the crustacean STNS (Figure 1-2) (Marder and Bucher 2006). The STNS is a peripheral nervous system whose sole function is to control the movements of the striated muscles surrounding the gut. The neurons in the STNS comprise multiple CPG circuits that drive different sets of muscles around the gut to produce a rhythmic, patterned motor activity associated with a specific function, such as chewing or swallowing.

DA acts as both a neuromodulator and a neurohormone in the STNS (Kushner and Maynard 1977; Sullivan et al. 1977a; Barker et al. 1979; Kushner and Barker 1983; Bucher et al. 2003a). DA is found in descending modulatory input fibers that travel through the *stn* to terminate in the neuropil of the STG (Figure 1-2). The somata of these fibers originate in both the commissural ganglia (COG) and the brain. Neurons in the STG do not themselves contain DA. Additionally, DA is secreted directly into the hemolymph by the pericardial organs, which are not shown in Figure 1-2 (Sullivan et al. 1977a; Fort et al. 2004). Importantly, the STG resides in an artery, and STG neurons are constantly bathed by hemolymph and therefore receive neurohormonal dopaminergic input.

DA's effects on the pyloric CPG have been particularly well characterized. The fourteen pyloric neurons are located exclusively within the STG. Specific dopaminergic inputs to pyloric neurons have not been defined, but DA is known to reconfigure pyloric circuit output by altering component neuron intrinsic firing properties, synaptic strengths and axonal spike initiation (Selverston and Miller 1980; Anderson and Barker 1981; Eisen and Marder 1984; Marder and Eisen 1984b; Flamm and Harris-Warrick 1986a, b; Harris-Warrick and Flamm 1987; Johnson

and Harris-Warrick 1990; Johnson et al. 1995; Ayali and Harris-Warrick 1998, 1999; Bucher et al. 2003a; Johnson et al. 2005; Szucs et al. 2005). Many types of voltage dependent ionic conductances are modified by bath applied DA, including a variety of K^+-, Ca^{2+}- and non-specific cation, or H-currents (Harris-Warrick et al. 1995a; Harris-Warrick et al. 1995b; Kloppenburg et al. 1999; Kloppenburg et al. 2000; Peck et al. 2001; Johnson et al. 2003a; Gruhn et al. 2005; Peck et al. 2006). DA also modulates ionotropic receptors including a glutamate gated chloride channel (Cleland and Selverston 1995, 1997, 1998). DA can modify multiple currents in a single cell type, and its effect on a given current is cell specific; thus, DA evokes a unique response from each of the six pyloric cell types. The molecular mechanisms underlying these DA-induced cellular and circuit reconfigurations are poorly understood.

Dopaminergic responses are mediated by multiple, highly conserved DARs that belong to the superfamily of G protein coupled receptors (GPCRs). GPCRs often exist in multiprotein complexes, and their signaling pathways are constrained and shaped by proteins that co-localize in the receptor complex (Bockaert et al. 2003). GPCR signaling is context dependent. Whereas the inherent properties of the GPCR are important, signaling pathways change according to the cellular milieu (Clark and Baro 2007). Moreover, GPCR signaling is not constant within a given cell type. Rather, GPCR performance can vary with its history of prior activation (Gainetdinov et al. 2004).

DARs are broadly classified into two subfamilies on the basis of conserved structure and signaling mechanisms: D_1 and D_2 (Neve et al. 2004). Traditionally, DARs are thought to couple with trimeric G proteins: D_1 receptors activate $G\alpha_s$, whereas D_2 receptors couple with $G\alpha_{i/o}$ proteins. In addition to these two canonical cascades, DARs can couple with multiple G proteins (Sidhu and Niznik 2000), and signal through a variety of other means, including $G\beta\gamma$- (Clark and

Baro 2007) and even G protein independent-pathways (Beaulieu et al. 2005; Lefkowitz and Shenoy 2005; Zou et al. 2005). DARs can display agonist independent activity (Hall and Strange 1997), and homo- and hetero-multimers can form between DARs within a subfamily

There are three known DARs in arthropods. We have cloned the spiny lobster orthologs, $D_{1\alpha Pan}$, $D_{1\beta Pan}$ and $D_{2\alpha Pan}$, and characterized them in a heterologous expression system (Clark and Baro 2006, 2007). We found that when stably expressed in human embryonic kidney (HEK) cells, $D_{1\alpha Pan}$ receptors coupled with Gs to increase cAMP, and $D_{1\beta Pan}$ receptors coupled with Gs and Gz to increase cAMP (Clark and Baro 2006). On the other hand, $D_{2\alpha Pan}$ receptors coupled with multiple members of the Gi/o family in HEK cells. Once activated, the Gα subunits of the trimeric Gi/o proteins acted to decrease cAMP, while the Gβγ subunits caused an increase in cAMP. Under the experimental conditions, the two effects summed. Thus, an increase or decrease in cAMP could be observed depending upon which cascade dominated the response, and the dominant cascade varied with the cell line (Clark and Baro 2007). The latter study emphasizes that DAR signaling is context dependent, and dopaminergic transduction cascades must therefore be delineated in the native system. Here we define DAR-G protein couplings and localization in the STNS.

Materials and Methods

Production of receptor specific antagonists (RSAs)

Each of the three peptides shown below served as an antigen in the production of a rabbit, polyclonal, affinity-purified antibody that then functioned as the indicated RSA. The peptides and antibodies were generated by the designated commercial establishments.

$D_{1\alpha}$ RSA antigen: CLDRYWAITDPFSYPSRM (Bethyl Laboratories Inc., Montgomery, TX)

$D_{1\beta}$ RSA antigen: CDRYIHIKDPLRYGRWMTKRI (Bethyl Laboratories Inc.)

$D_{2\alpha}$ RSA antigen: CDRYIAVTQPIKYAQSKNNKR (Alpha Diagnostic International, San Antonio, TX)

In addition to the antibodies that served as RSAs, an additional rabbit, polyclonal, affinity purified antibody was generated against each receptor using the following extracellular antigens.

anti-D1α-AB.b: WRAVSDPHPVGACPFTEDL (Alpha Diagnostic)

anti-D1β-AB.b: VNDLLGYWPFGSQFCNIWIA (Alpha Diagnostic)

anti-D2α-AB.b: VNAISKKTQNPSLEPGC + CLAQTLPVLKVPNLKY (21^{ST} Century Biochemicals, Marlboro, MA)

Membrane preparations

Membrane preparations for G protein assays on HEK cell lines were as previously described (Clark and Baro 2006, 2007). For G protein assays on native tissue, an STNS was dissected from an animal and immediately frozen at -70°C. STNS were homogenized on ice using a 2 ml Wheaton glass tissue grinder and ice cold homogenizing buffer (120mM NaCl, 5mM KCl, 1.6mM KH_2PO_4, 1.2mM $MgSO_4$, 25mM $NaHCO_3$, 7.5mM dextrose, 2mM EGTA, 5µg/ml leupeptin, 10µg/ml aprotinin, 5µg/ml pepstatin, 0.5mg/ml Pefablock, 50µl/ml Pefablock protector, 5mM iodoacetamide, and 1mM EDTA, pH 7.4). The homogenate was spun for 2 minutes at 2000 rpm. The supernatant was recovered and centrifuged at 15,000 rpm for 30 minutes at 4°C. Pellets were resuspended in 20mM HEPES (pH 7.4) containing 0.5% 3-[(3-cholamidopropyl) dimethylammonio]-1-propanesulfonate (CHAPS), and 2mM EDTA, and shaken on ice for 1 hour. Samples were then centrifuged for 1 minute at 2000 rpm, and

supernatant was transferred to a fresh tube for storage at -70°C. Protein concentrations were determined using a BCA Protein Assay Kit (Pierce).

G protein activation assay

Agonist-induced activation of specific G proteins was determined as previously described (Clark and Baro 2006, 2007). In this assay binding of GTPγS^{35} to a given G protein is used as an index of G protein activation in the presence and absence of DA. This method employs commercially available antibodies against human G proteins (anti-Gs, anti-Gi and anti-Gq). This is valid because, the antibodies were raised against the C-termini of human $G\alpha_s$, $G\alpha_q$ and $G\alpha_{i1/2}$, which are completely conserved with lobster $G\alpha_s$, $G\alpha_q$ and $G\alpha_i$, respectively (Clark and Baro 2006), and the antibodies specifically recognize their cognate lobster G proteins in immunoblot experiments (Figure 5-1.). In addition, a scan of the NCBI protein sequence database shows that $G\alpha_s$ and $G\alpha_q$ have also been sequenced from a penaeid shrimp (Dendrobranchiata, Figure 5-3), and the C-termini are completely conserved. Literature and the insect genome database searches suggest that there are six Gα proteins in arthropods: $G\alpha_s$, $G\alpha_f$, $G\alpha_q$, $G\alpha_i$, $G\alpha_o$, and $G\alpha_{12}$ (a.k.a. concertina).We did not examine receptor coupling with $G\alpha_f$, $G\alpha_o$ and $G\alpha_{12}$ in this work for lack of the appropriate sequence information and/or antibodies.

Immunoblots and immunocytochemistry (ICC)

Antibodies were used in immunoblot and immunocytochemistry protocols as previously described (Baro et al. 2000; Clark et al. 2004). Controls in which the antibodies were preabsorbed with their cognate peptide antigens were performed for all antibodies in both types of experiments. In the case of the western blots and the ICC experiments using anti-$D_{2\alpha}$,-AB.b, all immunoreactivity was lost upon preabsorption (not shown). In the case of ICC experiments

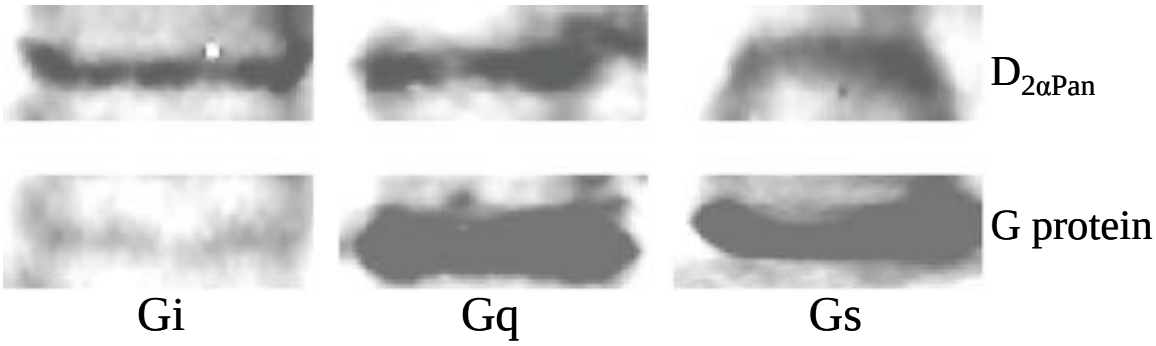

Figure 5-1: Gs, Gi and Gq are differentially expressed in the lobster. Western blots containing protein extracts from the lobster nervous system were probed with antibodies against $D_{2\alpha Pan}$ and Gαi**,** Gαq, or Gαs. The human G protein antibodies recognized lobster G proteins of predicted molecular weights (Gαi ~ 36 kD**,** Gαq ~ 36 kD, Gαs ~ 37 kD).

using anti-$D_{1\alpha}$-AB.b or anti-$D_{1\beta}$ RSA, most immunoreactivity was lost upon preabsorption, however, there was still some non-specific immunoreactivity homogeneously dispersed throughout the STG (not shown). In these cases, antibody specificity was confirmed with quantitative ICC experiments. Six independent experiments were performed for each antibody: 3 using the antibody and 3 using preabsorbed antibody. For a given animal, five confocal stacks (10μm) were obtained from the fine neuropil where receptors appeared to reside (see Results). Receptor staining was quantified by counting all puncta in every 1μm optical section in each confocal stack. Significant differences between experimental and preabsorbed controls were determined with two-tailed, unpaired Student t-tests. As expected, the number of puncta in the synaptic neuropil was significantly increased by 5 ± 0.002 fold ($D_{1\alpha Pan}$, $p = 0.0014$) and 4.7 ± 0.008 fold ($D_{1\beta Pan}$, $p < 10^{-5}$), in the experimental compared to the preabsorbed control.

In some ICC experiments, prior to fixation a neuron was filled with a lysine fixable, dextran coupled Texas Red fluorophore that cannot pass through gap junctions (M.W. 10,000; Molecular Probes). This was accomplished by pressure injecting a 1% solution of the fluorophore in 0.2M KCl using 20msec pulses at 0.05 Hz and 28 psi for 10 minutes. The fluorophore was allowed to diffuse at room temperature for > 2hrs. The ganglion was then fixed and the standard ICC protocol performed.

Semi-quantitative measurement of G protein abundance

The aforementioned G protein antibodies were used to quantify levels of G proteins in membrane preparations from the lobster nervous system relative to $D_{2\alpha Pan}$ receptor proteins. Two sets of experiments were performed. First, immunoblots containing lobster nervous system membrane protein extracts were probed with anti-D2α-AB.b and either anti-Gs, anti-Gi or anti-Gq (Figure 5-2). The optical density (OD) for each signal was obtained, and the G protein signal

was normalized by the $D_{2\alpha Pan}$ signal. These experiments were repeated three times with three different membrane protein extracts to obtain a relative measure of average G protein abundance for Gs (3.7±1.1), Gi (0.5±0.1) and Gq (2.1±0.3). In order to compare these relative measures across G protein subtypes, a second set of experiments was performed to determine the efficiency of each G protein antibody. Dot blots containing 50μg of each of the three antigenic G protein peptides were generated (www.abcam.com/technical) and subjected to the standard immunoblot protocol. For a given experiment (i.e., 3 dot blots: Gs, Gi, Gq), after removing the primary antibody, the dot blots were processed together and treated in an identical fashion for the remainder of the protocol. These experiments were repeated three times and the average OD of the immunogenic signal produced by each primary was found to be 414 ± 71, 381 ± 65 and 563 ± 119 for anti-Gs, anti-Gi and anti-Gq, respectively. The data suggest that there were no statistically significant differences in antibody efficiencies (One Way ANOVA, p=0.49). Nevertheless the anti-Gq signal was 1.35 times more intense than Gs and 1.48 times more intense than Gi. To compensate for the differences in efficiencies, the average, relative G protein abundance determined in the first set of experiments was multiplied by 1.35 (Gs) or 1.48 (Gi). Data were analyzed with a one-way ANOVA.

Animals

Pacific spiny lobsters (*Panulirus interruptus*) were obtained from Don Tomlinson Commercial Fishing (San Diego, CA). Lobsters were maintained at 16°C in constantly aerated and filtered seawater. Freshwater prawns (*Macrobrachium rosenbergii*) were obtained from the Kentucky State University Aquaculture Program (Frankfort, KY). Animals were kept in filtered, aerated freshwater and sacrificed within 24 hours of arrival. Pink shrimp (*Penaeus duorarum*)

were obtained from Gulf Specimen Marine Laboratories, Inc (Panacea, FL). Animals were kept in filtered, aerated seawater and sacrificed within 48 hours of arrival. Live American lobsters (*Homarus americanus*) and blue crabs (*Callinectes sapidus*) were obtained from the Dekalb Farmer's Market (Decatur, GA) and kept on ice for up to four hours from the time of purchase before sacrificing. All animals were anesthetized by cooling on ice prior to experiments.

Statistical analyses and curve fitting

Student t-tests were performed with Excel software. Curve fitting and Kruskall-wallis (ANOVA on ranks) tests were performed with Prism software. In all cases, statistical significance was determined as $p < 0.05$.

Results

DA activates Gs, Gi and Gq in STNS membranes in all species examined

DA-induced signal transduction cascades have never been defined in crustaceans. Although DARs can transduce signals through a variety of pathways, G protein cascades remain a major form of DAR mediated signal transduction in all species examined. As a first step in characterizing DAR transduction cascades in the crustacean STNS, we examined DA-induced G protein activation in STNS membrane preparations from multiple crustacean species (Figure 5-2). Recent studies on the phylogenetic relationships between Decapod crustaceans are summarized in the cladogram shown in Figure 5-2A (Richter and Scholtz 2001; Dixon et al. 2003). STNS circuits have been described for Dendrobranchiata (Tazaki and Tazaki 2000), Caridea (Meyrand and Moulins 1988) and Reptantia (Selverston and Moulins 1987; Harris-Warrick et al. 1992b; Katz and Tazaki 1992). We examined five species spanning these three

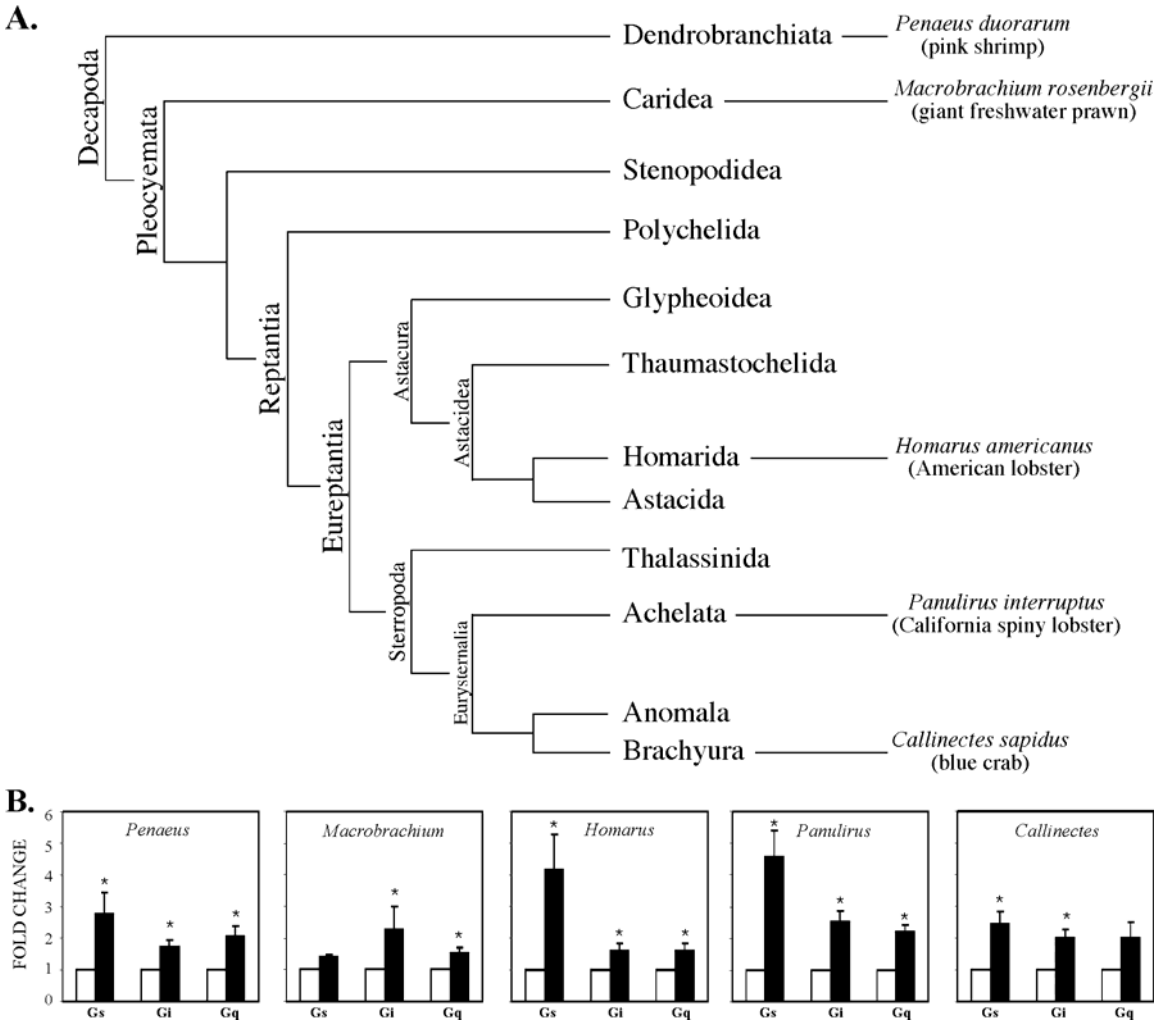

Figure 5-2: Dopaminergic responses in the STNS are mediated by Gs, Gi and Gq in all species of Decapod crustaceans examined. (A) Phylogenetic classification scheme for Decapod crustaceans modified from (Dixon et al. 2003). Branches are not drawn to scale. **(B)** DA activates Gs, Gi and Gq in all species examined. G protein activity in the absence (open bar) vs. the presence (filled bar) of 10^{-5}M DA was measured for Gs, Gi, and Gq in STNS membrane preparations from multiple species, as indicated. For each species, the total number of animals used for all experiments, and the total number of independent experiments are: 25 *Penaeus*, n = 5 experiments; 13 *Machrobrachium*, n = 3; 30 *Panulirus*, n = 17; 10 *Homarus*, n = 7; 20 *Callinectes*, n = 5. The activities of all three G proteins were measured in each experiment. Data are represented as the mean $\pm$ S.E.M. Statistically significant differences in the activity of a given G protein are indicated with an asterisk ($p < 0.05$). For Gq activity in *Callinectes*, $p < 0.051$ and for Gs activity in *Machrobrachium*, $p < 0.07$.

taxa. The data indicate that dopaminergic responses in the STNS are mediated by Gs, Gi, and Gq in all species examined (Figure 5-2B), as is the case in the mammalian and C. elegans CNS. Although the mean DA-induced increase in Gs activity varied greatly with the species (e.g., compare the DA-induced fold change in Gs activity in lobster vs. freshwater prawn), there were no statistically significant differences in DA-induced G protein activity across species, as determined with one-way ANOVAs for Gs ($p > 0.078$), Gi ($p > 0.3$) and Gq ($p > 0.48$).

In some cases, the level of G protein activation within a given species varied according to the G protein. For example, Figure 5-2B indicates that on average, DA increased Gs activity 4.6-fold, Gi activity 2.6-fold and Gq activity 2.2-fold in *Panulirus* membrane preparations. This could reflect differences in DAR and/or G protein abundances or efficacies. To determine if these changes correlated with the number of G proteins in the membrane preparation, we performed a semi-quantitative immunoblot analysis as described in Materials & Methods, and found that Gs was approximately 2.4-fold more abundant than Gq ($p>0.05$) and roughly 6.4-fold more abundant than Gi ($p<0.03$), while Gq was about 4.0-fold more abundant than Gi ($p>0.05$). These data suggest that the level of G protein activation did not strictly correlate with G protein abundance in the membrane preparation.

STG DARs are localized to the synaptic neuropil

DA-induced activation of multiple G proteins is consistent with the fact that there are three known DARs in arthropods. In order to determine which DARs might contribute to the dopaminergic effects observed in Figure 5-2B, we ascertained receptor distributions in the spiny lobster STG. First, affinity purified antibodies for each of the spiny lobster DARs were generated as described in Materials and Methods. The immunoblots in Figure 5-3 demonstrate that each of

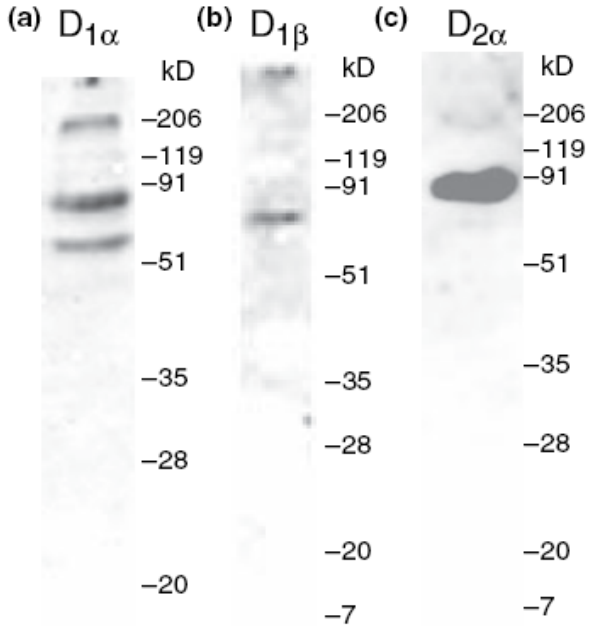

Figure 5-3: Affinity purified antibodies specifically recognize their respective proteins. Western blots containing protein extracts from the lobster nervous system were probed with anti-$D_{1\alpha Pan}$ **(A)** or anti-$D_{1\beta Pan}$ **(B)** or anti-$D_{2\alpha Pan}$ **(C)** antibodies. For each antibody, nervous systems from multiple lobsters were individually examined ($n \geq 3$). The molecular weight standards for each western blot are indicated. The predicted molecular weights of the receptors are: $D_{1\alpha Pan}$ ~ 76 kD, $D1_{\beta Pan}$ ~ 48 kD, $D_{2\alpha Pan}$ ~ 66KD.

the antibodies recognized a protein larger than the predicted molecular weight, indicating putative post-translational processing of the receptor (glycosylation, phosphorylation, etc). The two bands recognized by the antibody against $D_{1\alpha Pan}$ most likely represent alternate splicing of receptor transcripts (Clark and Baro 2006, 2007).

The antibodies were next used to determine receptor distributions in the native system. The STG is a highly structured ganglion containing roughly 30 neurons. STG anatomy has been well-characterized at the level of light and electron microscopy (King 1976a, b; Kilman and Marder 1996; Cabirol-Pol et al. 2002), and is diagramed in Figure 5-4, A-B. The STG can be divided into three regions. The outer or peripheral layer contains the neuronal cell bodies. The central core, or coarse neuropil, contains large diameter neurites. The fine neuropil, which contains small diameter neurites, lies between the central coarse neuropil and the outer peripheral layer. STG synapses are exclusively confined to this region, so it is also known as the synaptic neuropil (King 1976a). As shown in Figure 5-4A, a monopolar STG neuron, whose soma lies in the peripheral layer, sends its primary process into the central coarse neuropil where it divides to produce several large diameter secondary and tertiary processes. These neurites then extend into the fine neuropil where they further divide and make synaptic contacts with other STG neurons, as well as the terminals of sensory and projection neurons. In sum, each of the three layers of the STG contains distinct neuronal subcellular compartments.

The well-defined STG architecture allows subcellular localization of neuronal proteins using confocal microscopy in conjunction with ICC experiments on STG wholemounts (Baro et al. 2000; Clark et al. 2004). Using this approach we discovered that DARs were localized exclusively to neurolemma in the STG synaptic neuropil. Low magnification confocal stacks through the STG suggested that DARs were found predominantly in the fine neuropil (e.g.,

compare region of obvious immunostaining in Figure 5-4C with horizontal section in Figure 5-4B). Projections of high magnification confocal stacks from the fine neuropil showed that each of the three DARs displayed a punctate distribution throughout this region (Figure 5-4D-F). STG neurons are entirely ensheathed by glial cells except at their synaptic terminals (King 1976a).

We were interested in whether DARs localized to neurons and/or glia; therefore, in some experiments a single neuron was dye-filled prior to fixation and ICC. Examples of these experiments are shown in Figure 5-4G-I. The data illustrated that DARs were located in the terminals of $\leq$ 1μm diameter processes, as well as in 3-10μm bulbous structures emanating from fine neurites (arrowheads in Figure 5-4H-I). Light and electron microscopic studies have previously shown that presynaptic compartments of spiny lobster STG neurons appear as 3-10μm bulbous structures emanating from finer neurites, whereas post-synaptic compartments appear as ~1μm finger-like projections extending from the presynaptic compartments (King 1976a). Thus, the most parsimonious interpretation of our data is that DARs are in neuronal synaptic compartments located exclusively in the fine neuropil. Additionally, the DARs that were not located in the filled neurons (i.e., green immunoreactivity in Figure 5-4G-I) exhibited the same staining pattern found for the filled neurons, suggesting that these DARs were most likely also localized to neurons, and not to glial cells. Finally, careful examination of 1μm optical slices throughout an entire filled neuron and ganglia ($n \geq 3$ per antibody) indicated that DARs were never found in the plasma membrane surrounding the soma or large diameter neurites (not shown).

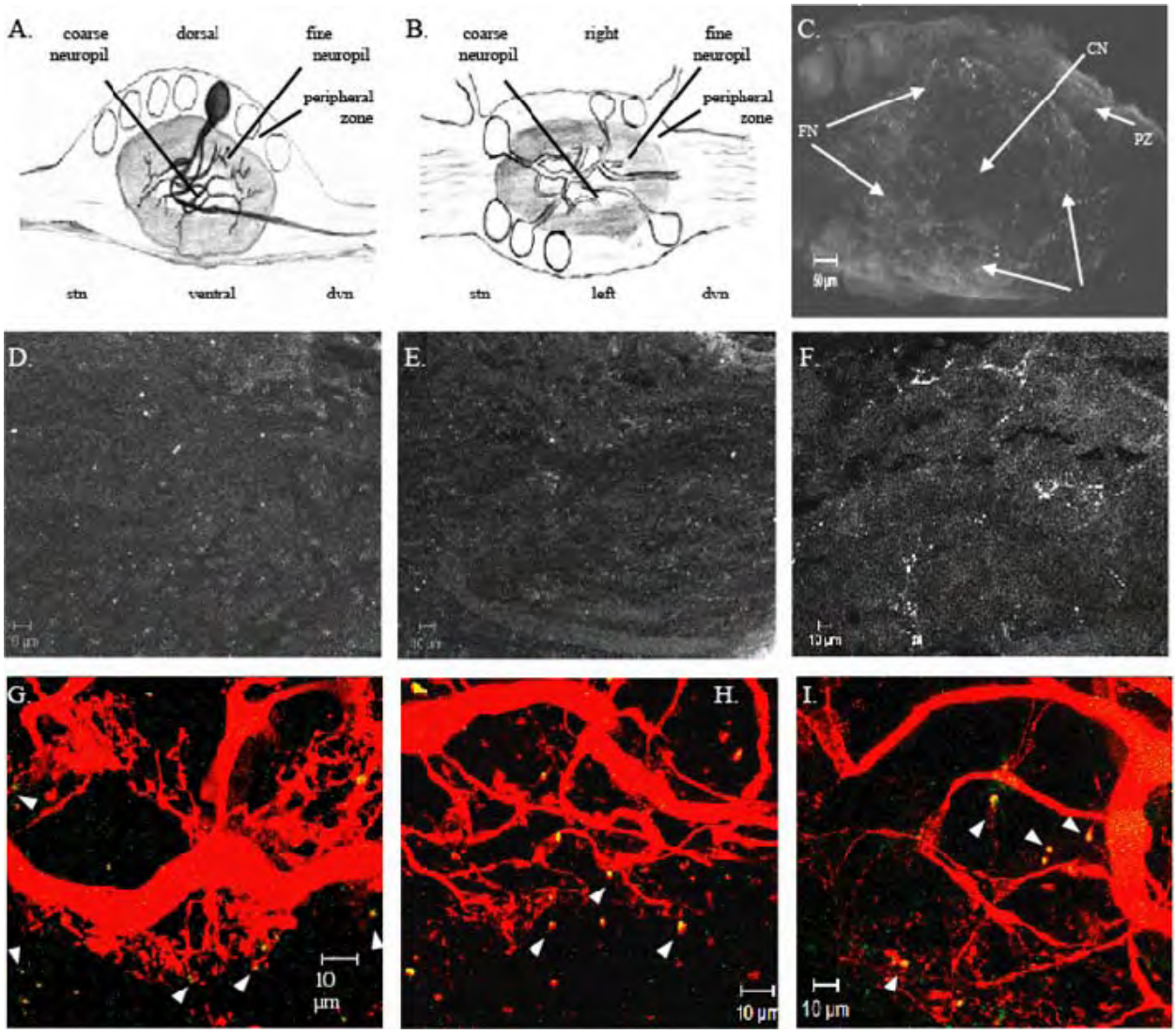

Figure 5-4: DARs are localized to the STG synaptic neuropil. (A) Diagrammatic representation of a midsagittal section through the STG, with a single neuron highlighted. **(B)** Diagram of a horizontal section through the STG. **(C)** 21µm confocal projection from a wholemount STG preparation showing DAR staining in the STG. 3µm confocal slices from the center of the ganglion were used to construct the low magnification projection shown. Mounting was such that all confocal slices represent horizontal sections through the STG, as shown in B. The arrows point to: fine neuropil (FN), coarse neuropil (CN), and peripheral zone (PZ). Staining appears as white puncta. **D-F,** Whole-mount STG preparations stained with anti-$D_{1\alpha Pan}$, n = 9 (**D)** or anti-$D_{1\beta Pan}$, n = 11 (**E)** or anti-$D_{2\alpha Pan}$, n = 11 (**F)** were used to obtain stacks of serial 1um confocal optical sections through the synaptic neuropil. The stacks were used to make the 10µm projections shown. **G-I**, Merged confocal projections of STG neurons that were filled with Texas red and stained with anti-$D_{1\alpha Pan}$ **(G)** or anti-$D_{1\beta Pan}$ **(H)** or anti-$D_{2\alpha Pan}$ **(I).** Yellow indicates DAR staining in the filled neurons. Green shows DAR staining in unfilled cells. Projections are 30µm **(G)**, 26µm **(H)**, or 48µm **(I)**. Arrowheads point to putative synaptic terminals containing DARs.

Generating receptor specific antibody antagonists

The DA induced increases in G protein activity observed in Figure 5-2B represent the sum of all DAR-G protein couplings in the STNS. We next wanted to determine specific G protein couplings for each of the three lobster DARs. A receptor specific antagonist (RSA) will subtract the contribution of an individual receptor from the summed DA-induced G protein activation, and thereby define receptor-G protein coupling. Accordingly, we set out to acquire a specific antagonist for each of the three DARs.

Since the pharmacology of invertebrate DARs is not well-characterized, and RSAs have not been identified, we created a specific antagonist for each receptor. The domains involved in receptor activation and G protein coupling have been fairly well defined and include the intracellular face of the third transmembrane domain and the adjacent intracellular loop 2 (*i2*) (Limbird 2004). The *i2* region is not highly conserved between the three DAR paralogs ($D_{1\alpha}$, $D_{1\beta}$, $D_{2\alpha}$) (Clark and Baro 2006, 2007); thus, an anti-*i2* antibody could theoretically bind to its corresponding receptor and prevent it from activating G proteins.

To create RSAs, we generated three custom, affinity-purified antibodies against *i2*, one for each of the three *Panulirus* DARs: $D_{1\alpha}$ RSA, $D_{1\beta}$ RSA, and $D2_{\alpha}$ RSA. We tested each of the three potential RSAs for its ability to specifically block its cognate receptor in membrane preparations from previously described HEK cell lines, each stably expressing one of the three lobster DARs: HEK $D_{1\alpha Pan}$; HEK $D_{1\beta Pan}$; HEK $D_{2\alpha.1Pan}$ (Clark and Baro 2006, 2007). Figures 5-5 through 5-7 illustrate that each antibody acts as an RSA.

The $D_{1\alpha Pan}$ receptor exclusively couples with Gs in HEK cells, but not members of the Gi/o, Gq, or G12 families of G proteins (Clark and Baro 2006). Figure 5-5A shows the effect of each RSA on $D_{1\alpha Pan}$-Gs coupling at the highest [RSA] tested (300ng/ml). DA (10^{-5}M) produced a

significant, roughly 2-fold increase in Gs activity in these cells. The $D_{1\alpha}$ RSA completely blocked the DA induced increase in Gs activity, while the $D_{1\beta}$ and the $D_{2\alpha}$ RSAs had no significant effect. Thus, only the $D_{1\alpha}$ RSA can uncouple the $D_{1\alpha Pan}$ receptor from Gs. Preabsorption with its peptide antigen prevented $D_{1\alpha}$ RSA antagonism and the $D_{1\alpha}$ RSA had no significant effect on its own. Figure 5-5B illustrates the dose dependencies of the 3 RSAs. Together these data indicate that only the $D_{1\alpha}$ RSA can uncouple the $D_{1\alpha Pan}$ receptor from Gs.

Next we tested the effect of the three RSAs on $D_{1\beta Pan}$ receptor-G protein coupling. When expressed in HEK cells, the $D_{1\beta Pan}$ receptor couples with Gs and Gz, but not members of the Gq, or G12 families of G proteins, nor any member of the Gi/o family except Gz (Clark and Baro 2006). We performed G protein activation assays for Gs (Figure 5-6A-B) and Gz (Figure 5-6C-D) using HEK $D_{1\beta Pan}$ membranes with increasing concentrations of the RSAs. The $D_{1\beta}$ RSA blocked both of these couplings in a dose-dependent manner such that Gs and Gz activities in 10^{-5} M DA plus 300ng/ml $D_{1\beta}$ RSA were not significantly different than under baseline conditions. The $D_{1\beta}$ RSA could be inhibited by preabsorption with its peptide antigen and had no effect on its own (Figure 5-6A and 5-6C). As expected, the $D_{1\alpha}$ and $D_{2\alpha}$ RSAs had no significant effect on $D_{1\beta Pan}$ receptor-G protein couplings at any concentration tested. Together these data indicate that only the $D_{1\beta}$ RSA can prevent the $D_{1\beta Pan}$ receptor from coupling with G proteins.

The $D_{2\alpha Pan}$ receptor couples with multiple members of the Gi/o family, but not members of the Gs, Gq, or G12 families of G proteins (Clark and Baro 2007). Figure 5-7 demonstrates that the $D_{2\alpha}$ RSA disrupts all of these couplings in a dose-dependent manner, and reduces Gi/o activity to levels that are not significantly different from baseline. The $D_{2\alpha}$ RSA had no effect on its own and preabsorption of the $D_{2\alpha}$ RSA with its peptide antigen prevented receptor antagonism

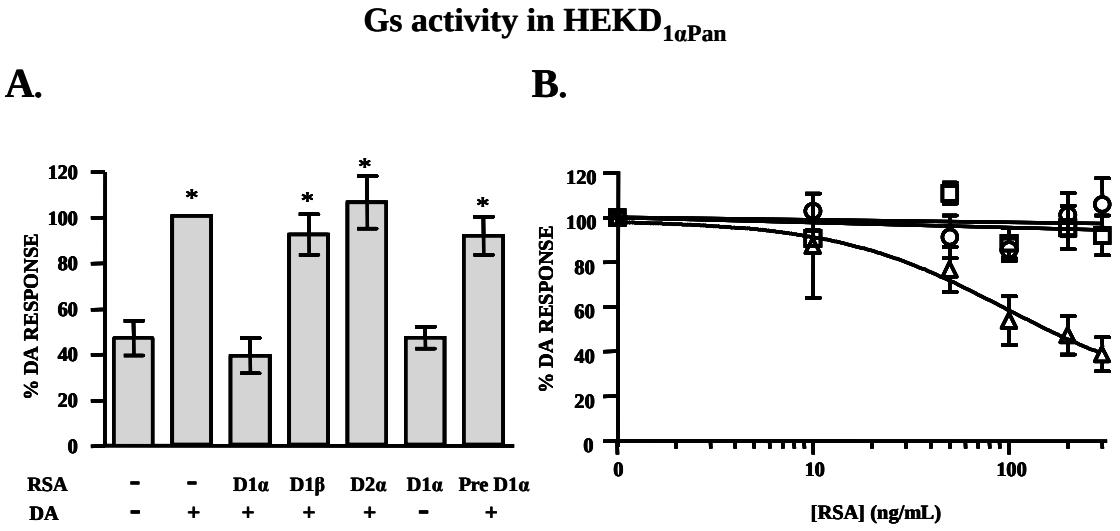

Figure 5-5: Only the $D_{1\alpha}$ RSA can uncouple the $D_{1\alpha Pan}$ receptor from Gs. (**A)** The left panel shows the effect of each RSA on D_{1Pan} receptor-G protein coupling. Gs activity was measured in HEK $D_{1\alpha Pan}$ membrane preparations in the presence (+) or absence (-) of 10^{-5}M DA and 300ng/ml of an RSA as indicated under each bar. Data were normalized by G protein activity in the presence of 10^{-5}M DA without RSA, and are plotted as the percent of the response in 10^{-5}M DA without RSA. Pre $D_{1\alpha}$ indicates that the $D_{1\alpha}$ RSA was preabsorbed with its peptide antigen. Asterisks indicate a significant difference from no DA no RSA ($p < 0.05$). Data represent the mean $\pm$ S.E.M, $n \geq 3$. (**B)** The right panel shows the dose dependency of RSA uncoupling. Gs activity was measured in HEK $D_{1\alpha Pan}$ membrane preparations in the presence of 10^{-5}M DA and increasing concentrations of an RSA ($D_{1\alpha}$, open triangles; $D_{1\beta}$, open squares, $D_{2\alpha}$ open circles). Data represent the mean $\pm$ S.E.M, $n \geq 3$.

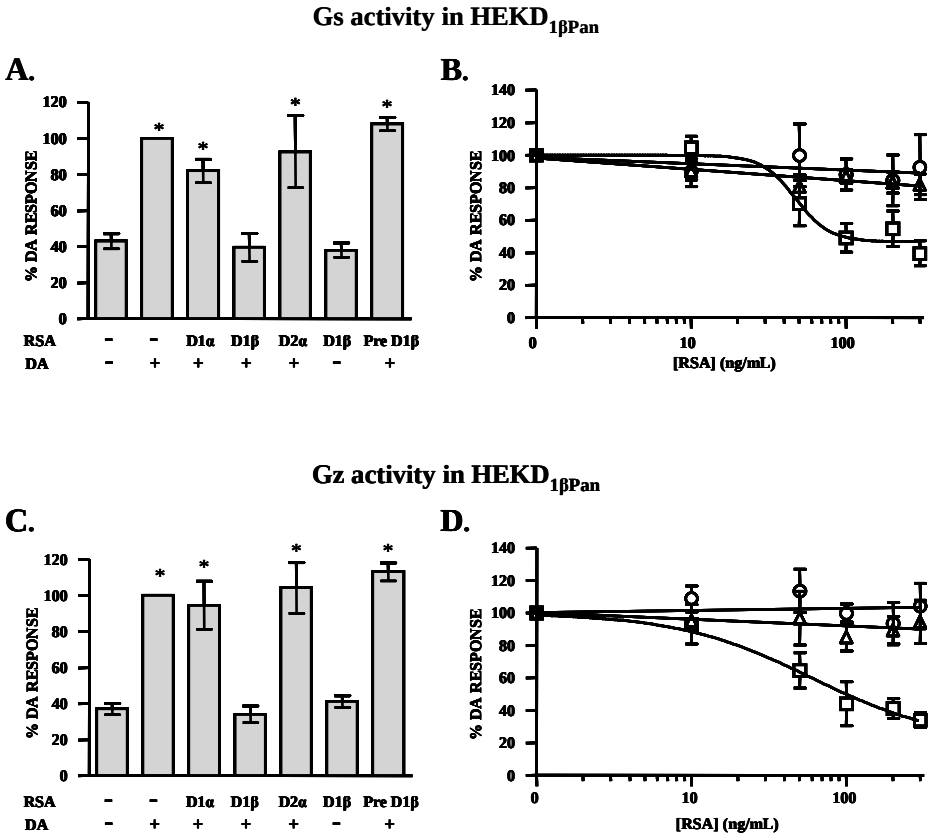

Figure 5-6: Only the $D_{1\beta}$ RSA can significantly uncouple the $D_{1\beta Pan}$ receptor from Gs and Gz. The left panels show the effect of each RSA on $D_{1\beta Pan}$ receptor-G protein coupling. Gs **(A)** or Gz **(C)** activities were measured in HEK $D_{1\alpha Pan}$ membrane preparations in the presence (+) or absence (-) of 10^{-5}M DA and 300ng/ml of an RSA as indicated under each bar. Asterisks indicate a significant difference from no DA no RSA ($p < 0.05$). Data represent the mean $\pm$ S.E.M, $n \geq 3$. The right panels show that RSA uncoupling exhibits a dose-dependency. Gs **(B)** or Gz **(D)** activities were measured in HEK $D_{1\beta Pan}$ membrane preparations in the presence of 10^{-5}M DA and increasing concentrations of an RSA ($D_{1\alpha}$, open triangles; $D_{1\beta}$, open squares, $D_{2\alpha}$ open circles). Data represent the mean $\pm$ S.E.M, $n \geq 3$.

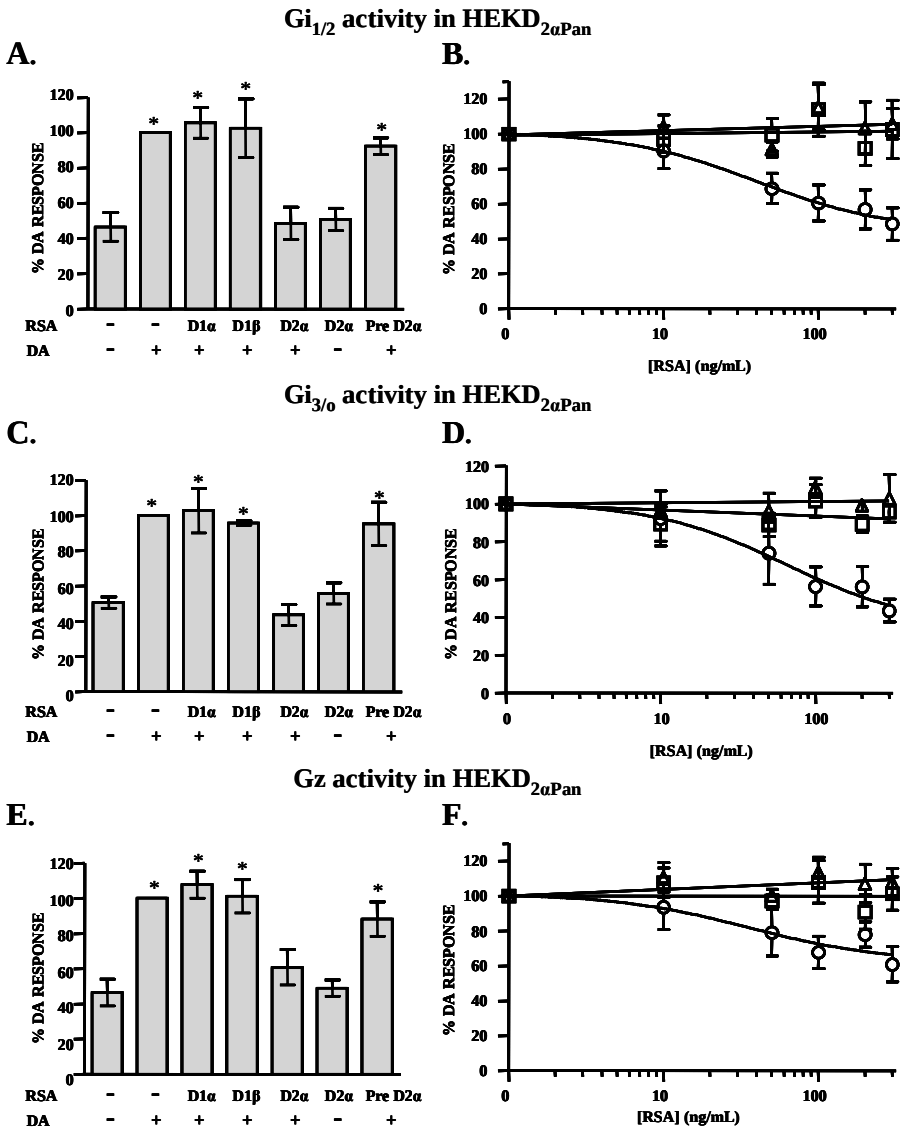

Figure 5-7: Only the $D_{2\alpha}$ RSA can uncouple the $D_{2\alpha Pan}$ receptor from the Gi/o family of G proteins. The left panels show the effect of each RSA on $D_{2\alpha Pan}$ receptor-G protein coupling. Gi_1 and Gi_2 **(A)** or Gz **(C)** or Gi_3 and Go **(E)** were measured in HEK $D_{2\alpha Pan}$ membrane preparations in the presence (+) or absence (-) of 10^{-5}M DA and 300ng/ml of an RSA as indicated under each bar. Asterisks indicate a significant difference from no DA, no RSA ($p < 0.05$). Data represent the mean $\pm$ S.E.M, $n \geq 3$. The right panels show that RSA uncoupling exhibits a dose-dependency. Gi_1 and Gi_2 **(B)** or Gz **(D)** or Gi_3 and Go **(F)** activities were measured in HEK $D_{2\alpha Pan}$ membrane preparations in the presence of 10^{-5}M DA and increasing concentrations of an RSA ($D_{1\alpha}$, open triangles; $D_{1\beta}$, open squares, $D_{2\alpha}$ open circles). Data represent the mean $\pm$ S.E.M, $n \geq 3$.

(Figures 5-7A, 5-7C, 5-7E). In contrast to the $D_{2\alpha}$ RSA, the $D_{1\alpha}$ and $D_{1\beta}$ RSAs had no significant effects on $D_{2\alpha Pan}$ coupling at any concentration tested. Thus, only the $D_{2\alpha Pan}$ RSA can uncouple the $D_{2\alpha Pan}$ receptor from G proteins. In summary, the data indicate that each of the three antibodies produces a significant dose dependent decrease in receptor-G protein coupling for its cognate DAR, but not for any other DAR examined. Therefore, each antibody is a bona fide RSA.

$D_{1\alpha Pan}$ couples with Gs and Gq, $D_{1\beta Pan}$ couples with Gs and $D_{2\alpha Pan}$ couples with Gi in Panulirus STNS membranes

To determine DAR-G protein coupling in the lobster STNS, we performed G protein activation assays on lobster STNS membrane preparations in the presence and absence of DA and each of the RSAs. We reasoned that if an RSA could partially block some aspect of the DA response seen in Figure 5-2B, it would suggest that the corresponding receptor signals through the G protein whose activity had been reduced. These experiments are shown in Figure 5-8. For a given experiment, the membrane preparations were tested with no DA and no RSA (baseline conditions, right panels in Figures 5-8A-C) and with 10^{-5}M DA and increasing concentrations of the indicated RSA (left panels in Figures 5-8A-C). For each experiment all of the data were normalized by G protein activity in the presence of 10^{-5}M DA without RSA. Multiple experiments were averaged and the data are plotted as the percent of the response in 10^{-5}M DA without RSA

Figure 5-.8A illustrates that DA increased Gs activity by 3.1$\pm$0.08-fold ($p < 10^{-4}$, n = 4), Gq activity by 1.9$\pm$0.06- fold ($p < 10^{-4}$, n = 4) and Gi activity by 3.2$\pm$0.05-fold ($p < 10^{-5}$, n = 4). The $D_{1\alpha}$ RSA dose-dependently reduced the DA-induced increase in Gs and Gq, but not Gi

activities. The DA induced increase in Gs activity was significantly reduced by 300ng/ml $D_{1\alpha}$ RSA ($p < 0.005$ for 0 vs. 300ng/ml RSA) such that it was not significantly different from baseline ($p > 0.17$ for 300ng/ml RSA vs. baseline). Similarly, the DA-induced increase in Gq activity was significantly reduced by 300ng/ml $D_{1\alpha}$ RSA ($p < 0.002$) such that it was not significantly different from baseline ($p > 0.35$). On the other hand, 300ng/ml $D_{1\alpha}$ RSA had no significant effect on the DA-induced increase in Gi activity ($p > 0.7$). In sum, the data indicate that the $D_{1\alpha Pan}$ receptor couples with both Gs and Gq.

Figure 5-8B shows that the $D_{1\beta Pan}$ receptor couples solely with Gs in the spiny lobster STNS. Gs activity was significantly reduced in a dose-dependent fashion by the $D_{1\beta}$ RSA ($p < 10^{-4}$ for 0 vs. 300ng/ml $D_{1\beta}$ RSA, n= 3). The $D_{1\beta}$ RSA reduced Gs activity to levels that were not significantly different than baseline ($p > 0.08$). On the other hand, there were no statistically significant changes in Gq ($p > 0.2$) or Gi ($p > 0.4$) activities in response to increasing concentrations of the RSA. Further, although it appears that Gi activity increases with increasing [D1β RSA], perhaps suggesting an interaction between Gs and Gi (e.g. competition for Gβγ subunits), a linear regression did not reveal a statistically significant correlation between the rise in Gi and the reduction in Gs activities with increasing [RSA].

Figure 5-8C illustrates that the lobster $D_{2\alpha Pan}$ receptor couples with Gi alone. At 200ng/ml the $D_{2\alpha}$ RSA significantly reduced the DA induced increase in Gi activity ($p < 0.02$, n = 3). Furthermore, at concentrations of 10ng/ml or higher, the $D_{2\alpha}$ RSA reduced Gi activity to levels that were not significantly different than baseline ($p > 0.88$). On the other hand, the D2α RSA had no significant effect on DA-induced increases in Gs ($p > 0.9$) or Gq ($p > 0.68$) activities. In summary, the data suggest that $D_{1\alpha Pan}$ couples with Gs and Gq, $D_{1\beta Pan}$ couples with Gs and $D_{2\alpha Pan}$ couples with Gi in STNS membrane preparations.

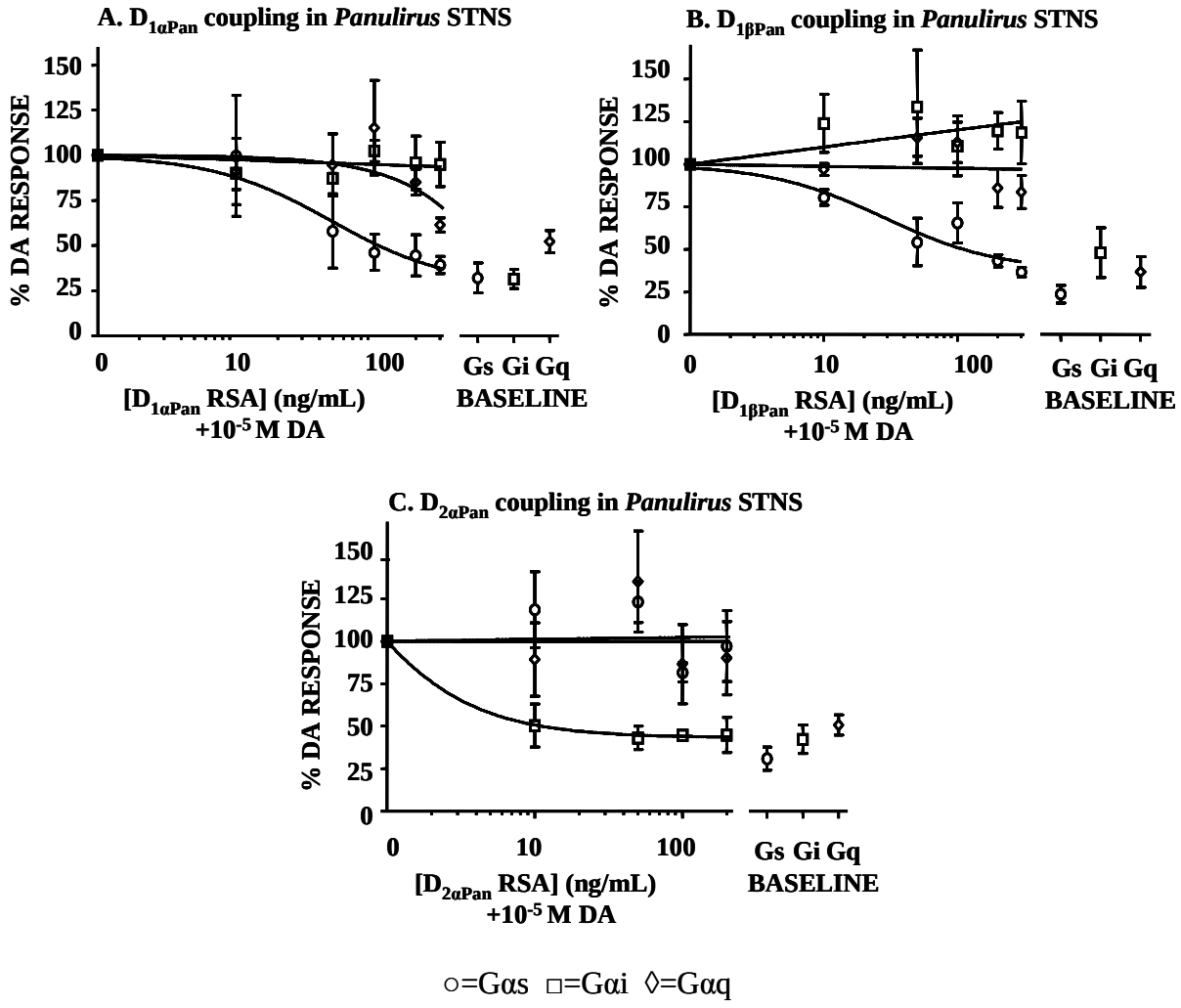

Figure 5-8: DAR-G protein couplings in *Panulirus* STNS membranes. (A) The $D_{1\alpha Pan}$ receptor couples with Gs and Gq, but not Gi, in *Panulirus* STNS membranes. G protein activities in *Panulirus* STNS membrane preparations were measured either in the presence of 10^{-5}M DA and increasing concentrations of the $D_{1\alpha}$ RSA, or in the absence of DA and the RSA (baseline conditions). Two STNS were used per experiment, and the experiment was repeated four times. Thus, each data point in panel A represents 8 lobsters. **(B)** The $D_{1\beta Pan}$ receptor couples with Gs, but not Gq or Gi, in *Panulirus* STNS membranes. G protein activities in *Panulirus* STNS membrane preparations were measured either in the presence of 10^{-5}M DA and increasing concentrations of the $D_{1\beta}$ RSA or in the absence of DA and the RSA (baseline conditions). Two STNS were used per experiment, and the experiment was repeated three times. Thus, each data point in panel B represents 6 lobsters. **(C)** The $D_{2\alpha Pan}$ receptor couples with Gi, but not Gs or Gq, in *Panulirus* STNS membrane preparations. G protein activities in *Panulirus* STNS membrane preparations were measured either in the presence of 10^{-5}M DA and increasing concentrations of the $D_{2\alpha}$ RSA or in the absence of DA and the RSA (baseline conditions). Two STNS were used per experiment, and the experiment was repeated three times. Thus each data point in panel C represents six lobsters. In all, 20 lobsters were used in these experiments (8, panel A + 6, panel B + 6, panel C). Data are represented as the mean $\pm$ S.E.M.

Discussion

The crustacean STNS is an important model system for understanding the involvement of neuromodulators in motor control. It was previously shown that DA can alter CPG output by modulating multiple ionic conductances in component neurons in a cell specific manner. DA altered the biophysical properties of ion channels throughout neurons, including channels in the soma and the neuropil. Here we begin to define the molecular mechanisms underlying these changes. We found that DA activates Gs, Gi and Gq in the STNS of all five crustacean species examined. Further, we demonstrated that the three known DARs were all expressed in the spiny lobster STG and were exclusively localized to the synaptic neuropil where the $D_{1\alpha Pan}$ receptor coupled with Gs and Gq, the $D_{1\beta Pan}$ receptor coupled with Gs and the $D_{2\alpha Pan}$ receptor coupled with Gi. The expression of multiple receptors with distinct G protein couplings in the STNS can help to explain the previously documented, cell specific modulation of ionic conductances by DA.

In other systems DARs are known to alter local target protein activity through multiple G protein-dependent and -independent mechanisms. Our data suggest that STNS DARs can also alter cell function locally through G protein transduction cascades. Unfortunately, our data do not predict how a given receptor will alter second messengers, but the literature suggests that STNS DARs will most likely modulate [cAMP] and [Ca^{2+}]. Regardless of the details, both Gα and Gβγ subunits will indirectly modulate local second messenger levels, and this in turn will alter kinase and phosphatase activities, which will modify the phosphorylation states of ion channels and thereby change neuronal excitability and circuit output. Independent of second messengers, the Gβγ subunits can also directly modulate ion channels (Dascal 2001). In addition, Gβγ subunits are known to directly regulate the synaptic release machinery (Blackmer et al.

2005; Gerachshenko et al. 2005), which could partially account for DA induced alterations in synaptic strengths within the circuit (Johnson and Harris-Warrick 1990).

STNS DARs may also generate more global signals. On the one hand, we have shown that DA-Rs are not in the plasma membrane surrounding pyloric somata or primary neurites. Indeed, DARs are at least hundreds of microns away from the primary neurite and are found exclusively in the neurolemma encompassing fine neurites and/or terminals in the synaptic neuropil (Figure 5-4). On the other hand, two electrode voltage clamp studies suggest that DA alters somatic ion channels within seconds of application (Hartline et al. 1993; Kloppenburg et al. 1999). Together these data suggest that pyloric DARs might transduce constant bath applied DA into a global signal. Second messengers have the potential for rapid diffusion and could therefore propagate a global signal. One possibility is that at least some STNS DA-Rs produce global changes in cAMP since (1) previous imaging studies on STG neurons revealed that neuromodulator-induced increases in $[cAMP]_i$ were initially generated in the fine neurites and diffused to the soma with time (Hempel et al. 1996a), (2) STNS DA-Rs activate G protein cascades that modulate $[cAMP]_i$ (Clark and Baro 2006, 2007), and (3) experimental and computational studies on a variety of cell types have shown that GPCRs that couple with Gs can generate small and sustained global changes in $[cAMP]_i$ (Rich et al. 2001; Dyachok et al. 2006; Nikolaev et al. 2006; Rochais et al. 2006; Gervasi et al. 2007). Alternatively, DA-Rs may produce global changes in Ca^{2+}. Mammalian and arthropod D_1 (Reale et al. 1997) and D_2 receptors, including $D_{2\alpha Pan}$ (Tsu and Wong 1996; Clark and Baro 2007), are known to activate PLCβ via Gβγ subunits, and in some cases increase $[Ca^{2+}]_i$ (Nishi et al. 1997; Hernandez-Lopez et al. 2000). In addition, $D_{1\alpha Pan}$ receptors couple with Gq, which is traditionally thought to release Ca^{2+} stores. It might also be argued that second messenger effectors (i.e. proteins) rather than the

second messengers themselves diffuse to the soma. Given the size difference, protein diffusion should be a much slower process. Moreover, it has been shown that in *Aplysia* neurons PKA is distinct in the soma (PKA I) and terminals (PKA II), and PKA I is responsible for activating nuclear CREB in response to neuromodulators acting at distant terminals (Liu et al. 2004).

Our work reinforces the idea that receptor-G protein interactions are highly preserved throughout evolution. Spiny lobster DARs are not only highly conserved at the amino acid level, but they show the same couplings in native and heterologous systems as is observed with receptors from other species (Clark and Baro 2006, 2007). Interestingly, DA seemed to activate Gs to a lesser extent in *M. rosenbergii* than in other species (Figure 2B). This could reflect a difference in DAR and/or G protein distribution patterns across species, but without sequence data we cannot rule out technical reasons for the variation. For example, the anti-Gs antibody used in the G protein assay may not recognize the *M. rosenbergii* Gs protein as well as the Gs protein in other species.

Finally, the data demonstrate that lobster DAR signaling is context dependent. G protein couplings in the native system are different from that in HEK cell lines. The $D_{1\alpha Pan}$ receptor only couples with Gs in HEK cells (Clark and Baro 2006), but Gs and Gq in the lobster STNS. $D_{1\beta Pan}$ couples with Gs and Gi/o protein families in HEK cells, but only Gs in the STNS. Differential coupling according to cell type has been reported for DARs from a variety of species and cell types (Sidhu and Niznik 2000). Together, these data suggest that a given DAR can interact with a limited repertoire of G proteins, and that the cellular environment further restricts the range of interactions and helps to define the specific DAR-G protein couplings that occur in a given cell type.

CHAPTER SIX

DA RECEPTOR EXPRESSION IN IDENTIFIED PYLORIC NEURONS

NOTE: I PERFORMED ALL EXPERIMENTS IN THIS CHAPTER

Introduction

DA reconfigures pyloric circuit output by altering component neuron intrinsic firing properties, synaptic strengths, and axonal spike initiation (Selverston and Miller 1980; Anderson and Barker 1981; Eisen and Marder 1984; Marder and Eisen 1984; Flamm and Harris-Warrick 1986a, b; Harris-Warrick and Flamm 1987; Johnson and Harris-Warrick 1990; Johnson et al. 1995; Ayali and Harris-Warrick 1998, 1999; Bucher et al. 2003; Johnson et al. 2005; Szucs et al. 2005). As previously stated, many types of voltage dependent ionic conductances are differentially modified by bath applied DA (Table 1-1) (Harris-Warrick et al. 1995a; Harris-Warrick et al. 1995b; Kloppenburg et al. 1999; Kloppenburg et al. 2000; Peck et al. 2001; Johnson et al. 2003; Gruhn et al. 2005; Peck et al. 2006). The differential modulation of ionic conductances in pyloric neurons plays a key role in sculpting cell-type specific responses to DA.

The LP and PD neurons represent two pyloric neurons that are differentially modulated by DA. DA enhances spiking activity in the LP neuron and causes it to fire earlier in the cycle then under control conditions (Eisen and Marder 1984; Flamm and Harris-Warrick 1986a). DA's excitatory effects in the LP are partially due to a decrease in I_A, and an increase in I_h and I_{Ca} (Harris-Warrick et al. 1995b; Johnson et al. 2003). In contrast, DA has purely inhibitory effects on the PD neuron, which is partially due to an increase in I_A, and a decrease in I_{Ca} (Kloppenburg et al. 1999; Johnson et al. 2003). DA has no effect on I_h in the PD neuron (Peck et al. 2006). The fact that DA modulates two currents in opposing directions in these two neurons may suggest a common pathway. Interestingly, DA modulation of I_h is not exactly opposite in these two cell types, suggesting that perhaps I_h is modulated by a distinct pathway.

We have previously shown that dopaminergic responses in the lobster STNS are mediated by multiple, highly conserved DARs that signal via G protein transduction cascades. We demonstrated that the three known DARs ($D_{1\alpha Pan}$, $D_{1\beta Pan}$, and $D_{2\alpha Pan}$) are all expressed in the spiny lobster STG and are exclusively localized to the synaptic neuropil. Depending on the cellular environment, both type-

1 and type-2 lobster DARs can produce an increase or a decrease in cAMP. To explain the fact that DA has opposite effects on I_A and I_{Ca} in LP and PD, we hypothesized that the LP and PD neurons express DARs that have opposing effects on cAMP (e.g., cAMP is increased via type-1 DARs in the LP and decreased via type-2 DARs in the PD). As a first step toward testing this hypothesis, we set out to define DAR distribution patterns in LP and PD neurons.

We used our previously published single cell RT-PCR protocol (Baro et al. 1996) to determine which DAR transcripts are expressed in the PD and LP neurons. We found that the PD neuron expresses only $D_{2\alpha Pan}$ transcripts (n=5, Baro, unpublished), while the LP neuron expresses only $D_{1\alpha Pan}$, and $D_{1\beta Pan}$ transcripts (n=1, Baro, unpublished). Here, we investigate DAR protein expression and localization in the LP and PD neurons. We demonstrate that receptor expression profiles are cell-type specific, and are consistent with previously described cell-specific, DA-induced electrophysiological changes. Further, DAR distributions within pyloric neurons are regulated such that expression is restricted to putative synaptic terminals.

Materials and Methods

Immunocytochemistry (ICC) and cell fills

The STNS was dissected from the lobster, desheathed, and pinned in a Sylgard-lined dish. The STG was desheathed, and the preparation was constantly bathed in *Panulirus* saline (479 mM NaCl, 12.8 mM KCl, 13.7 mM $CaCl_2$, 39 mM Na_2SO_4, 10 mM $MgSO_4$, 2 mM glucose, 4.99 mM HEPES, 5 mM TES; pH 7.4). Using standard intracellular and extracellular recordings, neurons were identified by correlating action potentials from somatic intracellular recordings with extracellularly recorded action potentials on identified motor nerves, and by their characteristic shape and timing of oscillations (Figure 1-4). Identified neurons were filled with a lysine fixable, dextran coupled Texas Red fluorophore that cannot pass through gap junctions

(M.W. 10,000; Molecular Probes). This was accomplished by pressure injecting a 1% solution of the fluorophore in 0.2 M KCl using 20 msec pulses at 0.05 Hz and 28 psi for 10 min. The fluorophore was allowed to diffuse at room temperature for 2-24 hours at room temperature. The STG was then fixed in 3.2% paraformaldehyde (in 1X PBST; PBS plus 0.3% Triton X-100) for 30 minutes at room temperature.

Antibodies were used in ICC protocols as previously described (Baro et al. 2000; Clark et al. 2004). Following fixation, samples were washed with 8 changes (15 minutes each) of PBST at 4°C with continuous shaking. The preparation then received primary antibody (anti- $D_{1\alpha Pan}$, $D_{1\beta Pan}$ or $D_{2\alpha Pan}$) plus 5% normal goat serum in PBST. Samples were incubated at 4°C overnight. Primary antibody was washed out over 2-8 hours with 8 changes of PBST at 4°C with constant shaking. The secondary antibody (goat anti-rabbit IgG conjugated to FITC) was then added, and samples were incubated overnight 4°C. Secondary antibody was washed out over 2-8 hours with 8 changes of PBS at 4°C with constant shaking. Samples were then mounted on poly-L-lysine coated coverslips and dehydrated using an ethanol series (2 X 30%, 10 min; 2 X 50%, 10 min; 2 X 75%, 10 min; 3X 100%, 10 min). Samples were cleared 2 times in xylene (10 min. each), and mounted on slides using DPX mounting media. Slides were dried 2-3 days and visualized using confocal microscopy.

In some experiments, fixed ganglia were imbedded in 40°C warm, 4% low melting point agarose (Sigma, St. Louis, MO) in *Panulirus* saline prior to antibody treatment. Slices (50-70 µm) were made with a Lancer Series 1000 vibratome (Vibratome, St. Louis, MO) and transferred to PBST filled wells. Antibody treatment was performed on the floating agarose sections, as described above.

Confocal imaging

All images were obtained with a Zeiss LSM510 confocal imaging system (Oberkochen, Germany). Confocal projections were constructed using the LSM510 Image Examiner or Image Browser software (version 4.2.0.121, Zeiss). Color enhancements were performed with Adobe Photoshop 7.0 software (Adobe Systems, Mountain View, CA).

3D Reconstruction and analysis of PD neurons

To render 3D models of PD neurons, we obtained overlapping confocal stacks (13-17 stacks per animal) spanning the entire neuron, up to the point where the axon exits the STG via the dvn (n=3). Each stack was comprised of 1 µm dorsal to ventral confocal slices. After imaging the entire neuron, the stacks were imported into the Neurolucida imaging software package (MicroBrightField, Inc.). Neurolucida was used to manually trace the PD neuron, keeping the length and diameter of the soma and all traced neurites matched to the actual filled structures. Neurolucida compiled volume measurements for each traced structure, and recorded the 3D position of each branch origin and ending. These values were then imported into the NeuroExplorer software program (MicroBrightField, Inc.), which constructed a morphological model of the cell as a composition of cylinders. As neuronal branches were traced, markers were placed to indicate the presence or the absence of the $D_{2\alpha Pan}$ receptor. We additionally placed markers where we observed varicosities at the end of or along neurites, representing putative synaptic terminals. The position of any markers that were placed was stored by the Neurolucida program, and those 3D values were also imported into the NeuroExplorer program to perform an analysis of $D_{2\alpha Pan}$ distribution in completed PD tracings.

For comparison of the spatial distribution of neuronal branches for three PD neurons, we used 3D Grapher software (version 1.21; RomanLab, Vancouver, BC, Canada). Data for each terminal point (obtained from the Neurolucida program, described above) were imported into the 3D grapher program to generate a 3D plot for all terminals for each of the three PDs. To construct figure 6-8, the position where the dvn begins (i.e., the most posterior point of the ganglion) was set to zero for three dimensions (X=0, Y=0, Z=0) for each PD. Thus, all X, Y, Z values for a given PD terminal are relative to the dvn for the same PD. In this way, we could compare PD terminal distributions across three preparations.

Animals

Pacific spiny lobsters (*Panulirus interruptus*) were obtained from Don Tomlinson Commercial Fishing (San Diego, CA). Lobsters were maintained at 16°C in constantly aerated and filtered seawater. All animals were anesthetized by cooling on ice prior to experiments.

Results

The $D_{2\alpha}$ receptor is transported to putative synaptic sites in the PD neuron

There are 3 known DARs that could potentially mediate DA-induced changes in pyloric neurons: $D_{1\alpha}$, $D_{1\beta}$, and $D_{2\alpha}$. We previously found that all of these receptors are expressed in the STG, and they each couple with distinct signaling cascades (Clark et al. 2008). We further found that the PD neuron expresses only $D_{2\alpha Pan}$ transcripts, while the LP neuron expresses only $D_{1\alpha Pan}$, and $D_{1\beta Pan}$ transcripts (not shown). To determine whether protein distributions in the PD and LP neurons were consistent with our previous RT-PCR studies, we performed

immunocytochemistry (ICC) experiments on STG wholemount preparations containing dye-filled PD neurons, as described in Materials and Methods.

Figure 6-1A shows a monopolar STG neuron. As described in Chapter 5, the single process extending from the soma is termed the primary neurite. The primary neurite (1) branches in the STG (shown in Figure 6-1) and (2) extends beyond the STG and into the dvn, at which point it is termed an axon (not shown in Figure 6-1). A neuron's processes can be broadly classified as large diameter and small diameter. The large and small diameter neuronal processes are found in the central core and periphery of the STG, respectively (Figure 5-4A-B). We determined $D_{2\alpha Pan}$ subcellular distributions within the PD by performing ICC experiments on dye-filled PD neurons (n=5). We observed $D_{2\alpha Pan}$ immunoreactivity in organelles within the soma, likely the ER and Golgi apparatus, and in cytoplasmic transport vesicles in the primary neurite (Figure 6-1B). There was no staining in the plasma membrane of the soma or primary neurite.

The receptor appeared to be transported to some, but not all higher order neurites. The arrows in Figure 6-1C indicate neurites without $D_{2\alpha Pan}$. For this figure, we constructed a maximum intensity confocal projection of the same PD neuron shown in Figure 6-1B in order to detect receptors present in low abundance. At lower intensity, vesicles in the primary neurite showed a punctuate distribution as in Figure 6-1B. The staining intensity among higher order neurites did not vary according to distance from the soma, and our data suggest that $D_{2\alpha Pan}$ receptors are differentially transported through PD neurites (see below, and Discussion). Whereas $D_{2\alpha Pan}$ receptors were clearly in the cytoplasm of higher order processes, careful examination of 1 µm optical sections throughout a neuron suggested that they were not in the plasma membrane of these processes (n=3 neurons).

The $D_{2\alpha Pan}$ receptor was localized to the plasma membrane of varicosities and/or neurites less than 2μm in diameter. These regions could represent synaptic structures. Synaptic contacts within the STG are found at specialized swellings along neural processes and at the terminals of fine neurites (King 1976b, a; Kilman and Marder 1996). Synaptic structures are bulbous with diameters of 3-10 μm. As diagrammed in Figure 6-1D, a single synaptic structure contains both pre- and post-synaptic elements. Electron microscopy studies showed that a single varicosity contains multiple presynaptic release sites, while postsynaptic elements are housed within fingerlike projections extending from the presynaptic varicosity (King 1976a). These projections can be less than 1 μm in diameter. At low magnification, we observed patches of $D_{2\alpha Pan}$ immunoreactivity in several putative synaptic varicosities (e.g. arrowheads in Figure 6-1C). Higher magnification images taken from deep within the synaptic neuropil also revealed dense $D_{2\alpha Pan}$ staining in the varicosities of PD neurons (arrowheads in Figure 6-1E, n=5 ganglia), as well as in unidentified neurons (green staining in Figure 6-1E). It is not clear if the receptor is located in the pre- and/or post-synaptic compartments, or if it is in the membrane or the cytosol of these varicosities. To further examine $D_{2\alpha Pan}$ distribution in putative synaptic terminals, we obtained high magnification images of clusters of PD varicosities (n=3 neurons). Figure 6-1F shows a 4 μm confocal projection of one such cluster. $D_{2\alpha Pan}$ receptors appear to be localized to the plasma membrane in some varicosities. In this image, the cytoplasmic ridge seen in Figures 6-1C and 6-1E is absent, and receptor staining is not concentrated toward the center of the varicosities. Rather, immunoreactivity is seen in dense patches along the periphery, and in some cases, toward one side of a given varicosity. At this magnification, we also observed tufts of green on some varicosities (arrows in Figure 6-1F). As the antibody used in our ICC experiments

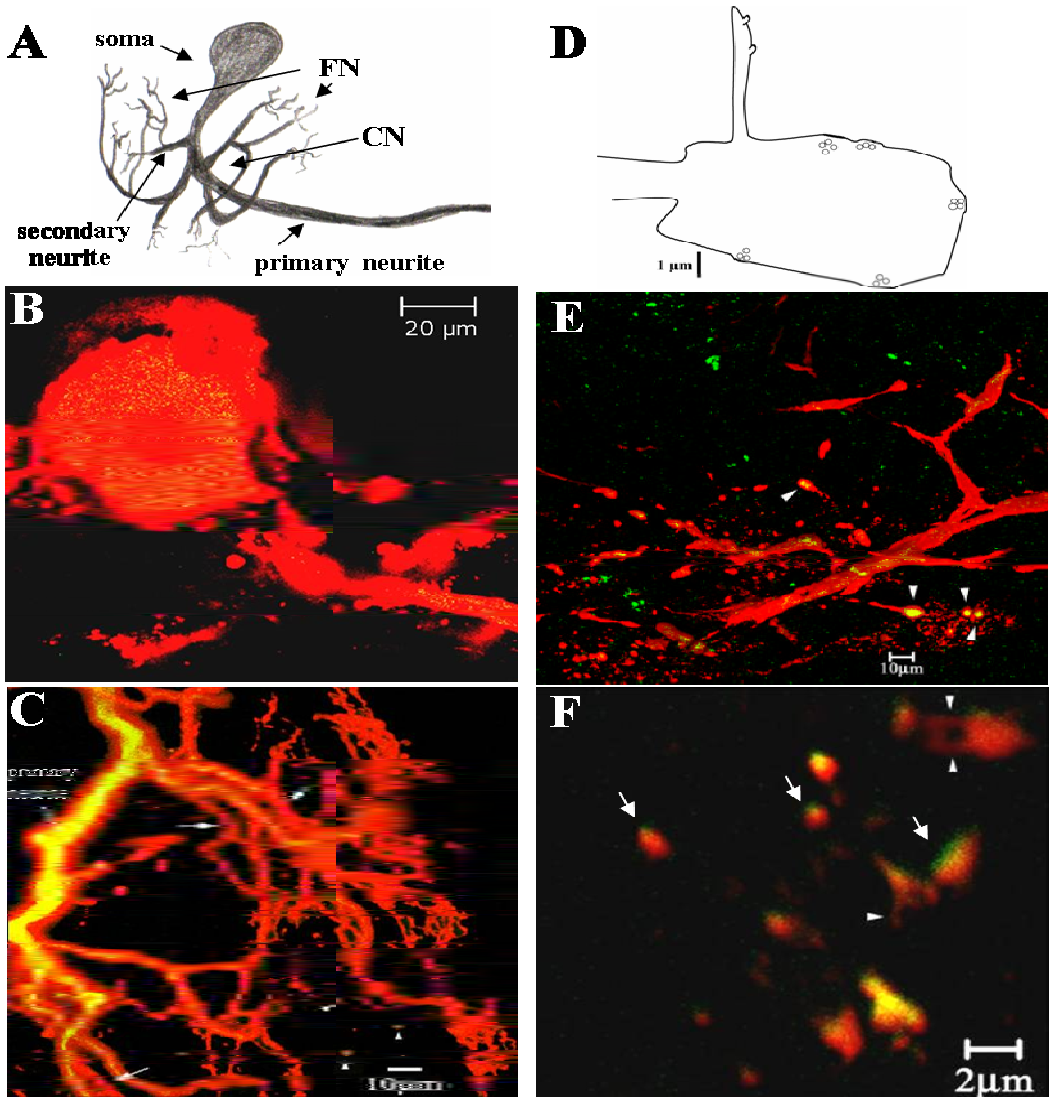

Figure 6-1: $D_{2\alpha}$ expression in the PD neuron (n=5). (**A**) Drawing of a monopolar STG neuron. A single primary process gives rise to large diameter neurites in the central, coarse neuropil (CN) of the ganglion. Fine neurites (FN) and synapses are in the outer, fine neuropil. The primary neurite leaves the STG posteriorly, via the dvn. (**B**) Merged confocal slice (1µm) of a PD neuron filled with texas red. Yellow staining indicates $D_{2\alpha}$ expression in the soma and primary neurite. (**C**) 34µm merged confocal projection of the same PD as in A. $D_{2\alpha}$ receptors are in cytoplasmic transport vesicles in the primary neurite, and some higher order neurites. Arrows indicate neurites lacking the receptor. Arrowheads show $D_{2\alpha}$ in putative synaptic terminals. (**D**) STG synaptic terminal drawn to scale. The bulbous structure contains multiple presynaptic release sites. A fingerlike projection extending from the bulb houses 2 postsynaptic contacts. (**E**) 29µm merged confocal projection from deep within the synaptic neuropil shows a single tertiary and higher order neurites. Arrowheads as in C. Green staining shows $D_{2\alpha}$ in unidentified neurons. (**F**) High magnification 4 µm projection from synaptic neuropil showing a cluster of putative PD terminals, some of which contain $D_{2\alpha}$. Fingerlike processes extend from the bulbous structure (arrowheads).

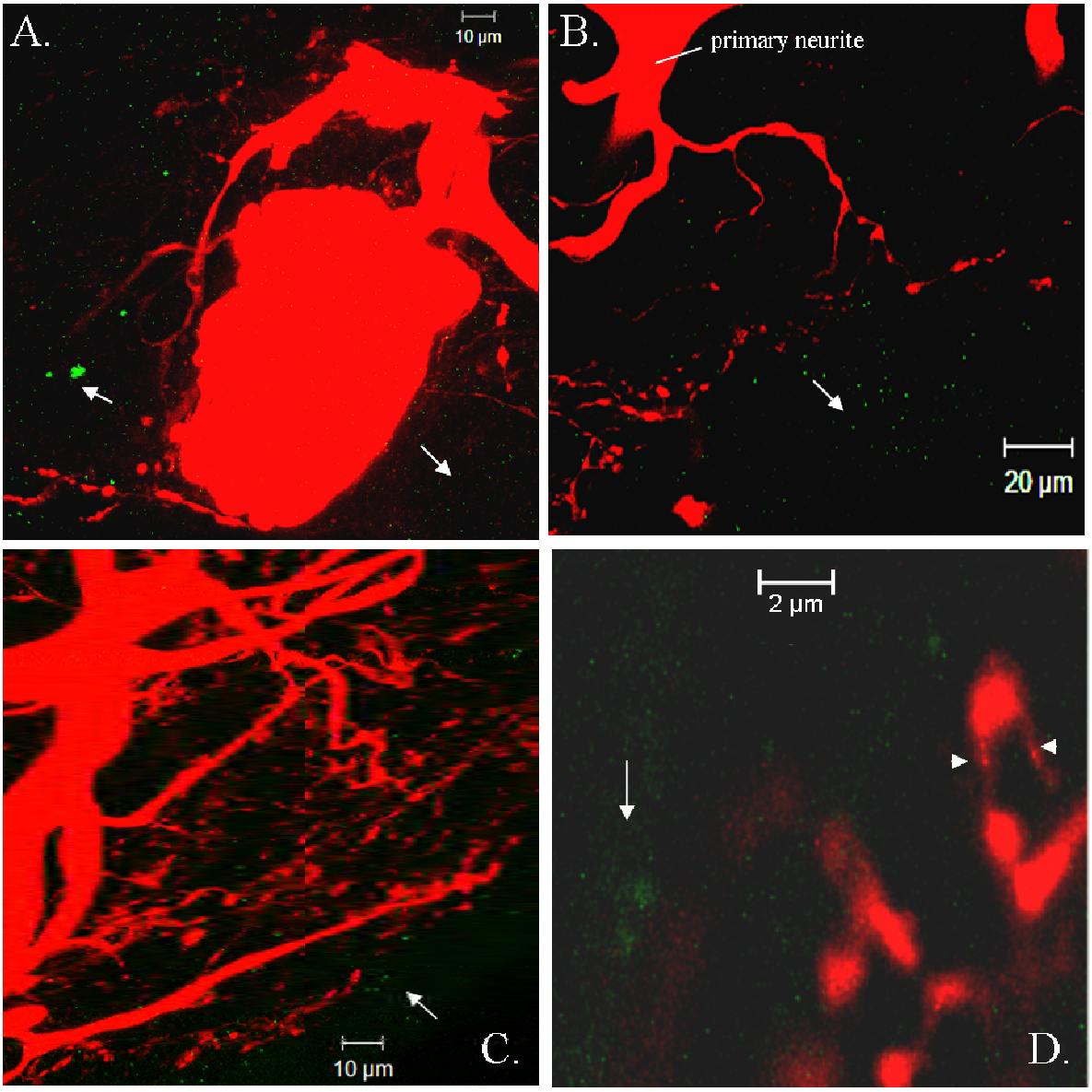

Figure 6-2: $D_{1\alpha Pan}$ is not expressed in the PD neuron. PD neurons were filled with texas red, then processed for ICC using anti-$D_{1\alpha Pan}$ (n=3). Green staining shows $D_{1\alpha Pan}$ in unidentified neurons (arrows in all panels). (**A**) Merged confocal projection (22µm) showing the PD soma and neurites. (**B**) 10µm merged confocal projection of another filled PD neuron. Primary neurite is indicated. (**C**) Merged confocal projection (35µm) from deep within the neuropil. (**D**) High magnification 5µm projection from synaptic neuropil showing a cluster of putative PD terminals. Fingerlike processes extend from the bulbous structure (arrowheads).

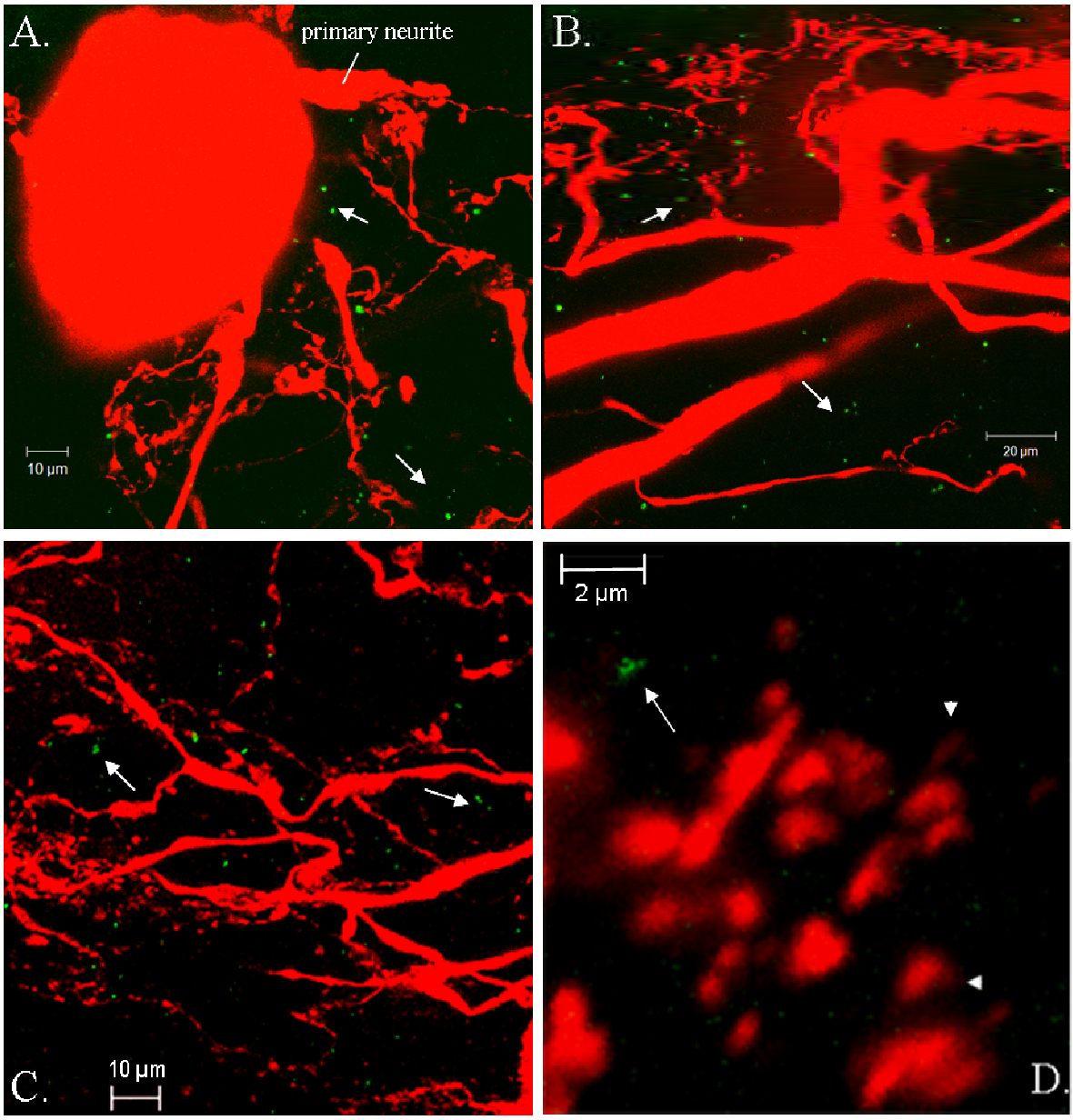

Figure 6-3: $D_{1\beta Pan}$ is not expressed in the PD neuron. PD neurons were filled with texas red, then processed for ICC using anti-$D_{1\beta Pan}$ (n=3). In all panels, green staining shows $D_{1\beta Pan}$ in unidentified neurons (arrows in all panels). (**A**) Merged confocal projection (16µm) shows the PD soma and primary neurite. (**B**) 30µm merged confocal projection of the same PD as in A. (**C**) Merged confocal projection (30µm) from deep within the neuropil. (**D**) High magnification 6µm projection from synaptic neuropil showing a cluster of putative PD terminals. Fingerlike processes extend from the bulbous structure (arrowheads).

recognizes extracellular epitopes, this staining may underscore the extracellular localization of the protein and further imply that $D_{2\alpha Pan}$ receptors are inserted into the synaptic membrane. Arrowheads in this figure indicate the finger-like putative postsynaptic structures described by King (1976a) (Figure 6-1D). Unfortunately, we cannot confirm if $D_{2\alpha Pan}$ is localized to pre- and/or postsynaptic sites without performing electron microscopy.

We tested for $D_{1\alpha Pan}$ immunoreactivity in the PD neuron (n=3). Figure 6-2 shows confocal images of a filled PD neuron that was processed for ICC using the $D_{1\alpha Pan}$ antibody. We observed no $D_{1\alpha Pan}$ staining in the soma or primary neurite (Figure 6-2A-B) or in fine neurites (Figure 6-2B-C), though green staining in these images shows $D_{1\alpha Pan}$ immunoreactivity in unidentified neurons (arrows in Figure 6-2). High magnification images taken from deep within the neuropil show that $D_{1\alpha Pan}$ receptor staining is absent in putative PD terminals (Figure 6-2D). Thus, consistent with the results of the single cell RT-PCR experiments, it appears that the PD neuron does not express the $D_{1\alpha Pan}$ protein.

We also tested for expression of the $D_{1\beta Pan}$ receptor in PD neurons. Figure 6-3 shows filled PD neurons that were imaged after performing ICC experiments using the $D_{1\beta Pan}$ antibody (n=3). The receptor is not present in the soma or primary neurite (Figure 6-3:A-B), neuronal branches (Figure 6-3:B-C), or putative synaptic terminals (Figure 6-3:D). Thus, the PD neuron expresses the $D_{2\alpha Pan}$, but not the $D_{1\alpha Pan}$ or $D_{1\beta Pan}$ receptors.

The LP neuron expresses $D_{1\alpha}$ and $D_{1\beta}$ receptors at putative synaptic terminals

We next examined receptor expression patterns in the LP neuron using the same methods as described above for the PD. Figure 6-4 shows a filled LP neuron that was processed for ICC using an antibody against the $D_{1\alpha Pan}$ receptor (n=3). We did not identify receptor staining in the

soma or larger order branches of the LP neuron. However, we did observe $D_{1\alpha Pan}$ immunoreactivity in several putative synaptic terminals (Figure 6-4A-C, arrows indicate $D_{1\alpha Pan}$ staining in putative terminals). A high magnification image shows $D_{1\alpha Pan}$ immunoreactivity in dense patches near the edge of varicosities, and green tufts are visible on some of these patches (Figure 6-4D). Thus, the LP neuron expresses the $D_{1\alpha Pan}$ receptor at putative synaptic terminals.

$D_{1\beta Pan}$ immunoreactivity in the LP neuron is shown in Figure 6-5 (n=3). The staining pattern is similar to that of the $D_{1\alpha Pan}$ antibody (Figure 6-4). $D_{1\beta Pan}$ immunoreactivity is absent from the soma or larger order branches of the LP neuron (Figure 6-5A-B), but dense staining is evident in several putative synaptic terminals at low (Figure 6-5C) and high (Figure 6-5D) magnification. The high magnification image (Figure 6-5D) shows that $D_{1\beta Pan}$ staining occurs in patches toward the edges of LP varicosities. We did not observe green tufts on the edge of the varicosities, which is consistent with the fact that this antibody recognizes an intracellular epitope. Together, the data suggest that the LP neuron expresses $D_{1\beta Pan}$ in putative synaptic terminals.

Interestingly, the D_1 antibodies did not recognize receptors in organelles and transport vesicles as did the D_2 antibody. Differences are not unexpected because all three antibodies were generated against different regions of the receptors, and one vs. two peptide antigens was used to produce the D_1 vs. D_2 antibodies. Perhaps the epitopes used to generate the D_1 antibodies were inaccessible during receptor transport. Alternatively, the receptors may be in a highly diffuse state during transport and only detectable when concentrated in the terminals.

Figure 6-6 shows images of LP neurons that were tested for $D_{2\alpha Pan}$ expression. We observed no $D_{2\alpha Pan}$ immunoreactivity in the LP neuron (Figure 6-6A-C, n=3). High magnification images of a cluster of LP varicosities confirm that the $D_{2\alpha Pan}$ receptor is absent

from putative synaptic terminals in the LP (Figure 6-6D), though receptor immunoreactivity was observed in terminals of unidentified neurons (arrows in all panels). Collectively, these data show that in *Panulirus interruptus*, the LP neuron expresses $D_{1\alpha Pan}$ and $D_{1\beta Pan}$, but not $D_{2\alpha Pan}$ receptors.

3D renderings of the PD neuron

Our ICC results revealed that $D_{2\alpha Pan}$ expression is not homogenous within the PD neuron, and functional receptors are most likely localized to synaptic terminals (Figure 6-1). These findings led us to further explore $D_{2\alpha Pan}$ distribution in the PD. To this end, we rendered 3D models of dye-filled PD neurons that were stained with anti-$D_{2\alpha Pan}$.We imported confocal images (for examples, see Figure 6-1) into a software program (Neurolucida, MicroBrightField, Inc.) that enabled us to manually trace a filled neuron. The program calculated the three dimensional position of each point traced along the neuron based on an original reference location, so that an accurate 3D representation was created. We designated a hierarchical branch order based on point of origin: secondary branches arose from a single primary neurite, which emerged from the soma and left the STG posteriorly. Secondary branches gave rise solely to tertiary branches, which then gave rise to quaternary, and so on. Similar to Bucher et al. (2007), we observed cases where two secondary branches emerged from the primary neurite at an enlarged region containing multiple nodes. These were less extensive than the “hand-like” branching structure, described in *Homarus americanus* (Bucher et al. 2007), however, and we were able to clearly identify the branch origin point for all secondaries. The origin and ending of the finest neurites (< 1 μm diameter) was not always obvious. In all cases, branches were only traced if the origin

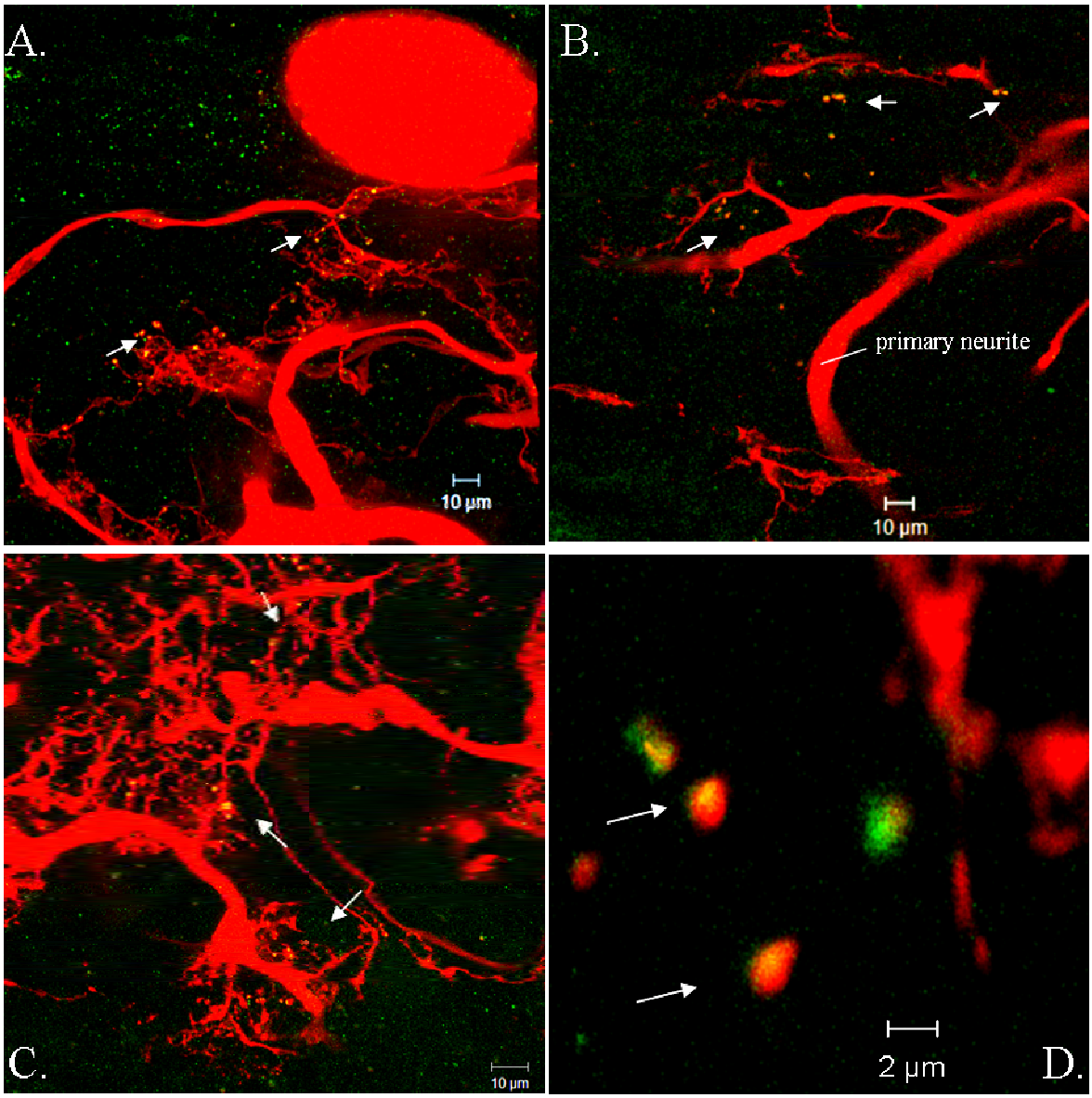

Figure 6-4: $D_{1\alpha Pan}$ expression in the LP neuron. LP neurons were filled with texas red, then processed for ICC using anti-$D_{1\alpha Pan}$ (n=3). Yellow staining shows $D_{1\alpha Pan}$ expression within the neuron. In A-C, green staining shows $D_{1\alpha Pan}$ in unidentified neurons.Clusters of putative terminals expressing the receptor are indicated by arrows in all panels. (**A**) Merged confocal projection (50µm) showing the LP soma and neurites. (**B**) 8µm merged confocal projection of another filled LP neuron. Primary neurite is indicated. (**C**) Merged confocal projection (36µm) of the same LP shown in A. Image is from deep within the neuropil. (**D**) High magnification 6µm projection from synaptic neuropil showing a cluster of putative LP terminals.

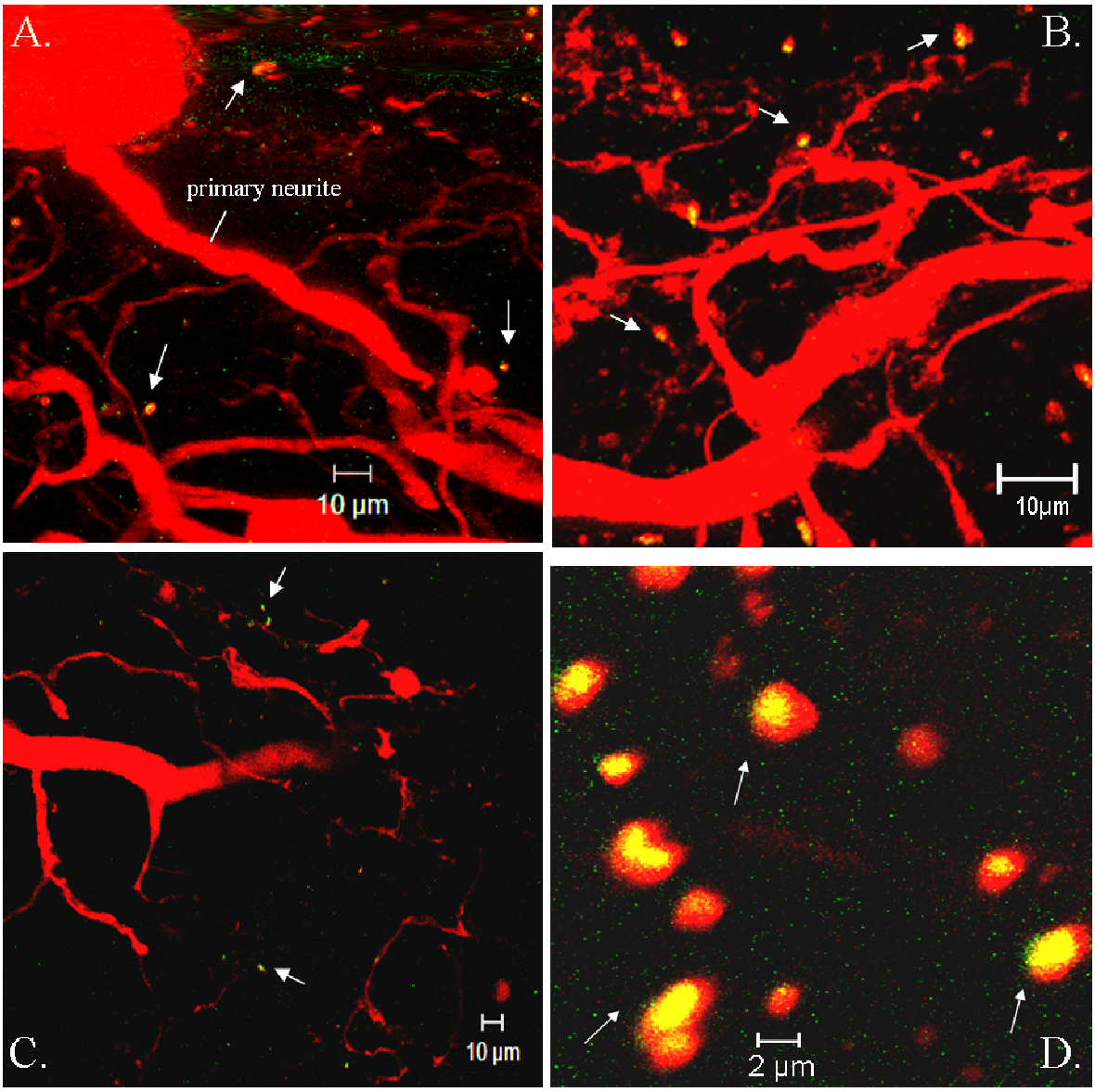

Figure 6-5: $D_{1\beta Pan}$ expression in the LP neuron. LP neurons were filled with texas red, then processed for ICC using anti-$D_{1\beta Pan}$ (n=3). Yellow staining shows $D_{1\beta Pan}$ expression within the neuron. Clusters of putative terminals expressing the receptor are indicated by arrows in all panels. (**A**) Merged confocal projection (60µm) showing the LP soma and primary neurite. (**B**) 26µm merged confocal projection of another filled LP neuron. (**C**) Merged confocal projection (30µm) of the same LP shown in A. Image is from deep within the neuropil. (**D**) High magnification 5µm projection from synaptic neuropil showing a cluster of putative LP terminals. In A-C, green staining shows $D_{1\beta Pan}$ in unidentified neurons.

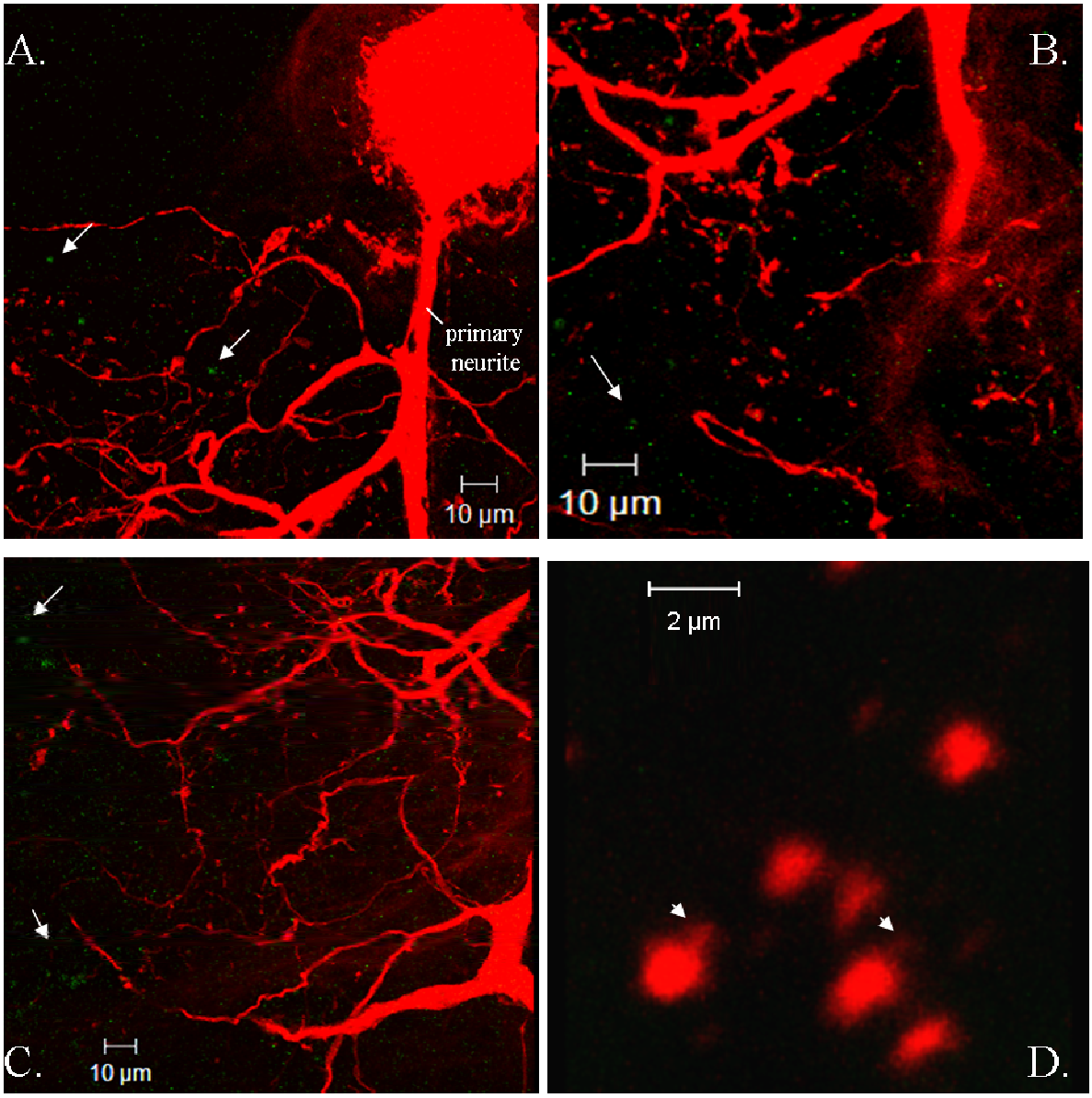

Figure 6-6: $D_{2\alpha Pan}$ is not expressed in the LP neuron. LP neurons were filled with texas red, then processed for ICC using anti-$D_{2\alpha Pan}$ (n=3). In A-C, green staining shows $D_{2\alpha Pan}$ in unidentified neurons (arrows). (**A**) Merged confocal projection (40µm) showing the LP soma and neurites. (**B**) 10µm merged confocal projection of another filled LP neuron. Primary neurite is indicated. (**C**) Merged confocal projection (48µm) of the same LP shown in A. Image is from deep within the neuropil. (**D**) High magnification 4µm projection from synaptic neuropil showing a cluster of putative LP terminals. Fingerlike processes extend from the bulbous structure (arrowheads).

and ending were clear. Questionable neurites were either left untraced or were traced as far as they could be seen. A comparison of volumes obtained with confocal imaging (calculated using Zeiss LSM510 software) versus those obtained with the tracing software (Neurolucida) suggests that we traced 87-94% of a given neuron (Table 6-1).

Figure 6-7 shows completed traces of PD neurons from 3 animals. The primary neurite was traced to the point where it exited the STG at the posterior end of the ganglion, via the dvn. The length and trajectory of the primary neurite varied among three PDs, possibly due to the position of the soma (Table 6-1). For example, the PD soma in the top panel of Figure 6-7 is situated centrally, and the primary neurite makes a short loop toward the anterior end of the ganglion before crossing toward the posterior end. The PD soma in the middle panel is near the posterior end of the ganglion, thus the primary neurite projects toward the anterior end of the ganglion before looping around and exiting at the posterior end. In the bottom panel, the soma is located anteriorly, and the neurite twists twice, then projects directly across to exit the STG posteriorly.

Each PD neuron had 9-10 secondary branches arising from the primary neurite. We designated a secondary branch plus all branches stemming from that secondary as a secondary branch cluster. Each secondary branch cluster is shown in a different color, where the color indicates the order in which the secondary branched from the primary neurite. For example, in all 3 PDs, the red cluster is the first secondary to emerge from the primary neurite; thus, it is closest to the soma (Figure 6-7). We used a 3-D graphing software to analyze the terminal fields for each secondary cluster. Since all 3 tracings end at the point where the primary neurite leaves the STG via the dvn, this location was set to zero in all 3 dimensions (x, y, z) for each of the 3 PD

Table 6-1: PD neuron volumes

	Volume of 3D tracing (μm^3)	Confocal volume (μm^3)	% traced	Length of primary neurite (µm)
PD-1	3.7×10^5	4.1×10^5	89%	766.2
PD-2	4.7×10^5	5.5×10^5	87%	1167.4
PD-3	4.1×10^5	4.4×10^5	94%	1015.1

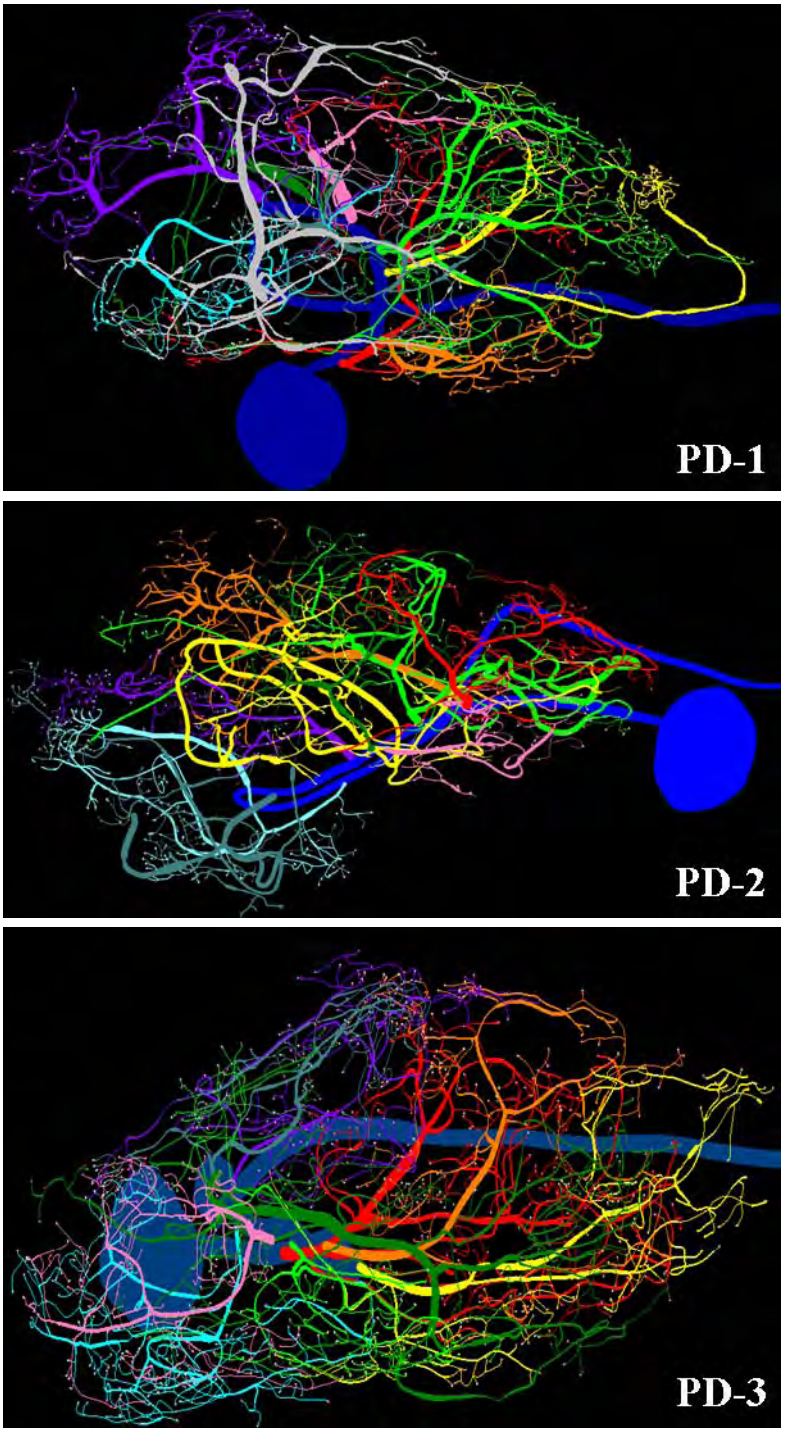

Figure 6-7: 3D renderings of a PD neuron from three different animals. In all panels: left = anterior, right = posterior. Secondary branch clusters are color coded according to the order they emerged from the primary neurite: red=1st, orange=2nd, yellow=3rd, bright green=4th, pink=5th, dark green=6th, purple=7th, teal=8th, light blue=9th. The top PD has a 10th secondary branch (grey). Secondary branches were detached from the primary neurite to construct this figure, but were not moved.

neurons. Using this method, the position of any branch terminal relative to the dvn could be calculated. Figure 6-8 shows scatter plots generated for each of the three PD tracings. Each branch terminal is represented in the 3D space as a circle of the color corresponding to the appropriate cluster. For example, the yellow cluster from PD-1 has a total of 46 branch terminals, which are represented by 46 yellow circles on the graph in panel A. These figures show that the terminal fields for all clusters are largely non-overlapping, and further, that the terminals of a given cluster are restricted to a portion of the STG.

To facilitate interpretation of the 3D tracings, we detached secondary branch clusters and ordered them in Figure 6-9. A given cluster showed extensive arborization, with branches extending to the 13^{th}-16^{th} branch order (Figure 6-9, Table 6-2). As branches were traced, markers were placed to indicate synaptic varicosities. These markers appear as pale blue circles in figure 6-9. Putative synaptic varicosities were found on all branch orders, with the exception of the primary neurite. In some cases, a single neurite contained multiple varicosities, which were most often clustered in one region of the branch. In accordance with previous reports, varicosities appeared along neurites that continued to arborize (King 1976a; Marder and Bucher 2007), but in most cases, varicosities were seen at or near the end of the neurite. As shown in Table 6-2, the number of varicosities per branch increased with increasing branch order.

Mapping $D_{2\alpha}$ in the PD neuron

Having identified general anatomical similarities and differences among the PD neurons, we next sought to define $D_{2\alpha Pan}$ subcellular distributions. We placed markers to indicate the presence (orange triangles, Figure 6-9) or absence (red crosses, Figure 6-9) of $D_{2\alpha Pan}$ immunoreactivity within a branch or varicosity as the neurons were traced. In all cases, $D_{2\alpha Pan}$

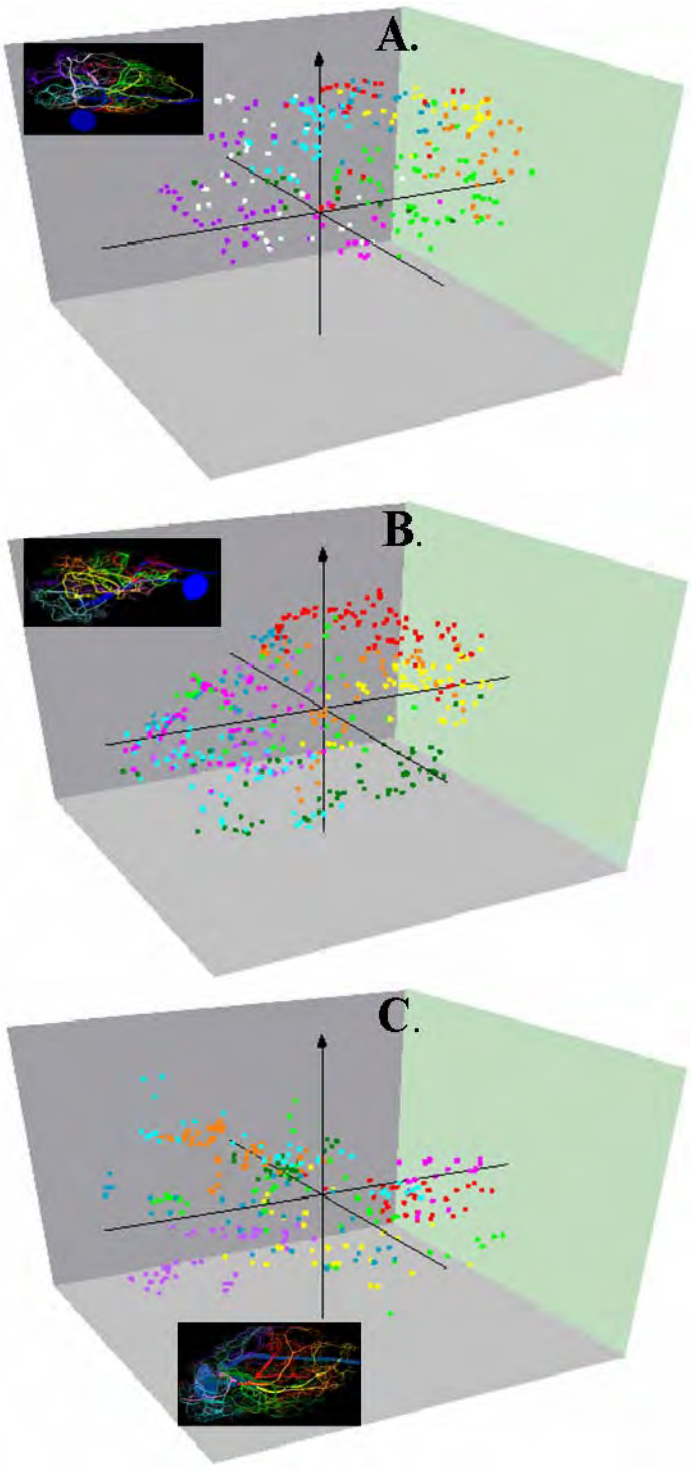

Figure 6-8: PD terminals are largely non-overlapping and restricted within the STG. PD terminals are shown in three dimensional space relative to the dvn. Each circle corresponds to a single terminal. The color of a terminal corresponds to the color of the secondary branch cluster from which it emerged. The corresponding PD tracing for each plot is shown as an inset. (A) PD-1; (B) PD-2 (C) PD-3.

Table 6-2: Average values for 3 PDs

* values are exclusively from PD-1, as PD-2 and PD-3 did not have branches above the 13th order.

Branch order	mean # of branches (n=3)	mean % of branches with $D_{2\alpha Pan}$ (n=3)	mean # of varicosities per branch (n=3)	% of varicosities with $D_{2\alpha Pan}$ (n=3)
2	9 ± 0.3	97 ± 3	0.04 ± 0.04	33 ± 33
3	24 ± 3.9	79 ± 5	0.25 ± 0.10	75 ± 13
4	56 ± 7.2	65 ± 5	0.48 ± 0.18	54 ± 12
5	110 ± 7.4	55 ± 5	0.52 ± 0.15	44 ± 4
6	175 ± 17.7	45 ± 5	0.64 ± 0.06	42 ± 2
7	211 ± 21.0	42 ± 5	0.65 ± 0.06	38 ± 5
8	195 ± 33.0	37 ± 5	0.67 ± 0.03	40 ± 3
9	162 ± 35.4	40 ± 4	0.67 ± 0.06	35 ± 3
10	113 ± 19.5	32 ± 4	0.71 ± 0.10	34 ± 4
11	61 ± 6.2	32 ± 8	0.80 ± 0.01	43 ± 12
12	32 ± 4.9	25 ± 11	0.79 ± 0.07	24 ± 7
13	16 ± 0.3	58 ± 17	0.96 ± 0.05	43 ± 11
14	10*	40*		38*
15	4*	50*		67*
16	3*	100*		100*

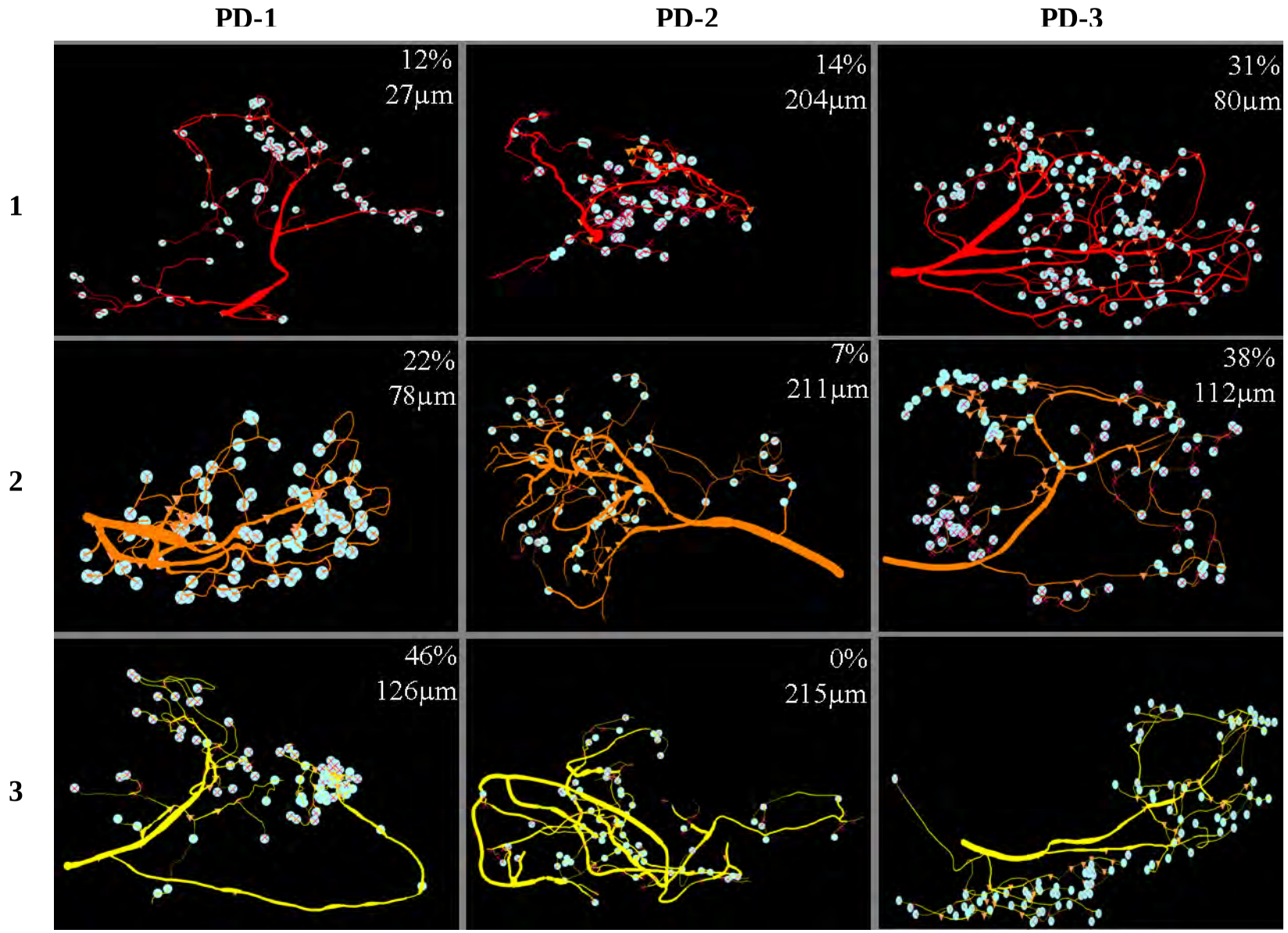
PD-1
PD-2
PD-3
1
2
3
12%
27µm
14%
204µm
31%
80µm
22%
78µm
7%
211µm
38%
112µm
46%
126µm
0%
215µm

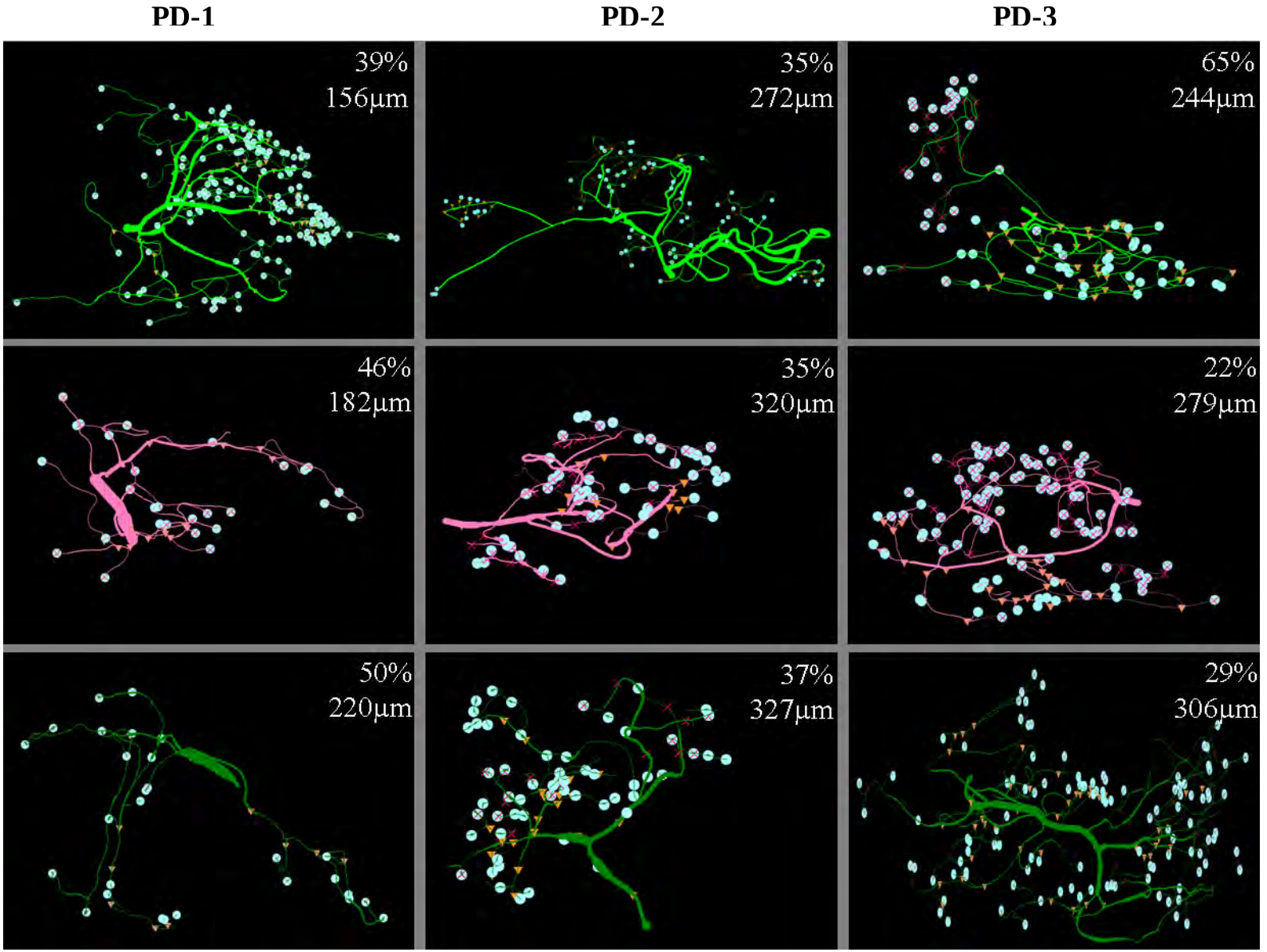
PD-1
PD-2
PD-3
4
5
6
39%
156µm
35%
272µm
65%
244µm
46%
182µm
35%
320µm
22%
279µm
50%
220µm
37%
327µm
29%
306µm

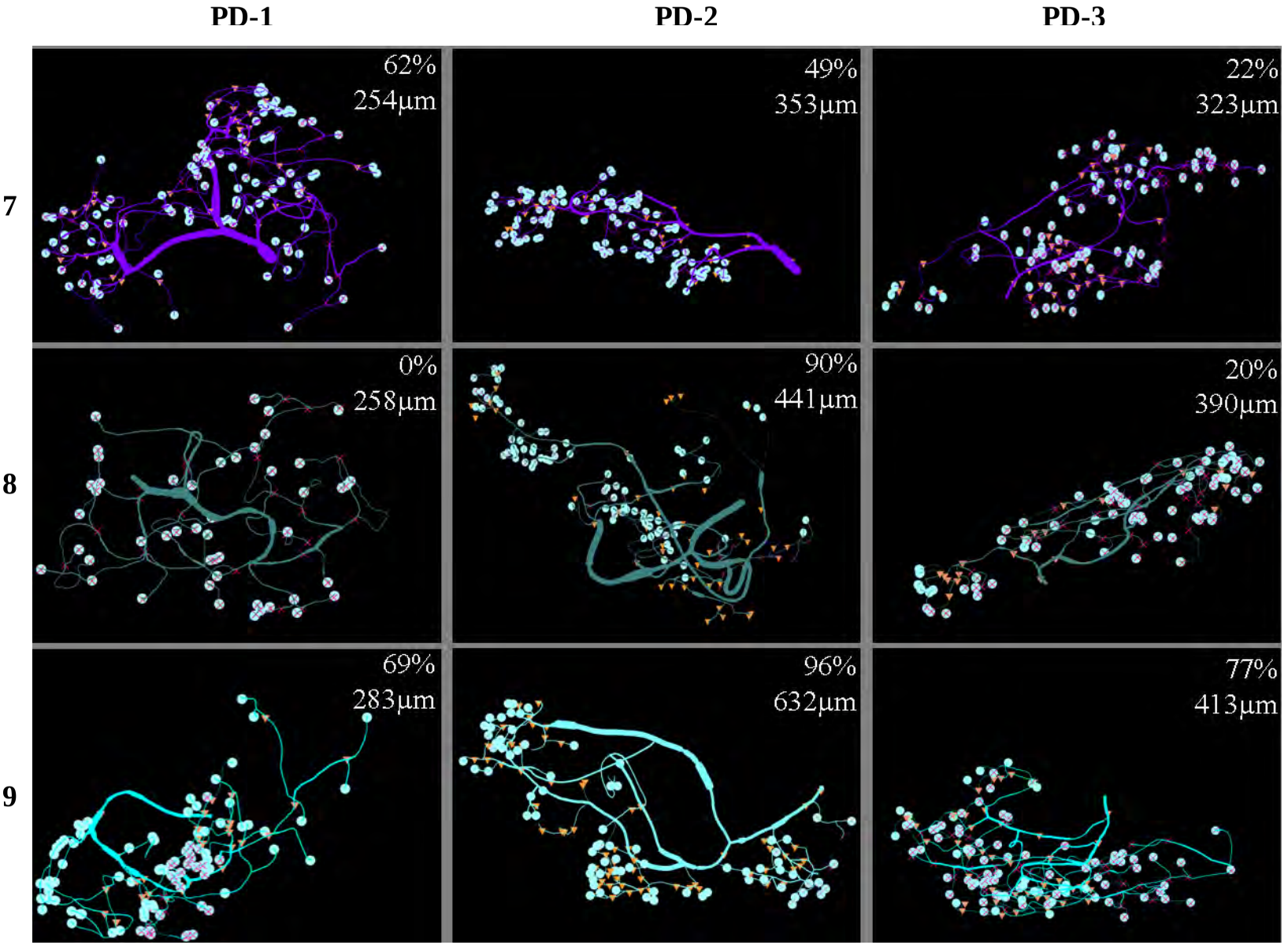
PD-1
PD-2
PD-3
7
8
9
62%
254µm
49%
353µm
22%
323µm
0%
258µm
90%
441µm
20%
390µm
69%
283µm
96%
632µm
77%
413µm

PD-1

10

Figure 6-9: $D_{2\alpha Pan}$ distribution in PD neurites. Ordered clusters for 3 PDs are shown. Upper right corners of each panel list (1) the percentage of varicosities with $D_{2\alpha Pan}$ and (2) the distance between the soma and the point on the primary process from which the secondary emerges. Markers: ● = varicosity; ▲ = branch or varicosity with $D_{2\alpha Pan}$; X = branch or varicosity without $D_{2\alpha Pan}$. Note that some ▲ or X may not be visible, as they are behind the ●.

staining in a branch occurred only when it was also observed in the branches from which it originated. For example, a marker indicating the absence of $D_{2\alpha Pan}$ in a branch or varicosity is never followed by a marker indicating the presence of the receptor in the next branch order (Figure 6-9; see PD3, cluster 4 for clearest example). Our markers did not discriminate between $D_{2\alpha Pan}$ staining in the cytoplasm versus the membrane; however, as mentioned above, confocal stacks were inspected to determine receptor distributions, and there was no obvious staining in the membrane of large diameter neuronal branches, nor was there evidence for receptor expression the somatic membrane. Instead, the $D_{2\alpha Pan}$ receptors were located exclusively in the terminal/varicosity plasma membrane.

$D_{2\alpha Pan}$ receptors were non-uniformly distributed. This is emphasized in Figure 6-9 where, for each secondary branch cluster, the percentage of varicosities containing $D_{2\alpha Pan}$ receptors is indicated in the upper right-hand corner of each panel. The fraction of $D_{2\alpha Pan}$ containing varicosities did not vary according to branch order (Table 6-2), and ranged from 0-96% for a given secondary branch cluster (compare values in individual panels, Figure 6-9). Interestingly, in two of the PDs, one secondary branch cluster completely lacked $D_{2\alpha Pan}$ in the varicosities (Figure 6-9: PD1, teal cluster 8; PD2, yellow cluster 3). In the 3rd PD, the secondary branch giving rise to cluster 5 (Figure 6-9: PD3, pink cluster) immediately split into two tertiary processes, and $D_{2\alpha Pan}$ receptors were associated with only one of the two branches. As seen in Figure 6-8, the terminal fields of these secondary branch clusters were not located in same region of the STG (compare location of teal, yellow and pink circles in A, B and C, respectively). The function of this feature (i.e., lack of receptors on one entire branch) is not clear.

On average, $D_{2\alpha Pan}$ expression was limited to 40 ± 3% of the total number of PD varicosities (n=3). These data are consistent with previous imaging and electrophysiological

studies, which showed that DA had an effect on depolarization induced changes in [Ca^{2+}] at roughly half of the PD varicosities (Kloppenburg et al. 2000). Nevertheless, we performed control experiments to show that this was not an artifact of poor antibody penetration. For these controls, we identified and filled a PD neuron, embedded the STG in agarose, obtained 70 μm sections and performed the ICC experiments on the sectioned ganglion. The logic was that penetration should not be an issue in these thinner slices. Figure 6-10 shows $D_{2\alpha Pan}$ immunoreactivity in a PD neuron that was filled with texas red, then sliced prior to performing ICC. We did not observe $D_{2\alpha Pan}$ staining in the membrane of the soma or large diameter processes using this technique, and $D_{2\alpha Pan}$ staining intensity was consistent throughout the synaptic neuropil. Moreover, we counted the number of terminals in this slice, and determined that roughly 35% were immunopositive for $D_{2\alpha Pan}$ (n=1). We are currently repeating these experiments to increase the sample number.

DISCUSSION

The electrophysiological effects of DA in the LP and PD neurons have been well characterized, but until my dissertation work, nothing was known about the signal transduction cascades operating in pyloric neurons. Here, I show that LP and PD differentially express DARs that couple with G proteins that regulate [cAMP] in opposing directions. The LP neuron expresses $D_{1\alpha Pan}$ and $D_{1\beta Pan}$, which couple with Gs and Gq, or Gs, respectively. The PD neuron expresses $D_{2\alpha Pan}$ receptors, which couple with Gi/o. This suggests that some of the opposing effects of DA on these two cell types could be mediated by cAMP. DAR expression in these neurons is restricted to the cell membrane encompassing varicosities and/or terminals in the synaptic neuropil. Further, receptors are differentially expressed at terminals. This work

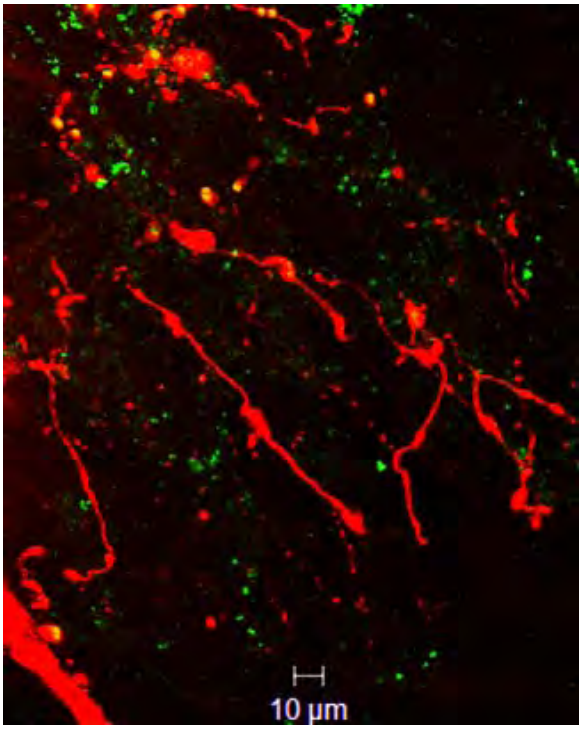

6-10: $D_{2\alpha Pan}$ is expressed at a percentage of PD terminals. Figure shows a 50µm merged confocal projection of a PD neuron that was sectioned prior to performing ICC with anti-$D_{2\alpha Pan}$. Confocal slices used for this projection were obtained from the fine neuropil.

represents the first description of receptor expression profiles in any crustacean system. When considered in light of existing data, our results imply that remote receptors can differentially regulate local activity in PD terminals as well as generate a global signal to modulate ion channels located in the soma.

Implications of DAR distribution patterns: local versus global signals

Our data show that DARs are targeted exclusively to terminals and varicosities. This subcellular distribution pattern has important implications for receptor signaling when considered together with previously described dopaminergic effects and modes of transmission. Specifically, it suggests that DARs can produce both local and global signals. This is in keeping with a rapidly growing cell biology literature indicating that GPCRs can simultaneously generate a large, rapid local signal that is chiefly restricted to the membrane, as well as a small, sustained global signal that diffuses to distal compartments in the cell (Figure 1-8). First we consider the local signal.

DA transmission via modulatory inputs to the STG may be synaptic or paracrine. If the inputs are synaptic, and assuming reuptake mechanisms are rapid, then DA would generate a large, rapid, transient change in second messengers in the terminals where $D_{2\alpha Pan}$ receptors are expressed (e.g., Figure 1-8, trace 1). This, in turn, would cause momentary changes in local signal transduction cascades to alter target protein function in only a fraction of the terminals. We can only speculate as to what transduction cascades mediate the local signals. $D_{2\alpha Pan}$ receptors in the PD activate Gαi/o to decrease cAMP (Chapter 5). Thus, the activity of PKA and exchange proteins activated by cAMP (Epacs) may be restricted, and the fraction of open cyclic nucleotide sensitive channels could be reduced in PD. The opposite would be true for the LP

because it contains D_1 receptors, which activate Gs to increase cAMP. In addition, $D_{1\alpha Pan}$ receptors may also couple with Gq to alter local [Ca^{++}] and thus the activity of local Ca^{++}-binding proteins. GPCRs signal via subunits other than Gα. For example, we and others have shown that G$\beta\gamma$ may also target PLCβ to alter Ca^{++} and/or cAMP (Hernandez-Lopez et al. 2000). In addition, $\beta\gamma$ subunits may act directly to alter ion channel function (Logothetis et al. 1987) or the vesicle release machinery, and thereby synaptic transmission (Blackmer et al. 2005). Finally, DARs themselves can physically interact with effectors such as ion channels (Liu et al. 2000; Lee and Liu 2004; Pei et al. 2004; Zou et al. 2005). Again, we emphasize that terminals lacking the receptor would not experience these types of changes. Thus, synaptic DA can have local effects. The situation is even further complicated in the LP where a terminal can have one of four types of receptor arrangements ($D_{1\alpha}$, $D_{1\beta}$, both, or neither).

On the other hand, DA may also reach the PD neuron as a circulating hormone, or through paracrine release from modulatory inputs. Hormonal concentrations of DA are several orders of magnitude lower than those at modulatory release sites (Fort et al. 2004; Fort et al. 2007). Further, the effects of hormonal DA should be continuous given that DA reuptake mechanisms are usually localized to synaptic regions (Iversen 2006). The distributed nature of $D_{2\alpha Pan}$ receptors in the PD neuron suggests that hormonal DA could synchronously modulate multiple distant compartments. This type of slow transmission most likely generates global signals throughout the cell (Figure 1-8, trace 2).

The idea that hormonal DA produces global changes is substantiated by the fact that constant bath application of DA alters somatic ion channels in all pyloric neurons. It is easy to understand how DA might generate a global signal in the LP neuron, because we postulate that D_1 receptors appear to increase cAMP, and a neuromodulatory-induced increase in cAMP

diffuses from the fine neurites to the soma (Hempel et al. 1996). It is less clear how a $D_{2\alpha Pan}$ receptor mediated decrease in cAMP could produce a diffusible signal in the PD neuron. One possibility is that cAMP constantly diffuses toward the soma due to compartmentalized somatic PDEs that act as a "sink" to drain the second messenger from discrete locations (Terrin et al. 2006). A $D_{2\alpha Pan}$ mediated decrease in cAMP at the terminals would then automatically cause a decrease in cAMP diffusing to the soma and thereby lower somatic [cAMP]. Another possibility is that Ca^{++} is the diffusible second messenger. D_2 receptors activate PLCβ via Gβγ subunits, which in some cases triggers the mobilization of intracellular Ca^{++} stores (Hernandez-Lopez et al. 2000).

DARs exist in multiprotein complexes (Hall and Lefkowitz 2002), and the complexes producing local vs. global signals may be distinct. Perhaps neuromodulatory (local) vs. hormonal (global) receptor complexes maintain the receptor in a low vs. high affinity conformational state, respectively. Complexes could also differ with regard to the number and/or type of signaling terminating molecules (Nikolaev et al. 2006; Rochais et al. 2006). Neuromodulatory complexes may contain signal terminating molecules (i.e., PDEs) and produce transient, non-diffusible signals. Neurohormonal complexes, on the other hand, may lack signal terminating molecules, and generate sustained, diffusible signals. The second messenger that is modified in each type of cascade could also vary depending on the colocalization of PLCβ (changes in Ca^{++}) and AC (changes in cAMP), as could the final targets (e.g., ion channels, pumps, etc.).

Mechanisms by which DAR signals could modulate ion channel activity in pyloric neurons

I_A is expressed in the somatodendritic membrane of pyloric neurons (i.e., in the soma as well as in the neuropil) (Baro et al. 2000). A-channels localized to terminals may receive local

DA signals, but channels located in the soma must receive a global signal generated by remote DARs in the terminals. Since DA alters somatic channels within seconds, and since protein diffusion should be relatively restricted due to size considerations, it is most likely that second messengers and not proteins carry the global signal. This appears to be the case for *Aplysia* where distinct types of PKA are found in the soma and terminals. Application of neuromodulator at the terminals produces somatic changes that are mediated exclusively by the somatic form of PKA (Liu et al. 2004).

DA decreases and increases the amplitudes of the somatic I_A in LP (Harris-Warrick et al. 1995b) and PD (Kloppenburg et al. 1999) neurons, respectively. The most parsimonious explanation of this differential modulation is that opposing global signals are generated in LP (via D_1Rs) versus PD (via $D_{2\alpha Pan}$). If the traditional DAR signaling cascades are maintained in LP and PD, cAMP levels will be altered in opposing directions in the two cells upon DAR activation. In the LP, a Gs-mediated increase in cAMP may lead to PKA activation, while in the PD, a Gi/o-mediated decrease in cAMP should decrease PKA activity. Alternately, as mentioned above, the diffusible signal in the PD neuron may be Ca^{++}. An increase in Ca^{++} may stimulate protein phosphatase 2B (PP2B, calcineurin), as is the case for D_2 receptors in mammalian striatal neurons (Hernandez-Lopez et al. 2000). Since PP2B is a serine-threonine phosphatase, and PKA is a serine-threonine kinase, activation of PP2B would have the same effect as decreased PKA activity.

DA increases I_{Ca} in the LP neuron and decreases I_{Ca} in the PD (Kloppenburg et al. 1999; Johnson et al. 2003). Unlike I_A, I_{Ca} is expressed in the neuropil, but not in the soma (Graubard and Hartline 1991). Voltage sensitive Ca^{++} channels are localized to putative synaptic varicosities in the PD neuron (Kloppenburg et al. 2000). We predict that DARs produce opposing changes in I_{Ca} by differentially regulating cAMP in the terminals. Regulation of Ca^{++} channels is most likely local, as

Kloppenburg et al. have shown that DA application alters Ca^{++} concentration in only ~50% of varicosities in PD, (Kloppenburg et al. 2000) and LP neurons (Kloppenburg et al. 2007).

The effect of DA on I_h is less easy to understand in terms of the underlying transduction cascades in LP and PD. DA increases I_h in the LP neuron (Harris-Warrick et al. 1995b) and has no effect on I_h in the PD cell (Peck et al. 2006). I_h is a small current, most likely expressed in the neuropil, but not the somata of pyloric neurons (Peck et al. 2006). Since I_h is larger in LP than PD (Harris-Warrick et al. 1995b; Peck et al. 2006), it is possible that DA-induced changes in I_h are not readily detected in TEVC recordings measured in the PD soma. Alternatively, I_h localization may be different in LP versus PD. I_h may be localized to terminals containing D_1 receptors in LP so that it can be regulated by local transduction cascades. On the other hand, the PD neuron may not co-express I_h and $D_{2\alpha Pan}$ in the same terminal, and local transduction cascades may have no effect on I_h. Another possibility is that I_h is modulated by a Gq-mediated cascade in LP, and there is no parallel cascade in the PD cell.

Lobster DARs display a high degree of structural and functional conservation with their mammalian homologs, but we do not know to what extent DAR cascades are conserved with regard to downstream components and effectors. I_{Ca} and I_A are modulated similarly in the PD neuron and D_2-expressing medium spiny neurons (Hernandez-Lopez et al. 2000; Perez et al. 2006). D_1 receptors are known to decrease I_A and increase I_{Ca} in LP and multiple mammalian neurons (Hernandez-Lopez et al. 1997; Dong and White 2003; Hopf et al. 2003). In general, D_1 and D_2 receptors are thought to increase and decrease cell excitability, respectively. Thus, it is possible that some signaling modules have been conserved throughout evolution, from the receptor to the target. However, there will always be exceptions to the rule, and a more complete characterization of the signaling cascades is required before drawing firm conclusions.

Relationship between terminal distribution and DA induced changes in synaptic efficacy

The $D_{2\alpha Pan}$ receptor was found at 40%$\pm$3% of the PD terminals, and D_1 receptors in LP were also found at a subset of terminals. However, it is difficult to interpret these findings with regard to DA induced changes in synaptic transmission without additional experiments. For example, DA reduces graded transmission at all PD output synapses (Johnson and Harris-Warrick 1990), but this does not necessarily mean that $D_{2\alpha Pan}$ receptors are located at all PD-LP, LP-PD, PD-PY and PD-IC synapses (see Figure 1-6). DA-induced synaptic changes were measured from the soma, and could reflect global changes in input resistance rather than localization of receptors to PD synapses. Moreover, Bucher at al. (2007) recently found that not all terminals of STG neurons contain chemical synapses. Thus, in one scenario $D_{2\alpha Pan}$ receptors could be localized to all synapses. Alternatively, at the opposite extreme, all $D_{2\alpha Pan}$ receptor complexes may be designed for hormone or paracrine input and reside exclusively on terminals without synapses. Similar scenarios could describe the situation for D_1 receptors in the LP. Additional experiments involving electron microscopy and two filled neurons are needed to further resolve receptor localization and function.

PD branching within the STG

Our 3D renderings of the PD neuron produced notable results. Consistent with previous studies (Wilensky et al. 2003) we observed a clear segregation of PD neurites within the STG neuropil (Figures 6-7 and 6-8). No secondary cluster covered the entire ganglion, and there was little overlap among secondary clusters. Thus, while PD terminals are broadly distributed throughout the STG, inputs are regionally segregated to specific secondary branch clusters.

Unlike previous reports (Wilensky et al. 2003), we did not find that a given branch consistently arborized within a specific region of the STG. We found that in any given animal, regions of the neuropil were innervated by particular subsets of PD terminals, but the secondary branch cluster innervating a given region was not consistent from animal to animal. Since Wilensky et al. (2003) examined the branching pattern of the VD neuron, which has a distinct morphology from that of the PD neuron in that it gives rise to two axons, the discrepancy may reflect cell type differences in the spatial segregation of neuronal branches. It could also be the case that branching patterns for a given neuron are species-specific, as the former study was performed in the crab, *Cancer borealis*.

CHAPTER SEVEN

GENERAL DISCUSSION

Evolutionary conservation of monoaminergic transduction cascades

Comparison of functional domains

The transmembrane domains of monoaminergic receptors cloned from *Panulirus interruptus* display high homology to their arthropod and mammalian homologs at the level of the DNA sequence. Further, key functional domains involved in G protein coupling and receptor activation are highly conserved across species. Consistent with the distinct pharmacological profiles reported for vertebrate versus invertebrate receptors (Tierney 2001; Mustard et al. 2005), amino acids involved in binding natural ligands (e.g. monoamines) are also highly conserved, while those involved in binding synthetic ligands are not.

In contrast to most other functional domains, the DRY motif, which is involved in receptor activation and is highly conserved among all monoamine receptors, is altered to DRF in the $5HT_{2\beta Pan}$ receptor. Our work shows that this evolutionary alteration leads to constitutive activity in HEK cells, but whether this receptor displays agonist-independent activity *in vivo* is unknown. One might speculate that the mutation is somehow associated with the fact that all 5-HT transmission in the *Panulirus* STG is hormonal. Interestingly, the crayfish homolog of this receptor also contains a DRF motif. Crayfish sensory neurons contain 5-HT (Tierney et al. 1999), but these neurons may release the transmitter in a paracrine fashion (Katz and Harris-Warrick 1990) In any event, the $5HT_{2\beta Pan}$ receptor is most likely expressed in other regions of

the nervous system where 5-HT transmission is synaptic, making it less likely that this change is related to mode of transmission. Thus, the function of the Y/F transition is unclear at this time.

Signaling properties

Given the high degree of structural conservation among receptor homologs, it is not surprising that the classical G protein couplings for a given receptor are completely conserved across species. Indeed, when expressed in a mammalian cell line, the lobster receptors behave exactly like their mammalian counterparts. Furthermore, a single receptor can initiate multiple cascades, and the predominant signaling cascade can vary with the cellular milieu. Thus, our results on lobster receptors support the well-established concept that GPCR transduction cascades are largely influenced by the cellular environment. My characterization of crustacean monoamine receptors will provide a strong framework for future investigations on the molecular and cellular underpinnings of neuromodulation of CPGs. The recent identification of pharmacological profiles for crustacean 5-HT receptors (Spitzer et al. 2008) and the use of pharmacological agents to delineate the components of the 5-HT response system controlling network cycle frequency (Spitzer, in revision) were built upon my studies. These tools can be used in the future to study other 5-HT-mediated effects including aggression (Kravitz 2000) and social status (Edwards et al. 1999), in addition to motor pattern generation.

Surprisingly, our results indicate that a given receptor can produce opposite intracellular responses. For example, $D_{1\beta Pan}$ couples with Gs and Gz proteins and may therefore produce an increase or a decrease in cAMP. Similarly, the $D_{2\alpha Pan}$ receptor can signal via Gαi and Gβγ to produce an increase or decrease in cAMP, respectively. What is the functional significance of producing opposing responses? In the case of the mammalian D_5 receptor, which like $D_{1\beta Pan}$

couples to Gs and Gz, Gz activation may be secondary to Gs activation (Sidhu 1998). Since the rate of nucleotide exchange is much faster for Gs than for Gz (Fields and Casey 1997), the Gz response could serve to dampen an initial Gs response, thus preventing large changes in cAMP. Alternately, D_5 may be preferentially localized in brain regions where it has only an inhibitory effect due to co-localization with Gz and/or specific AC subtypes (Sidhu 1998). Similarly, the cascades may be spatially segregated within the cell so that their effects are highly localized and non-interacting. Of course there is no Gz protein in crustaceans. Nevertheless, future studies on receptor couplings in identified neurons may yield important insights into the functional significance of multiple and seemingly paradoxical G protein couplings.

Monoamine receptor localization in the STG

Cells show unique receptor expression profiles.

Zhang and Harris-Warrick (1994) predicted that pyloric cells should show unique 5-HT receptor expression patterns in the somatodendritic compartment. In contrast, we found that 5-$HT_{2\beta Pan}$ was expressed in all pyloric neurons. Nevertheless, when combined with recent pharmacological studies (Spitzer et al., in revision), the data indicate that 5-$HT_{2\beta Pan}$ is uniquely expressed in pyloric neurons. The receptor is only expressed in the somatodendritic compartment of the AB neuron, while in all other pyloric cells it is found in peripheral compartments, such as the axon. Similarly, DARs appear to be differentially expressed in LP and PD. These findings correspond neatly with the previously reported electrophysiological effects of DA on the LP versus PD neuron (Harris-Warrick et al. 1995; Johnson et al. 2003; Peck et al. 2006) and support the idea of receptor expression as an underlying mechanism for cell-type specific effects of a given monoamine.

Receptors are targeted to specific locations

We found that receptors are distributed to a subset of varicosities in neurons, which suggests regulated distribution. It is understandable that receptors are not expressed in the soma or large diameter processes of the PD or LP neurons, since these large structures are surrounded by thick glial sheaths in *P. interruptus* (King 1976b, a). It will be interesting to discern distribution patterns in species where pyloric neurons have less extensive glial coverings. Receptor distribution patterns in the PD cell suggest that individual terminals may differentially process synaptic input and/or differentially release neurotransmitter when DA is present. It may be the case that local differences segregate according to cell type. For example, perhaps all receptors are located at PD-LP synapses and are excluded from all PD-PY synapses. Future ICC studies involving two filled neurons will further address the significance of DAR distribution patterns with regard to specific input/ouput sites.

Variable receptor expression as a mechanism for state-dependent responses

One interesting idea that is emerging in the field is that modulatory and/or sensory inputs can have state dependent effects (Yeh et al. 1997; Katz and Edwards 1999; Edwards et al. 2002; Mesce 2002; Birmingham et al. 2003; Mitchell and Johnson 2003). Receptor expression and function can be state dependent (Wohlpart and Molinoff 1998; Ango et al. 2001; Anji et al. 2001; Riad et al. 2001; Bockaert et al. 2003; Cirelli and Tononi 2004; Dwivedi et al. 2005). Interestingly, variable 5-$HT_{1\alpha}$ receptor expression levels occur in the crayfish nervous system (Spitzer et al. 2005). Further, we found that 5-$HT_{2\beta Pan}$ receptor targeting to the NMJ may be variable in the PY neuron, although more work is needed to substantiate this idea. On the other hand, $D_{2\alpha Pan}$ expression does not appear to vary in the PD neuron from five preparations obtained

throughout the course of one year. Thus, only some receptors might be associated with state dependent effects. The techniques that I developed can be extended to study this question in the future.

If receptor expression is not variable, then changes in the expression of other proteins in a transduction cascade may underlie state-dependent effects. For example, targets of the cascade, such as ion channels, vary considerably across individuals (Schulz et al. 2006). Removing modulatory input can cause changes in ionic current, channel expression, and co-regulation of ionic conductances (Thoby-Brisson and Simmers 1998; Mizrahi et al. 2001; Khorkova and Golowasch 2007). This suggests that neuromodulators may control ion channel transcription and translation in neurons. Some changes in expression could be local, but there is no evidence for ion channel transcripts in pyloric terminals. The most parsimonious interpretation of these collective findings is that a global signal regulates the genetic program through hormonal receptors.

Summary

A description of the spatial and temporal characteristics of transduction cascades operating in cells is a prerequisite for understanding how modulatory inputs alter or maintain cellular phenotypes. The work presented in the preceding chapters offers insight into the molecular underpinnings of neural circuit modulation. By characterizing receptor signaling cascades and defining receptor expression patterns in identified neurons, I have provided an understanding of how the differential effects of neuromodulators are mediated. My findings also suggest that different types of signals can be generated by a single receptor. Questions remain as to what transduction cascades mediate the monoaminergic effects *in vivo*, and to what extent

transduction cascades vary among neurons. My work has provided a sound framework for addressing these issues.

LITERATURE CITED

Albert P. R. and Tiberi M. (2001) Receptor Signaling and Structure: Insights from Serotonin-1 Receptors. *Trends Endocrinol.Metab* **12,** 453-460.

Almaula N., Ebersole B. J., Zhang D., Weinstein H. and Sealfon S. C. (1996a) Mapping the Binding Site Pocket of the Serotonin 5-Hydroxytryptamine2a Receptor. Ser3.36(159) Provides a Second Interaction Site for the Protonated Amine of Serotonin but Not of Lysergic Acid Diethylamide or Bufotenin. *J Biol Chem* **271,** 14672-14675.

Almaula N., Ebersole B. J., Ballesteros J. A., Weinstein H. and Sealfon S. C. (1996b) Contribution of a Helix 5 Locus to Selectivity of Hallucinogenic and Nonhallucinogenic Ligands for the Human 5-Hydroxytryptamine2a and 5-Hydroxytryptamine2c Receptors: Direct and Indirect Effects on Ligand Affinity Mediated by the Same Locus. *Mol Pharmacol* **50,** 34-42.

Anderson W. W. and Barker D. L. (1981) Synaptic Mechanisms That Generate Network Oscillations in the Absence of Discrete Postsynaptic Potentials. *J Exp Zool* **216,** 187-191.

Ango F., Prezeau L., Muller T., Tu J. C., Xiao B., Worley P. F., Pin J. P., Bockaert J. and Fagni L. (2001) Agonist-Independent Activation of Metabotropic Glutamate Receptors by the Intracellular Protein Homer. *Nature* **411,** 962-965.

Angstadt J. D. and Calabrese R. L. (1989) A Hyperpolarization-Activated Inward Current in Heart Interneurons of the Medicinal Leech. *J Neurosci* **9,** 2846-2857.

Angstadt J. D. and Calabrese R. L. (1991) Calcium Currents and Graded Synaptic Transmission between Heart Interneurons of the Leech. *J Neurosci* **11,** 746-759.

Anji A., Sullivan Hanley N. R., Kumari M. and Hensler J. G. (2001) The Role of Protein Kinase C in the Regulation of Serotonin-2a Receptor Expression. *J Neurochem* **77,** 589-597.

Arakawa S., Gocayne J. D., McCombie W. R., Urquhart D. A., Hall L. M., Fraser C. M. and Venter J. C. (1990) Cloning, Localization, and Permanent Expression of a Drosophila Octopamine Receptor. *Neuron* **4,** 343-354.

Arbas E. A. and Calabrese R. L. (1987a) Slow Oscillations of Membrane Potential in Interneurons That Control Heartbeat in the Medicinal Leech. *J Neurosci* **7,** 3953-3960.

Arbas E. A. and Calabrese R. L. (1987b) Ionic Conductances Underlying the Activity of Interneurons That Control Heartbeat in the Medicinal Leech. *J Neurosci* **7,** 3945-3952.

Arbas E. A. and Calabrese R. L. (1990) Leydig Neuron Activity Modulates Heartbeat in the Medicinal Leech. *J Comp Physiol [A]* **167,** 665-671.

Atwood H. L., Govind C. K. and Jahromi S. S. (1977) Excitatory Synapses of Blue Crab Gastric Mill Muscles. *Cell Tiss Res* **177,** 145-158.

Ausubel a., Brent R., Kinston R., Moore D., Seidman J., JA J. S. and Struhl K. (1990) *Current Protocols in Molecular Biology*. Greene Publishing Associates and Wiley Interscience., New York.

Ayali A. and Harris-Warrick R. M. (1998) Interaction of Dopamine and Cardiac Sac Modulatory Inputs on the Pyloric Network in the Lobster Stomatogastric Ganglion. *Brain Res* **794,** 155-161.

Ayali A. and Harris-Warrick R. M. (1999) Monoamine Control of the Pacemaker Kernel and Cycle Frequency in the Lobster Pyloric Network. *J Neurosci* **19,** 6712-6722.

Ayali A., Johnson B. R. and Harris-Warrick R. M. (1998) Dopamine Modulates Graded and Spike-Evoked Synaptic Inhibition Independently at Single Synapses in Pyloric Network of Lobster. *J Neurophysiol* **79,** 2063-2069.

Baillie G. S., Sood A., McPhee I., Gall I., Perry S. J., Lefkowitz R. J. and Houslay M. D. (2003) Beta-Arrestin-Mediated Pde4 Camp Phosphodiesterase Recruitment Regulates Beta-Adrenoceptor Switching from Gs to Gi. *Proc Natl Acad Sci U S A* **100,** 940-945.

Banihashemi B. and Albert P. R. (2002) Dopamine-D2s Receptor Inhibition of Calcium Influx, Adenylyl Cyclase, and Mitogen-Activated Protein Kinase in Pituitary Cells: Distinct Galpha and Gbetagamma Requirements. *Mol Endocrinol* **16,** 2393-2404.

Barker D. L., Kushner P. D. and Hooper N. K. (1979) Synthesis of Dopamine and Octopamine in the Crustacean Stomatogastric Nervous System. *Brain Res* **161,** 99-113.

Baro D. J., Cole C. L. and Harris-Warrick R. M. (1996a) Rt-Pcr Analysis of Shaker, Shab, Shaw, and Shal Gene Expression in Single Neurons and Glial Cells. *Receptors Channels* **4,** 149-159.

Baro D. J., Cole C. L., Zarrin A. R., Hughes S. and Harris-Warrick R. M. (1994) Shab Gene Expression in Identified Neurons of the Pyloric Network in the Lobster Stomatogastric Ganglion. *Receptors Channels* **2,** 193-205.

Baro D. J., Coniglio L. M., Cole C. L., Rodriguez H. E., Lubell J. K., Kim M. T. and Harris-Warrick R. M. (1996b) Lobster Shal: Comparison with Drosophila Shal and Native Potassium Currents in Identified Neurons. *J Neurosci* **16,** 1689-1701.

Baro D. J., Ayali A., French L., Scholz N. L., Labenia J., Lanning C. C., Graubard K. and Harris-Warrick R. M. (2000) Molecular Underpinnings of Motor Pattern Generation: Differential Targeting of Shal and Shaker in the Pyloric Motor System. *J Neurosci* **20,** 6619-6630.

Beaulieu J. M., Sotnikova T. D., Marion S., Lefkowitz R. J., Gainetdinov R. R. and Caron M. G. (2005) An Akt/Beta-Arrestin 2/Pp2a Signaling Complex Mediates Dopaminergic Neurotransmission and Behavior. *Cell* **122,** 261-273.

Becamel C., Figge A., Poliak S., Dumuis A., Peles E., Bockaert J., Lubbert H. and Ullmer C. (2001) Interaction of Serotonin 5-Hydroxytryptamine Type 2c Receptors with Pdz10 of the Multi-Pdz Domain Protein Mupp1. *J.Biol.Chem.* **276,** 12974-12982.

Becamel C., Alonso G., Galeotti N., Demey E., Jouin P., Ullmer C., Dumuis A., Bockaert J. and Marin P. (2002) Synaptic Multiprotein Complexes Associated with 5-Ht(2c) Receptors: A Proteomic Approach. *EMBO J.* **21,** 2332-2342.

Beenhakker M. P. and Nusbaum M. P. (2004) Mechanosensory Activation of a Motor Circuit by Coactivation of Two Projection Neurons. *J Neurosci* **24,** 6741-6750.

Beenhakker M. P., DeLong N. D., Saideman S. R., Nadim F. and Nusbaum M. P. (2005) Proprioceptor Regulation of Motor Circuit Activity by Presynaptic Inhibition of a Modulatory Projection Neuron. *J Neurosci* **25,** 8794-8806.

Beltz B., Eisen J. S., Flamm R., Harris-Warrick R. M., Hooper S. L. and Marder E. (1984) Serotonergic Innervation and Modulation of the Stomatogastric Ganglion of Three Decapod Crustaceans (Panulirus Interruptus, Homarus Americanus and Cancer Irroratus). *J Exp Biol* **109,** 35-54.

Beltz B. S. (1999) Distribution and Functional Anatomy of Amine-Containing Neurons in Decapod Crustaceans. *Microsc.Res.Tech.* **44,** 105-120.

Berg K. A., Maayani S., Goldfarb J. and Clarke W. P. (1998) Pleiotropic Behavior of 5-Ht2a and 5-Ht2c Receptor Agonists. *Ann.N.Y.Acad.Sci.* **861,** 104-110.

Berrada K., Plesnicher C. L., Luo X. and Thibonnier M. (2000) Dynamic Interaction of Human Vasopressin/Oxytocin Receptor Subtypes with G Protein-Coupled Receptor Kinases and Protein Kinase C after Agonist Stimulation. *J Biol Chem* **275,** 27229-27237.

Bezprozvanny I. and Maximov A. (2001) Classification of Pdz Domains. *FEBS Lett.* **509,** 457-462.

Birmingham J. T., Billimoria C. P., DeKlotz T. R., Stewart R. A. and Marder E. (2003a) Differential and History-Dependent Modulation of a Stretch Receptor in the Stomatogastric System of the Crab, Cancer Borealis. *J.Neurophysiol.*

Birmingham J. T., Billimoria C. P., DeKlotz T. R., Stewart R. A. and Marder E. (2003b) Differential and History-Dependent Modulation of a Stretch Receptor in the Stomatogastric System of the Crab, Cancer Borealis. *J Neurophysiol* **90,** 3608-3616.

Bjarnadottir T. K., Gloriam D. E., Hellstrand S. H., Kristiansson H., Fredriksson R. and Schioth H. B. (2006) Comprehensive Repertoire and Phylogenetic Analysis of the G Protein-Coupled Receptors in Human and Mouse. *Genomics* **88,** 263-273.

Blackmer T., Larsen E. C., Bartleson C., Kowalchyk J. A., Yoon E. J., Preininger A. M., Alford S., Hamm H. E. and Martin T. F. (2005) G Protein Betagamma Directly Regulates Snare Protein Fusion Machinery for Secretory Granule Exocytosis. *Nat Neurosci* **8,** 421-425.

Blenau W. and Baumann A. (2001) Molecular and Pharmacological Properties of Insect Biogenic Amine Receptors: Lessons from Drosophila Melanogaster and Apis Mellifera. *Arch.Insect Biochem.Physiol* **48,** 13-38.

Blenau W., Erber J. and Baumann A. (1998) Characterization of a Dopamine D1 Receptor from Apis Mellifera: Cloning, Functional Expression, Pharmacology, and Mrna Localization in the Brain. *J Neurochem* **70,** 15-23.

Blitz D. M. and Nusbaum M. P. (1997) Motor Pattern Selection Via Inhibition of Parallel Pathways. *J Neurosci* **17,** 4965-4975.

Blitz D. M. and Nusbaum M. P. (1999) Distinct Functions for Cotransmitters Mediating Motor Pattern Selection. *J Neurosci* **19,** 6774-6783.

Blitz D. M., Beenhakker M. P. and Nusbaum M. P. (2004) Different Sensory Systems Share Projection Neurons but Elicit Distinct Motor Patterns. *J Neurosci* **24,** 11381-11390.

Blitz D. M., Christie A. E., Coleman M. J., Norris B. J., Marder E. and Nusbaum M. P. (1999) Different Proctolin Neurons Elicit Distinct Motor Patterns from a Multifunctional Neuronal Network. *J Neurosci* **19,** 5449-5463.

Bockaert J. and Pin J. P. (1999) Molecular Tinkering of G Protein-Coupled Receptors: An Evolutionary Success. *Embo J* **18,** 1723-1729.

Bockaert J., Marin P., Dumuis A. and Fagni L. (2003a) The 'Magic Tail' of G Protein-Coupled Receptors: An Anchorage for Functional Protein Networks. *FEBS Lett* **546,** 65-72.

Bockaert J., Marin P., Dumuis A. and Fagni L. (2003b) The 'Magic Tail' of G Protein-Coupled Receptors: An Anchorage for Functional Protein Networks. *FEBS Lett.* **546,** 65-72.

Bockaert J., Claeysen S., Becamel C., Pinloche S. and Dumuis A. (2002) G Protein-Coupled Receptors: Dominant Players in Cell-Cell Communication. *Int.Rev.Cytol.* **212,** 63-132.

Bockaert J., Claeysen S., Becamel C., Dumuis A. and Marin P. (2006) Neuronal 5-Ht Metabotropic Receptors: Fine-Tuning of Their Structure, Signaling, and Roles in Synaptic Modulation. *Cell Tissue Res* **326,** 553-572.

Brown T. G. (1924) Studies in the Physiology of the Nervous System. Xxviii.: Absence of Algebraic Equality between the Magnitudes of Central Excitation and Effective Central Inhibition Given in the Reflex Centre of a Single Limb by the Same Reflex Stimulus, pp 1-23.

Bucher D., Thirumalai V. and Marder E. (2003a) Axonal Dopamine Receptors Activate Peripheral Spike Initiation in a Stomatogastric Motor Neuron. *J Neurosci* **23,** 6866-6875.

Bucher D., Thirumalai V. and Marder E. (2003b) Axonal Dopamine Receptors Activate Peripheral Spike Initiation in a Stomatogastric Motor Neuron. *J.Neurosci.* **23,** 6866-6875.

Bucher D., Johnson C. D. and Marder E. (2007) Neuronal Morphology and Neuropil Structure in the Stomatogastric Ganglion of the Lobster, Homarus Americanus. *J Comp Neurol* **501,** 185-205.

Burgess G. M. (1992) Analysis of Protein Kinase C Function, in *Neuromethods: Intracellular Messengers,* Vol. 20 (Boulton A., Baker G. and Taylor C., eds), pp 231-271. Humana Press.

Burns C. M., Chu H., Rueter S. M., Hutchinson L. K., Canton H., Sanders-Bush E. and Emeson R. B. (1997) Regulation of Serotonin-2c Receptor G-Protein Coupling by Rna Editing. *Nature* **387,** 303-308.

Cabirol-Pol M. J., Combes D., Fenelon V. S., Simmers J. and Meyrand P. (2002) Rare and Spatially Segregated Release Sites Mediate a Synaptic Interaction between Two Identified Network Neurons. *J Neurobiol* **50,** 150-163.

Cabrera-Vera T. M., Vanhauwe J., Thomas T. O., Medkova M., Preininger A., Mazzoni M. R. and Hamm H. E. (2003) Insights into G Protein Structure, Function, and Regulation. *Endocr Rev* **24,** 765-781.

Callier S., Snapyan M., Le Crom S., Prou D., Vincent J. D. and Vernier P. (2003) Evolution and Cell Biology of Dopamine Receptors in Vertebrates. *Biol Cell* **95,** 489-502.

Ceccaldi H. J. (1989) Anatomy and Physiology of Digestive Tract of Crustaceans Decapods Reared in Aquaculture. *Actes de Colloque, AQUACOP IFREMER* **9,** 243-259.

Chase D. L., Pepper J. S. and Koelle M. R. (2004) Mechanism of Extrasynaptic Dopamine Signaling in Caenorhabditis Elegans. *Nat Neurosci* **7,** 1096-1103.

Choudhary M. S., Craigo S. and Roth B. L. (1993) A Single Point Mutation (Phe340-->Leu340) of a Conserved Phenylalanine Abolishes 4-[125i]Iodo-(2,5-Dimethoxy)Phenylisopropylamine and [3h]Mesulergine but Not [3h]Ketanserin Binding to 5-Hydroxytryptamine2 Receptors. *Mol Pharmacol* **43,** 755-761.

Choudhary M. S., Sachs N., Uluer A., Glennon R. A., Westkaemper R. B. and Roth B. L. (1995) Differential Ergoline and Ergopeptine Binding to 5-Hydroxytryptamine2a Receptors: Ergolines Require an Aromatic Residue at Position 340 for High Affinity Binding. *Mol Pharmacol* **47,** 450-457.

Christie A. E., Skiebe P. and Marder E. (1995) Matrix of Neuromodulators in Neurosecretory Structures of the Crab Cancer Borealis. *J Exp Biol* **198 (Pt 12),** 2431-2439.

Cirelli C. and Tononi G. (2004) Locus Ceruleus Control of State-Dependent Gene Expression. *J Neurosci* **24,** 5410-5419.

Clark M. C. and Baro D. J. (2006) Molecular Cloning and Characterization of Crustacean Type-One Dopamine Receptors: D1alphapan and D1betapan. *Comp Biochem Physiol B Biochem Mol Biol* **143,** 294-301.

Clark M. C. and Baro D. J. (2007) Arthropod D2 Receptors Positively Couple with Camp through the Gi/O Protein Family. *Comp Biochem Physiol B Biochem Mol Biol* **146,** 9-19.

Clark M. C., Khan R. and Baro D. J. (2008) Crustacean Dopamine Receptors: Localization and G Protein Coupling in the Stomatogastric Ganglion. *J Neurochem* **104,** 1006-1019.

Clark M. C., Dever T. E., Dever J. J., Xu P., Rehder V., Sosa M. A. and Baro D. J. (2004) Arthropod 5-Ht2 Receptors: A Neurohormonal Receptor in Decapod Crustaceans That Displays Agonist Independent Activity Resulting from an Evolutionary Alteration to the Dry Motif. *J Neurosci* **24,** 3421-3435.

Cleland T. A. and Selverston A. I. (1995) Glutamate-Gated Inhibitory Currents of Central Pattern Generator Neurons in the Lobster Stomatogastric Ganglion. *J Neurosci* **15,** 6631-6639.

Cleland T. A. and Selverston A. I. (1997) Dopaminergic Modulation of Inhibitory Glutamate Receptors in the Lobster Stomatogastric Ganglion. *J Neurophysiol* **78,** 3450-3452.

Cleland T. A. and Selverston A. I. (1998) Inhibitory Glutamate Receptor Channels in Cultured Lobster Stomatogastric Neurons. *J Neurophysiol* **79,** 3189-3196.

Clemens S., Combes D., Meyrand P. and Simmers J. (1998a) Long-Term Expression of Two Interacting Motor Pattern-Generating Networks in the Stomatogastric System of Freely Behaving Lobster. *J Neurophysiol* **79,** 1396-1408.

Clemens S., Massabuau J. C., Legeay A., Meyrand P. and Simmers J. (1998b) In Vivo Modulation of Interacting Central Pattern Generators in Lobster Stomatogastric Ganglion: Influence of Feeding and Partial Pressure of Oxygen. *J Neurosci* **18,** 2788-2799.

Colas J. F., Launay J. M., Kellermann O., Rosay P. and Maroteaux L. (1995) Drosophila 5-Ht2 Serotonin Receptor: Coexpression with Fushi-Tarazu During Segmentation. *Proc Natl Acad Sci U S A* **92,** 5441-5445.

Coleman M. J. and Nusbaum M. P. (1994) Functional Consequences of Compartmentalization of Synaptic Input. *J Neurosci* **14,** 6544-6552.

Coleman M. J., Meyrand P. and Nusbaum M. P. (1995) A Switch between Two Modes of Synaptic Transmission Mediated by Presynaptic Inhibition. *Nature* **378,** 502-505.

Coleman M. J., Nusbaum M. P., Cournil I. and Claiborne B. J. (1992) Distribution of Modulatory Inputs to the Stomatogastric Ganglion of the Crab, Cancer Borealis. *J Comp Neurol* **325,** 581-594.

Cooper R. L., Hampson D. R. and Atwood H. L. (1995) Synaptotagmin-Like Expression in the Motor Nerve Terminals of Crayfish. *Brain Res* **703,** 214-216.

Cooper R. L., Donmezer A. and Shearer J. (2003) Intrinsic Differences in Sensitivity to 5-Ht between High- and Low-Output Terminals Innervating the Same Target. *Neurosci Res* **45,** 163-172.

Cropper E. C., Evans C. G., Hurwitz I., Jing J., Proekt A., Romero A. and Rosen S. C. (2004) Feeding Neural Networks in the Mollusc Aplysia. *Neurosignals* **13,** 70-86.

Cymbalyuk G. S., Gaudry Q., Masino M. A. and Calabrese R. L. (2002) Bursting in Leech Heart Interneurons: Cell-Autonomous and Network-Based Mechanisms. *J Neurosci* **22,** 10580-10592.

Daaka Y., Luttrell L. M. and Lefkowitz R. J. (1997) Switching of the Coupling of the Beta2-Adrenergic Receptor to Different G Proteins by Protein Kinase A. *Nature* **390,** 88-91.

Dascal N. (2001) Ion-Channel Regulation by G Proteins. *Trends Endocrinol Metab* **12,** 391-398.

Del Negro C. A., Wilson C. G., Butera R. J., Rigatto H. and Smith J. C. (2002) Periodicity, Mixed-Mode Oscillations, and Quasiperiodicity in a Rhythm-Generating Neural Network. *Biophys J* **82,** 206-214.

Demchyshyn L. L., McConkey F. and Niznik H. B. (2000) Dopamine D5 Receptor Agonist High Affinity and Constitutive Activity Profile Conferred by Carboxyl-Terminal Tail Sequence. *J.Biol.Chem.* **275,** 23446-23455.

Dickinson P. S. (2006) Neuromodulation of Central Pattern Generators in Invertebrates and Vertebrates. *Curr Opin Neurobiol* **16,** 604-614.

Dixon C. J., Ahyong S. T. and Schram F. R. (2003) A New Hypothesis of Decapod Phlogeny. *Crustaceana* **76,** 935-975.

Dixon D. and Atwood H. L. (1989) Phosphatidylinositol System's Role in Serotonin-Induced Facilitation at the Crayfish Neuromuscular Junction. *J Neurophysiol* **62,** 239-246.

Dodge-Kafka K. L., Soughayer J., Pare G. C., Carlisle Michel J. J., Langeberg L. K., Kapiloff M. S. and Scott J. D. (2005) The Protein Kinase a Anchoring Protein Makap Coordinates Two Integrated Camp Effector Pathways. *Nature* **437,** 574-578.

Dong Y. and White F. J. (2003) Dopamine D1-Class Receptors Selectively Modulate a Slowly Inactivating Potassium Current in Rat Medial Prefrontal Cortex Pyramidal Neurons. *J Neurosci* **23,** 2686-2695.

Dwivedi Y., Mondal A. C., Payappagoudar G. V. and Rizavi H. S. (2005) Differential Regulation of Serotonin (5ht)2a Receptor Mrna and Protein Levels after Single and Repeated Stress in Rat Brain: Role in Learned Helplessness Behavior. *Neuropharmacology* **48,** 204-214.

Dyachok O., Isakov Y., Sagetorp J. and Tengholm A. (2006) Oscillations of Cyclic Amp in Hormone-Stimulated Insulin-Secreting Beta-Cells. *Nature* **439,** 349-352.

Edwards D. H., Heitler W. J. and Krasne F. B. (1999) Fifty Years of a Command Neuron: The Neurobiology of Escape Behavior in the Crayfish. *Trends Neurosci* **22,** 153-161.

Edwards D. H., Yeh S. R., Musolf B. E., Antonsen B. L. and Krasne F. B. (2002) Metamodulation of the Crayfish Escape Circuit. *Brain Behav Evol* **60,** 360-369.

Eisen J. S. and Marder E. (1982) Mechanisms Underlying Pattern Generation in Lobster Stomatogastric Ganglion as Determined by Selective Inactivation of Identified Neurons. Iii. Synaptic Connections of Electrically Coupled Pyloric Neurons. *J Neurophysiol* **48,** 1392-1415.

Eisen J. S. and Marder E. (1984) A Mechanism for Production of Phase Shifts in a Pattern Generator. *J Neurophysiol* **51,** 1375-1393.

Erlenbach I. and Wess J. (1998) Molecular Basis of V2 Vasopressin Receptor/Gs Coupling Selectivity. *J Biol Chem* **273,** 26549-26558.

Feldman J. L. and Janczewski W. A. (2006a) Point:Counterpoint: The Parafacial Respiratory Group (Pfrg)/Pre-Botzinger Complex (Prebotc) Is the Primary Site of Respiratory Rhythm Generation in the Mammal. Counterpoint: The Prebotc Is the Primary Site of Respiratory Rhythm Generation in the Mammal. *J Appl Physiol* **100,** 2096-2097; discussion 2097-2098, 2103-2098.

Feldman J. L. and Janczewski W. A. (2006b) The Last Word: Point:Counterpoint Authors Respond to Commentaries On "The Parafacial Respiratory Group (Pfrg)/Pre-Botzinger Complex (Prebotc) Is the Primary Site of Respiratory Rhythm Generation in the Mammal". *J Appl Physiol* **101,** 689.

Feldman J. L., Mitchell G. S. and Nattie E. E. (2003) Breathing: Rhythmicity, Plasticity, Chemosensitivity. *Annu Rev Neurosci* **26,** 239-266.

Fenelon V. S., Kilman V., Meyrand P. and Marder E. (1999) Sequential Developmental Acquisition of Neuromodulatory Inputs to a Central Pattern-Generating Network. *J Comp Neurol* **408,** 335-351.

Feng G., Hannan F., Reale V., Hon Y. Y., Kousky C. T., Evans P. D. and Hall L. M. (1996) Cloning and Functional Characterization of a Novel Dopamine Receptor from Drosophila Melanogaster. *J Neurosci* **16,** 3925-3933.

Fields T. A. and Casey P. J. (1997) Signalling Functions and Biochemical Properties of Pertussis Toxin-Resistant G-Proteins. *Biochem J* **321 (Pt 3),** 561-571.

Flamm R. E. and Harris-Warrick R. M. (1986a) Aminergic Modulation in Lobster Stomatogastric Ganglion. I. Effects on Motor Pattern and Activity of Neurons within the Pyloric Circuit. *J Neurophysiol* **55,** 847-865.

Flamm R. E. and Harris-Warrick R. M. (1986b) Aminergic Modulation in Lobster Stomatogastric Ganglion. Ii. Target Neurons of Dopamine, Octopamine, and Serotonin within the Pyloric Circuit. *J Neurophysiol* **55,** 866-881.

Fort T. J., Brezina V. and Miller M. W. (2004) Modulation of an Integrated Central Pattern Generator-Effector System: Dopaminergic Regulation of Cardiac Activity in the Blue Crab Callinectes Sapidus. *J Neurophysiol* **92,** 3455-3470.

Fort T. J., Garcia-Crescioni K., Agricola H. J., Brezina V. and Miller M. W. (2007) Regulation of the Crab Heartbeat by Crustacean Cardioactive Peptide (Ccap): Central and Peripheral Actions. *J Neurophysiol* **97,** 3407-3420.

Fredriksson R. and Schioth H. B. (2005) The Repertoire of G-Protein-Coupled Receptors in Fully Sequenced Genomes. *Mol Pharmacol* **67,** 1414-1425.

Fredriksson R., Lagerstrom M. C., Lundin L. G. and Schioth H. B. (2003) The G-Protein-Coupled Receptors in the Human Genome Form Five Main Families. Phylogenetic Analysis, Paralogon Groups, and Fingerprints. *Mol Pharmacol* **63,** 1256-1272.

Friend B. (1976) Morphology and Location of Dense-Core Vesicles in the Stomatogastric Ganglion of the Lobster, Panulirus Interruptus. *Cell Tiss. Res.* **175,** 369-390.

Gainetdinov R. R., Premont R. T., Bohn L. M., Lefkowitz R. J. and Caron M. G. (2004) Desensitization of G Protein-Coupled Receptors and Neuronal Functions. *Annu Rev Neurosci* **27,** 107-144.

Gao Q. B. and Wang Z. Z. (2006) Classification of G-Protein Coupled Receptors at Four Levels. *Protein Eng Des Sel* **19,** 511-516.

Gerachshenko T., Blackmer T., Yoon E. J., Bartleson C., Hamm H. E. and Alford S. (2005) Gbetagamma Acts at the C Terminus of Snap-25 to Mediate Presynaptic Inhibition. *Nat Neurosci* **8,** 597-605.

Gervasi N., Hepp R., Tricoire L., Zhang J., Lambolez B., Paupardin-Tritsch D. and Vincent P. (2007) Dynamics of Protein Kinase a Signaling at the Membrane, in the Cytosol, and in the Nucleus of Neurons in Mouse Brain Slices. *J Neurosci* **27,** 2744-2750.

Ghahremani M. H., Cheng P., Lembo P. M. and Albert P. R. (1999) Distinct Roles for Galphai2, Galphai3, and Gbeta Gamma in Modulation Offorskolin- or Gs-Mediated Camp Accumulation and Calcium Mobilization by Dopamine D2s Receptors. *J Biol Chem* **274,** 9238-9245.

Gola M. and Selverston A. (1981) Ionic Requirements for Bursting Activity in Lobster Stomatogastric Neurons. *J Comp Physiol* **145,** 191-207.

Golowasch J., Abbott L. F. and Marder E. (1999) Activity-Dependent Regulation of Potassium Currents in an Identified Neuron of the Stomatogastric Ganglion of the Crab Cancer Borealis. *J Neurosci (Online)* **19,** RC33.

Gotzes F., Balfanz S. and Baumann A. (1994) Primary Structure and Functional Characterization of a Drosophila Dopamine Receptor with High Homology to Human D1/5 Receptors. *Receptors Channels* **2,** 131-141.

Govind C. K. and Atwood H. L. (1975) Innervation and Neuromuscular Physiology of Intrinsic Foregut Muscles in the Blue Crab and Spiny Lobster. *Journal of Comparative Physiology* **96,** 185-204.

Graubard K. and Hartline D. K. (1991) Voltage Clamp Analysis of Intact Stomatogastric Neurons. *Brain Res* **557,** 241-254.

Graubard K., Raper J. A. and Hartline D. K. (1983) Graded Synaptic Transmission between Identified Spiking Neurons. *J Neurophysiol* **50,** 508-521.

Gray P. A., Janczewski W. A., Mellen N., McCrimmon D. R. and Feldman J. L. (2001) Normal Breathing Requires Prebotzinger Complex Neurokinin-1 Receptor-Expressing Neurons. *Nat Neurosci* **4,** 927-930.

Grillner S. (1985) Neurobiological Bases of Rhythmic Motor Acts in Vertebrates. *Science* **228,** 143-149.

Grillner S., Wallen P., Hill R., Cangiano L. and El Manira A. (2001) Ion Channels of Importance for the Locomotor Pattern Generation in the Lamprey Brainstem-Spinal Cord. *J Physiol* **533,** 23-30.

Grillner S., Ekeberg, El Manira A., Lansner A., Parker D., Tegner J. and Wallen P. (1998) Intrinsic Function of a Neuronal Network - a Vertebrate Central Pattern Generator. *Brain Res Brain Res Rev* **26,** 184-197.

Gruhn M., Guckenheimer J., Land B. and Harris-Warrick R. M. (2005) Dopamine Modulation of Two Delayed Rectifier Potassium Currents in a Small Neural Network. *J Neurophysiol* **94,** 2888-2900.

Hall D. A. and Strange P. G. (1997) Evidence That Antipsychotic Drugs Are Inverse Agonists at D2 Dopamine Receptors. *Br J Pharmacol* **121,** 731-736.

Hall R. A. and Lefkowitz R. J. (2002) Regulation of G Protein-Coupled Receptor Signaling by Scaffold Proteins. *Circ.Res.* **91,** 672-680.

Han K. A., Millar N. S. and Davis R. L. (1998) A Novel Octopamine Receptor with Preferential Expression in Drosophila Mushroom Bodies. *J Neurosci* **18,** 3650-3658.

Han K. A., Millar N. S., Grotewiel M. S. and Davis R. L. (1996) Damb, a Novel Dopamine Receptor Expressed Specifically in Drosophila Mushroom Bodies. *Neuron* **16,** 1127-1135.

Harris-Warrick R. M. (2002) Voltage-Sensitive Ion Channels in Rhythmic Motor Systems. *Curr.Opin.Neurobiol.* **12,** 646-651.

Harris-Warrick R. M. and Flamm R. E. (1987) Multiple Mechanisms of Bursting in a Conditional Bursting Neuron. *J Neurosci* **7,** 2113-2128.

Harris-Warrick R. M., Nagy F. and Nusbaum M. P. (1992a) Neuromodulation of Stomatogastric Networks by Identified Neurons and Transmitters, in *Dynamic Biological Networks: The Stomatogastric Nervous System* (Harris-warrick R. M., Marder E., Selverston A. I. and Moulins M., eds), pp 87-137. MIT Press, Cambridge.

Harris-Warrick R. M., Marder E., Selverston A. I. and Moulins M., eds (1992b) *Dynamic Biological Networks: The Stomatogastric Nervous System*. MIT Press, Cambridge.

Harris-Warrick R. M., Coniglio L. M., Barazangi N., Guckenheimer J. and Gueron S. (1995a) Dopamine Modulation of Transient Potassium Current Evokes Phase Shifts in a Central Pattern Generator Network. *J Neurosci* **15,** 342-358.

Harris-Warrick R. M., Coniglio L. M., Levini R. M., Gueron S. and Guckenheimer J. (1995b) Dopamine Modulation of Two Subthreshold Currents Produces Phase Shifts in Activity of an Identified Motoneuron. *J Neurophysiol* **74,** 1404-1420.

Harris-Warrick R. M., Johnson B. R., Peck J. H., Kloppenburg P., Ayali A. and Skarbinski J. (1998) Distributed Effects of Dopamine Modulation in the Crustacean Pyloric Network. *Ann N Y Acad Sci* **860,** 155-167.

Hartline D. K. and Maynard D. M. (1975) Motor Patterns in the Stomatogastric Ganglion of the Lobster Panulirus Argus. *J Exp Biol* **62,** 405-420.

Hartline D. K. and Russell D. F. (1984) Endogenous Burst Capability in a Neuron of the Gastric Mill Pattern Generator of the Spiny Lobster Panulirus Interruptus. *J Neurobiol* **15,** 345-364.

Hartline D. K., Gassie D. V. and Jones B. R. (1993) Effects of Soma Isolation on Outward Currents Measured under Voltage Clamp in Spiny Lobster Stomatogastric Motor Neurons. *J Neurophysiol* **69,** 2056-2071.

Hearn M. G., Ren Y., McBride E. W., Reveillaud I., Beinborn M. and Kopin A. S. (2002) A Drosophila Dopamine 2-Like Receptor: Molecular Characterization and Identification of Multiple Alternatively Spliced Variants. *Proc.Natl.Acad.Sci.U.S.A* **99,** 14554-14559.

Hempel C. M., Vincent P., Adams S. R., Tsien R. Y. and Selverston A. I. (1996a) Spatio-Temporal Dynamics of Cyclic Amp Signals in an Intact Neural Circuitm. *Nature* **384,** 166-169.

Hempel C. M., Vincent P., Adams S. R., Tsien R. Y. and Selverston A. I. (1996b) Spatio-Temporal Dynamics of Cyclic Amp Signals in an Intact Neural Circuit. *Nature* **384,** 166-169.

Hernandez-Lopez S., Bargas J., Surmeier D. J., Reyes A. and Galarraga E. (1997) D1 Receptor Activation Enhances Evoked Discharge in Neostriatal Medium Spiny Neurons by Modulating an L-Type Ca2+ Conductance. *J Neurosci* **17,** 3334-3342.

Hernandez-Lopez S., Tkatch T., Perez-Garci E., Galarraga E., Bargas J., Hamm H. and Surmeier D. J. (2000) D2 Dopamine Receptors in Striatal Medium Spiny Neurons Reduce L-Type Ca2+ Currents and Excitability Via a Novel Plc[Beta]1-Ip3-Calcineurin-Signaling Cascade. *J Neurosci* **20,** 8987-8995.

Ho M. K. and Wong Y. H. (2001) G(Z) Signaling: Emerging Divergence from G(I) Signaling. *Oncogene* **20,** 1615-1625.

Hooper S. L. and DiCaprio R. A. (2004) Crustacean Motor Pattern Generator Networks. *Neurosignals* **13,** 50-69.

Hopf F. W., Cascini M. G., Gordon A. S., Diamond I. and Bonci A. (2003) Cooperative Activation of Dopamine D1 and D2 Receptors Increases Spike Firing of Nucleus Accumbens Neurons Via G-Protein Betagamma Subunits. *J Neurosci* **23,** 5079-5087.

Hoyer D., Hannon J. P. and Martin G. R. (2002) Molecular, Pharmacological and Functional Diversity of 5-Ht Receptors. *Pharmacol.Biochem.Behav.* **71,** 533-554.

Huang K. P., Huang F. L. and Chen H. C. (1993) Characterization of a 7.5-Kda Protein Kinase C Substrate (Rc3 Protein, Neurogranin) from Rat Brain. *Arch Biochem Biophys* **305,** 570-580.

Huang X., Xiao H., Rex E. B., Hobson R. J., Messer W. S., Komuniecki P. R. and Komuniecki R. W. (2002) Functional Characterization of Alternatively Spliced 5-Ht2 Receptor Isoforms from the Pharynx and Muscle of the Parasitic Nematode, Ascaris Suum. *J Neurochem* **83,** 249-258.

Insel P. A., Head B. P., Ostrom R. S., Patel H. H., Swaney J. S., Tang C. M. and Roth D. M. (2005) Caveolae and Lipid Rafts: G Protein-Coupled Receptor Signaling Microdomains in Cardiac Myocytes. *Ann N Y Acad Sci* **1047,** 166-172.

Ivanov A. I. and Calabrese R. L. (2006) Graded Inhibitory Synaptic Transmission between Leech Interneurons: Assessing the Roles of Two Kinetically Distinct Low-Threshold Ca Currents. *J Neurophysiol* **96,** 218-234.

Iversen L. (2006) Neurotransmitter Transporters and Their Impact on the Development of Psychopharmacology. *Br J Pharmacol* **147 Suppl 1,** S82-88.

Janczewski W. A. and Feldman J. L. (2006) Distinct Rhythm Generators for Inspiration and Expiration in the Juvenile Rat. *J Physiol* **570,** 407-420.

Johnson B. R. and Harris-Warrick R. M. (1990) Aminergic Modulation of Graded Synaptic Transmission in the Lobster Stomatogastric Ganglion. *J Neurosci* **10,** 2066-2076.

Johnson B. R. and Hooper S. L. (1992) Overview of the Stomatogastric Nervous System, in *Dynamic Biological Networks* (Harris-Warrick R.M., Marder E., Selverston A.I. and Moulins M., eds), pp 1-30. MIT Press, Cambridge.

Johnson B. R., Peck J. H. and Harris-Warrick R. M. (1993a) Dopamine Induces Sign Reversal at Mixed Chemical-Electrical Synapses. *Brain Res* **625,** 159-164.

Johnson B. R., Peck J. H. and Harris-Warrick R. M. (1993b) Amine Modulation of Electrical Coupling in the Pyloric Network of the Lobster Stomatogastric Ganglion. *J Comp Physiol [A]* **172,** 715-732.

Johnson B. R., Peck J. H. and Harris-Warrick R. M. (1994) Differential Modulation of Chemical and Electrical Components of Mixed Synapses in the Lobster Stomatogastric Ganglion. *J Comp Physiol [A]* **175,** 233-249.

Johnson B. R., Peck J. H. and Harris-Warrick R. M. (1995) Distributed Amine Modulation of Graded Chemical Transmission in the Pyloric Network of the Lobster Stomatogastric Ganglion. *J Neurophysiol* **74,** 437-452.

Johnson B. R., Kloppenburg P. and Harris-Warrick R. M. (2003a) Dopamine Modulation of Calcium Currents in Pyloric Neurons of the Lobster Stomatogastric Ganglion. *J Neurophysiol* **90,** 631-643.

Johnson B. R., Schneider L. R., Nadim F. and Harris-Warrick R. M. (2005) Dopamine Modulation of Phasing of Activity in a Rhythmic Motor Network: Contribution of Synaptic and Intrinsic Modulatory Actions. *J Neurophysiol* **94,** 3101-3111.

Johnson M. P., Wainscott D. B., Lucaites V. L., Baez M. and Nelson D. L. (1997) Mutations of Transmembrane Iv and V Serines Indicate That All Tryptamines Do Not Bind to the Rat 5-Ht2a Receptor in the Same Manner. *Brain Res Mol Brain Res* **49,** 1-6.

Johnson M. S., Lutz E. M., Firbank S., Holland P. J. and Mitchell R. (2003b) Functional Interactions between Native Gs-Coupled 5-Ht Receptors in Hek-293 Cells and the Heterologously Expressed Serotonin Transporter. *Cell Signal.* **15,** 803-811.

Jorge-Rivera J. C., Sen K., Birmingham J. T., Abbott L. F. and Marder E. (1998) Temporal Dynamics of Convergent Modulation at a Crustacean Neuromuscular Junction. *J.Neurophysiol.* **80,** 2559-2570.

Kapsimali M., Le Crom S. and Vernier P. (2003) A Natural History of Vertebrate Dopamine Receptors, in *Dopamine Receptors and Transporters: Function, Imaging and Clinical Implication,* second Edition (A S., M L. and P V., eds), pp 1-43. Marcel Dekker, Inc, New York.

Karhunen T., Vilim F. S., Alexeeva V., Weiss K. R. and Church P. J. (2001) Targeting of Peptidergic Vesicles in Cotransmitting Terminals. *J Neurosci* **21,** RC127.

Katz P. S. and Harris-Warrick R. M. (1989) Serotonergic/Cholinergic Muscle Receptor Cells in the Crab Stomatogastric Nervous System. Ii. Rapid Nicotinic and Prolonged Modulatory Effects on Neurons in the Stomatogastric Ganglion. *J Neurophysiol* **62,** 571-581.

Katz P. S. and Harris-Warrick R. M. (1990a) Actions of Identified Neuromodulatory Neurons in a Simple Motor System. *Trends Neurosci* **13,** 367-373.

Katz P. S. and Harris-Warrick R. M. (1990b) Neuromodulation of the Crab Pyloric Central Pattern Generator by Serotonergic/Cholinergic Proprioceptive Afferents. *J Neurosci* **10,** 1495-1512.

Katz P. S. and Tazaki K. (1992) Comparative and Evolutionary Aspects of the Crustacean Stomatogastric System, in *Dynamic Biological Networks: The Stomoatogatric Nervous System* (Harris-Warrick R. M., Marder E., Selverston A. I. and Moulins M., eds), pp 221-262. MIT Press, Cambridge.

Katz P. S. and Frost W. N. (1997) Removal of Spike Frequency Adaptation Via Neuromodulation Intrinsic to the Tritonia Escape Swim Central Pattern Generator. *J Neurosci* **17,** 7703-7713.

Katz P. S. and Edwards D. H. (1999) Metamodulation: The Control and Modulation of Neuromodulation, in *Beyond Neurotransmission: Neuromodulation and Its Importance for Information Processing* (Katz P. S., ed.), pp 339-381. Oxford Univ. Press, New York.

Katz P. S., Eigg M. H. and Harris-Warrick R. M. (1989) Serotonergic/Cholinergic Muscle Receptor Cells in the Crab Stomatogastric Nervous System. I. Identification and Characterization of the Gastropyloric Receptor Cells. *J Neurophysiol* **62,** 558-570.

Katz P. S., Getting P. A. and Frost W. N. (1994) Dynamic Neuromodulation of Synaptic Strength Intrinsic to a Central Pattern Generator Circuit. *Nature* **367,** 729-731.

Khorkova O. and Golowasch J. (2007) Neuromodulators, Not Activity, Control Coordinated Expression of Ionic Currents. *J Neurosci* **27,** 8709-8718.

Kiehn O. (2006) Locomotor Circuits in the Mammalian Spinal Cord. *Ann. Rev. Neurosci.* **29,** 279-306.

Kiehn O. and Harris-Warrick R. M. (1992a) Serotonergic Stretch Receptors Induce Plateau Properties in a Crustacean Motor Neuron by a Dual-Conductance Mechanism. *J Neurophysiol* **68,** 485-495.

Kiehn O. and Harris-Warrick R. M. (1992b) 5-Ht Modulation of Hyperpolarization-Activated Inward Current and Calcium-Dependent Outward Current in a Crustacean Motor Neuron. *J Neurophysiol* **68,** 496-508.

Kiehn O., Kjaerulff O., Tresch M. C. and Harris-Warrick R. M. (2000) Contributions of Intrinsic Motor Neuron Properties to the Production of Rhythmic Motor Output in the Mammalian Spinal Cord. *Brain Res Bull* **53,** 649-659.

Kilman V., Fenelon V. S., Richards K. S., Thirumalai V., Meyrand P. and Marder E. (1999) Sequential Developmental Acquisition of Cotransmitters in Identified Sensory Neurons of the Stomatogastric Nervous System of the Lobsters, Homarus Americanus and Homarus Gammarus. *J Comp Neurol* **408,** 318-334.

Kilman V. L. and Marder E. (1996) Ultrastructure of the Stomatogastric Ganglion Neuropil of the Crab, *Cancer Borealis*. *J Comp Neurol* **374,** 362-375.

Kimura K., White B. H. and Sidhu A. (1995a) Coupling of Human D-1 Dopamine Receptors to Different Guanine Nucleotide Binding Proteins. Evidence That D-1 Dopamine Receptors Can Couple to Both Gs and G(O). *J Biol Chem* **270,** 14672-14678.

Kimura K., Sela S., Bouvier C., Grandy D. K. and Sidhu A. (1995b) Differential Coupling of D1 and D5 Dopamine Receptors to Guanine Nucleotide Binding Proteins in Transfected Gh4c1 Rat Somatomammotrophic Cells. *J Neurochem* **64,** 2118-2124.

King D. G. (1976a) Organization of Crustacean Neuropil. Ii. Distribution of Synaptic Contacts on Identified Motor Neurons in Lobster Stomatogastric Ganglion. *J Neurocytol* **5,** 239-266.

King D. G. (1976b) Organization of Crustacean Neuropil. I. Patterns of Synaptic Connections in Lobster Stomatogastric Ganglion. *J Neurocytol* **5,** 207-237.

Kirby M. S. and Nusbaum M. P. (2007) Peptide Hormone Modulation of a Neuronally Modulated Motor Circuit. *J Neurophysiol* **98,** 3206-3220.

Kloppenburg P., Levini R. M. and Harris-Warrick R. M. (1999) Dopamine Modulates Two Potassium Currents and Inhibits the Intrinsic Firing Properties of an Identified Motor Neuron in a Central Pattern Generator Network. *J Neurophysiol* **81,** 29-38.

Kloppenburg P., Zipfel W. R., Webb W. W. and Harris-Warrick R. M. (2000) Highly Localized Ca(2+) Accumulation Revealed by Multiphoton Microscopy in an Identified Motoneuron and Its Modulation by Dopamine. *J Neurosci* **20,** 2523-2533.

Kloppenburg P., Zipfel W. R., Webb W. W. and Harris-Warrick R. M. (2007) Heterogeneous Effects of Dopamine on Highly Localized, Voltage-Induced Ca2+ Accumulation in Identified Motoneurons. *J Neurophysiol* **98,** 2910-2917.

Koshiya N. and Smith J. C. (1999) Neuronal Pacemaker for Breathing Visualized in Vitro. *Nature* **400,** 360-363.

Kravitz E. A. (2000) Serotonin and Aggression: Insights Gained from a Lobster Model System and Speculations on the Role of Amine Neurons in a Complex Behavior. *J Comp Physiol [A]* **186,** 221-238.

Krenz W. D., Nguyen D., Perez-Acevedo N. L. and Selverston A. I. (2000) Group I, Ii, and Iii Mglur Compounds Affect Rhythm Generation in the Gastric Circuit of the Crustacean Stomatogastric Ganglion. *J Neurophysiol* **83,** 1188-1201.

Kristiansen K., Kroeze W. K., Willins D. L., Gelber E. I., Savage J. E., Glennon R. A. and Roth B. L. (2000) A Highly Conserved Aspartic Acid (Asp-155) Anchors the Terminal Amine Moiety of Tryptamines and Is Involved in Membrane Targeting of the 5-Ht(2a) Serotonin Receptor but Does Not Participate in Activation Via A "Salt-Bridge Disruption" Mechanism. *J Pharmacol Exp Ther* **293,** 735-746.

Kroeze W. K., Kristiansen K. and Roth B. L. (2002) Molecular Biology of Serotonin Receptors Structure and Function at the Molecular Level. *Curr.Top.Med.Chem.* **2,** 507-528.

Kurrasch-Orbaugh D. M., Watts V. J., Barker E. L. and Nichols D. E. (2003) Serotonin 5-Hydroxytryptamine 2a Receptor-Coupled Phospholipase C and Phospholipase A2 Signaling Pathways Have Different Receptor Reserves. *J.Pharmacol.Exp.Ther.* **304,** 229-237.

Kushner P. D. and Maynard E. A. (1977) Localization of Monoamine Fluorescence in the Stomatogastric Nervous System of Lobsters. *Brain Res* **129,** 13-28.

Kushner P. D. and Barker D. L. (1983) A Neurochemical Description of the Dopaminergic Innervation of the Stomatogastric Ganglion of the Spiny Lobster. *J.Neurobiol.* **14,** 17-28.

Laugwitz K. L., Allgeier A., Offermanns S., Spicher K., Van Sande J., Dumont J. E. and Schultz G. (1996) The Human Thyrotropin Receptor: A Heptahelical Receptor Capable of Stimulating Members of All Four G Protein Families. *Proc Natl Acad Sci U S A* **93,** 116-120.

Le Crom S., Kapsimali M., Barome P. O. and Vernier P. (2003) Dopamine Receptors for Every Species: Gene Duplications and Functional Diversification in Craniates. *J Struct Funct Genomics* **3,** 161-176.

Le Feuvre Y., Fenelon V. S. and Meyrand P. (1999) Central Inputs Mask Multiple Adult Neural Networks within a Single Embryonic Network. *Nature* **402,** 660-664.

Lee F. J. and Liu F. (2004) Direct Interactions between Nmda and D1 Receptors: A Tale of Tails. *Biochem Soc Trans* **32,** 1032-1036.

Lefkowitz R. J. (1998) G Protein-Coupled Receptors. Iii. New Roles for Receptor Kinases and Beta-Arrestins in Receptor Signaling and Desensitization. *J Biol Chem* **273,** 18677-18680.

Lefkowitz R. J. and Shenoy S. K. (2005) Transduction of Receptor Signals by Beta-Arrestins. *Science* **308,** 512-517.

Lembo P. M., Ghahremani M. H., Morris S. J. and Albert P. R. (1997) A Conserved Threonine Residue in the Second Intracellular Loop of the 5-Hydroxytryptamine 1a Receptor Directs Signaling Specificity. *Mol Pharmacol* **52,** 164-171.

Lezcano N., Mrzljak L., Eubanks S., Levenson R., Goldman-Rakic P. and Bergson C. (2000) Dual Signaling Regulated by Calcyon, a D1 Dopamine Receptor Interacting Protein. *Science***,** 1660-1664.

Li X. C., Giot J. F., Kuhl D., Hen R. and Kandel E. R. (1995) Cloning and Characterization of Two Related Serotonergic Receptors from the Brain and the Reproductive System of Aplysia That Activate Phospholipase C. *J Neurosci* **15,** 7585-7591.

Limbird L. E. (2004) The Receptor Concept: A Continuing Evolution. *Mol Interv* **4,** 326-336.

Littleton J. T., Bellen H. J. and Perin M. S. (1993) Expression of Synaptotagmin in Drosophila Reveals Transport and Localization of Synaptic Vesicles to the Synapse. *Development* **118,** 1077-1088.

Liu F., Wan Q., Pristupa Z. B., Yu X. M., Wang Y. T. and Niznik H. B. (2000) Direct Protein-Protein Coupling Enables Cross-Talk between Dopamine D5 and Gamma-Aminobutyric Acid a Receptors. *Nature* **403,** 274-280.

Liu J. and Wess J. (1996) Different Single Receptor Domains Determine the Distinct G Protein Coupling Profiles of Members of the Vasopressin Receptor Family. *J Biol Chem* **271,** 8772-8778.

Liu J., Hu J. Y., Schacher S. and Schwartz J. H. (2004) The Two Regulatory Subunits of Aplysia Camp-Dependent Protein Kinase Mediate Distinct Functions in Producing Synaptic Plasticity. *J Neurosci* **24,** 2465-2474.

Liu W. S. and Heckman C. A. (1998) The Sevenfold Way of Pkc Regulation. *Cell Signal* **10,** 529-542.

Livingstone M. S., Harris-Warrick R. M. and Kravitz E. A. (1980) Serotonin and Octopamine Produce Opposite Postures in Lobsters. *Science* **208,** 76-79.

Logothetis D. E., Kurachi Y., Galper J., Neer E. J. and Clapham D. E. (1987) The Beta Gamma Subunits of Gtp-Binding Proteins Activate the Muscarinic K+ Channel in Heart. *Nature* **325,** 321-326.

Luttrell L. M., Roudabush F. L., Choy E. W., Miller W. E., Field M. E., Pierce K. L. and Lefkowitz R. J. (2001) Activation and Targeting of Extracellular Signal-Regulated Kinases by Beta-Arrestin Scaffolds. *Proc Natl Acad Sci U S A* **98,** 2449-2454.

Luttrell L. M., Ferguson S. S., Daaka Y., Miller W. E., Maudsley S., Della Rocca G. J., Lin F., Kawakatsu H., Owada K., Luttrell D. K., Caron M. G. and Lefkowitz R. J. (1999) Beta-Arrestin-Dependent Formation of Beta2 Adrenergic Receptor-Src Protein Kinase Complexes. *Science* **283,** 655-661.

Manivet P., Schneider B., Smith J. C., Choi D. S., Maroteaux L., Kellermann O. and Launay J. M. (2002) The Serotonin Binding Site of Human and Murine 5-Ht2b Receptors: Molecular Modeling and Site-Directed Mutagenesis. *J Biol Chem* **277,** 17170-17178.

Marder E. and Eisen J. S. (1984a) Transmitter Identification of Pyloric Neurons: Electrically Coupled Neurons Use Different Transmitters. *J Neurophysiol* **51,** 1345-1361.

Marder E. and Eisen J. S. (1984b) Electrically Coupled Pacemaker Neurons Respond Differently to Same Physiological Inputs and Neurotransmitters. *J Neurophysiol* **51,** 1362-1374.

Marder E. and Calabrese R. L. (1996) Principles of Rhythmic Motor Pattern Generation. *Physiol Rev* **76,** 687-717.

Marder E. and Bucher D. (2001) Central Pattern Generators and the Control of Rhythmic Movements. *Curr.Biol.* **11,** R986-R996.

Marder E. and Bucher D. (2006) Understanding Circuit Dynamics Using the Stomatogastric Nervous System of Lobsters and Crabs. *Annu Rev Physiol* **69,** 291-316.

Marder E. and Bucher D. (2007) Understanding Circuit Dynamics Using the Stomatogastric Nervous System of Lobsters and Crabs. *Annu Rev Physiol* **69,** 291-316.

Marder E., Christie A. E. and Kilman V. L. (1995) Functional Organization of Cotransmission Systems: Lessons from Small Nervous Systems. *Invert Neurosci* **1,** 105-112.

McClintock T. S., Byrnes A. P. and Lerner M. R. (1992) Molecular Cloning of a G-Protein Alpha I Subunit from the Lobster Olfactory Organ. *Brain Res Mol Brain Res* **14,** 273-276.

McClintock T. S., Xu F., Quintero J., Gress A. M. and Landers T. M. (1997) Molecular Cloning of a Lobster G Alpha(Q) Protein Expressed in Neurons of Olfactory Organ and Brain. *J Neurochem* **68,** 2248-2254.

Mee C. J., Pym E. C., Moffat K. G. and Baines R. A. (2004) Regulation of Neuronal Excitability through Pumilio-Dependent Control of a Sodium Channel Gene. *J Neurosci* **24,** 8695-8703.

Mellen N. M., Janczewski W. A., Bocchiaro C. M. and Feldman J. L. (2003) Opioid-Induced Quantal Slowing Reveals Dual Networks for Respiratory Rhythm Generation. *Neuron* **37,** 821-826.

Mesce K. A. (2002) Metamodulation of the Biogenic Amines: Second-Order Modulation by Steroid Hormones and Amine Cocktails. *Brain Behav Evol* **60,** 339-349.

Meyrand P. and Moulins M. (1988) Phylogenetic Plasticity of Crustacean Stomatogastric Circuits. I. Pyloric Opatterns and Pyloric Circuit of the Shrimp Palaemon Serratus. *Journal of Experimental Biology* **138,** 107-132.

Meyrand P., Simmers J. and Moulins M. (1991) Construction of a Pattern-Generating Circuit with Neurons of Different Networks. *Nature* **351,** 60-63.

Meyrand P., Weimann J. M. and Marder E. (1992) Multiple Axonal Spike Initiation Zones in a Motor Neuron: Serotonin Activation. *J Neurosci* **12,** 2803-2812.

Michel J. J. and Scott J. D. (2002) Akap Mediated Signal Transduction. *Annu Rev Pharmacol Toxicol* **42,** 235-257.

Miller J. P. (1987) Pyloric Mechanisms, in *The Crustacean Stomatogastric System* (Selverston A. I. and Moulins M., eds), pp 109-146. Springer-Verlag, New York.

Missale C., Nash S. R., Robinson S. W., Jaber M. and Caron M. G. (1998) Dopamine Receptors: From Structure to Function. *Physiol Rev.* **78,** 189-225.

Mitchell G. S. and Johnson S. M. (2003) Neuroplasticity in Respiratory Motor Control. *J Appl Physiol* **94,** 358-374.

Mizrahi A., Dickinson P. S., Kloppenburg P., Fenelon V., Baro D. J., Harris-Warrick R. M., Meyrand P. and Simmers J. (2001) Long-Term Maintenance of Channel Distribution in a Central Pattern Generator Neuron by Neuromodulatory Inputs Revealed by Decentralization in Organ Culture. *J.Neurosci.* **21,** 7331-7339.

Morisset S., Rouleau A., Ligneau X., Gbahou F., Tardivel-Lacombe J., Stark H., Schunack W., Ganellin C. R., Schwartz J. C. and Arrang J. M. (2000) High Constitutive Activity of Native H3 Receptors Regulates Histamine Neurons in Brain. *Nature* **408,** 860-864.

Morris L. G. and Hooper S. L. (1997) Muscle Response to Changing Neuronal Input in the Lobster (*Panulirus Interruptus*) Stomatogastric System: Spike Number- Versus Spike Frequency-Dependent Domains. *J Neurosci* **17,** 5956-5971.

Morris L. G. and Hooper S. L. (1998) Muscle Response to Changing Neuronal Input in the Lobster (*Panulirus Interruptus*) Stomatogastric System: Slow Muscle Properties Can Transform Rhythmic Input into Tonic Output. *J Neurosci* **18,** 3433-3442.

Morris L. G., Thuma J. B. and Hooper S. L. (2000) Muscles Express Motor Patterns of Non-Innervating Neural Networks by Filtering Broad-Band Input. *Nat Neurosci* **3,** 245-250.

Mustard J. A., Beggs K. T. and Mercer A. R. (2005) Molecular Biology of the Invertebrate Dopamine Receptors. *Arch Insect Biochem Physiol* **59,** 103-117.

Mustard J. A., Blenau W., Hamilton I. S., Ward V. K., Ebert P. R. and Mercer A. R. (2003) Analysis of Two D1-Like Dopamine Receptors from the Honey Bee Apis Mellifera Reveals Agonist-Independent Activity. *Brain Res.Mol.Brain Res.* **113,** 67-77.

Nagy F. and Miller J. P. (1987) Pyloric Pattern Generation in *Panulirus Interruptus* Is Terminated by Blockade of Activity through the Stomatogastric Nerve, in *The Crustacean Stomatogastric System* (Selverston A. I. and Moulins M., eds), pp 136-139. Springer, Berlin.

Neve K. A., Seamans J. K. and Trantham-Davidson H. (2004) Dopamine Receptor Signaling. *J Recept Signal Transduct Res* **24,** 165-205.

Newman-Tancredi A., Cussac D., Audinot V., Pasteau V., Gavaudan S. and Millan M. J. (1999) G Protein Activation by Human Dopamine D3 Receptors in High-Expressing Chinese Hamster Ovary Cells: A Guanosine-5'-O-(3-[35s]Thio)- Triphosphate Binding and Antibody Study. *Mol Pharmacol* **55,** 564-574.

Newton A. C. (1995) Protein Kinase C: Structure, Function, and Regulation. *J Biol Chem* **270,** 28495-28498.

Newton A. C. (2001) Protein Kinase C: Structural and Spatial Regulation by Phosphorylation, Cofactors, and Macromolecular Interactions. *Chem Rev* **101,** 2353-2364.

Nikolaev V. O., Bunemann M., Schmitteckert E., Lohse M. J. and Engelhardt S. (2006) Cyclic Amp Imaging in Adult Cardiac Myocytes Reveals Far-Reaching Beta1-Adrenergic but Locally Confined Beta2-Adrenergic Receptor-Mediated Signaling. *Circ Res* **99,** 1084-1091.

Nishi A., Snyder G. L. and Greengard P. (1997) Bidirectional Regulation of Darpp-32 Phosphorylation by Dopamine. *J Neurosci* **17,** 8147-8155.

Niswender C. M., Copeland S. C., Herrick-Davis K., Emeson R. B. and Sanders-Bush E. (1999) Rna Editing of the Human Serotonin 5-Hydroxytryptamine 2c Receptor Silences Constitutive Activity. *J Biol Chem* **274,** 9472-9478.

Nusbaum M. P. (2002) Regulating Peptidergic Modulation of Rhythmically Active Neural Circuits. *Brain Behav Evol* **60,** 378-387.

Nusbaum M. P. and Beenhakker M. P. (2002) A Small-Systems Approach to Motor Pattern Generation. *Nature* **417,** 343-350.

Nusbaum M. P., Weimann J. M., Golowasch J. and Marder E. (1992) Presynaptic Control of Modulatory Fibers by Their Neural Network Targets. *J Neurosci* **12,** 2706-2714.

Nusbaum M. P., Blitz D. M., Swensen A. M., Wood D. and Marder E. (2001) The Roles of Co-Transmission in Neural Network Modulation. *Trends Neurosci.* **24,** 146-154.

O'Sullivan G. J., Roth B. L., Kinsella A. and Waddington J. L. (2004) Sk&F 83822 Distinguishes Adenylyl Cyclase from Phospholipase C-Coupled Dopamine D1-Like Receptors: Behavioural Topography. *Eur J Pharmacol* **486,** 273-280.

Oakley R. H., Laporte S. A., Holt J. A., Barak L. S. and Caron M. G. (2001) Molecular Determinants Underlying the Formation of Stable Intracellular G Protein-Coupled Receptor-Beta-Arrestin Complexes after Receptor Endocytosis*. *J Biol Chem* **276,** 19452-19460.

Obadiah J., Avidor-Reiss T., Fishburn C. S., Carmon S., Bayewitch M., Vogel Z., Fuchs S. and Levavi-Sivan B. (1999) Adenylyl Cyclase Interaction with the D2 Dopamine Receptor Family; Differential Coupling to Gi, Gz, and Gs. *Cell Mol Neurobiol* **19,** 653-664.

Onimaru H. and Homma I. (2003) A Novel Functional Neuron Group for Respiratory Rhythm Generation in the Ventral Medulla. *J Neurosci* **23,** 1478-1486.

Onimaru H. and Homma I. (2006) Point:Counterpoint: The Parafacial Respiratory Group (Pfrg)/Pre-Botzinger Complex (Prebotc) Is the Primary Site of Respiratory Rhythm Generation in the Mammal. Point: The Pfrg Is the Primary Site of Respiratory Rhythm Generation in the Mammal. *J Appl Physiol* **100,** 2094-2095.

Ostrom R. S., Liu X., Head B. P., Gregorian C., Seasholtz T. M. and Insel P. A. (2002) Localization of Adenylyl Cyclase Isoforms and G Protein-Coupled Receptors in Vascular Smooth Muscle Cells: Expression in Caveolin-Rich and Noncaveolin Domains. *Mol Pharmacol* **62,** 983-992.

Palczewski K., Kumasaka T., Hori T., Behnke C. A., Motoshima H., Fox B. A., Le Trong I., Teller D. C., Okada T., Stenkamp R. E., Yamamoto M. and Miyano M. (2000) Crystal Structure of Rhodopsin: A G Protein-Coupled Receptor. *Science* **289,** 739-745.

Pauwels P. J. (2000) Diverse Signalling by 5-Hydroxytryptamine (5-Ht) Receptors. *Biochem Pharmacol* **60,** 1743-1750.

Peck J. H., Nakanishi S. T., Yaple R. and Harris-Warrick R. M. (2001) Amine Modulation of the Transient Potassium Current in Identified Cells of the Lobster Stomatogastric Ganglion. *J.Neurophysiol.* **86,** 2957-2965.

Peck J. H., Gaier E., Stevens E., Repicky S. and Harris-Warrick R. M. (2006) Amine Modulation of Ih in a Small Neural Network. *J Neurophysiol* **96,** 2931-2940.

Pei L., Lee F. J., Moszczynska A., Vukusic B. and Liu F. (2004) Regulation of Dopamine D1 Receptor Function by Physical Interaction with the Nmda Receptors. *J Neurosci* **24,** 1149-1158.

Perez M. F., White F. J. and Hu X. T. (2006) Dopamine D(2) Receptor Modulation of K(+) Channel Activity Regulates Excitability of Nucleus Accumbens Neurons at Different Membrane Potentials. *J Neurophysiol* **96,** 2217-2228.

Perry S. J., Baillie G. S., Kohout T. A., McPhee I., Magiera M. M., Ang K. L., Miller W. E., McLean A. J., Conti M., Houslay M. D. and Lefkowitz R. J. (2002) Targeting of Cyclic Amp Degradation to Beta 2-Adrenergic Receptors by Beta-Arrestins. *Science* **298,** 834-836.

Pierce K. L. and Lefkowitz R. J. (2001) Classical and New Roles of Beta-Arrestins in the Regulation of G-Protein-Coupled Receptors. *Nat Rev Neurosci* **2,** 727-733.

Prinz A. A., Bucher D. and Marder E. (2004) Similar Network Activity from Disparate Circuit Parameters. *Nat Neurosci*.

Quigley P. A., Msghina M., Govind C. K. and Atwood H. L. (1999) Visible Evidence for Differences in Synaptic Effectiveness with Activity-Dependent Vesicular Uptake and Release of Fm1-43. *J Neurophysiol* **81,** 356-370.

Ramakers G. M., Gerendasy D. D. and de Graan P. N. (1999) Substrate Phosphorylation in the Protein Kinase Cgamma Knockout Mouse. *J Biol Chem* **274,** 1873-1874.

Ramirez J. M., Tryba A. K. and Pena F. (2004) Pacemaker Neurons and Neuronal Networks: An Integrative View. *Curr Opin Neurobiol* **14,** 665-674.

Reale V., Hannan F., Hall L. M. and Evans P. D. (1997) Agonist-Specific Coupling of a Cloned Drosophila Melanogaster D1-Like Dopamine Receptor to Multiple Second Messenger Pathways by Synthetic Agonists. *J Neurosci* **17,** 6545-6553.

Rekling J. C. and Feldman J. L. (1998) Prebotzinger Complex and Pacemaker Neurons: Hypothesized Site and Kernel for Respiratory Rhythm Generation. *Annu Rev Physiol* **60,** 385-405.

Rezer E. and Moulins M. (1983) Expression of the Pyloric Pattern Generator in the Intact Animal. *Journal of Comparative Physiology* **153,** 17-28.

Riad M., Watkins K. C., Doucet E., Hamon M. and Descarries L. (2001) Agonist-Induced Internalization of Serotonin-1a Receptors in the Dorsal Raphe Nucleus (Autoreceptors) but Not Hippocampus (Heteroreceptors). *J Neurosci* **21,** 8378-8386.

Rich T. C., Fagan K. A., Tse T. E., Schaack J., Cooper D. M. and Karpen J. W. (2001) A Uniform Extracellular Stimulus Triggers Distinct Camp Signals in Different Compartments of a Simple Cell. *Proc Natl Acad Sci U S A* **98,** 13049-13054.

Richards K. S., Simon D. J., Pulver S. R., Beltz B. S. and Marder E. (2003) Serotonin in the Developing Stomatogastric System of the Lobster, Homarus Americanus. *J.Neurobiol.* **54,** 380-392.

Richter S. and Scholtz G. (2001) Phylogenetic Analyses of the Malacostraca (Crustacea). *J. Zool. Systemat. Res.* **39,** 1-23.

Rochais F., Abi-Gerges A., Horner K., Lefebvre F., Cooper D. M., Conti M., Fischmeister R. and Vandecasteele G. (2006) A Specific Pattern of Phosphodiesterases Controls the Camp Signals Generated by Different Gs-Coupled Receptors in Adult Rat Ventricular Myocytes. *Circ Res* **98,** 1081-1088.

Rosendorff A., Ebersole B. J. and Sealfon S. C. (2000) Conserved Helix 7 Tyrosine Functions as an Activation Relay in the Serotonin 5ht(2c) Receptor. *Brain Res Mol Brain Res* **84,** 90-96.

Roth B. L., Choudhary M. S., Khan N. and Uluer A. Z. (1997a) High-Affinity Agonist Binding Is Not Sufficient for Agonist Efficacy at 5-Hydroxytryptamine2a Receptors: Evidence in Favor of a Modified Ternary Complex Model. *J Pharmacol Exp Ther* **280,** 576-583.

Roth B. L., Shoham M., Choudhary M. S. and Khan N. (1997b) Identification of Conserved Aromatic Residues Essential for Agonist Binding and Second Messenger Production at 5-Hydroxytryptamine2a Receptors. *Mol Pharmacol* **52,** 259-266.

Saideman S. R., Blitz D. M. and Nusbaum M. P. (2007a) Convergent Motor Patterns from Divergent Circuits. *J Neurosci* **27,** 6664-6674.

Saideman S. R., Ma M., Kutz-Naber K. K., Cook A., Torfs P., Schoofs L., Li L. and Nusbaum M. P. (2007b) Modulation of Rhythmic Motor Activity by Pyrokinin Peptides. *J Neurophysiol* **97,** 579-595.

Saudou F., Amlaiky N., Plassat J. L., Borrelli E. and Hen R. (1990) Cloning and Characterization of a Drosophila Tyramine Receptor. *EMBO J.* **9,** 3611-3617.

Saudou F., Boschert U., Amlaiky N., Plassat J. L. and Hen R. (1992) A Family of Drosophila Serotonin Receptors with Distinct Intracellular Signalling Properties and Expression Patterns. *EMBO J.* **11,** 7-17.

Schioth H. B. and Fredriksson R. (2005) The Grafs Classification System of G-Protein Coupled Receptors in Comparative Perspective. *Gen Comp Endocrinol* **142,** 94-101.

Schulz D. J., Goaillard J. M. and Marder E. (2006) Variable Channel Expression in Identified Single and Electrically Coupled Neurons in Different Animals. *Nat Neurosci* **9,** 356-362.

Schulz D. J., Goaillard J. M. and Marder E. E. (2007) Quantitative Expression Profiling of Identified Neurons Reveals Cell-Specific Constraints on Highly Variable Levels of Gene Expression. *Proc Natl Acad Sci U S A* **104,** 13187-13191.

Sealfon S. C., Chi L., Ebersole B. J., Rodic V., Zhang D., Ballesteros J. A. and Weinstein H. (1995) Related Contribution of Specific Helix 2 and 7 Residues to Conformational Activation of the Serotonin 5-Ht2a Receptor. *J Biol Chem* **270,** 16683-16688.

Seifert R. and Wenzel-Seifert K. (2002) Constitutive Activity of G-Protein-Coupled Receptors: Cause of Disease and Common Property of Wild-Type Receptors. *Naunyn Schmiedebergs Arch Pharmacol.* **366,** 381-416.

Selverston A. I. (1977) Neural Circuitry Underlying Oscillatory Motor Output. *J Physiol* **73,** 463-470.

Selverston A. I. (2005) A Neural Infrastructure for Rhythmic Motor Patterns. *Cell Mol Neurobiol* **25,** 223-244.

Selverston A. I. and Mulloney B. (1974) Organization of the Stomatogastric Ganglion of the Spiny Lobster. *Journal of Comparative Physiology A: Neuroethology, Sensory, Neural, and Behavioral Physiology* **91,** 33-51.

Selverston A. I. and Miller J. P. (1980) Mechanisms Underlying Pattern Generation in Lobster Stomatogastric Ganglion as Determined by Selective Inactivation of Identified Neurons. I. Pyloric System. *J Neurophysiol* **44,** 1102-1121.

Selverston A. I. and Moulins M., eds (1987) *The Crustacean Stomatogastric System.* Springer, Berlin.

Setterblad N., Onyango I., Pihlgren U., Rask L. and Andersson G. (1998) The Role of Protein Kinase C Signaling in Activated Dra Transcription. *J Immunol* **161,** 4819-4824.

Sgourakis N. G., Bagos P. G., Papasaikas P. K. and Hamodrakas S. J. (2005) A Method for the Prediction of Gpcrs Coupling Specificity to G-Proteins Using Refined Profile Hidden Markov Models. *BMC Bioinformatics* **6,** 104.

Shapiro D. A., Kristiansen K., Kroeze W. K. and Roth B. L. (2000) Differential Modes of Agonist Binding to 5-Hydroxytryptamine(2a) Serotonin Receptors Revealed by Mutation and Molecular Modeling of Conserved Residues in Transmembrane Region 5. *Mol Pharmacol* **58,** 877-886.

Shapiro D. A., Kristiansen K., Weiner D. M., Kroeze W. K. and Roth B. L. (2002) Evidence for a Model of Agonist-Induced Activation of 5-Hydroxytryptamine 2a Serotonin Receptors That Involves the Disruption of a Strong Ionic Interaction between Helices 3 and 6. *J Biol Chem* **277,** 11441-11449.

Sidhu A. (1998) Coupling of D1 and D5 Dopamine Receptors to Multiple G Proteins: Implications for Understanding the Diversity in Receptor-G Protein Coupling. *Mol Neurobiol* **16,** 125-134.

Sidhu A. and Niznik H. B. (2000) Coupling of Dopamine Receptor Subtypes to Multiple and Diverse G Proteins. *Int J Dev Neurosci* **18,** 669-677.

Sidhu A., Laruelle M. and Vernier P., eds (2003) *Dopamine Receptors and Transporters: Function , Imaging and Clinical Implication,* second Edition. Marcel Dekker, Inc., New York.

Sidhu A., Kimura K., Uh M., White B. H. and Patel S. (1998) Multiple Coupling of Human D5 Dopamine Receptors to Guanine Nucleotide Binding Proteins Gs and Gz. *J Neurochem* **70,** 2459-2467.

Smith J. C., Ellenberger H. H., Ballanyi K., Richter D. W. and Feldman J. L. (1991) Pre-Botzinger Complex: A Brainstem Region That May Generate Respiratory Rhythm in Mammals. *Science* **254,** 726-729.

Smith J. C., Butera R. J., Koshiya N., Del Negro C., Wilson C. G. and Johnson S. M. (2000) Respiratory Rhythm Generation in Neonatal and Adult Mammals: The Hybrid Pacemaker-Network Model. *Respir Physiol* **122,** 131-147.

Sosa M. A., Spitzer N., Edwards D. H. and Baro D. J. (2004) A Crustacean Serotonin Receptor: Cloning and Distribution in the Thoracic Ganglia of Crayfish and Freshwater Prawn. *J Comp Neurol* **473,** 526-537.

Sossin W. S., Sweet-Cordero A. and Scheller R. H. (1990) Dale's Hypothesis Revisited: Different Neuropeptides Derived from a Common Prohormone Are Targeted to Different Processes. *Proc Natl Acad Sci U S A* **87,** 4845-4848.

Spitzer N., Antonsen B. L. and Edwards D. H. (2005) Immunocytochemical Mapping and Quantification of Expression of a Putative Type 1 Serotonin Receptor in the Crayfish Nervous System. *J Comp Neurol* **484,** 261-282.

Spitzer N., Edwards D. H. and Baro D. J. (2008) Conservation of Structure, Signaling and Pharmacology between Two Serotonin Receptor Subtypes from Decapod Crustaceans, Panulirus Interruptus and Procambarus Clarkii. *J Exp Biol* **211,** 92-105.

Srivastava D. P., Yu E. J., Kennedy K., Chatwin H., Reale V., Hamon M., Smith T. and Evans P. D. (2005) Rapid, Nongenomic Responses to Ecdysteroids and Catecholamines Mediated by a Novel Drosophila G-Protein-Coupled Receptor. *J Neurosci* **25,** 6145-6155.

Stein W., DeLong N. D., Wood D. E. and Nusbaum M. P. (2007) Divergent Co-Transmitter Actions Underlie Motor Pattern Activation by a Modulatory Projection Neuron. *Eur J Neurosci* **26,** 1148-1165.

Sugamori K. S., Demchyshyn L. L., McConkey F., Forte M. A. and Niznik H. B. (1995) A Primordial Dopamine D1-Like Adenylyl Cyclase-Linked Receptor from Drosophila Melanogaster Displaying Poor Affinity for Benzazepines. *FEBS Lett* **362,** 131-138.

Sullivan R. E., Friend B. J. and Barker D. L. (1977a) Structure and Function of Spiny Lobster Ligamental Nerve Plexuses: Evidence for Synthesis, Storage, and Secretion of Biogenic Amines. *J.Neurobiol.* **8,** 581-605.

Sullivan R. E., Friend B. J. and Barker D. L. (1977b) Structure and Function of Spiny Lobster Ligamental Nerve Plexuses: Evidence for Synthesis, Storage, and Secretion of Biogenic Amines. *J Neurobiol* **8,** 581-605.

Swensen A. M. and Marder E. (2000) Multiple Peptides Converge to Activate the Same Voltage-Dependent Current in a Central Pattern-Generating Circuit. *J.Neurosci.* **20,** 6752-6759.

Swensen A. M. and Marder E. (2001) Modulators with Convergent Cellular Actions Elicit Distinct Circuit Outputs. *J.Neurosci.* **21,** 4050-4058.

Szucs A., Abarbanel H. D., Rabinovich M. I. and Selverston A. I. (2005) Dopamine Modulation of Spike Dynamics in Bursting Neurons. *Eur J Neurosci* **21,** 763-772.

Tabor J. N. and Cooper R. L. (2002) Physiologically Identified 5-Ht2-Like Receptors at the Crayfish Neuromuscular Junction. *Brain Res* **932,** 91-98.

Tazaki K. and Tazaki Y. (2000) Multiple Motor Patterns in the Stomatogastric Ganglion of the Shrimp Penaeus Japonicus. *J Comp Physiol [A]* **186,** 105-118.

Terrin A., Di Benedetto G., Pertegato V., Cheung Y. F., Baillie G., Lynch M. J., Elvassore N., Prinz A., Herberg F. W., Houslay M. D. and Zaccolo M. (2006) Pge(1) Stimulation of Hek293 Cells Generates Multiple Contiguous Domains with Different [Camp]: Role of Compartmentalized Phosphodiesterases. *J Cell Biol* **175,** 441-451.

Thibonnier M., Plesnicher C. L., Berrada K. and Berti-Mattera L. (2001) Role of the Human V1 Vasopressin Receptor Cooh Terminus in Internalization and Mitogenic Signal Transduction. *Am J Physiol Endocrinol Metab* **281,** E81-92.

Thoby-Brisson M. and Simmers J. (1998) Neuromodulatory Inputs Maintain Expression of a Lobster Motor Pattern-Generating Network in a Modulation-Dependent State: Evidence from Long-Term Decentralization in Vitro. *J Neurosci* **18,** 2212-2225.

Thoby-Brisson M. and Ramirez J. M. (2000) Role of Inspiratory Pacemaker Neurons in Mediating the Hypoxic Response of the Respiratory Network in Vitro. *J Neurosci* **20,** 5858-5866.

Thoby-Brisson M. and Ramirez J. M. (2001) Identification of Two Types of Inspiratory Pacemaker Neurons in the Isolated Respiratory Neural Network of Mice. *J Neurophysiol* **86,** 104-112.

Thoby-Brisson M. and Simmers J. (2002) Long-Term Neuromodulatory Regulation of a Motor Pattern-Generating Network: Maintenance of Synaptic Efficacy and Oscillatory Properties. *J Neurophysiol* **88,** 2942-2953.

Thuma J. B. and Hooper S. L. (2002) Quantification of Gastric Mill Network Effects on a Movement Related Parameter of Pyloric Network Output in the Lobster. *J Neurophysiol* **87,** 2372-2384.

Thuma J. B. and Hooper S. L. (2003) Quantification of Cardiac Sac Network Effects on a Movement-Related Parameter of Pyloric Network Output in the Lobster. *J Neurophysiol* **89,** 745-753.

Thuma J. B., Morris L. G., Weaver A. L. and Hooper S. L. (2003) Lobster (Panulirus Interruptus) Pyloric Muscles Express the Motor Patterns of Three Neural Networks, Only One of Which Innervates the Muscles. *J Neurosci* **23,** 8911-8920.

Tierney A. J. (2001) Structure and Function of Invertebrate 5-Ht Receptors: A Review. *Comp Biochem.Physiol A Mol.Integr.Physiol* **128,** 791-804.

Tierney A. J., Godleski M. S. and Rattananont P. (1999) Serotonin-Like Immunoreactivity in the Stomatogastric Nervous Systems of Crayfishes from Four Genera. *Cell Tissue Res* **295,** 537-551.

Tohgo A., Choy E. W., Gesty-Palmer D., Pierce K. L., Laporte S., Oakley R. H., Caron M. G., Lefkowitz R. J. and Luttrell L. M. (2003) The Stability of the G Protein-Coupled Receptor-Beta-Arrestin Interaction Determines the Mechanism and Functional Consequence of Erk Activation. *J Biol Chem* **278,** 6258-6267.

Tsu R. C. and Wong Y. H. (1996) Gi-Mediated Stimulation of Type Ii Adenylyl Cyclase Is Augmented by Gq-Coupled Receptor Activation and Phorbol Ester Treatment. *J Neurosci* **16,** 1317-1323.

Turrigiano G. G. and Selverston A. I. (1990) A Cholecystokinin-Like Hormone Activates a Feeding-Related Neural Circuit in Lobster. *Nature* **344,** 866-868.

Turrigiano G. G. and Marder E. (1993) Modulation of Identified Stomatogastric Ganglion Neurons in Primary Cell Culture. *J Neurophysiol* **69,** 1993-2002.

Undie A. S., Berki A. C. and Beardsley K. (2000) Dopaminergic Behaviors and Signal Transduction Mediated through Adenylate Cyclase and Phospholipase C Pathways. *Neuropharmacology* **39,** 75-87.

Vilim F. S., Cropper E. C., Price D. A., Kupfermann I. and Weiss K. R. (1996) Release of Peptide Cotransmitters in Aplysia: Regulation and Functional Implications. *J Neurosci* **16,** 8105-8114.

Visiers I., Hassan S. A. and Weinstein H. (2001) Differences in Conformational Properties of the Second Intracellular Loop (Il2) in 5ht(2c) Receptors Modified by Rna Editing Can Account for G Protein Coupling Efficiency. *Protein Eng* **14,** 409-414.

Wang C. D., Gallaher T. K. and Shih J. C. (1993) Site-Directed Mutagenesis of the Serotonin 5-Hydroxytrypamine2 Receptor: Identification of Amino Acids Necessary for Ligand Binding and Receptor Activation. *Mol Pharmacol* **43,** 931-940.

Watt A. J., van Rossum M. C., MacLeod K. M., Nelson S. B. and Turrigiano G. G. (2000) Activity Coregulates Quantal Ampa and Nmda Currents at Neocortical Synapses. *Neuron* **26,** 659-670.

Watt A. J., Sjostrom P. J., Hausser M., Nelson S. B. and Turrigiano G. G. (2004) A Proportional but Slower Nmda Potentiation Follows Ampa Potentiation in Ltp. *Nat Neurosci* **7,** 518-524.

Way K. J., Chou E. and King G. L. (2000) Identification of Pkc-Isoform-Specific Biological Actions Using Pharmacological Approaches. *Trends Pharmacol Sci* **21,** 181-187.

Wersinger C., White B. H., Sidhu A. and Senogles S. E. (2003) Physiology, Pharmacology, and Pathophysiology of the D1-Like Family of Dopamine Receptors in the Central Nervous System, in *Dopamine Receptors and Transporters: Function, Imagin and Clinical Implication* (Sidhu A., Laruelle M. and Vernier P., eds), pp 145-210. Marcel Dekker, Inc, New York.

Wilensky A. E., Baldwin D. H., Christie A. E. and Graubard K. (2003) Stereotyped Neuropil Branching of an Identified Stomatogastric Motor Neuron. *J Comp Neurol* **466,** 554-563.

Willoughby D., Wong W., Schaack J., Scott J. D. and Cooper D. M. (2006) An Anchored Pka and Pde4 Complex Regulates Subplasmalemmal Camp Dynamics. *Embo J* **25,** 2051-2061.

Witz P., Amlaiky N., Plassat J. L., Maroteaux L., Borrelli E. and Hen R. (1990) Cloning and Characterization of a Drosophila Serotonin Receptor That Activates Adenylate Cyclase. *Proc.Natl.Acad.Sci.U.S.A* **87,** 8940-8944.

Wohlpart K. L. and Molinoff P. B. (1998) Regulation of Levels of 5-Ht2a Receptor Mrna. *Ann N Y Acad Sci* **861,** 128-135.

Wong S. K. (2003) G Protein Selectivity Is Regulated by Multiple Intracellular Regions of Gpcrs. *Neurosignals* **12,** 1-12.

Wong W. and Scott J. D. (2004) Akap Signalling Complexes: Focal Points in Space and Time. *Nat Rev Mol Cell Biol* **5,** 959-970.

Wood D. E. and Nusbaum M. P. (2002) Extracellular Peptidase Activity Tunes Motor Pattern Modulation. *J Neurosci* **22,** 4185-4195.

Xia Z., Gray J. A., Compton-Toth B. A. and Roth B. L. (2003) A Direct Interaction of Psd-95 with 5-Ht2a Serotonin Receptors Regulates Receptor Trafficking and Signal Transduction. *J Biol Chem* **278,** 21901-21908.

Xu F., Hollins B., Gress A. M., Landers T. M. and McClintock T. S. (1997) Molecular Cloning and Characterization of a Lobster G Alphas Protein Expressed in Neurons of Olfactory Organ and Brain. *J Neurochem* **69,** 1793-1800.

Yamada M., Inanobe A. and Kurachi Y. (1998) G Protein Regulation of Potassium Ion Channels. *Pharmacol Rev* **50,** 723-760.

Yeagle P. L. and Albert A. D. (2007) G-Protein Coupled Receptor Structure. *Biochim Biophys Acta* **1768,** 808-824.

Yeh S.-R., Musolf B. E. and Edwards D. H. (1997) Neuronal Adaptations to Changes in the Social Dominance Status of Crayfish. *J Neurosci* **17,** 697-708.

Zaccolo M. and Pozzan T. (2002) Discrete Microdomains with High Concentration of Camp in Stimulated Rat Neonatal Cardiac Myocytes. *Science* **295,** 1711-1715.

Zhang B. and Harris-Warrick R. M. (1994) Multiple Receptors Mediate the Modulatory Effects of Serotonergic Neurons in a Small Neural Network. *J Exp Biol* **190,** 55-77.

Zhang B. and Harris-Warrick R. M. (1995) Calcium-Dependent Plateau Potentials in a Crab Stomatogastric Ganglion Motor Neuron. I. Calcium Current and Its Modulation by Serotonin. *J Neurophysiol* **74,** 1929-1937.

Zhang B., Wootton J. F. and Harris-Warrick R. M. (1995) Calcium-Dependent Plateau Potentials in a Crab Stomatogastric Ganglion Motor Neuron. Ii. Calcium-Activated Slow Inward Current. *J Neurophysiol* **74,** 1938-1946.

Zhen X., Goswami S., Abdali S. A., Gil M., Bakshi K. and Friedman E. (2004) Regulation of Cyclin-Dependent Kinase 5 and Calcium/Calmodulin-Dependent Protein Kinase Ii by Phosphatidylinositol-Linked Dopamine Receptor in Rat Brain. *Mol Pharmacol* **66,** 1500-1507.

Zheng S., Yu P., Zeng C., Wang Z., Yang Z., Andrews P. M., Felder R. A. and Jose P. A. (2003) Galpha12- and Galpha13-Protein Subunit Linkage of D5 Dopamine Receptors in the Nephron. *Hypertension* **41,** 604-610.

Zhou H. and Murthy K. S. (2004) Distinctive G Protein-Dependent Signaling in Smooth Muscle by Sphingosine 1-Phosphate Receptors S1p1 and S1p2. *Am J Physiol Cell Physiol* **286,** C1130-1138.

Zou S., Li L., Pei L., Vukusic B., Van Tol H. H., Lee F. J., Wan Q. and Liu F. (2005) Protein-Protein Coupling/Uncoupling Enables Dopamine D2 Receptor Regulation of Ampa Receptor-Mediated Excitotoxicity. *J Neurosci* **25,** 4385-4395.